

Departamento de Tecnología y Química Farmacéuticas

Facultad de Farmacia y Nutrición

UNIVERSIDAD DE NAVARRA



**“Systems Pharmacology in Modelling Complex Scenarios:
Opportunities and Challenges”**

María Leire Ruiz Cerdá

Pamplona, 2019

Departamento de Tecnología y Química Farmacéuticas

Facultad de Farmacia y Nutrición

UNIVERSIDAD DE NAVARRA



TESIS DOCTORAL

**“Systems Pharmacology in Modelling Complex Scenarios:
Opportunities and Challenges”**

Trabajo presentado por María Leire Ruiz Cerdá para obtener el grado
de Doctor en Farmacia

Fdo. María Leire Ruiz Cerdá

Pamplona, 2019



UNIVERSIDAD DE NAVARRA

FACULTAD DE FARMACIA Y NUTRICIÓN

Departamento de Tecnología y Química Farmacéuticas

D. JOSÉ IGNACIO FERNÁNDEZ DE TROCÓNIZ FERNÁNDEZ, Doctor en Farmacia y Catedrático del Departamento de Tecnología y Química Farmacéuticas, certifica:

Que el presente trabajo, titulado “Systems Pharmacology in Modelling Complex Scenarios: Opportunities and Challenges”, presentado por DÑA. MARÍA LEIRE RUIZ CERDÁ, para optar al grado de Doctor en Farmacia, ha sido realizado bajo su dirección en el Departamento de Tecnología y Química Farmacéuticas. Considerando finalizado el trabajo autorizan su presentación a fin de que pueda ser juzgado y calificado por el Tribunal correspondiente.

Y para que así conste, firma la presente:

Fdo: Dr. José Ignacio Fernández de Trocóniz Fernández

Pamplona, 2019

A mi padre

“Sólo una cosa vuelve a un sueño imposible: el miedo a fracasar”

- Paulo Coelho

AGRADECIMIENTOS

Comienzo expresando mi agradecimiento a la Universidad de Navarra y al Departamento de Tecnología y Química Farmacéuticas por darme la oportunidad de realizar la tesis doctoral.

Al Prof. Iñaki Fernández de Trocóniz, por haberme dado la oportunidad de desarrollarme tanto profesional como personalmente. Por su comprensión y su generosidad, por buscar siempre lo mejor para mí y apoyarme en los momentos difíciles. Y como no, por haberme enseñado tanto de este campo. También a María Jesús por haber formado parte de este aprendizaje.

A mis PKPDitas, gracias a cada una de vosotras por todo lo que me habéis dado. A María Nonmem, la más veterana, por desprender siempre tanta alegría. A Itziar, de gran estómago pero de mayor corazón, que tras pasar una dura entrevista, empezó esta aventura conmigo. A Vio Pío por su bondad y generosidad, por preocuparte tanto de mí. A Bel por transmitirme esa paz y tranquilidad.

A las personas que forman parte del grupo PSP, gracias por enseñarme como debe funcionar un grupo, como debemos ayudarnos los unos a los otros. Zinnia, gracias por todos tus consejos y cariño, sobre todo en los momentos de caos. Edu, por guiarme de la mejor forma y tener siempre la puerta abierta cuando lo necesito. Diego, por poner ese toque de humor entre modelo y modelo. Nicolás, por luchar por nuestros derechos. Fernando, por tu alegría. Sara, por tus dosis de motivación y alegría en las comidas.

A las personas que han pasado por el grupo, que aunque ya no forman parte de él, sí de mi corazón: Nuria, María Merino, Ana Margarita, Víctor, Nacho, Aziz, Aurelia... pero en especial a JD, por llenarme de positividad y tirar de mí hacia delante, por apoyarme en todas mis decisiones y buscar lo mejor para mí, aunque estés lejos me acuerdo mucho de ti.

A todos los compañeros y profesores del Departamento, a los que ya terminaron, a los que están y a los que empiezan. A Hugo, y tal. Han sido muchos cafés durante estos 4 años, os deseo lo mejor.

A Ioritz, por estar a mi lado durante este largo camino, por haberme dado lo más bonito de este mundo. Ainhoa, cariño, gracias por traer tanta alegría a nuestras vidas, por cada sonrisa, cada beso, cada abrazo, por llenar de luz mis días más oscuros. Tú me haces más fuerte.

A mi madre, eres lo más grande que tengo. De ti he aprendido a querer desinteresadamente, a ser cada día mejor persona y una luchadora. Gracias por hacer de madre y de padre a la vez y convertirme en lo que soy. A mi padre, que nos cuida y guía desde su estrella. No sabes lo que te echo en falta. A mi hermano, por apoyarme y defenderme siempre, hacerme entrar en razón y hacerme ver las cosas desde la tranquilidad y el sosiego. Al resto de mi familia, abuelos, tíos y primos, gracias por estar siempre ahí. A mi familia de Pamplona, Loli, Pedro e Ibai por quererme y tratarme como una hija más.

A Anaïs, gracias por tu amistad, por tu apoyo incondicional, por haber estado SIEMPRE, en los momentos buenos, pero sobretodo en los malos. Por no dejar que toque fondo y aceptarme tal y como soy. No sé qué será de nosotras, lo que sí que sé es que voy a tener una hermana toda la vida.

A mis amigos y amigas. Gracias por poder contar con vosotros.

TABLE OF CONTENTS

ABBREVIATIONS	1
PREFACE	5
INTRODUCTION	9
SYSTEMS PHARMACOLOGY	11
1. PHARMACOMETRICS AND SYSTEMS PHARMACOLOGY APPROACHES	15
2. TYPES OF SYSTEMS PHARMACOLOGY MODELS	16
3. SYSTEMS PHARMACOLOGY MODELS VALIDATION	25
4. SYSTEMS PHARMACOLOGY MODELS REDUCTION	26
5. PHARMACOMETRICS AND SYSTEMS PHARMACOLOGY IN THE WORLD	27
6. REFERENCES	29
OBJECTIVES	37
CHAPTER 1	41
SYSTEMIC LUPUS ERYTHEMATOSUS OVERVIEW	43
1. SYSTEMIC LUPUS ERYTHEMATOSUS DEFINITION	43
2. EPIDEMIOLOGY	43
3. ETIOLOGY	43
4. DIAGNOSIS	44
5. TREATMENT	45
6. MODELLING EFFORTS APPLIED TO SLE	47
7. REFERENCES	50
TOWARDS PATIENT STRATIFICATION AND TREATMENT IN THE AUTOIMMUNE DISEASE LUPUS ERYTHEMATOSUS USING A SYSTEMS PHARMACOLOGY APPROACH	55
ABSTRACT.....	57
1. INTRODUCTION.....	59
2. METHODS.....	65
2.1 LITERATURE SEARCH, SELECTION, ANNOTATION AND SYSTEM REPRESENTATION.....	65
2.2 BOOLEAN NETWORK BUILDING	68

2.3 SIMULATIONS.....	70
3. RESULTS	74
3.1 NETWORK DYNAMICS SIMULATIONS	76
3.2. PERTURBATION ANALYSIS AND CLUSTERING	77
3.3. EVALUATION OF THERAPEUTIC TARGETS	78
4. DISCUSSION.....	81
5. CONCLUSIONS.....	85
6. REFERENCES.....	87
SUPPLEMENTARY MATERIAL	93
CHAPTER 2.....	123
COAGULATION OVERVIEW.....	125
1. COAGULATION GENERALITIES	125
2. COAGULATION MECHANISMS	125
3. COAGULATION REGULATION	127
4. COAGULATION TESTS.....	127
5. COAGULATION ALTERATIONS	130
6. THERAPEUTIC ALTERNATIVES	132
7. REFERENCES.....	135
DESCRIBING THE COAGULATION CASCADE: FROM A SYSTEMS PHARMACOLOGY MODEL TO A SEMI-MECHANISTIC APPROACH	137
1. INTRODUCTION.....	139
2. METHODS.....	143
LITERATURE SEARCH OF QUANTITATIVE SYSTEMS PHARMACOLOGY MODELS FOR COAGULATION	143
MODEL IMPLEMENTATION AND EVALUATION	143
CLINICAL DATA.....	145
SIMULATIONS.....	146
SEMI-MECHANISTIC PKPD MODEL BUILDING	147
3. RESULTS	151
MODEL IMPLEMENTATION AND EVALUATION OF THE IMPLEMENTATION	151
CLINICAL DATA INTEGRATION IN THE MODELS AND SIMULATION	152
MODELLING THROMBIN PROFILES	156

SEMI-MECHANISTIC PKPD MODEL FOR THE COAGULATION PROCESS.....	158
4. DISCUSSION.....	163
5. REFERENCES.....	166
SUPPLEMENTARY MATERIAL	169
CHAPTER 3.....	187
THE LONG NEGLETED PLAYER: MODELING TUMOR UPTAKE TO GUIDE OPTIMAL	
DOSING	189
ABSTRACT.....	191
MAIN TEXT	193
REFERENCES.....	197
GENERAL DISCUSSION	199
CONCLUSIONS/CONCLUSIONES	211
ANNEX I	217

ABBREVIATIONS

Abbreviation	Definition
ACoP	American Conference of Pharmacometrics
ACR	American College of Rheumatology
AIC	Akaike Information Criteria
APC	Antigen Presenting Cell
aPTT	Activated partial thromboplastin time
ATIII	Antithrombin III
AUC	Area under the concentration vs time curve
B7H1	Programmed death-ligand 1
BAFF	B-cell activating factor
BSV	Between subject variability
CAT	Calibrated automated thrombogram
C _{max}	Maximun drug concentration
COLOMOTO	Consortium for Logical Models and Tools
CPT:PSP	Clinical Pharmacology & Therapeutics: Pharmacometrics & Systems Pharmacology
CTLA4	Cytotoxic T-lymphocyte-associated protein 4
DC	Dendritic cell
DDMoRe	Drug Disease Model Resources
DIL	Drug induced lupus
DLE	Discoid lupus erythematosus
DNA	Deoxyribonucleic acid
EBV	Epstein-Barr virus
F	Fibrin
FDA	Food and Drug administration
Fg	Fibrinogen
FII	Factor II
FIIa	Factor II activated
FIX	Factor IX
FIXa	Factor IX activated
FOCE	First Order Conditional Estimation
FVII	Factor VII

FVIIa	Factor VII activated
FVIII	Factor VIII
FVIIIa	Factor VIII activated
FX	Factor X
FXa	Factor X activated
FXI	Factor XI
FXIa	Factor XI activated
FXII	Factor XII
FXIIa	Factor XII activated
GINsim	Gene Interaction Network simulation
GOF	Goodness of fit
ICOS	Inducible T-cell COStimulator
IFN	Interferon
IIV	Inter Individual Variabilty
IL	Interleukin
INR	International normalized ratio
ISI	International sensitivity index
ISOP	International Society of Pharmacometrics
K	Kallikrein
LMWH	Low molecular weight heparins
mAb	Monoclonal antibody
MeSH	Medical Subject Headings
MHCII	Major histocompatibility complex class II
MID3	Model-informed Drug Discovery and Development
MTD	Maximum tolerated dose
NET	Neutrophil Extracellular Traps
NLE	Neonatal lupus erythematosus
NONMEM	Nonlinear Mixed Effect Models
NSAID	Nonsteroidal anti-inflammatory drug
ODE	Ordinary differential equation
OFV	Objective function value
PAGANZ	Population Approach Group in Australia and New Zealand
PAGE	Population Approach Group in Europe

PAGJa	Population Approach Group in Japan
PAGK	Population Approach Group in Korea
PBPK	Physiologically based pharmacokinetic modelling
PCPC	Pharmacometrics in China
PD1	Programmed cell death-1
PharmML	Pharmacometrics Markup Language
PI	Perturbation Index
Pk	Prekallikrein
popPKPD	Population pharmacokinetic pharmacodynamic
PPP	Platelet-rich plasma
PRP	Platelet-poor plasma
PsN	Perl-speaks-Nonmem
PT	Prothrombin time
QSP	Quantitative systems pharmacology
RE	Residual error
SB	Systems Biology
SBML	Systems Biology Markup Language
SCM	Stepwise covariate modelling
SLE	Systemic Lupus Erythematosus
SNP	Single Nucleotide Polymorphism database
SP	Systems Pharmacology
SPIDDOR	Systems Pharmacology for efficient Drug Development On R
TF	Tissue factor
TFPI	Tissue factor pathway inhibitor
TGA	Thrombin generation assay
TMDD	Target-Mediated Drug Disposition
TNF	Tumor Necrosis Factor
UH	Unfractionated heparin
UV	Ultraviolet
VPC	Visual Predictive Check
WCOP	World Conference of Pharmacometrics

PREFACE

The treatment of complex diseases represents currently a major challenge. In this context systems pharmacology (SP) is an emergent discipline that provides an opportunity to get deeper insights in this type of diseases by integrating different areas of knowledge including biology, pharmacology, pharmacometrics, statistics, and computational modelling.

Nowadays, SP has relevance throughout the entire process of drug development, since it has been able to show that systems computational models allow increasing the understanding of different mechanisms of action and regulatory processes, demonstrating their usefulness for organizing large biological data sets and extracting significant information. These models are useful for (i) the identification and validation of new therapeutic targets, (ii) the discovery of new biomarkers, (iii) patient stratification, (iv) dose individualization, (v) the identification of new sources of variability and (vi) the prediction of toxicity and adverse effects.

In this thesis, different types of mechanistic models were explored showing its capabilities and drawbacks.

The *Introduction* section provides a brief description and uses of systems pharmacology models.

Chapter 1 presents a systems pharmacology model for Systemic Lupus Erythematosus. This model, based in Boolean equations, allows identifying different patient subpopulations according to their molecular alterations, predicting the variability in the progression of the disease and designing individualized drug therapies with a high likelihood of success.

In *Chapter 2* two systems pharmacology models for coagulation cascade published in the literature are implemented and reproduced. Then, experimental data obtained from the literature was incorporated in both models to reproduce coagulation tests. Finally, a semi-mechanistic pharmacokinetic/pharmacodynamic (PKPD) model was built to fit this experimental data.

Chapter 1 and *Chapter 2* provide an overview of the characteristics of the disease or biological system and their therapeutic alternatives as well as the description of the

information and methodology used to develop the SP models, together with the corresponding results.

On the other hand, *Chapter 3* discusses the impact of considering exposure at the target site with regard to systemic concentrations, a piece of information that usually remains forgotten in mechanistic modelling.

The *General Discussion* highlights the most relevant aspects of the three chapters, followed by the *Conclusions* section, which summarizes the main findings of this thesis.

Finally, in the Annex, an article of a systems pharmacology model developed for inflammatory bowel disease, recently published in PLOS ONE journal is enclosed.

INTRODUCTION

SYSTEMS PHARMACOLOGY

In the last years, drug development is becoming more challenging and costly. Despite the advances in scientific knowledge, the gap between bench discovery and bedside application is increasing; in fact, less than 10% of the drugs starting a phase 1 clinical program are finally approved by the FDA (Food and Drug Administration). This percentage is even lower in oncology or cardiovascular diseases among others^a (Figure 1). Additionally, the cost of bringing a new drug to market is estimated to be around \$1.7 billion^b. As a consequence, regulatory agencies like FDA proposed several initiatives for optimizing drug development.

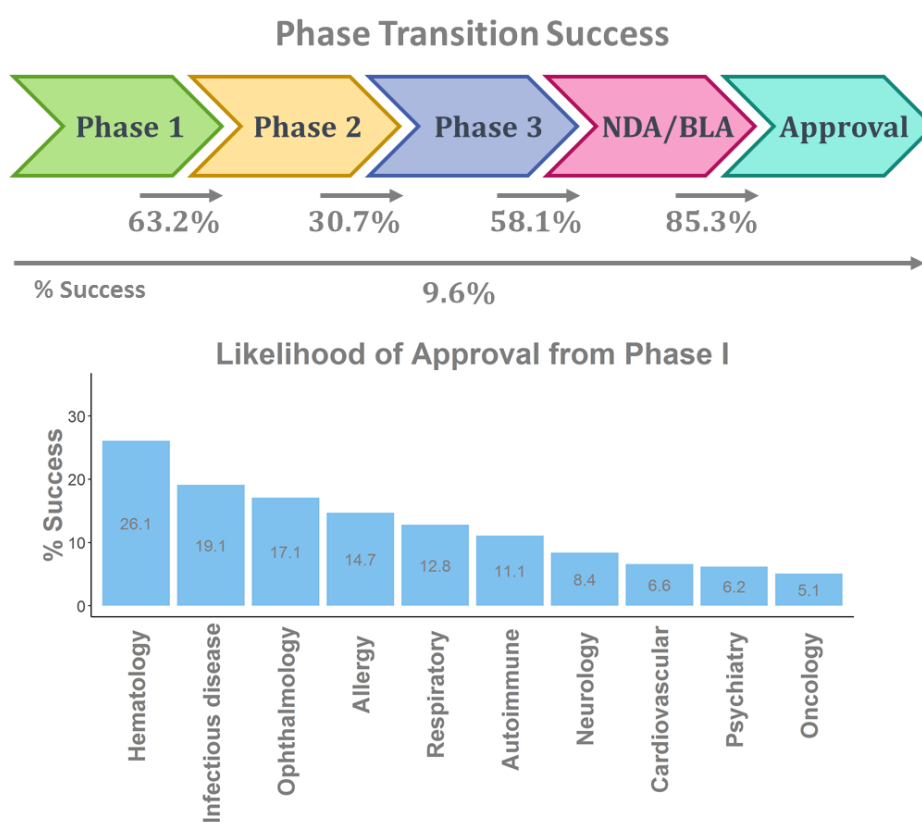


Figure 1. Phase transition success of drugs during drug development and the likelihood of approval from phase I by disease. NDA (New drug application), BLA (Biologic license application).

One of these initiatives was the *Critical Path Initiative* launched by the FDA in March 2004. This initiative aimed to modernize the scientific and technical tools for evaluating and predicting the safety, effectiveness and manufacturability of innovative medical products and thus accelerate the drug development process.

^a<https://www.bio.org/sites/default/files/Clinical%20Development%20Success%20Rates%202006-2015%20-%20BIO,%20Biomedtracker,%20Amplion%202016.pdf>

^b http://www2.bain.com/bainweb/PDFs/cms/Marketing/rebuilding_big_pharma.pdf

These strategies and tools were summarized in the report “*Innovation/Stagnation: Challenge and Opportunity on the Critical Path to New Medical Products*”^c. In addition to this report, an opportunity list^d with specific tasks for driving this modernization was provided. This opportunity list was subsequently divided into six broad topic areas (Figure 2).

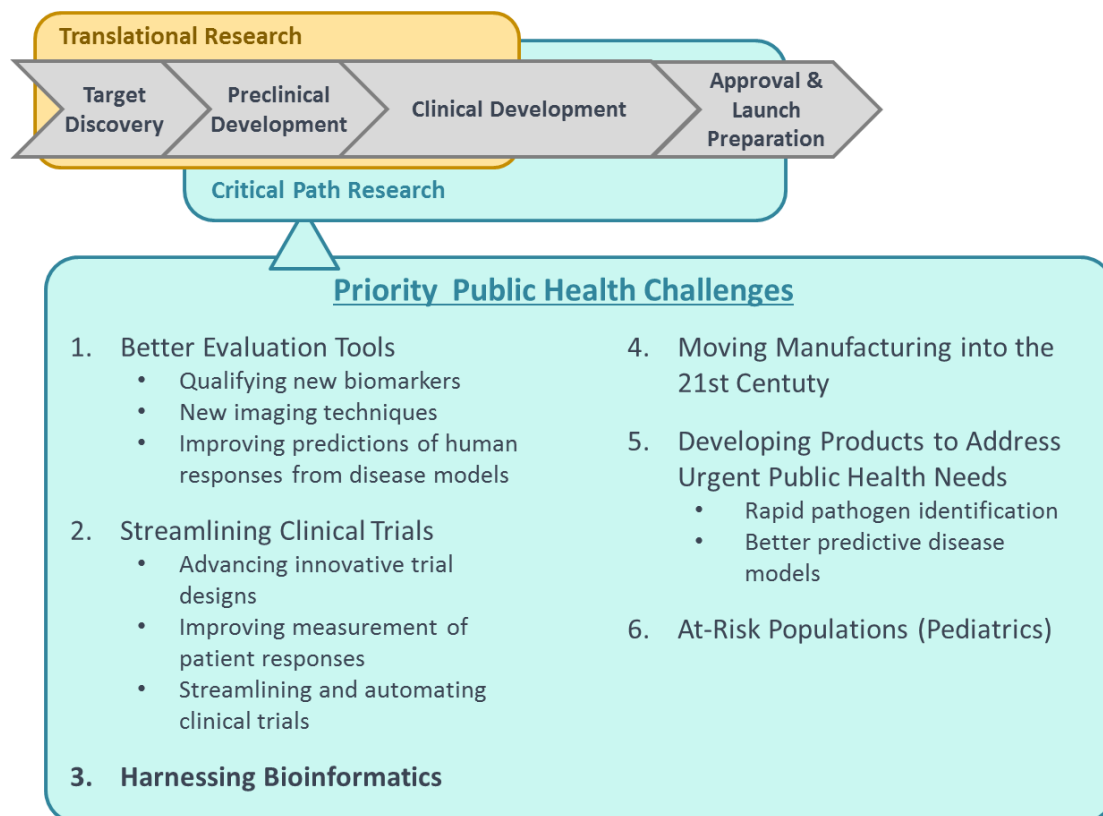


Figure 2. Translational research consists on transfer the discoveries into preclinical and clinical analysis whereas critical path research is focused on improving the drug development process. The FDA released an opportunity list to facilitate this process. It is divided into six different areas.

The focus of the current thesis is the third challenge area, bioinformatics. This area aims to improve drug development efficacy and predictability of results through the application of mathematics, statistics and computational analysis.

One opportunity suggested within the bioinformatics area was “Model-based drug development”. Defined as “a mathematical and statistical approach that constructs, validates, and utilizes different type of models to facilitate drug development”¹, this approach is also known as pharmacometrics. Pharmacometrics includes: (i) population pharmacokinetic/ pharmacodynamic (popPKPD) models, (ii) disease models, (iii)

^c<http://wayback.archive-it.org/7993/20180125142845/https://www.fda.gov/downloads/ScienceResearch/SpecialTopics/CriticalPathInitiative/CriticalPathOpportunitiesReports/UCM077254.pdf>

^d<http://wayback.archive-it.org/7993/20180125035449/https://www.fda.gov/downloads/ScienceResearch/SpecialTopics/CriticalPathInitiative/CriticalPathOpportunitiesReports/UCM077258.pdf>

evaluation and formal validation methodologies and (iv) optimized design of clinical trials. Additionally, through simulation exercises, is possible to understand biologic systems as well as explore possible dosage scenarios. This definition of pharmacometrics establishes links between other challenging areas as can be seen from figure 2.

Currently, most public and private institutions consider pharmacometrics a fundamental element within any drug development program as it aims to reduce the time and the cost of bringing a new drug to the market significantly. Furthermore, a properly evaluated and validated popPKPD model can be used to (i) establish individualized dosage regimens, (ii) explore different scenarios and (iii) reuse the acquired knowledge and apply to different conditions and situations, among others.

Although the predictive capacity of popPKPD models is contrasted and confirmed in the context of interpolation, prediction of the clinical outcome in complex scenarios is associated with a big uncertainty. For example, the emergence of immuno-oncology drugs has resulted in a revolution, becoming to cease different tumors that years ago were devastating, like melanoma. However, some part of the population does not respond to the treatment. The possibility to anticipate which type of patients are going to respond as well as discover the reason of this lack of response opening the possibility to an alternative treatment has an extraordinary repercussion. Besides the need of patient stratification, the difficulty to identify the best candidates for combination treatments, identification of predictive biomarkers and new therapeutic targets represents additional complexities. These needs/challenges could not be accomplished just by applying or developing data-driven popPKPD modelling, and thus a new discipline has emerged, systems pharmacology (SP) (Figure 3).

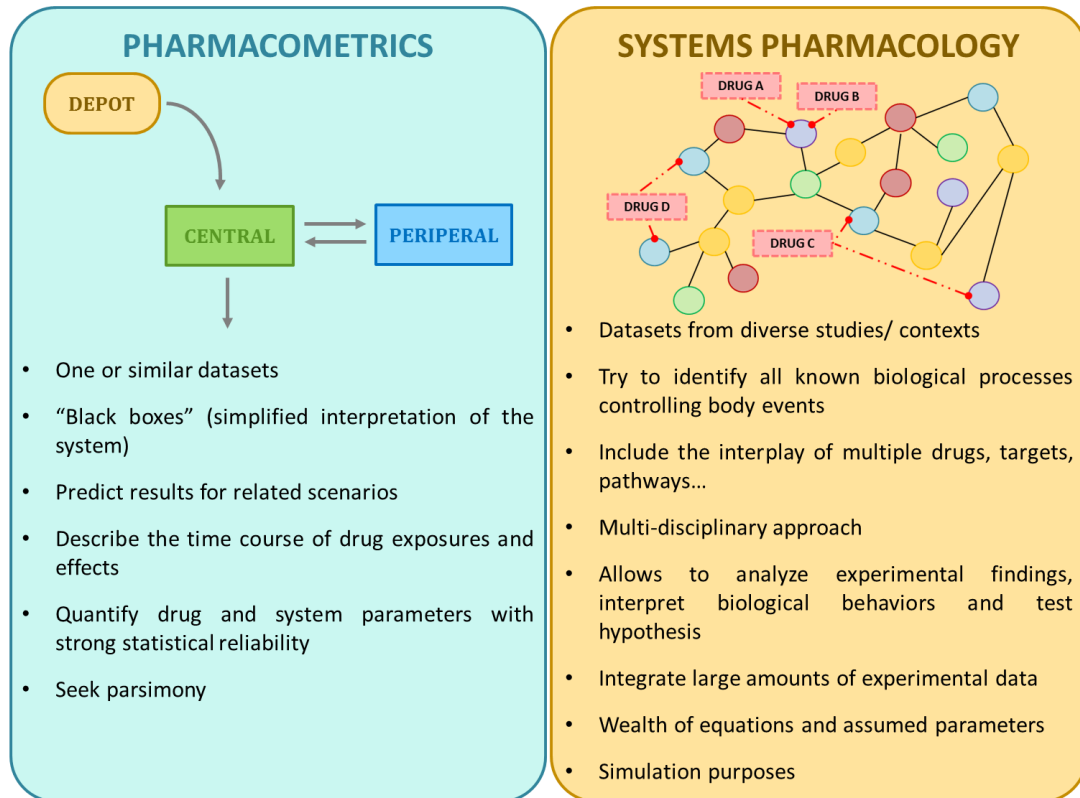


Figure 3. Differences between pharmacometrics and systems pharmacology.

Frequently, systems pharmacology term is associated with pharmacometrics. As Figure 4 shows, these disciplines are complementary and they are connected by the translational nexus. The aim of systems pharmacology is bridging together systems biology, engineering and pharmacokinetic/ pharmacodynamic (PKPD) modelling to understand the mechanism of action of drugs and therefore, making possible the interpretation of drug efficacy and adverse events².

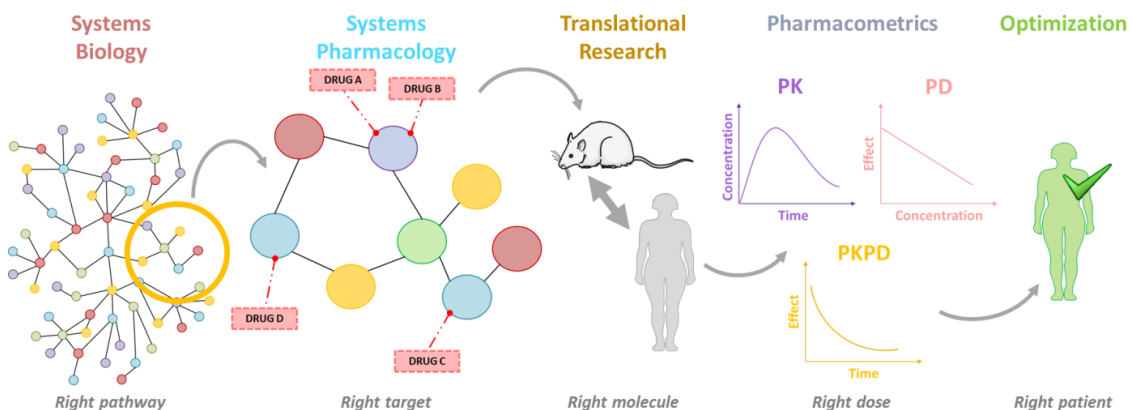


Figure 4. The relationship between PKPD modelling and systems pharmacology during new drug development and patient use.

As it is represented in Figure 4, systems pharmacology discipline has relevance during all drug development process because allows: (i) identifying and validating new targets, (ii) discovering new biomarkers, (iii) stratifying patients, (iv) individualizing dosage regimens, (v) identifying response variability sources, and (vi) predicting toxicity and adverse events.

The combination of pharmacometrics and systems pharmacology during the last decade has recently led to “Model Informed Drug Discovery and Development” (MID3), which is defined as “a quantitative framework for prediction and extrapolation, centered on knowledge and inference generated from integrated models of compound, mechanism and disease level data and aimed at improving the quality, efficiency and cost effectiveness of decision making”³.

1. Pharmacometrics and systems pharmacology approaches

There are two main strategies for data analysis and integration of knowledge (Figure 5), the bottom up and the top down approaches⁴. The distinction lies in the way in which the system is view. The bottom-up approach joins small systems to derive complex biological systems. In this type of approach, the individual elements of the system are first specified in great detail, conferring a maximum level of granularity. On the contrary, the top-down approach consists of breaking down a top-level system to get insights of the sub-systems. It is considered data-driven and represents the approach followed by most semi-mechanistic popPKPD models. One disadvantage of this approach is that sometimes the models may lack interpretability regarding mechanisms.

Generally, SP models use the bottom-up approach, allowing building exhaustive computational structures based on the knowledge of the physiologic systems and integrating different types of information obtained from diverse sources. Furthermore, they are not limited by quantitative and longitudinal data as it will be discussed below.

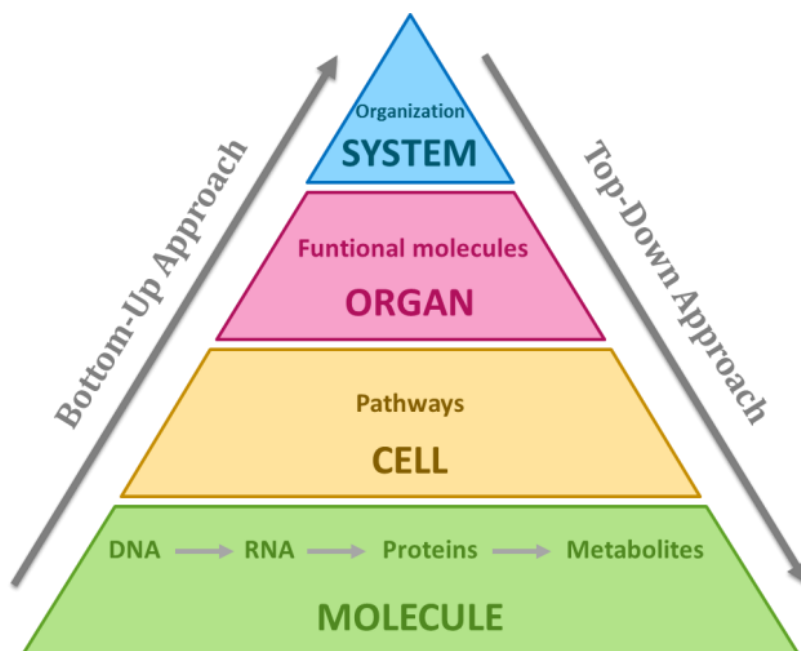


Figure 5. Bottom-up approach vs top-down approach. Adapted from Shalhoub et al.⁵

2. Types of systems pharmacology models

Generalizing, we can distinguish between two types of systems pharmacology models⁶ which are not mutually exclusive: (i) (semi-) qualitative networks based on Boolean operators and, (ii) quantitative models based on ordinary differential equations (ODEs) and algebraic equations.

Boolean networks

Boolean networks were introduced by Kauffman in 1969⁷. A network is a way of representing related data which is composed of nodes that are the network components (molecules, proteins, genes...) and the relationships between these nodes⁶. Through this type of networks, it is possible to represent complex biological processes.

In this type of models, the nodes (elements) only can assume two states, activated or inactivated, represented by logic values “1” or “0”, respectively. The connections (relationships) are built through the Boolean operators “AND”, “OR”, and “NOT”. Once the nodes and the relationships are identified, the Boolean equations are built. Each node has its Boolean equation, through its state is calculated.

- Updating methods: synchronous/ asynchronous

In Boolean models, time is a discrete entity that specifies the instances in which the state of the nodes may change. In each time step, the state of each node is updated and it is determined by the states of the nodes regulating it according to the corresponding Boolean equation.

There are two strategies that differ in the way in which the nodes are updated (as it is explained in Figure 6), the synchronous or asynchronous updating methods⁸. In the synchronous method, the state of the nodes at time t is calculated just by the states of its regulatory nodes at time $t-1$. On the other hand, with the asynchronous method, the state of a node at time t is updated according to the last update (time $t-1$ or t if it has already been updated) of its regulatory nodes. In both cases, the order in which the nodes are updated at each step is selected randomly. However, when using the synchronous method, the output at time t always depends on the state of the nodes at time $t-1$, obtaining the same output in each time step. Contrary, when using the asynchronous method the output may vary depending on the updated order in time t , thus introducing stochasticity in the model (as can be seen in Figure 6).

BOOLEAN EQUATIONS

- A = 1
- B = A
- C = NOT A
- D = A
- E = D OR C
- F = E AND B

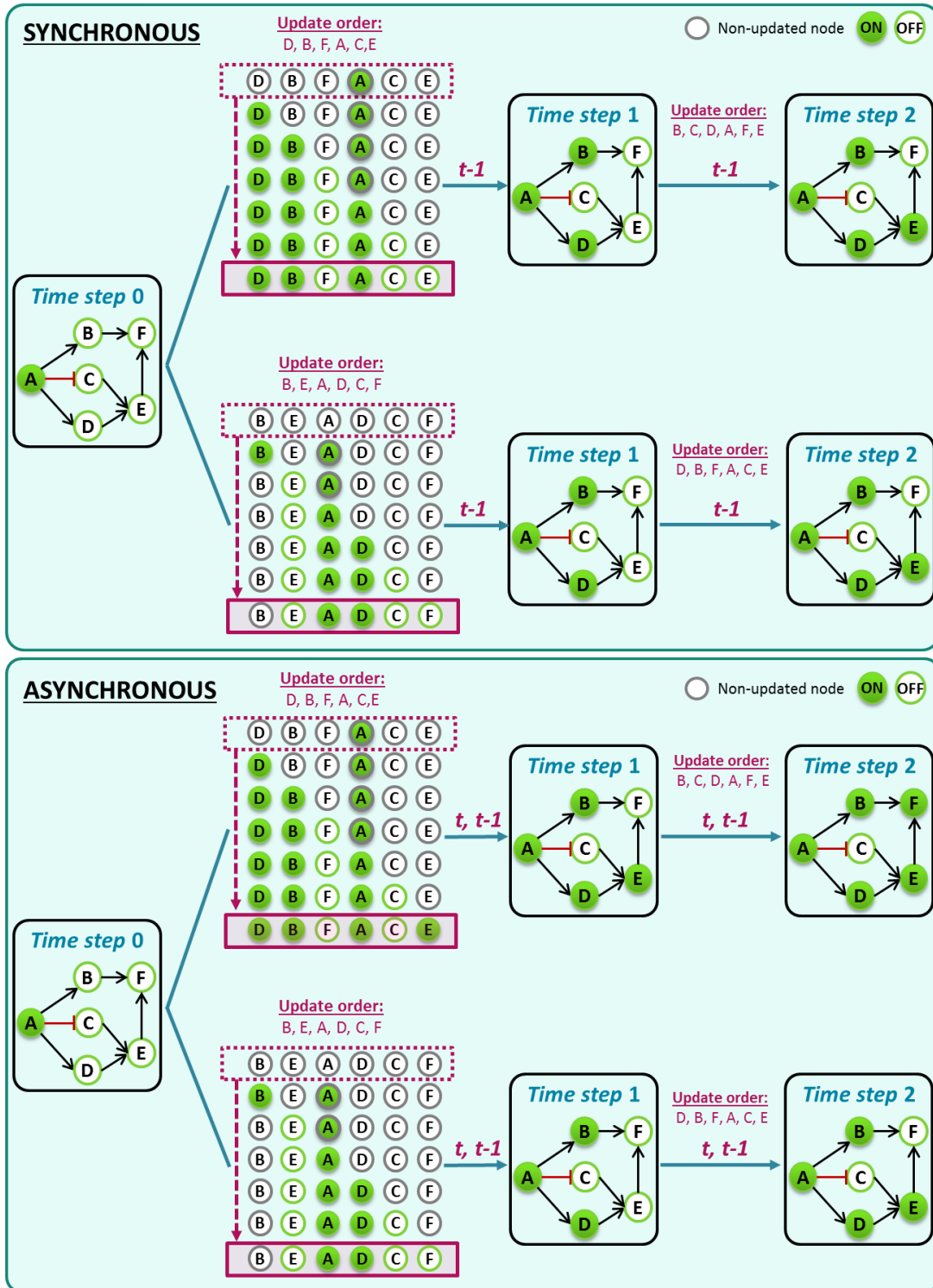


Figure 6. Explanation of the synchronous and asynchronous updating methods. Adapted from Irurzun-Arana I. et al.⁹

- Attractors

The behavior of a Boolean network is explored by means of simulations, once the initial conditions of the system are specified. The system eventually results in a set of stable states called attractors. Attractors can be classified in different groups: (i) a fixed-point if it consists of only one state, (ii) a simple cycle if it is composed by more than one state that oscillates in a cycle or (iii) a complex attractor if the set of states oscillate irregularly¹⁰. Usually, large-scale or highly interconnected networks using the asynchronous method converge into complex attractors.

- Models

The development of Boolean network models in the area of pharmacology is recent and still scarce. Some examples are summarized in Table 1. As we can observe, they represent complex networks in which a great number of nodes and relationships are involved.

Our research group has developed recently two Boolean networks corresponding to systemic lupus erythematosus¹¹ and inflammatory bowel diseases¹², the former as a part of the current Ph.D. thesis.

Usually, this type of models can be built with qualitative or discrete data, that is when the quantitative and longitudinal data is limited and parameter estimation is not possible. Furthermore, they can be used as the starting point in the development of quantitative models. For example, Chudasama et al.¹³ built a Boolean network of signal transduction pathways in multiple myeloma cells, and they converted it into an ODEs based model in order study bortezomib effects on signal transduction in multiple myeloma cells. Years later, Ramakrishnan and Mager¹⁴, extended Chudasama et al. model adding additional signaling pathways. Also, the model was converted to a quantitative model to evaluate the heterogeneity in the pharmacological response to bortezomib.

Table 1. Boolean systems biology and systems pharmacology models published in the literature. SB (Systems Biology) SP (Systems Pharmacology).

Author(s)	Type	Pathway/Disease	Components		Method	Tool	Year	Ref
			Nodes	Interactions				
Sáez-Rodríguez et al.	SB	T cell receptor signaling	94	123	Synchronous/ Asynchronous	Cell Net Analyzer	2007	15
Thakar et al.	SB	B. bronchiseptica and B. pertussis	Not specified	Not specified	Asynchronous	Custom Python code	2007	16
Zhang et al.	SB	T cell large granular lymphocyte leukemia	58	123	Asynchronous	Custom Python code	2008	17
Sahin et al.	SP	ERbb signaling	20	46	Not specified	GINsim	2009	18
Calzone et al.	SB	Cell-Fate Decision in Response to Death Receptor Engagement	11	28	Asynchronous	GINsim	2010	19
Saadatpour et al.	SB	T cell large granular lymphocyte leukemia	60	142	Asynchronous	BooleanNet	2011	8
Saez-Rodríguez et al.	SP	Immediate-early signaling in liver cells	78	112	Synchronous	Cell Net Optimizer	2011	20
Rodríguez et al.	SB	FA/BRCA pathway	28	122	Synchronous	BoolNet	2012	21
Singh et al.	SP	Signaling pathway in HGF-induced keratinocyte migration	66	66	Synchronous	BoolNet	2012	22
Helikar et al.	SP	ErbB Receptor Signal Transduction	245	1100	Synchronous	Cell Collective	2013	23
Conroy et al.	SB	CD4+ T-cell	188	Not specified	Synchronous	Cell Collective	2014	24
von der Heyde et al.	SP	Breast Cancer	96	356	Synchronous/ Asynchronous	BoolNet	2014	25
Steinway et al.	SP	TGFβ signaling in hepatocellular carcinoma	70	135	Asynchronous	BooleanNet	2014	26
Oyeyemi et al.	SP	HIV-1	137	336	Not specified	Cell Net Analyzer	2015	27
Rodríguez et al.	SP	FA/BRCA pathway	15	66	Synchronous/ Asynchronous	BoolNet	2015	28
Remy et al.	SB	Bladder cancer	30	84	Asynchronous	GINsim	2015	29
Flobak et al.	SP	Gastric cancer	73	142	Asynchronous	GINsim	2015	30
Lu et al.	SP	Colitis-associated colon cancer	70	153	Asynchronous	SimpleBool	2015	31
Vasaikar et al.	SP	Apoptotic pathway in neuronal cells	21	37	Synchronous	Matlab	2015	32
Ruiz-Cerdá et al.	SP	Systemic Lupus Erythematosus	52	296	Asynchronous	Custom R code	2016	11
Méndez & Mendoza	SB	B cells terminal differentiation	22	39	Synchronous	BoolNet	2016	33
Udyavar et al.	SB	Small-Cell Lung Cancer	33	361	Asynchronous	NetworkX	2017	34
Balbás-Martínez et al.	SP	Inflammatory Bowel Disease	43	298	Asynchronous	SPIDDOR	2018	12
Ramakrishnan & Mager	SP	Multiple Myeloma	19	37	-	Odefy	2018	14

- Tools

As can be seen in Table 1, there are different tools and software packages to develop and explore Boolean networks. The following provides a brief description of some of them:

SPIDDOR: Systems Pharmacology for efficient Drug Development On R³⁵ (SPIDDOR) is an R package to perform Boolean modelling. It was developed in our laboratory. This software, allows (i) simulating activation profiles with corresponding confidence intervals, (ii) performing attractor analysis, (iii) including perturbations in the system and, (iv) making sensitivity analysis. It has implemented synchronous and asynchronous updating methods. Furthermore, this tool offers the possibility to introduce new types of regulatory interactions, like up-regulation or down-regulation, as well as polymorphisms.

Cell Net Analyzer: Cell Net Analyzer³⁶ is a Matlab toolbox which provides a graphical user interface and allows structural analysis of different types of cellular networks (metabolic, signaling and regulatory).

BoolNet: BoolNet³⁷ is an R package that allows analyzing Boolean networks using synchronous and asynchronous updating schemes, as well as probabilistic Boolean Networks. It also includes different methods to identify attractors. The nodes can be temporarily knocked out and overexpressed.

Cell Collective: Cell collective³⁸ is a software which is implemented in Java and the simulation tool is based on ChemChains. This web-based platform^e allows scientists over the world to share experimental data to build mathematical models of biological processes. Cell Collective is formed by (i) biological databases from different resources, like Uniprot, WikiPathways, among others which contain information about data experiments, (ii) a software which allows performing simulations with dynamical models, (iii) the first repository for qualitative models, (iv) the option to use Systems Biology Markup Language (SBML) to facilitate the exchange between investigation groups, and (v) tools for visualization and analysis different types of networks.

GINsim: Gene Interaction Network simulation (GINsim)³⁹ is a user-friendly modelling software for logical networks analysis which can include perturbations. The software

^e <http://www.thecellcollective.org>

was presented in 2006⁴⁰ but currently, there are different versions. It is composed by a graphical user interface, a simulation core and a graph analysis toolbox. The main advantages of GINsim are the possibility of multilevel modelling and the updating schemes that can be used are synchronous, asynchronous and mixed schemes.

SQUAD: SQUAD⁴¹ is a software which is written in Java version 1.6. Before using SQUAD, the topology (nodes and their relationships representation) of the network has to be established. SQUAD accepts different types of input formats, but they included the possibility of using CellDesigner^f, which is a graphical tool to build and edit biological networks. Once the network is loaded into SQUAD, it converts the network into a discrete dynamical system and identifies all stable states of the network. Then, it is converted into a continuous dynamical system using the steady states found in the discrete model. Finally, simulations with or without perturbations can be performed.

- CoLoMoTo consortium

CoLoMoTo (Consortium for Logical Models and Tools)^g is a consortium formed by different research groups working in the field of logical modelling. It comprises modelers as well as tools developers. A priority in this consortium is to define standards for (i) model representation and interchange, (ii) methods comparison, (iii) models and (iv) tools.

Quantitative models

Quantitative systems pharmacology is described as the quantitative analysis of dynamic interactions between drugs and biologic systems to discover how the drugs modulate the dynamics of biologic components in molecular and cellular networks and the impact of these perturbations in human physiopathology⁴².

Quantitative systems pharmacology models are mechanistic models which describe physiologic processes through ODEs. For that, extensive knowledge of the parameters involved in the processes is needed⁶. These models are a great tool to enhance the understanding of different mechanisms of action and regulation processes, demonstrating its utility to organize large dimension data sets allowing to obtain relevant information⁴³.

^f <http://www.celldesigner.org/>

^g <http://www.colomoto.org/>

○ Models

In the last decade, the development of quantitative systems pharmacology (QSP) models has increased⁴⁴. Some examples are shown in Table 2. These models describe dynamic systems through mathematical equations that characterize biological mechanisms. Some of them present similarities to mechanistic PKPD models, in fact, there are still some controversies when it comes to distinguishing between them.

Table 2. Examples of QSP models published in the literature.

Author(s)	Pathway/Disease	Tool	Year	Ref
Wajima et al.	Coagulation	Matlab	2009	45
Peterson & Riggs	Calcium homeostasis and bone remodelling	Berkeley Madonna	2010	46
Benson et al.	Nerve growth factor pathway	Simbiology	2013	47
Demin et al.	5-Lipoxygenase Inhibitors	DBSolve	2013	48
Nayak et al.	Coagulation	Simbiology	2014	49
Lu et al.	Lipoprotein Metabolism	Matlab	2014	50
Gadkar et al.	Mechanisms of action of statin and anti-PCSK9 therapies	Simbiology	2014	51
Benson et al.	Development of fatty acid amide hydrolase inhibitors for pain	Simbiology	2014	52
Toni et al.	Nerve growth factor signaling through p75 and TrkA receptors	Simbiology	2014	53
Sharan & Woo	The relationship between circulating angiogenic factors dynamics and in vivo antitumor activity in response to anti-VEGF (vascular endothelial growth factor) agents	Berkeley Madonna	2014	54
Wronowska et al.	Sphingolipid metabolism	Simbiology	2015	55
Garmaroudi et al.	Nitric Oxide–Cyclic GMP Signaling Pathway	Simbiology	2016	56
Karelina et al.	Effect of Anti-Interleukin Therapy on Eosinophils	DBSolve	2016	57
Gotta et al.	Drug-induced QTc interval prolongation	NONMEM	2016	58
Clausznitzer et al.	Alzheimer	Simbiology	2018	59
Thiel et al.	Drug efficacy of COX-2 and 5-LOX inhibitors	MoBi	2018	60

The lack of standardization to develop a QSP model, as well as the establishment of the most efficient tools, may hinder the use of this methodology in drug development. To overcome some of these limitations, the DDMoRe (Drug Disease Model Resources) project^h developed a specific language, called the Pharmacometrics Markup Language (PharmML). What aims this project is to establish a standard language for PKPD and QSP modelling, making easier the exchange and the reusability of the models between research groups. Moreover, it has a freely available repository to submit models and

^h <http://www.ddmore.eu/content/project>

share them. Another repository to share models is BioModels Databaseⁱ, a platform created in 2006. The published models are divided into two groups, manually curated or non-curated. One advantage of this type of resources is that they enhance models visibility.

- Tools

Matlab: Matlab^j is a programming platform that allows analyzing data, developing algorithms and creating models and applications.

Simbiology: Simbiology^k is an application of Matlab that uses ODEs and stochastic solvers. It allows modelling, simulating, and analyzing dynamic systems and also using population data to estimate model parameters.

MoBi: MoBi^l is a systems biology software tool which can be used in R or Matlab and was developed by Bayer technologies. It is a potent tool for modelling and simulation of biological systems.

NONMEM: NONMEM^m (non-linear mixed effects modelling) is a software developed by Lewis B. Sheiner and Stuart L. Beal⁶¹ for popPK modelling. Nowadays, it can be used to fit different types of data and simulate data through mathematical models.

Berkeley Madonna: Berkeley Madonnaⁿ is a software to solve differential equations. The new version has a graphical interface for constructing mathematical models instead of write equations.

- ROSA

Rosa & Co.^o is a company that was founded in 2002 by Ron Beaver. It is characterized by its knowledge in biology and therapeutic sciences, as well as its modelling expertise. This company developed PhysioPD research platform which allows incorporating PK or

ⁱ <https://www.ebi.ac.uk/biomodels-main/termsfuse>

^j <https://es.mathworks.com/>

^k <https://es.mathworks.com/products/simbiology.html>

^l <http://www.systems-biology.com/products/pk-sim.html>

^m <https://www.iconplc.com/innovation/nonmem/>

ⁿ <https://berkeley-madonna.myshopify.com/>

^o <https://www.rosaandco.com/>

PKPD models integrated with physiological models to perform clinical trials simulations, in other words, it allows generating QSP models.

This platform can help the researcher in: (i) evaluate target mechanism of action, (ii) prioritize candidate targets, (iii) support lead compound selection, (iv) translate preclinical to clinical, (v) optimize therapy combinations among others.

The PhysioPD platform provides support to models in several diseases like Schizophrenia⁶², Parkinson⁶³, Psoriasis⁶⁴, lymphoblastic leukemia⁶⁵ and nervous systems central diseases⁶⁶ among others.

Since 2011 Rosa & Co. gives free webinars each month about aspects of research and drug development. These webinars are given by select speakers from academia, industry, Rosa client companies, and Rosa itself.

As on every scientific discipline, there are still open issues with SP models regardless if they are based on Boolean operators or quantitative dynamics, as shown below.

3. Systems pharmacology models validation

Contrary to popPKPD models where currently there is a consensus on how to evaluate and validate a model properly, there is not general agreement on how to validate QSP models.

One suggested strategy is the use of virtual populations⁶⁷. A virtual population is a family of parameter sets that reflect the characteristics of a population which allows exploring parametric uncertainty and reproducing the variability in response to perturbation⁶⁸.

On the other hand, regarding Boolean networks validation, Balbás-Martínez et al.¹² performed model simulations with different simulated therapies comparing the simulation outcomes against the results reported from clinical trials^P.

^P <https://www.clinicaltrials.gov/>

4. Systems pharmacology models reduction

In order to obtain simpler and more manageable SP models, several reduction techniques can be applied to convert them into mechanistic PKPD like models: (i) time-scale analysis, (ii) sensitivity analysis, (iii) lumping, (iv) balanced truncation, (v) singular value decomposition-based model reduction and (vi) miscellaneous methods, among others⁴⁷.

The first three methods are the most extensively used in systems pharmacology. Timescale analysis consists in the division of the system into different time scales depending on the speed of the reaction rates, defining slow and fast variables. This approach allows excluding one or other group of reactions and variables depending on the time scale of interest.

Sensitivity analysis determines the influence of parameters and initial states on a specific output variable. Then, those species or parameters eliciting little or no effect on the output of interest might be removed.

Finally, lumping is the most common method applied to this type of models. Through this method, several states of the model are lumped into a new pseudo-state, reducing the number of equations and parameters. Two different variants of this methodology have been described⁶⁹: proper and improper lumping. Although both variants can provide a reduced version of the model, proper lumping is more appropriate and more often used in systems biology models as it preserves a clear physiological interpretation. In this case, the original states contribute to only one of the pseudo-states of the reduced system, while in improper lumping the original states can correspond to one or more lumped states.

The work performed by Gulati⁷⁰ et al. represents a good example. They developed in 2009 a systems pharmacology model of coagulation process⁴⁵. Years later they reduced the 62-state systems model to a 5-state model through proper lumping method, to describe the time course of a factor recovery after a snake bite, maintaining an appropriate mechanistic relationship.

5. Pharmacometrics and systems pharmacology in the world

Conferences

The first PAGE (Population Approach Group in Europe) meeting^q was held in 1992 in Basel, Switzerland. Every year it is held in a different European country.

On the other hand, in 2005 ACOP (American Conference of Pharmacometrics) meeting^r was held for the first time.

WCOP (World Conference of Pharmacometrics)^s is a global meeting of pharmacometricians and was started in 2012 in Korea and it is held every four years. The last one was in Australia in 2016 and the next is going to take place in South Africa.

PAGANZ (Population Approach Group of Australia and New Zealand)^t scientific meeting has been held every year in the Southern hemisphere. In 2019 will take place the 20th meeting.

The 1st APC (Asian Pharmacometrics Conference)^u was held in 2017 at Kyoto University in collaboration with the Professional Committee of Pharmacometrics in China (PCPC), Population Approach Group in Korea (PAGK), and Population Approach Group in Japan (PAGJa).

The Iberoamerican Pharmacometrics Network Congress^v was held for the first time in 2017 in Montevideo (Uruguay). This congress targets people from Latin America to promote pharmacometrics in this area.

Journals

There are several journals that published this type of models like the Journal of Pharmacokinetics and Pharmacodynamics, European Journal of Pharmaceutical Sciences, Pharmaceutical Research, Journal of Pharmacology and Experimental Therapeutics, Clinical Pharmacology and Therapeutics, Plos One, Plos Computational Biology, Pharmacology Research and Perspectives, Cancer Research, Theoretical

^q <https://www.page-meeting.org/>

^r <http://www.go-acop.org/>

^s <https://go-wcop.org/>

^t <https://www.paganz.org/>

^u <http://www.pagja.org/apc-2017>

^v <http://www.redifar.org/events.html>

Biology and Medical Modelling and Bioinformatics among others, but they are not specific to this field.

In 2012, the first number of the “open access” journal *Clinical Pharmacology and Therapeutics: Pharmacometrics and Systems Pharmacology* (CPT:PSP)^w was published. It is a cross-disciplinary journal which covers the following areas: pharmacometrics, systems pharmacology modelling, disease modelling and physiologically-based pharmacokinetics (PBPK).

Society

The International Society of Pharmacometrics (ISOP)^x was founded in 2012. The purpose of this organization is to promote and advance the discipline of pharmacometrics and broaden its impact.

PAGANZ^y is an incorporated society founded on an interest in pharmacology and therapeutic applications using the population approach.

American Society for Clinical Pharmacology and Therapeutics (ASCPT)^z is a society which was founded in 1900. By using clinical pharmacology and translational medicine disciplines, this society focuses on improving the understanding and use of existing drug therapies and developing safer and more effective treatments for the future.

^w <https://ascpt.onlinelibrary.wiley.com/journal/21638306/>

^x <http://www.go-isop.org/>

^y <https://www.paganz.org/>

^z <https://www.ascpt.org/>

6. REFERENCES

1. Zhang, L. *et al.* Model-based drug development: The road to quantitative pharmacology. *J. Pharmacokinet. Pharmacodyn.* **33**, 369–393 (2006).
2. Gadkar, K., Kirouac, D., Mager, D., van der Graaf, P. & Ramanujan, S. A Six-Stage Workflow for Robust Application of Systems Pharmacology. *CPT Pharmacometrics Syst. Pharmacol.* **5**, 235–249 (2016).
3. Marshall, S. *et al.* Good Practices in Model-Informed Drug Discovery and Development: Practice, Application, and Documentation. *CPT Pharmacometrics Syst. Pharmacol.* **5**, 93–122 (2016).
4. Wang, R. S., Saadatpour, A. & Albert, R. Boolean modeling in systems biology: An overview of methodology and applications. *Phys. Biol.* **9**, (2012).
5. Shalhoub, J. *et al.* Systems biology of human atherosclerosis. *Vasc. Endovascular Surg.* **48**, 5–17 (2014).
6. Bloomingdale, P., Nguyen, V. A., Niu, J. & Mager, D. E. Boolean network modeling in systems pharmacology. *J. Pharmacokinet. Pharmacodyn.* **45**, 159–180 (2018).
7. Kauffman, S. A. Metabolic stability and epigenesis in randomly constructed genetic nets. *J. Theor. Biol.* **22**, 437–467 (1969).
8. Saadatpour, A. *et al.* Dynamical and Structural Analysis of a T Cell Survival Network Identifies Novel Candidate Therapeutic Targets for Large Granular Lymphocyte Leukemia. *PLoS Comput. Biol.* **7**, e1002267 (2011).
9. Irurzun-Arana, I., Gómez-mantilla, J. D. & Trocóniz, I. F. Attractor analysis of Boolean models for Systems Pharmacology Networks. *University of Navarra* (2013). at https://www.page-meeting.org/pdf_assets/6404-PAGE16_ITZIAR_IFT.pdf
10. Hopfensitz, M., Müssel, C., Maucher, M. & Kestler, H. A. Attractors in Boolean networks: A tutorial. *Comput. Stat.* **28**, 19–36 (2013).
11. Ruiz-Cerdá, M. L. *et al.* Towards patient stratification and treatment in the autoimmune disease lupus erythematosus using a systems pharmacology

- approach. *Eur. J. Pharm. Sci.* **94**, 46–58 (2015).
12. Balbas-Martinez, V. *et al.* A systems pharmacology model for inflammatory bowel disease. *PLoS One* **13**, 1–19 (2018).
 13. Chudasama, V. L., Ovacik, M. A., Abernethy, D. R. & Mager, D. E. Logic-Based and Cellular Pharmacodynamic Modeling of Bortezomib Responses in U266 Human Myeloma Cells. *J. Pharmacol. Exp. Ther.* **354**, 448–458 (2015).
 14. Ramakrishnan, V. & Mager, D. E. Network-Based Analysis of Bortezomib Pharmacodynamic Heterogeneity in Multiple Myeloma Cells. *J. Pharmacol. Exp. Ther.* **365**, 734–751 (2018).
 15. Saez-Rodriguez, J. *et al.* A logical model provides insights into T cell receptor signaling. *PLoS Comput. Biol.* **3**, 1580–1590 (2007).
 16. Thakar, J., Pilione, M., Kirimanjeswara, G., Harvill, E. T. & Albert, R. Modeling systems-level regulation of host immune responses. *PLoS Comput. Biol.* **3**, e109 (2007).
 17. Zhang, R. *et al.* Network model of survival signaling in large granular lymphocyte leukemia. *Proc. Natl. Acad. Sci. U. S. A.* **105**, 16308–16313 (2008).
 18. Sahin, Ö. *et al.* Modeling ERBB receptor-regulated G1/S transition to find novel targets for de novo trastuzumab resistance. *BMC Syst. Biol.* **3**, 1–20 (2009).
 19. Calzone, L. *et al.* Mathematical modelling of cell-fate decision in response to death receptor engagement. *PLoS Comput. Biol.* **6**, (2010).
 20. Saez-Rodriguez, J. *et al.* Comparing signaling networks between normal and transformed hepatocytes using discrete logical models. *Cancer Res.* **71**, 5400–5411 (2011).
 21. Rodríguez, A. *et al.* A Boolean network model of the FA/BRCA pathway. *Bioinformatics* **28**, 858–866 (2012).
 22. Singh, A., Nascimento, J. M., Kowar, S., Busch, H. & Boerries, M. Boolean approach to signalling pathway modelling in HGF-induced keratinocyte migration. *Bioinformatics* **28**, 495–501 (2012).

23. Helikar, T. *et al.* A Comprehensive, Multi-Scale Dynamical Model of ErbB Receptor Signal Transduction in Human Mammary Epithelial Cells. *PLoS One* **8**, (2013).
24. Conroy, B. D. *et al.* Design, Assessment, and in vivo Evaluation of a Computational Model Illustrating the Role of CAV1 in CD4+ T-lymphocytes. *Front. Immunol.* **5**, 1–9 (2014).
25. der Heyde, S. V. *et al.* Boolean ErbB network reconstructions and perturbation simulations reveal individual drug response in different breast cancer cell lines. *BMC Syst. Biol.* **8**, (2014).
26. Steinway, S. N. *et al.* Network Modeling of TGF Signaling in Hepatocellular Carcinoma Epithelial-to-Mesenchymal Transition Reveals Joint Sonic Hedgehog and Wnt Pathway Activation. *Cancer Res.* **74**, 5963–5977 (2014).
27. Oyeyemi, O. J., Davies, O., Robertson, D. L. & Schwartz, J. M. A logical model of HIV-1 interactions with the T-cell activation signalling pathway. *Bioinformatics* **31**, 1075–1083 (2015).
28. Rodríguez, A. *et al.* Fanconi anemia cells with unrepaired DNA damage activate components of the checkpoint recovery process. *Theor. Biol. Med. Model.* **12**, 1–22 (2015).
29. Remy, E. *et al.* A modeling approach to explain mutually exclusive and co-occurring genetic alterations in bladder tumorigenesis. *Cancer Res.* **75**, 4042–4052 (2015).
30. Flobak, Å. *et al.* Discovery of Drug Synergies in Gastric Cancer Cells Predicted by Logical Modeling. *PLoS Comput. Biol.* **11**, 1–20 (2015).
31. Lu, J. *et al.* Network modelling reveals the mechanism underlying colitis-associated colon cancer and identifies novel combinatorial anti-cancer targets. *Sci. Rep.* **5**, 1–15 (2015).
32. Vasaikar, S. V., Ghosh, S., Narain, P., Basu, A. & Gomes, J. HSP70 mediates survival in apoptotic cells—Boolean network prediction and experimental validation. *Front. Cell. Neurosci.* **9**, 1–12 (2015).

33. Méndez, A. & Mendoza, L. A Network Model to Describe the Terminal Differentiation of B Cells. *PLoS Comput. Biol.* **12**, 1–26 (2016).
34. Udyavar, A. R. *et al.* A transcription factor network model explains heterogeneity and reveals a novel hybrid phenotype in Small-Cell Lung Cancer. *Cancer Res.* **77**, 1063–1074 (2017).
35. Irurzun-Arana, I., Pastor, J. M., Trocóniz, I. F. & Gómez-Mantilla, J. D. Advanced Boolean modeling of biological networks applied to systems pharmacology. *Bioinformatics* **33**, 1040–1048 (2017).
36. Klamt, S., Saez-Rodriguez, J. & Gilles, E. D. Structural and functional analysis of cellular networks with CellNetAnalyzer. *BMC Syst. Biol.* **1**, 1–13 (2007).
37. Müssel, C., Hopfensitz, M. & Kestler, H. A. BoolNet-an R package for generation, reconstruction and analysis of Boolean networks. *Bioinformatics* **26**, 1378–1380 (2010).
38. Helikar, T. *et al.* The Cell Collective: toward an open and collaborative approach to systems biology. *BMC Syst. Biol.* **6**, 96 (2012).
39. Naldi, A. *et al.* Logical modelling of regulatory networks with GINsim 2.3. *BioSystems* **97**, 134–139 (2009).
40. Gonzalez, A. G., Naldi, A., Sánchez, L., Thieffry, D. & Chaouiya, C. GINsim: A software suite for the qualitative modelling, simulation and analysis of regulatory networks. *BioSystems* **84**, 91–100 (2006).
41. Di Cara, A., Garg, A., De Micheli, G., Xenarios, I. & Mendoza, L. Dynamic simulation of regulatory networks using SQUAD. *BMC Bioinformatics* **8**, 1–10 (2007).
42. van der Graaf, P. H. & Benson, N. Systems pharmacology: bridging systems biology and pharmacokinetics-pharmacodynamics (PKPD) in drug discovery and development. *Pharm. Res.* **28**, 1460–4 (2011).
43. Androulakis, I. P. Quantitative Systems Pharmacology: A Framework for Context. *Curr. Pharmacol. Reports* **2**, 152–160 (2016).

44. Knight-Schrijver, V. R., Chelliah, V., Cucurull-Sanchez, L. & Le Novère, N. The promises of quantitative systems pharmacology modelling for drug development. *Comput. Struct. Biotechnol. J.* **14**, 363–370 (2016).
45. Wajima, T., Isbister, G. K. & Duffull, S. B. A comprehensive model for the humoral coagulation network in humans. *Clin. Pharmacol. Ther.* **86**, 290–298 (2009).
46. Peterson, M. C. & Riggs, M. M. A physiologically based mathematical model of integrated calcium homeostasis and bone remodeling. *Bone* **46**, 49–63 (2010).
47. Benson, N. *et al.* Systems pharmacology of the nerve growth factor pathway: use of a systems biology model for the identification of key drug targets using sensitivity analysis and the integration of physiology and pharmacology. *Interface Focus* **3**, 20120071 (2013).
48. Demin, O. *et al.* Systems pharmacology models can be used to understand complex pharmacokinetic-pharmacodynamic behavior: an example using 5-lipoxygenase inhibitors. *CPT pharmacometrics Syst. Pharmacol.* **2**, e74 (2013).
49. Nayak, S. *et al.* Using a Systems Pharmacology Model of the Blood Coagulation Network to Predict the Effects of Various Therapies on Biomarkers. *CPT Pharmacometrics Syst. Pharmacol.* **4**, 396–405 (2015).
50. Lu, J., Hübner, K., Nanjee, M. N., Brinton, E. A. & Mazer, N. A. An In-Silico Model of Lipoprotein Metabolism and Kinetics for the Evaluation of Targets and Biomarkers in the Reverse Cholesterol Transport Pathway. *PLoS Comput. Biol.* **10**, (2014).
51. Gadkar, K. *et al.* A mechanistic systems pharmacology model for prediction of LDL cholesterol lowering by PCSK9 antagonism in human dyslipidemic populations. *CPT Pharmacometrics Syst. Pharmacol.* **3**, (2014).
52. Benson, N. *et al.* A Systems Pharmacology Perspective on the Clinical Development of Fatty Acid Amide Hydrolase Inhibitors for Pain. *CPT Pharmacometrics Syst. Pharmacol.* **3**, e91 (2014).
53. Toni, T., Dua, P. & Van Der Graaf, P. H. Systems pharmacology of the NGF

- signaling through p75 and TrkA receptors. *CPT Pharmacometrics Syst. Pharmacol.* **3**, 1–8 (2014).
54. Sharan, S. & Woo, S. Quantitative insight in utilizing circulating angiogenic factors as biomarkers for antiangiogenic therapy: Systems pharmacology approach. *CPT Pharmacometrics Syst. Pharmacol.* **3**, (2014).
 55. Wronowska, W., Charzyńska, A., Nienałtowski, K. & Gambin, A. Computational modeling of sphingolipid metabolism. *BMC Syst. Biol.* **9**, (2015).
 56. Garmaroudi, F. S., Handy, D. E., Liu, Y. Y. & Loscalzo, J. Systems Pharmacology and Rational Polypharmacy: Nitric Oxide–Cyclic GMP Signaling Pathway as an Illustrative Example and Derivation of the General Case. *PLoS Comput. Biol.* **12**, 1–16 (2016).
 57. Karelina, T., Voronova, V., Demin, O., Colice, G. & Agoram, B. M. A mathematical modeling approach to understanding the effect of anti-interleukin therapy on Eosinophils. *CPT Pharmacometrics Syst. Pharmacol.* **5**, 608–616 (2016).
 58. Gotta, V. *et al.* Application of a systems pharmacology model for translational prediction of hERG-mediated QTc prolongation. *Pharmacol. Res. Perspect.* **4**, 1–17 (2016).
 59. Clausznitzer, D. *et al.* Quantitative Systems Pharmacology Model for Alzheimer’s Disease Indicates Targeting Sphingolipid Dysregulation as Potential Treatment Option. *CPT Pharmacometrics Syst. Pharmacol.* 1–12 (2018). doi:10.1002/psp4.12351
 60. Thiel, C. *et al.* Using quantitative systems pharmacology to evaluate the drug efficacy of COX-2 and 5-LOX inhibitors in therapeutic situations. *npj Syst. Biol. Appl.* 1–12 (2018). doi:10.1038/s41540-018-0062-3
 61. Sheiner, L. B. & Beal, S. L. Evaluation of methods for estimating population pharmacokinetics parameters. I. Michaelis-Menten model: routine clinical pharmacokinetic data. *J. Pharmacokinet. Biopharm.* **8**, 553–71 (1980).
 62. Iadevaia, S. *et al.* Quantitative Systems Pharmacology Model to Quantify

- Benefits of DAAO Inhibition in Schizophrenia. *9th Am. Conf. Pharmacometrics (ACoP 9)* (2018).
63. Friedrich, C. M., Zago, W, Gardai, S, Tonn, G, Reed, M. A model qualification method for mechanistic physiological QSP models to support model-informed drug development. *World Preclin. Congr.* (2016).
64. Bansal, L. *et al.* Development of a Quantitative Systems Pharmacology (QSP) Model of Psoriasis : Overview and Challenges Map of Psoriasis Processes. *Am. Conf. Pharmacometrics 2015* (2015).
65. Indrajeet Singh, Theresa Yuraszeck, Matthias Klinger, Mike Reed, Christina Friedrich, Rukmini Kumar, Sharan Pagano, M. Z. A Systems Pharmacology Model to Characterize the Effect of Blinatumomab in Patients With Adult B-Precursor Acute Lymphoblastic Leukemia. *Am. Soc. Clin. Pharmacol. Ther.* (2014).
66. Friedrich, C. M. *et al.* Application of a quantitative systems pharmacology (QSP) model to evaluate xCT inhibition as a target for central nervous system diseases . *World Preclin. Congr.* (2016).
67. Kirouac, D. C., Du, J. Y., Lahdenranta, J. & Overland, R. Computational Modeling of ERBB2 -Amplified Breast Cancer Identifies Combined ErbB2 / 3 Blockade as Superior to the Combination of MEK and AKT Inhibitors. **6**, 2004008 (2013).
68. Rieger, T. R. *et al.* Improving the generation and selection of virtual populations in quantitative systems pharmacology models. *Prog. Biophys. Mol. Biol.* 1–20 (2018). doi:10.1016/j.pbiomolbio.2018.06.002
69. Knöchel, J., Kloft, C. & Huisinga, W. Understanding and reducing complex systems pharmacology models based on a novel input–response index. *J. Pharmacokinet. Pharmacodyn.* **45**, 139–157 (2018).
70. Gulati, a, Isbister, G. K. & Duffull, S. B. Scale reduction of a systems coagulation model with an application to modeling pharmacokinetic-pharmacodynamic data. *CPT pharmacometrics Syst. Pharmacol.* **3**, e90 (2014).

OBJECTIVES

The current investigation is focused on systems pharmacology (SP) models covering development, implementation, and validation/exploration.

The first objective was to develop a Boolean network model for Systemic Lupus Erythematosus integrating data from the literature and exploring the impact on the response of different therapeutic strategies. This work served as a proof of concept for the functionalities available in the tool SPIDDOR, which was internally developed.

The second objective was related to quantitative SP models and consisted first in the implementation of two already (and competing) published models corresponding to the coagulation process using the tool Simbiology. Then a comparison of the outcomes between the two models was performed. Finally, the application of the SP models to predict/describe the time course of thrombin and the results of different coagulation tests obtained from healthy and trauma patients were evaluated.

The third objective was to develop a semi-mechanistic PKPD model based on the coagulation systems pharmacology models to describe population data with high variability.

The other objectives were related to the pharmacological responses. However, little attention is paid in SP modelling to drug exposure in the target organ. This aspect of therapeutics is also covered in this thesis.

CHAPTER 1

SYSTEMIC LUPUS ERYTHEMATOSUS OVERVIEW

1. Systemic Lupus Erythematosus definition

Lupus is a severe and complex rheumatic disease which is classified in four main types: neonatal lupus erythematosus (NLE), discoid lupus erythematosus (DLE), drug-induced lupus (DIL) and systemic lupus erythematosus (SLE)¹.

This introduction is focused on SLE, which is the most common type of lupus¹. SLE is a chronic inflammatory autoimmune disease that can affect any organ/tissue in the body and presents a great patient heterogeneity reflected in the clinical profiles and serological alterations with periods of relapses and remissions. This disease is characterized by the production of autoantibodies that are directed against nuclear antigens (autoantigens) generating tissue damage and inflammation.

2. Epidemiology

SLE incidence (number of new cases in a year) ranges from 1 to 10 per 100,000 people-year and the prevalence (total individuals affected by the disease in a period) is about 20 to 70 per 100,000 people². This disease is up to 10 times more common in females than in males, being more frequent between 15 to 44 years³. Additionally, the incidence and prevalence in people of African or Asian background are approximately 2 to 3 times higher than in white populations. In the last decades, the life expectancy of SLE individuals has improved. However, the 15 to 20 years survival rate is still not greater than 80%².

3. Etiology

The mechanisms causing the development of SLE remain largely unknown. However, some factors have been postulated to play a crucial role in SLE⁴.

Genetic factors

Several single-nucleotide polymorphisms (SNPs) are associated with SLE. Most of them are within non-coding DNA regions of immune response-related genes⁴.

Environmental factors

Established environmental risk factors for SLE are silica exposure (crystalline silica or quartz), cigarette smoking and Epstein Barr virus (EBV) exposure. Less established environmental risk factors are metals, pesticides, persistent organic pollutants, asbestos, industrial chemicals and solvents, personal care products, UV radiation, and air pollution⁵.

Immunoregulatory factors

It has been found that SLE patients exhibit several immune alterations. Major histocompatibility complex (MHCII) expression in dendritic cells (DCs) of SLE patients have found to be upregulated⁶. Regarding T cells several costimulatory molecules are overexpressed, for examples the cytotoxic T-lymphocyte-associated antigen 4 (CTLA4)⁷, CD44⁸, programmed cell death-1 (PD1)⁹ while others are underexpressed like CD3 ζ chain or p65¹⁰ protein. Additionally, cytokines are also altered in SLE like interleukin 2 (IL-2)¹⁰, IL-4¹¹, IL-10¹², IL-6¹³, interferon γ (IFN γ)¹⁴, tumor necrosis factor α (TNF α)¹⁵ among others.

Hormones and sex

Females are more affected than males by SLE in a ratio of 9:1. This data suggests that steroids like estrogens can contribute to SLE pathogenesis. Several studies have found a correlation between early menarche, exogenous hormone use and surgical menopause and risk of SLE development^{16,17}. On the other hand, it has been observed that oral contraceptives do not affect disease activity¹⁸. Contrary, hormone therapy increases significantly mild/moderate flares^{19,20}.

Epigenetic factors

Several factors like some medications, diet, previous infections among others may result in epigenetic alterations. It has been seen that these alterations could be involved in the dysregulation of signaling molecules and receptors in SLE^{21,22}.

4. Diagnosis

Besides being a very complex disease, SLE is characterized by its heterogeneity. In fact, SLE is one of the most challenging diseases to diagnose by the clinicians due to the diverse clinical manifestations that the patients can present. The American College of

Rheumatology (ACR) made a list of symptoms in 1982 which was updated in 1997 (summarized in Figure 1). This list shows eleven criteria of which four are required for a formal diagnosis of SLE.

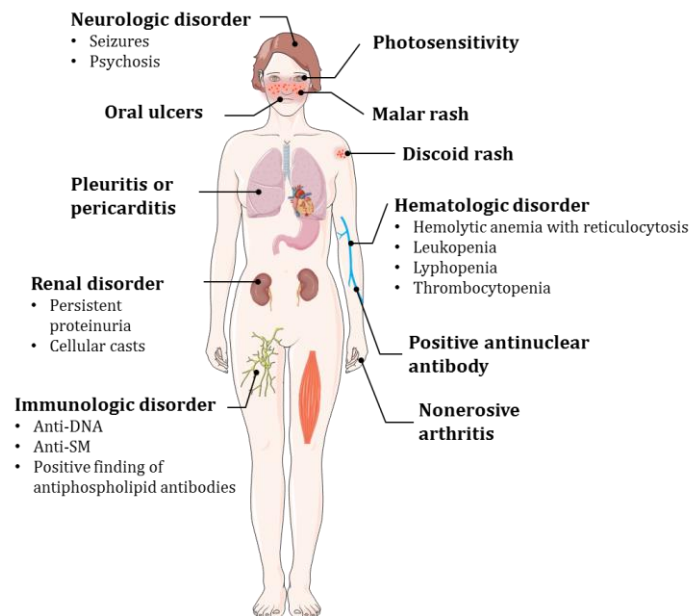


Figure 1. Diagnosis criteria for SLE by the American College of Rheumatology.

Considering this, there are 330 potential different types of SLE patients, and lot more if all the subcategories of the manifestations are considered. As a consequence SLE represents a big challenge for clinicians.

5. Treatment

Currently, the standard treatment consists of antimalarial drugs, non-steroidal anti-inflammatories, corticosteroids, cytotoxic and immunosuppressive drugs depending on disease severity, symptoms and involved organs (Table 1). None of these treatments are healing, but they prevent and treat relapses reducing organic damage. The only immunologic drug approved by the FDA so far is Belimumab which is a monoclonal antibody (mAb) targeted to a factor localized in B lymphocytes.

Table 1. Treatment recommendations for SLE.

Drug	Examples	Mechanism of action	Use	Ref
Antimalarial drugs	Chloroquine	Suppression of autoantigen presentation, blockade of Toll-like receptor signaling, reduced cytokine and prostaglandin synthesis, antiproliferative effects, photoprotection, decreased metalloproteinase activity and decreased leukocyte activation	<ul style="list-style-type: none"> • Long-term management of severe cutaneous manifestations • Improve survival and reduce disease activity • Pregnant patients with SLE 	23
	Hydroxychloroquine			
Non-steroidal anti-inflammatory drugs	COX-1 inhibitors	Act as nonselective inhibitors of COX-1 and COX-2 isoenzymes, which catalyze the formation of prostaglandins and thromboxane	<ul style="list-style-type: none"> • Mild symptoms like musculoskeletal symptoms, serositis, and headache 	24
	COX-2 inhibitors			
Corticosteroids	Prednisone	Glucocorticoids have broad inhibitory effects on specific immune responses mediated by T and B cell lymphocytes as well as potent suppressive effects on the effector functions of monocytes and neutrophils	<ul style="list-style-type: none"> • Acute management of discoid and other proliferative cutaneous lesions associated with dermal infiltration of lymphocytes • Alveolitis, bronchiolitis and interstitial pneumonitis • Renal lesions of lupus nephritis • Patients with acute central nervous system involvement • As initial therapy for hemolytic anemia or thrombocytopenia 	25
	Prednisolone			
	Methylprednisolone			
	Hydrocortisone			
Cytotoxic agents	Cyclophosphamide	Induce inhibition of DNA replication, leading to cell death.	<ul style="list-style-type: none"> • Patients with moderate to severe proliferative nephritis 	26
	Methotrexate	Folic acid antagonist. It interferes in processes of DNA synthesis, repair and cell replication.	<ul style="list-style-type: none"> • Long-term management of severe cutaneous manifestations for patients not being able to reduce steroids below doses acceptable for chronic use 	27
Immuno-suppressants	Azathioprine	Inhibit or prevent activity of the immune system.	<ul style="list-style-type: none"> • Long-term management of severe cutaneous manifestations for patients not being able to reduce steroids below doses acceptable for chronic use. • Pregnant patients with SLE 	27
	Cyclosporine A			
	Mycophenolate mofetil			
	Tacrolimus			
Monoclonal antibody	Belimumab	Human monoclonal antibody that inhibits B-cell activating factor (BAFF).	<ul style="list-style-type: none"> • In addition to standard therapy for reducing disease activity in adult patients with active, autoantibody-positive SLE which not have active lupus nephritis or CNS disease 	31
			<ul style="list-style-type: none"> • It has shown favorable results with a significant improvement in disease activity and an improvement in complement levels, leucopenia and thrombocytopenia • Treatment of patients with moderate and SLE who did not show a response to other immunosuppressive drugs • Lupus nephritis 	28 29 30

Targeted therapies

In the last years, several pharmaceutical companies have made major efforts to run clinical trials involving new biologic drugs to treat SLE patients that exhibited poor response to standard therapies. In Table 2 are listed several biologic drugs which are in different development phases. The main goal of these therapies is to induce disease remission and reestablish self-tolerance.

Table 2. Targeted therapies in SLE.

Drug	Target	Developer	Phase	ClinicalTrials.gov ID
Atacicept	B cells	EMD Serono	Phase 2	NCT01972568
AMG557	B7H2	Amgen	Phase 1	NCT01683695
Blisibimod	BAFF	Anthera Pharmaceuticals	Phase 3	NCT02514967
Tabalumab	BAFF	Eli Lilly and Company	Phase 3	NCT01205438
Rituximab	CD20	GlaxoSmithKline	Phase 3	NCT03312907
Epratuzumab	CD22	UCB Pharma	Phase 3	NCT01261793
Lulizumab Pegol	CD28	Bristol-Myers Squibb	Phase 2	NCT02265744
CDP7657	CD40L	UCB Pharma	Phase 1	NCT01093911
Abatacept	CD80 / CD86	Bristol-Myers Squibb	Phase 2	NCT02270957
AGS-009	IFN α	Argos Therapeutics	Phase 1	NCT00960362
Sifalimumab	IFN α	MedImmune LLC	Phase 2	NCT01283139
Anifrolumab	IFN α receptor 1	AstraZeneca	Phase 3	NCT02446912
Ustekinumab	IL12 / IL23	Janssen Research & Development, LLC	Phase 3	NCT03517722
NNC0114_0006	IL21	Novo Nordisk A/S	Phase 1	NCT01689025
ALX_0061	IL6	Ablynx	Phase 2	NCT02437890
Sirukumab	IL6	Centocor Research & Development	Phase 1	NCT01702740
Tocilizumab	IL6 receptor	National Institute of Arthritis and Musculoskeletal and Skin Diseases	Phase 1	NCT00046774
Rontalizumab	IFN α	Genentech Inc.	Phase 2	NCT00962832

6. Modelling efforts applied to SLE

In most cases, PK data belonging to clinical trials are analyzed through non-compartmental analysis (obtaining data descriptors such area under the concentration vs time curve (AUC) or maximum concentration drug (C_{MAX})). However, some drugs have

been analyzed by model-based compartmental analysis (estimating a set of parameters from data to describe and interpret the PK profiles), as it can be seen in Table 3.

During the clinical trial some pharmacodynamic data is also collected, as it is shown in Table 3. However, PKPD models that link drug concentrations with a response/effect are still scarce in SLE.

Table 3. Pharmacometric efforts performed in SLE.

Drug	Target	Pharmacokinetics	Pharmacodynamics	Year	Ref
AMG 811	IFN γ	A two-compartment model with linear elimination	TMDD model (relationship between the AMG 811 and IFN γ serum concentrations)	2015	32
Atacicept	BlyS and APRIL	Non-compartmental	<ul style="list-style-type: none"> • Mature B cells • Anti-dsDNA • Ig levels • C3 levels 	2009	33
		Non-compartmental	<ul style="list-style-type: none"> • Mature B cells • Anti-dsDNA • Ig levels • C3 levels 	2010	34
Belimumab	BlyS	Non-compartmental	Biologic biomarkers: <ul style="list-style-type: none"> • CD20+ B cells and CD38+ plasmacytoid cells • AntiDNAs ab and ANAS, Igs, Complement • SELENA SLEDAI score 	2008	35
		Two-compartment linear model	-	2013	36
		One compartment linear model with first order absorption and elimination Multiple dose	-	2013	37
Blisibimod	BlyS	Non-compartmental	<ul style="list-style-type: none"> • B cells • IgD+ CD27- naive cells • IgD+ CD27- memory cells 	2015	38
Rituximab	CD20	Serum rituximab levels	<ul style="list-style-type: none"> • CD19 lymphocytes as an indicator of B cell depletion • For the efficacy: SLAM score 	2004	39
Sifalimumab	IFN α	Two- compartment linear model with first order elimination	-	2013	40
		Two- compartment linear model with first order elimination	-	2016	41
PF-04236921	IL6	A two-compartment model with first order absorption and linear elimination	Mechanism-based indirect response model	2018	42

Regarding systems pharmacology in SLE, our research group has built an exhaustive model of the co-stimulation pathway in SLE disease⁴³ (a part of the current Ph.D.

thesis). This model consists of a Boolean network including 52 nodes and 296 interactions between them. As will be seen below, by perturbing the network nodes, it was possible to identify which could be the alterations that match reported observations in SLE patients. Additionally, SLE patients are grouped according to their molecular alterations to find if there are indeed different subpopulations of patients that may require different treatments.

7. REFERENCES

1. Maidhof, W. & Hilar, O. Lupus: an overview of the disease and management options. *P T* **37**, 240–9 (2012).
2. Pons-Estel, G. J., Alarcón, G. S., Scofield, L., Reinlib, L. & Cooper, G. S. Understanding the Epidemiology and Progression of Systemic Lupus Erythematosus. *Semin. Arthritis Rheum.* **39**, 257–268 (2010).
3. Cervera, R. *et al.* Morbidity and mortality in systemic lupus erythematosus during a 10-year period: A comparison of early and late manifestations in a cohort of 1,000 patients. *Medicine (Baltimore).* **82**, 299–308 (2003).
4. Tsokos, G. C. Systemic Lupus Erythematosus. *N. Engl. J. Med.* **365**, 2110–2121 (2011).
5. Kamen, D. L. Environmental Influences on Systemic Lupus Erythematosus Expression. *Rheum. Dis. Clin. North Am.* **40**, 401–412 (2014).
6. Gottenberg, J. E. & Chiochia, G. Dendritic cells and interferon-mediated autoimmunity. *Biochimie* **89**, 856–871 (2007).
7. Jury, E. C. *et al.* Abnormal CTLA-4 function in T cells from patients with systemic lupus erythematosus. *Eur. J. Immunol.* **40**, 569–78 (2010).
8. Crispín, J. C. *et al.* Expression of CD44 variant isoforms CD44v3 and CD44v6 is increased on T cells from patients with systemic lupus erythematosus and is correlated with disease activity. *Arthritis Rheum.* **62**, 1431–1437 (2010).
9. Jiao, Q. *et al.* Upregulated PD-1 expression is associated with the development of systemic lupus erythematosus, but not the PD-1.1 Allele of the PDCD1 gene. *Int. J. Genomics* **2014**, 10–12 (2014).
10. Moulton, V. R. & Tsokos, G. C. Abnormalities of T cell signaling in systemic lupus erythematosus. *Arthritis Res. Ther.* **13**, 207 (2011).
11. Sugimoto, K. *et al.* Decreased IL-4 producing CD4⁺ T cells in patients with active systemic lupus erythematosus-relation to IL-12R expression. *Autoimmunity* **35**, 381–7 (2002).

12. Park, Y. B. *et al.* Elevated interleukin-10 levels correlated with disease activity in systemic lupus erythematosus. *Clin. Exp. Rheumatol.* **16**, 283–8
13. Linker-Israeli, M. *et al.* Elevated levels of endogenous IL-6 in systemic lupus erythematosus. A putative role in pathogenesis. *J. Immunol.* **147**, 117–23 (1991).
14. Harigai, M. *et al.* Excessive Production of IFN- γ in Patients with Systemic Lupus Erythematosus and Its Contribution to Induction of B Lymphocyte Stimulator/B Cell-Activating Factor/TNF Ligand Superfamily-13B. *J. Immunol.* **181**, 2211–2219 (2008).
15. Ou, J.-N., Wiedeman, A. E. & Stevens, A. M. TNF- α and TGF- β counter-regulate PD-L1 expression on monocytes in systemic lupus erythematosus. *Sci. Rep.* **2**, 295 (2012).
16. Costenbader, K. H., Feskanich, D., Stampfer, M. J. & Karlson, E. W. Reproductive and menopausal factors and risk of systemic lupus erythematosus in women. *Arthritis Rheum.* **56**, 1251–1262 (2007).
17. Lateef, A. & Petri, M. Hormone replacement and contraceptive therapy in autoimmune diseases. *J. Autoimmun.* **38**, J170–J176 (2012).
18. Rojas-Villarraga, A., Torres-Gonzalez, J.-V. & Ruiz-Sternberg, Á.-M. Safety of Hormonal Replacement Therapy and Oral Contraceptives in Systemic Lupus Erythematosus: A Systematic Review and Meta-Analysis. *PLoS One* **9**, e104303 (2014).
19. Petri, M. Sex hormones and systemic lupus erythematosus. *Lupus* **17**, 412–415 (2008).
20. Ramsey-Goldman, R. Does hormone replacement therapy affect disease activity in patients with systemic lupus erythematosus? *Nat. Clin. Pract. Rheumatol.* **1**, 72–73 (2005).
21. Hedrich, C. M. & Tsokos, G. C. Epigenetic mechanisms in systemic lupus erythematosus and other autoimmune diseases. *Trends Mol. Med.* **17**, 714–724 (2011).
22. Hedrich, C. M., Mäbert, K., Rauen, T. & Tsokos, G. C. DNA methylation in

- systemic lupus erythematosus. *Epigenomics* **9**, 505–525 (2017).
23. Lee, S.-J., Silverman, E. & Bargman, J. M. The role of antimalarial agents in the treatment of SLE and lupus nephritis. *Nat. Rev. Nephrol.* **7**, 718–729 (2011).
 24. østensen, M. & Villiger, P. M. Nonsteroidal anti-inflammatory drugs in systemic lupus erythematosus. *Lupus* **9**, 566–572 (2000).
 25. Chatham, W. W. & Kimberly, R. P. Treatment of lupus with corticosteroids. *Lupus* **10**, 140–147 (2001).
 26. Takada, K., Illei, G. G. & Boumpas, D. T. Cyclophosphamide for the treatment of systemic lupus erythematosus. *Lupus* **10**, 154–161 (2001).
 27. Bertsias, G. *et al.* EULAR recommendations for the management of systemic lupus erythematosus. Report of a Task Force of the EULAR Standing Committee for International Clinical Studies Including Therapeutics. *Ann. Rheum. Dis.* **67**, 195–205 (2008).
 28. Griffiths, B. & Emery, P. The treatment of lupus with cyclosporin A. *Lupus* **10**, 165–170 (2001).
 29. Gaubitz, M., Schorat, a, Schotte, H., Kern, P. & Domschke, W. Mycophenolate mofetil for the treatment of systemic lupus erythematosus: an open pilot trial. *Lupus* **8**, 731–736 (1999).
 30. Yap, D. Y. *et al.* Pilot 24 month study to compare mycophenolate mofetil and tacrolimus in the treatment of membranous lupus nephritis with nephrotic syndrome. *Nephrology* **17**, 352–357 (2012).
 31. Askanase, A. D., Yazdany, J. & Molta, C. T. Post-marketing experiences with belimumab in the treatment of SLE patients. *Rheum. Dis. Clin. North Am.* **40**, 507–517 (2014).
 32. Chen, P. *et al.* Pharmacokinetic and Pharmacodynamic Relationship of AMG 811, An Anti-IFN- γ IgG1 Monoclonal Antibody, in Patients with Systemic Lupus Erythematosus. *Pharm. Res.* **32**, 640–653 (2014).
 33. Pena-Rossi, C. *et al.* An exploratory dose escalating study investigating the

- safety, Tolerability In, pharmacokinetics and pharmacodynamics of intravenous atacicept in patients with systemic lupus erythematosus. *Lupus* **18**, 547–55 (2009).
34. Nestorov, I., Papisoulitis, O., Pena Rossi, C. & Munafo, A. Pharmacokinetics and immunoglobulin response of subcutaneous and intravenous atacicept in patients with systemic lupus erythematosus. *J. Pharm. Sci.* **99**, 524–538 (2010).
 35. Furie, R. *et al.* Biologic activity and safety of belimumab, a neutralizing anti-B-lymphocyte stimulator (BLyS) monoclonal antibody: a phase I trial in patients with systemic lupus erythematosus. *Arthritis Res. Ther.* **10**, R109 (2008).
 36. Struemper, H., Chen, C. & Cai, W. Population pharmacokinetics of belimumab following intravenous administration in patients with systemic lupus erythematosus. *J. Clin. Pharmacol.* **53**, 711–720 (2013).
 37. Cai, W. W. *et al.* Bioavailability, pharmacokinetics, and safety of belimumab administered subcutaneously in healthy subjects. *Clin. Pharmacol. Drug Dev.* **2**, 349–357 (2013).
 38. Stohl, W. *et al.* Treatment of systemic lupus erythematosus patients with the BAFF antagonist ‘peptibody’ blisibimod (AMG 623/A-623): Results from randomized, double-blind phase 1a and phase 1b trials. *Arthritis Res. Ther.* **17**, 1–14 (2015).
 39. Looney, R. J. *et al.* B cell depletion as a novel treatment for systemic lupus erythematosus: A phase I/II dose-escalation trial of rituximab. *Arthritis Rheum.* **50**, 2580–2589 (2004).
 40. Narwal, R., Roskos, L. K. & Robbie, G. J. Population pharmacokinetics of sifalimumab, an investigational anti-interferon- γ monoclonal antibody, in systemic lupus erythematosus. *Clin. Pharmacokinet.* **52**, 1017–1027 (2013).
 41. Zheng, B., Yu, X.-Q., Greth, W. & Robbie, G. J. Population pharmacokinetic analysis of sifalimumab from a clinical phase IIb trial in systemic lupus erythematosus patients. *Br. J. Clin. Pharmacol.* **81**, 918–928 (2016).
 42. Li, C., Shoji, S. & Beebe, J. Pharmacokinetics and C-reactive protein modelling

- of anti-interleukin-6 antibody (PF-04236921) in healthy volunteers and patients with autoimmune disease. *Br. J. Clin. Pharmacol.* **84**, 2059–2074 (2018).
43. Ruiz-Cerdá, M. L. *et al.* Towards patient stratification and treatment in the autoimmune disease lupus erythematosus using a systems pharmacology approach. *Eur. J. Pharm. Sci.* **94**, 46–58 (2015).

Towards patient stratification and treatment in the autoimmune disease lupus erythematosus using a systems pharmacology approach

M. Leire Ruiz-Cerdá^{a,1}, Itziar Irurzun-Arana^{a,1}, Ignacio González-García^{a,b}, Chuanpu Hu^c, Honghui Zhou^c, An Vermeulen^d, Iñaki F. Trocóniz^{a,1} and José David Gómez-Mantilla^{a,1}

European Journal of Pharmaceutical Sciences 94 (2016) 46–58

(doi: <https://doi.org/10.1016/j.ejps.2016.04.010>)

^a Pharmacometrics & Systems Pharmacology, Department of Pharmacy and Pharmaceutical Technology, School of Pharmacy, University of Navarra, Pamplona 310890, Spain

^b Pharmacy and Pharmaceutical Technology Department, University of Valencia, Valencia, Spain

^c Clinical Pharmacology and Pharmacometrics, Janssen Research and Development, LLC, Spring House, PA 19477, USA

^d Janssen Research and Development, a division of Janssen Pharmaceutica NV, Beerse B-2340, Belgium

¹ These authors contributed equally to this work

ABSTRACT

Drug development in Systemic Lupus Erythematosus (SLE) has been hindered by poor translation from successful preclinical experiments to clinical efficacy. This lack of success has been attributed to the high heterogeneity of SLE patients and to the lack of understanding of disease pathophysiology. Modelling approaches could be useful for supporting the identification of targets, biomarkers and patient subpopulations with differential response to drugs. However, the use of traditional quantitative models based on differential equations is not justifiable by the sparse data available. Boolean Networks models are less demanding on the required data to be implemented and can provide insights into the dynamics of biological networks. This methodology allows the integration of all the available knowledge into a single framework to evaluate the behavior of the system under different conditions and test hypotheses about unknown aspects of the disease. In this proof-of-concept study, we explored the potential of a Systems Pharmacology model based on Boolean Networks to support drug development in SLE. We focused the analysis on the antigen presentation by the antigen presenting cells (APC) to the T-cells to evaluate the reach of this methodology in a medium size network before full implementation of the whole SLE pathway. The heterogeneity of SLE patients was replicated using this methodology simulating subjects with distinct pathway alterations. A perturbation analysis of the network coupled with clustering analysis showed potential to identify drug targets, optimal combinatorial regimens and subpopulations of responders and non-responders to drug treatment. We propose this approach as a first step towards the development of more quantitative platforms to address the current challenges in drug development for complex diseases.

1. INTRODUCTION

Systemic Lupus Erythematosus (SLE) is a chronic multiorgan relapsing-remitting autoimmune disease which is characterized by the production of autoantibodies that can affect the majority of organs¹. These autoantigens are suspected to be products of defective apoptosis, necrosis or NETosis (formation of Neutrophil Extracellular Traps [NETs]) of the body cells² and can be classified according their molecular structure³ (Table 1). The incidence of SLE is about 1 to 10 per 100,000 person/years and the prevalence 20 to 70 per 100,000 people. SLE cases have been reported in all continents but the incidence and prevalence in people of African or Asian background are approximately 2 to 3 times higher than in white populations, being more frequent among women than men (90% or more of patients are women). The 5-year survival rate among SLE patients has shifted from 50% in 1950 to 90% after the 1970s, but the 15 to 20 years survival rate is still approximately 80%⁴⁴. Among the factors that have been associated to the development of SLE are genetic, epigenetic, environmental, hormonal, and immunoregulatory among others⁵, but the underlying mechanisms of the disease remain largely unknown.

Table 1. Type of autoantigens in SLE and definition

Type	Autoantigen	Definition
DNA antigens	dsDNA	double-stranded DNA
	Nucleosomes	Fundamental subunit of chromatin
Non-DNA antigens	Ro	Ribonucleoprotein complex
	La	RNA-binding protein
	Sm	Nuclear particles consisting of several different polypeptides
	NMDA receptor	<i>N</i> -methyl-D-aspartate receptor
	Phospholipids	A lipid with one or more phosphate groups attached to it
	α -Actinin	Cytoskeletal actin-binding protein and a member of the spectrin superfamily
	C1q	Subunit of the C1 complement component

SLE is a complex disease involving different signaling pathways and characterized by a high clinical heterogeneity among patients. Currently, a patient has to exhibit at least

four out of eleven symptoms to be diagnosed with SLE. Symptoms include malar rash, photosensitivity, kidney disorder, blood disorder, abnormal antinuclear antibodies among others⁵. This gives an idea about the magnitude of different possible combinations of clinical manifestations in SLE. Additionally, more than 40 genes have been reported as predisposing to SLE. It is expected that SLE patients with different genetic backgrounds or different autoantigens will show different molecular alterations in their immune response. It seems reasonable to think that the pharmacological treatment of SLE should be personalized and probably should target more than one signaling pathway. Yet, current approaches follow the standard paradigm testing single drug hitting single specific targets while clinical trials has also been characterized by the lack of patient stratification prior to the studies.

The standard treatment for SLE consists of nonsteroidal anti-inflammatory drugs (NSAIDs), antimalarials, glucocorticoids, cytotoxic agents and immunosuppressive agents⁵⁻⁷. To date, only one monoclonal antibody (belimumab) has been approved by the FDA for SLE, which is used for mild to moderate SLE disease, in patients which do not present active lupus nephritis or central nervous system disease⁸. SLE treatment attempts to prevent and treat flares and reduce organ damage or other associated problems. SLE therapy depends on the symptoms and the tissue damage experienced by the patient. Several laboratories have investigated different compounds targeting different components of the immune response; several are still in development phases while others have not shown therapeutic success. Most of these research compounds have exhibited promising results in the preclinical development but this has not been translated into effective drugs for the treatment of SLE. Currently treatment of SLE is far from optimal and requires new paradigms in drug development, speeding selection and validation of active compounds and most promising drug combinations.

At the moment, there are not computational tools able to evaluate the effect of a drug in a “SLE like” system; target validation/invalidation have been made through costly empirical experiments and modelling have been limited to description of drug Pharmacokinetics (PK) and modest attempts to link SLE severity scores to drug exposure^{9,10}. In the last years, Systems Pharmacology has emerged as a new translational tool to study complex biological systems¹¹⁻¹⁸, with the aim of integrating information from different sources into a system level model that can be used for different purposes during the whole drug development pipeline, including target

identification and validation/invalidation, patient stratification, biomarkers identification, dosing selection, identification of sources of variability and prediction of toxicity and adverse effects^{11,19-26}. Due to the heterogeneity in SLE patients and the complexity of the disease, a Systems Pharmacology approach can support the drug development chain by identifying different patient subpopulations according to their molecular alterations and thus, predict the progression of the different patient subpopulations, allowing the design of individualized drug therapies with high likelihood of success.

In this work we propose a systems pharmacology model for the study of SLE pathogenesis and therapeutics than can be expanded or reduced to assess different questions during the drug development pipeline. In the SLE arena there are scarce longitudinal data, definitely not enough to build up and validate a mechanistic and predictive disease model. Therefore, in this initial attempt we modelled part of the immune response to autoantigens by a Boolean network, which is a logical model composed by several components (represented as nodes) and the interactions between them. The nodes of the network in a Boolean model present only two states, activated or deactivated, and the interactions between nodes can be: activation, inhibition, upregulation or downregulation. The main advantage of Boolean dynamic models is that they require far less parametrization than other quantitative models, capturing the essential dynamics of a system and allowing feasible scalability to larger systems²⁷.

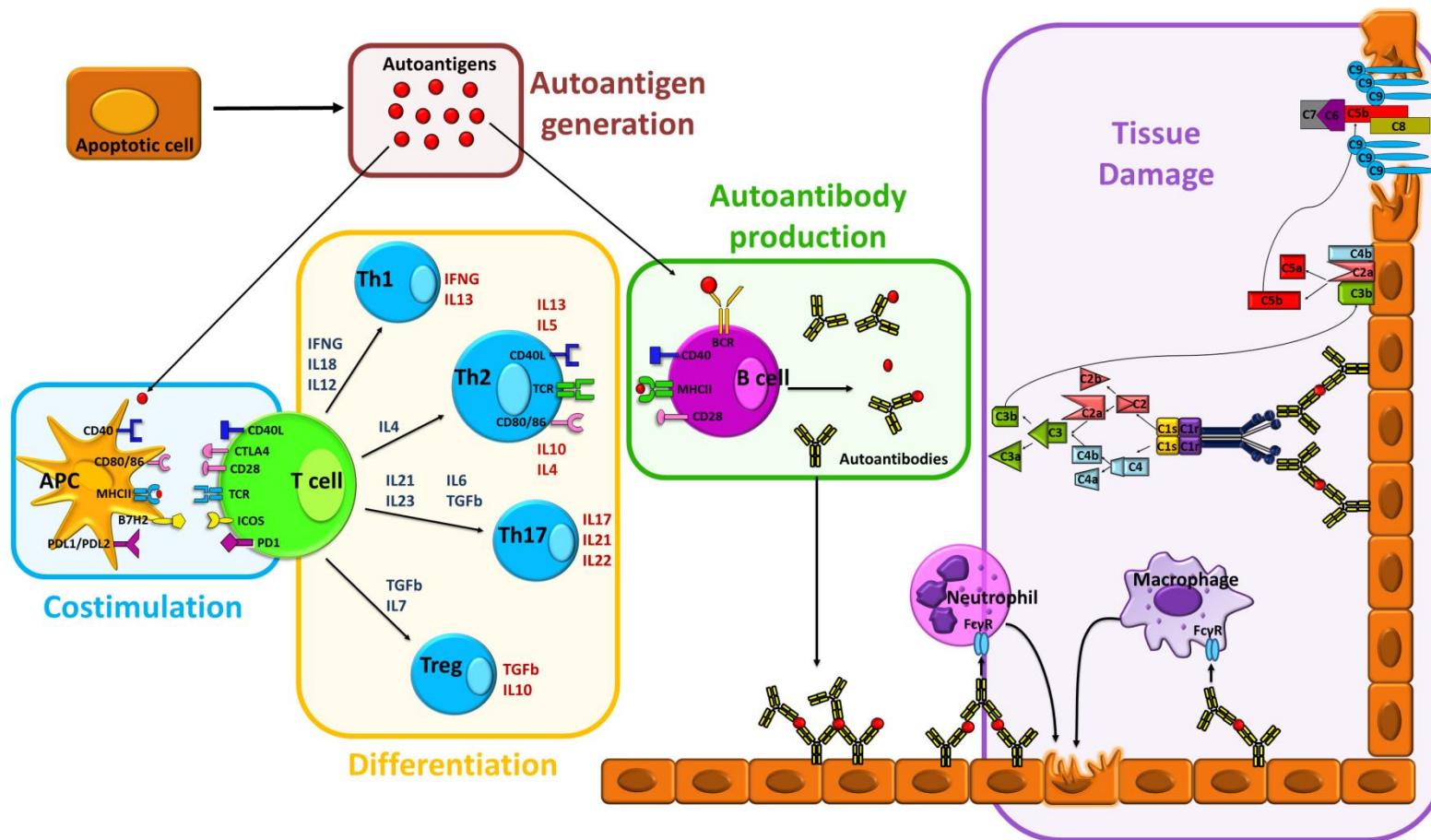


Figure 1. Assumed pathophysiology of SLE

For an unknown reason the body recognizes normal endogenous molecules as antigens, triggering an immune response. These autoantigens are recognized by the receptor of the antigen presenting cell (CD4+ type), processed and then expressed by the MHCII molecule which presents the autoantigen to the Th0 cell. APC molecules interact with their respective ligands on Th0 cell which triggers intracellular signals that will result in activation of Th0 cell. Once activated, depending on the cytokine environment and costimulation signals, it can differentiate into Th1, Th2, Th17 or Treg. Th2 cells interact with B cells which after maturation produce autoantibodies against these autoantigens. Subsequently, the immune complement and several macrophages and neutrophils recognize these autoantibodies attached to the autoantigens leading to a coordinated attack against tissues expressing those autoantigens causing tissue injury and damage.

Figure 1 illustrates a summary of the different molecular pathways present in SLE pathogenesis. In the current investigation we have focused our modelling efforts on the network involving the antigen presentation by the antigen presenting cells (APC) to the T cells. Several development programs are targeting molecules located in this stage and many of the alterations reported in SLE patients are present at this stage of the network.

The aims of this study were first to develop and evaluate the above mentioned network based on literature survey. Second to identify plausible altered pathways of the immune response that may explain the observed heterogeneous alterations in SLE patients, in order to classify SLE patients according to their molecular alterations. After a methodology for patient stratification was proposed, we aimed to use this information in the design of optimal therapy for each patient subpopulation.

2. METHODS

2.1 Literature search, selection, annotation and system representation

The network model is based on an exhaustive bibliographic review focused on the essential components of the antigen presentation. The review covered research in humans, including *in vitro*, *ex vivo* or *in vivo* studies. In few cases animal data were included to connect nodes of critical pathways when no human data was available. The review included around 300 papers published between 1993 and 2015. Medical Subject Headings (MeSH) terms were focused on: (i) relevant network components (nodes) involved in the pathogenesis of the autoimmune diseases, (ii) nodes that have been reported to be altered in SLE and (iii) nodes that directly affect the expression of the nodes selected in (i) and (ii). Only references with direct experimental evidence or widely accepted and cited in the literature were included.

The information from the literature review was annotated in a central repository. Annotation was key in developing these systems pharmacology models, it included: (i) identification of the main elements (i.e., cytokines, membrane receptors....) of the co-stimulation process, (ii) description of the functional interrelationship between these elements and their neighbors and (iii) identification of alteration of these elements in SLE patients. Figure 2a-b takes the Tumor Necrosis Factor alpha (TNF α) node as example to illustrate the processes of a) data extraction based on numerical data obtained from graphic evidence, and b) annotation and storage in a central repository. The same process was performed for all the nodes in the network.

Once the annotation was finalized, a graphical representation of the system was performed including all selected nodes and the corresponding inter-relationships and other relevant properties of the system of interest (Figure 3). Figure 2c provides a reduced version of a graphical representation of our system.

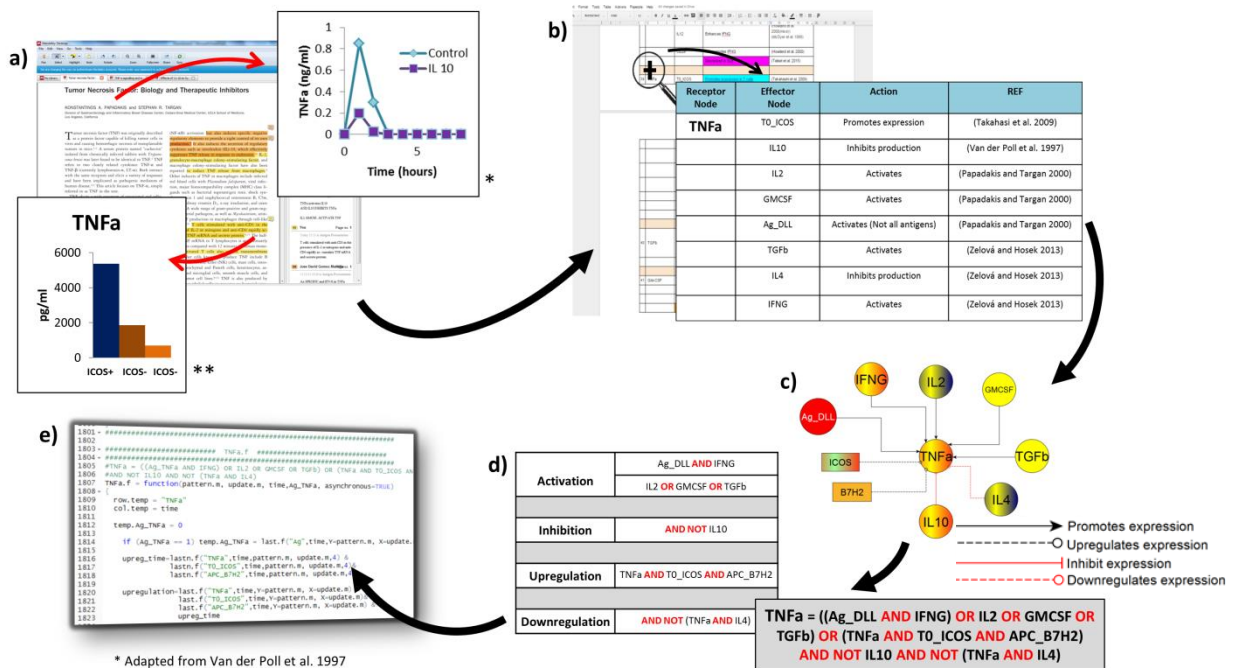


Figure 2. Development and implementation of a Boolean network model for SLE

a) An exhaustive literature review was performed aiming to find direct experimental evidence of relationships between nodes, using a multi-user online system based on Mendeley software. b) That information was annotated and structured in a table, which contains all the relationships between all the nodes, including link to bibliographic support to ensure traceability. c) A schematic representation of the relationships between the nodes was obtained using yEd Graph Editor. An illustrative example shows the relationships between TNFα regulator nodes and TNFα, different types of interaction were displayed by different connectors. d) Examples of four different types of interaction between nodes (activation, inhibition, upregulation and downregulation) and their corresponding Boolean expressions (Boolean operators shown in red). The final Boolean equation for each node was built considering all the available data simultaneously, inhibition was prioritized over activation unless it was proved otherwise in the bibliography. e) The Boolean equations were implemented into the R language according to Irurzun-Arana 2015²⁸.

* Adapted from Van der Poll et al. 1997²⁹

** Adapted from Takahashi et al. 2009³⁰

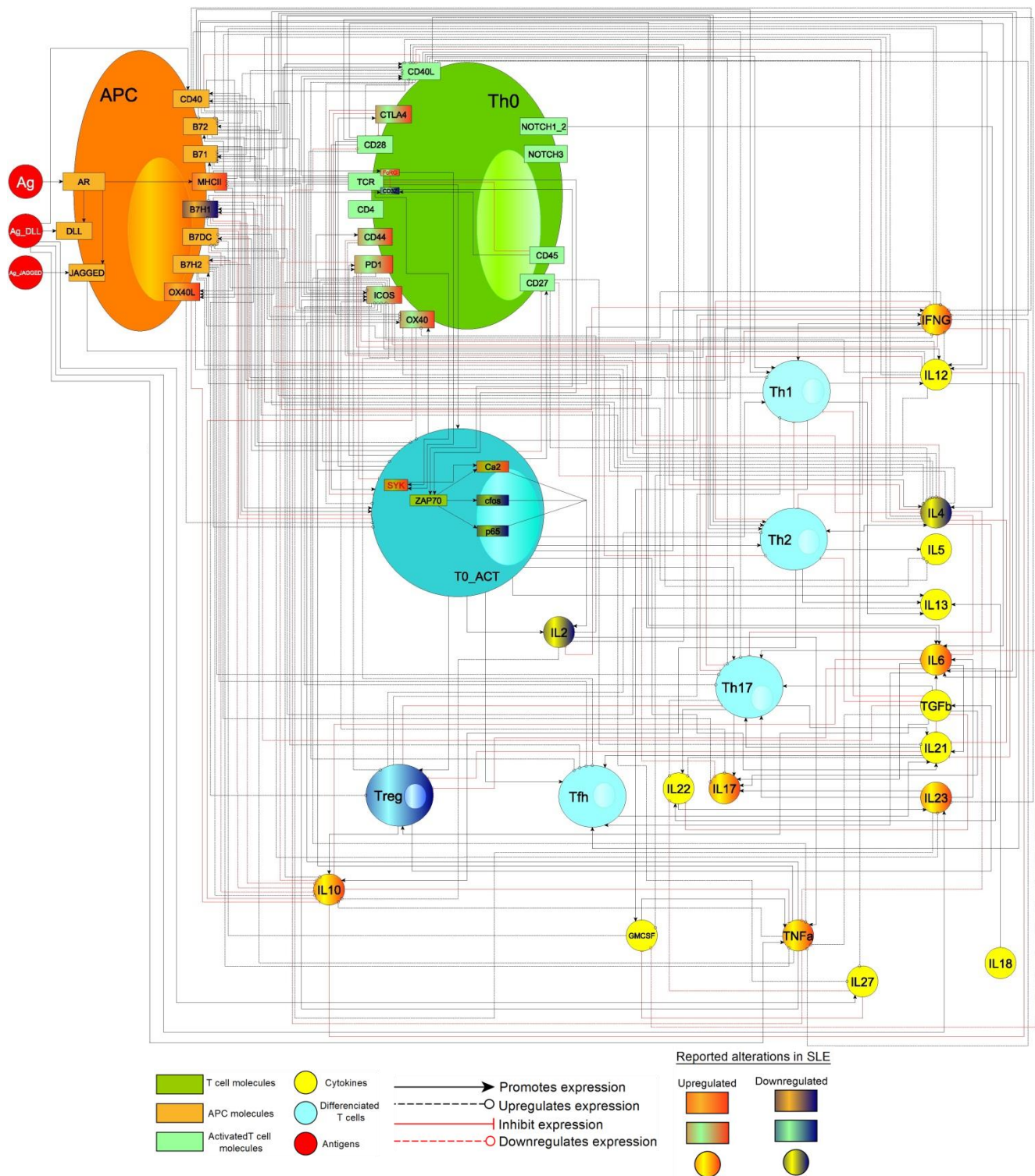


Figure 3. Graphical representation of SLE network

Nodes are represented with different shapes and colors depending on the nature and cellular location. Four types of relationships between nodes were represented by different edge colors or endings. Illustration made using yEd Graph Editor.

2.2 Boolean network building

The qualitative graphical representation of the system was transformed into a semi-quantitative framework using a methodology based on Boolean networks^{22,31}, which was introduced by Kauffman³². These logic models assume only two possible states for the nodes of the network: ON represented by 1, or OFF represented by 0. When a node of the system is ON, it means that it is activated whereas if the node is OFF it implies that it is deactivated or in basal state. The future state of the nodes is calculated based on the current states of its regulator nodes (the nodes that control its activation/deactivation) through Boolean equations. These equations are combinations of the logic operators AND, OR and NOT. Additionally, the \cap notation was used to model the nodes that need longer activation times of its regulator nodes to be activated.

The building of the Boolean functions followed two main steps: (i) equation definition (Supplementary data 1), and (ii) implementation in the R environment. Figure 2d shows an example of how the graphical representation shown in Figure 2c for the TNF α node was defined as a Boolean equation. The interactions between the nodes were classified in four different types: activation, inhibition, upregulation and downregulation. We introduced the upregulation and downregulation concepts because we were not able to capture all the information found in the literature only by using activation/inhibition interactions. An upregulation prolongs the activation of a node for a given number of time steps only when the node is already activated by its regulator nodes, whereas a downregulation inhibits the node once it is activated, producing a lessen in the expression of the component. Table 2 lists some examples of Boolean equations depending on the regulatory relationships (activation, inhibition, upregulation, downregulation) found in the literature and included in the current network.

The set of the defined Boolean expressions was implemented in R (Figure 2e) and forms part of a R framework²⁸ with several features as described in Supplementary Methods. We have developed a simulation algorithm to perform an analysis of the co-stimulation process, and in the following, we briefly describe how the system was initialized and perturbed, and how the signals were propagated and integrated.

Table 2. Examples to create Boolean equations

Type	Example	Explanation
Activation	<p>$T0_P65 = T0_ZAP70$</p> <p>$T0_CA2 = T0_ZAP70 \text{ OR } T0_SYK$</p> <p>$T0_ZAP70 = APC_MHCI \text{ AND } T0_TCR \text{ AND } T0_CD3Z$</p>	<p>T0_P65 needs T0_ZAP70 to be activated.</p> <p>T0_CA2 needs only one of the two activators. If T0_ZAP70 is activated then T0_CA2 will be activated.</p> <p>T0_ZAP70 needs the three activators activated. If one of them is not activated then T0_ZAP70 will not be activated.</p>
Longer time required for activation	$T0_CTLA4 = \cap T0_ACT$	T0_CTLA4 requires additional time for expression in the T cell surface.
Upregulation	$IL5 = Th2 \text{ OR } (IL5 \text{ AND } T0_ICOS \text{ AND } APC_B7H2)$	IL5 can be upregulated by the activation of T0_ICOS and APC_B7H2. By themselves, they are not able to activate IL5, so in the Boolean equation is necessary IL5 presence.
Downregulation	$IL17 = Th17 \text{ AND } IL6 \text{ AND } TGF\beta \text{ AND } IL23 \text{ OR } (IL17 \text{ AND } T0_ICOS \text{ AND } APC_B7H2) \text{ AND NOT } (IL17 \text{ AND } T0_CD27)$	The activation of the Th17 together with IL6, TGF β and IL23 activate the node IL17. T0_ICOS with APC_B7H2 upregulate IL17. If IL17 is activated and T0_CD27 becomes activated, activation of IL17 decreases over time.

In these models, there is no explicit notion of time, and the evolution of the Boolean network is studied using the concept of a time step, defined as the instance in which all the nodes in a network are updated based on the corresponding logic equations. To determine the state of a node in a time step, the random asynchronous updating method is used^{31,33,34}. This method computes the Boolean function of a node according to the last update of their regulator nodes (occurring either at previous or current time steps). The order in which the nodes are updated is selected randomly at each time step. Therefore, if for example node X depends on nodes A, B and C, the state of node X at time step $t + 1$ can be represented as: $X^{t+1} = F(A^{tu}, B^{tu}, C^{tu})$ being F , the corresponding Boolean function, tu the time step of the last update for nodes A, B and C which could be t or $t + 1$. Consequently, the same initial conditions may lead to different outcomes of the network dynamics. This method induces variability into the model and constitutes a more realistic representation of the biology as it assumes that biological processes of a system have aleatory timescales.

The initial conditions of our model (Table 3) are chosen in correspondence with the biological information found in the literature. At time step zero, all the nodes were set to 0 except the antigen and constitutive nodes. From time step one, the state of the nodes

depended on the state of its regulating nodes except antigen node which was kept activated to simulate continuous production of autoantigen as it is assumed in an autoimmune disease. At each time step and for each element (node) of the system the signal will be either 0 (OFF status) or 1 (ON status).

Table 3. Simulation initial conditions

Conditions	Th1- Polarizing	Th2- Polarizing	FcR γ chain translocation
1. Th1-Th2-polarizing FcR γ translocation	+	+	+
2.Th1-Th2-polarizing	+	+	-
3.Th1-polarizing FcR γ translocation	+	-	+
4.Th1-polarizing	+	-	-
5.Th2-polarizing FcR γ translocation	-	+	+
6.Th2-polarizing	-	+	-
7. Unpolarized FcR γ translocation	-	-	+
8. Unpolarized	-	-	-

2.3 Simulations

The SLE network inferred from the literature was simulated under continuous autoantigen exposure with asynchronous updating and the learned Boolean functions. First, we simulated the evolution of the network during 40 time steps, 30 of antigen exposure and 10 of washout, to obtain the relative activation profiles of the system nodes. Simulations consisted of 5000 random node updates per time step. Then, the average of the 5000 status (“0” or “1”) was calculated per node and time step. These profiles show the evolution of the nodes by plotting the fraction of simulations in which the node was in ON state at a given time step. Previous tests showed that running more than 5000 simulations and 30 time steps did not change the average of the dynamic trajectory of the network. We simulated different types and combinations of autoantigens, and also, the replacement of T0_CD3 ζ chain by T0_FcR γ chain, a translocation observed in many SLE patients³⁵. Depending on the type of antigen or the presence of the translocation of the FcR γ chain, 8 different initial conditions (Table 3) were studied initially.

Additional simulations were performed to accomplish different objectives as network validation (Supplementary Figure 1), attractor search or to explore system behavior under different type of perturbations.

2.3.1 Attractor analysis

To analyze the effect of perturbations or different initial conditions on the network dynamics, we studied the variations of the network attractor states. For any initial condition, the system eventually evolves into a limited set of stable states known as attractors^{33,36,37}. An attractor can be a fixed-point if it consists on only one state, a simple cycle if it is composed by more than one state that oscillate in a cycle or a complex attractor if the set of states oscillate irregularly.

Generally, large-scale or highly interconnected networks (like the one presented in this paper) converge into complex attractors when the asynchronous updating scheme is used. However, the interpretation of this type of attractors is not always easy due to the high number of stable states involved in them. An approach to overcome this problem is to generate the probability that a given node is in ON state inside the complex attractor. For example, for the “unpolarized” initial condition (Table 3) of the SLE model we found an attractor consisting of 7711 states, and we summarized all the information from the attractor state by including the activation probabilities of all the nodes in these 7711 states in a single vector.

As expected, identification of the exact attractor state was quite expensive regarding computational time. Alternatively, we found that the probabilities of being ON of the nodes almost did not change if we calculate the exact attractor or if we use an approximation, running the attractor search algorithm only 40 times during 5000 time steps, reducing computational times considerably. For more details about attractor identification see Supplementary Methods.

2.3.2 Network Perturbations and Clustering

The attractors of the system, and consequently, the activation probabilities of the nodes, may change when perturbations are introduced in the system. We introduced knockouts and over-expressions of single nodes in order to analyze which alterations could affect those stable patterns. A knockout of a node implies the deactivation of a component during all the simulation, whereas an over-expression generates a persistent activation of a node once it is activated for the first time.

The expression of 23 nodes of the network has been reported as altered in SLE patients (Supplementary Table 1). However, none of these alterations is shared among all SLE patients, and to our knowledge, there is no report of an SLE patient exhibiting all alterations. We attempted to simulate different individuals able to exhibit alterations in some of these 23 nodes. We simulated individuals with perturbations (knockouts or over-expressions) in each of the nodes of the network and checked which of these perturbations led to alterations in the activation pattern of the 23 nodes reported as altered in SLE patients. In the current investigation we limited our exploration to univariate perturbations (i.e., no combination of perturbed nodes in any simulation). We calculated the attractor of the system in normal conditions and evaluated how this attractor changed under each perturbation. If the activation level of a node in an attractor was decreased due to inclusion of a perturbation, it means that the perturbation caused a lower activation of the component compared to normal conditions. Conversely, if the activation probability of a node was increased due to a perturbation, it means that the perturbation caused a higher activation of the component compared to normal conditions. The ratio between the probabilities obtained in perturbed and unperturbed conditions were calculated to serve as input to the clustering analysis. We referred to this ratio as Perturbation Index (PI) of the nodes.

Hierarchical clustering methods determine clusters of similar items based on their distance and build a hierarchical structure, normally illustrated as a dendrogram. A hierarchical clustering method³⁸ was applied after the perturbation analysis to group the perturbed nodes that caused similar “lupus-like” manifestations on the network. We used the Euclidean distance to measure the similarities in the “lupus-like” alterations produced by the network perturbations, which are reflected in the PI of the nodes, and we employed the average-linkage strategy to merge the clusters of perturbed nodes

between each other. For a more detailed description of this process see Supplementary Methods. The objective of the clustering method is to group potential SLE patients according to the alterations in the attractor steady states that they share, in order to find different patient subpopulations that may require different treatments. Results of the clustering exercise are summarized as heatmaps in which the color indicates the effect of each perturbation compared to an unperturbed simulation, complemented by dendrograms to identify the perturbation clusters. Only the alterations elicited on any of the 23 nodes that have been reported as altered in SLE were considered for distance calculations in the cluster analysis.

2.3.3 Evaluation of Therapeutic Targets

Simulations of several potential treatments were performed following the assumption that receptor binding is complete and immediate. Two types of treatment were simulated: (i) inhibition of different signaling pathways or cytokines, driven by node knockouts or (ii) induction of certain molecules to upregulate a pathway using a constant activation of the node. Different doses of anti-ICOS treatment were simulated including a variable probability of inhibition in each time step in which the therapy was active.

3. RESULTS

After the process of bibliographic review, nodes selection, data annotation and description of the Boolean equations, the antigen presentation network model (Figure 3) consisted of 52 nodes (Supplementary Table 2), and contained 296 interactions between the nodes describing activation, inhibition, upregulation or downregulation processes. From de 52 nodes of the network, 23 have been reported as altered in SLE patients, 7 as downregulated and 16 as upregulated (Supplementary Table 1). The Boolean equations that control the network dynamics are listed in Table 4 and the biological explanation for these equations is presented in Supplementary data 1.

Table 4. Boolean equations

APC_AR = Ag
APC_MHCII = (Ag & APC_AR)
T0_TCR = 1
APC_B71 = (APC_MHCII & T0_TCR & Ag)
APC_B72 = (APC_MHCII & T0_TCR & Ag)
T0_NOTCH3 = 1
T0_NOTCH1_2 = 1
APC_DLL = APC_AR & Ag_DLL
APC_JAGGED = APC_AR & Ag_JAGGED
APC_CD40 = Ag_DLL & T0_TCR & APC_MHCII
T0_CD40L = ((APC_MHCII & T0_TCR & Ag & T0_ICOS & APC_B7H2) ((T0_CD40L & Th1 & (IL2 IL12))) &! ($\cap_{i=1}^{upreg=4} T0_CD40L^{t-i}$ & $\cap_{i=1}^{upreg=4} Th1^{t-i}$ & ($\cap_{i=1}^{upreg=4} IL2^{t-i}$ $\cap_{i=1}^{upreg=4} IL12^{t-i}$))) ((T0_CD40L & T0_CD28 & (APC_B71 APC_B72)) ($\cap_{i=1}^{upreg=4} T0_CD40L^{t-i}$ & $\cap_{i=1}^{upreg=4} T0_CD28$ & ($\cap_{i=1}^{upreg=4} APC_B71^{t-i}$ $\cap_{i=1}^{upreg=4} APC_B72^{t-i}$)))) &! ((APC_CD40 & T0_CD40L & ! Th1) (T0_CD40L & IL4))
T0_ICOS = (T0_TCR & APC_MHCII & Ag) TNFa ((T0_ICOS & (T0_CD28 & (APC_B71 APC_B72))) &! ($\cap_{i=1}^{upreg=4} T0_ICOS^{t-i}$ & ($\cap_{i=1}^{upreg=4} T0_CD28^{t-i}$ & ($\cap_{i=1}^{upreg=4} APC_B71^{t-i}$ $\cap_{i=1}^{upreg=4} APC_B72^{t-i}$)))) ((T0_ICOS & (IL12 IL23) & ! IL4) &! ($\cap_{i=1}^{upreg=4} T0_ICOS^{t-i}$ & ($\cap_{i=1}^{upreg=4} IL12^{t-i}$ $\cap_{i=1}^{upreg=4} IL23^{t-i}$))))
APC_B7H2 = (T0_ICOS & IFNG) & ! (APC_B7H2 & IL10)
T0_CD44 = T0_ACT
T0_CD28 = ! ($\cap_{i=1}^{THR_CTLA4_max_CD28=2} T0_CTLA4^{t-i}$ (T0_CD28 & $\cap_{i=1}^{THR_TNFa_max=3} TNFa^{t-i}$))
T0_CTLA4 = $\cap_{i=1}^{THR_T0_ACT_max_CTLA4=2} T0_ACT^{t-i}$
T0_OX40 = $\cap_{i=1}^{THR_T0_ACT_max_OX40=2} T0_ACT^{t-i}$ TNFa (T0_OX40 & IL2 & ! ($\cap_{i=1}^{upreg=4} T0_OX40^{t-i}$ & $\cap_{i=1}^{upreg=4} IL2^{t-i}$)) ((T0_OX40 & T0_CD28 & (APC_B71 APC_B72)) & ! ($\cap_{i=1}^{upreg=4} T0_OX40^{t-i}$ & $\cap_{i=1}^{upreg=4} T0_CD28^{t-i}$ & ($\cap_{i=1}^{upreg=4} APC_B71^{t-i}$ $\cap_{i=1}^{upreg=4} APC_B72^{t-i}$))))
APC_OX40L = APC_CD40 & T0_CD40L & APC_MHCII
APC_B7H1 = ($\cap_{i=1}^{THR_T0_ACT_max_B7H1=2} T0_ACT^{t-i}$ IFNG (APC_B7H1 & TNFa & ! ($\cap_{i=1}^{upreg=4} APC_B7H1^{t-i}$ & $\cap_{i=1}^{upreg=4} TNFa^{t-i}$)) (APC_B7H1 & IL12 & ! ($\cap_{i=1}^{upreg=4} APC_B7H1^{t-i}$ & $\cap_{i=1}^{upreg=4} IL12^{t-i}$)) (APC_B7H1 & IL4 & ! ($\cap_{i=1}^{upreg=4} APC_B7H1^{t-i}$ & $\cap_{i=1}^{upreg=4} IL4^{t-i}$))) & ! (APC_B7H1 & TGFb)

Table 4. Boolean equations (continued)

$\text{APC_B7DC} = \cap_{i=1}^{\text{THR_T0_ACT_max_B7DC}=2} \text{T0_ACT}^{t-i} \mid (\text{APC_B7DC} \& \text{GMCSF} \& \cap_{i=1}^{\text{upreg}=4} \text{APC_B7DC}^{t-i} \& \cap_{i=1}^{\text{upreg}=4} \text{GMCSF}^{t-i}) \mid (\text{APC_B7DC} \& \text{IL12} \& \cap_{i=1}^{\text{upreg}=4} \text{APC_B7DC}^{t-i} \& \cap_{i=1}^{\text{upreg}=4} \text{IL12}^{t-i}) \mid (\text{APC_B7DC} \& \text{IL4} \& \cap_{i=1}^{\text{upreg}=4} \text{APC_B7DC}^{t-i} \& \cap_{i=1}^{\text{upreg}=4} \text{IL4}^{t-i}) \mid (\text{APC_B7DC} \& \text{IL13} \& \cap_{i=1}^{\text{upreg}=4} \text{APC_B7DC}^{t-i} \& \cap_{i=1}^{\text{upreg}=4} \text{IL13}^{t-i})$
$\text{T0_PD1} = \cap_{i=1}^{\text{THR_T0_ACT_max_PD1}=2} \text{T0_PD1}^{t-i} \mid (\text{T0_PD1} \& \text{TNFa} \& \cap_{i=1}^{\text{upreg}=4} \text{T0_PD1}^{t-i} \& \cap_{i=1}^{\text{upreg}=4} \text{TNFa}^{t-i})$
$\text{T0_CD27} = \text{T0_ACT} \& \cap_{i=1}^{\text{THR_T0_ACT_max_CD27}=4} \text{T0_CD27}^{t-i}$
$\text{T0_ZAP70} = \text{APC_MHCII} \& \text{T0_TCR} \& \text{T0_CD3Z}$
$\text{T0_SYK} = \text{APC_MHCII} \& \text{Ag} \& \text{T0_TCR} \& \text{T0_FcRG}$
$\text{T0_cfos} = \text{T0_ZAP70}$
$\text{T0_CD3Z} = (\text{APC_MHCII} \& \text{Ag} \& \text{T0_TCR} \& \text{T0_CD45}) \& \text{T0_FcRG}$
$\text{T0_CA2} = \text{T0_ZAP70} \mid \text{T0_SYK}$
$\text{T0_FcRG} = \text{APC_MHCII} \& \text{Ag} \& \text{T0_TCR} \& \text{Lupus}$
$\text{T0_P65} = \text{T0_ZAP70}$
$\text{T0_CD45} = 1$
$\text{T0_ACT} = ((\text{APC_MHCII} \& \text{T0_TCR} \& (\text{T0_CD28} \& (\text{APC_B71} \mid \text{APC_B72}))) \mid (\text{T0_ACT} \& \text{T0_ICOS} \& \text{APC_B7H2} \& \cap_{i=1}^{\text{upreg}=4} \text{T0_ACT}^{t-i} \& \cap_{i=1}^{\text{upreg}=4} \text{T0_ICOS} \& \cap_{i=1}^{\text{upreg}=4} \text{APC_B7H2}^{t-i}) \mid (\text{T0_ACT} \& \text{T0_CD40L} \& \text{APC_CD40} \& \cap_{i=1}^{\text{upreg}=4} \text{T0_ACT}^{t-i} \& \cap_{i=1}^{\text{upreg}=4} \text{T0_CD40L}^{t-i} \& \cap_{i=1}^{\text{upreg}=4} \text{APC_CD40}^{t-i}) \mid (\text{T0_ACT} \& \text{T0_OX40} \& \text{APC_OX40L} \& \cap_{i=1}^{\text{upreg}=4} \text{T0_ACT}^{t-i} \& \cap_{i=1}^{\text{upreg}=4} \text{T0_OX40}^{t-i} \& \cap_{i=1}^{\text{upreg}=4} \text{APC_OX40L}^{t-i})) \& ((\text{T0_CTLA4} \& (\text{APC_B71} \mid \text{APC_B72})) \mid (\text{T0_PD1} \& (\text{APC_B7DC} \mid \text{APC_B7H1})))$
$\text{Th1} = ((\text{T0_ACT} \& \text{APC_CD40} \& \text{T0_CD40L} \& \text{IL12} \& \text{IFNG}) \mid (\text{Th1} \& \text{T0_CD44} \& \cap_{i=1}^{\text{upreg}=4} \text{Th1}^{t-i} \& \cap_{i=1}^{\text{upreg}=4} \text{T0_CD44}^{t-i})) \& ((\text{Th1} \& \text{Treg}) \& \text{Th2} \& \text{TGFb})$
$\text{Th2} = (\text{T0_ACT} \& (\text{T0_CD28} \& (\text{APC_B71} \mid \text{APC_B72}))) \& \text{IL4} \& ((\text{Th2} \& (\text{Treg} \mid \text{T0_CD44})) \& \text{IL12} \& \text{TGFb})$
$\text{Th17} = (((\text{T0_ACT} \& \text{TGFb} \& (\text{IL21} \mid \text{IL6} \mid \text{IL23})) \mid (\text{Th17} \& \text{T0_ICOS} \& \text{APC_B7H2} \& \cap_{i=1}^{\text{upreg}=4} \text{Th17}^{t-i} \& \cap_{i=1}^{\text{upreg}=4} \text{T0_ICOS}^{t-i} \& \cap_{i=1}^{\text{upreg}=4} \text{APC_B7H2}^{t-i})) \mid (\text{Th17} \& \text{T0_CD40L} \& \text{APC_CD40} \& \cap_{i=1}^{\text{upreg}=4} \text{Th17}^{t-i} \& \cap_{i=1}^{\text{upreg}=4} \text{T0_CD40L}^{t-i} \& \cap_{i=1}^{\text{upreg}=4} \text{APC_CD40}^{t-i})) \& ((\text{Treg} \& ((\text{IL21} \mid \text{IL6}))) \& ((\text{IL12} \mid \text{IFNG} \mid \text{IL4})))$
$\text{Tfh} = (\text{T0_ACT} \& \text{IL12} \& \text{IL21} \& \text{IL6}) \mid ((\text{Tfh} \& \text{APC_CD40} \& \text{T0_CD40L} \& \text{T0_ICOS} \& \text{APC_B7H2}) \& ((\cap_{i=1}^{\text{upreg}=4} \text{Tfh}^{t-i} \& \cap_{i=1}^{\text{upreg}=4} \text{APC_CD40}^{t-i} \& \cap_{i=1}^{\text{upreg}=4} \text{T0_CD40L}^{t-i} \& \cap_{i=1}^{\text{upreg}=4} \text{T0_ICOS}^{t-i} \& \cap_{i=1}^{\text{upreg}=4} \text{APC_B7H2}^{t-i})))$
$\text{Treg} = ((\text{T0_ACT} \& \text{TGFb}) \mid (\text{Treg} \& \text{T0_PD1} \& \text{APC_B7H1} \& ((\cap_{i=1}^{\text{upreg}=4} \text{Treg}^{t-i} \& \cap_{i=1}^{\text{upreg}=4} \text{T0_PD1}^{t-i} \& \cap_{i=1}^{\text{upreg}=4} \text{APC_B7H1}^{t-i}))) \& ((\text{IL6} \mid \text{IL21})))$
$\text{IL2} = \text{T0_ACT} \& \text{T0_cfos} \& \text{T0_P65} \& \text{T0_CA2} \& ((\text{T0_CTLA4} \& (\text{APC_B71} \mid \text{APC_B72})))$
$\text{IL4} = (\text{Th2} \mid (\text{T0_ACT} \& \text{APC_JAGGED} \& \text{T0_NOTCH1_2}) \mid ((\text{IL4} \& \text{T0_ICOS} \& \text{APC_B7H2}) \& ((\cap_{i=1}^{\text{upreg}=4} \text{IL4}^{t-i} \& \cap_{i=1}^{\text{upreg}=4} \text{T0_ICOS}^{t-i} \& \cap_{i=1}^{\text{upreg}=4} \text{APC_B7H2}^{t-i}))) \mid ((\text{IL4} \& \text{APC_OX40L} \& \text{T0_OX40}) \& ((\cap_{i=1}^{\text{upreg}=4} \text{IL4}^{t-i} \& \cap_{i=1}^{\text{upreg}=4} \text{APC_OX40L}^{t-i} \& \cap_{i=1}^{\text{upreg}=4} \text{T0_OX40}^{t-i}))) \mid (\text{IL4} \& \text{T0_CD27} \& ((\cap_{i=1}^{\text{upreg}=4} \text{IL4}^{t-i} \& \cap_{i=1}^{\text{upreg}=4} \text{T0_CD27}^{t-i}))) \& ((\text{IL4} \& (\text{T0_PD1} \& \text{APC_B7DC})))$
$\text{IL6} = ((\text{T0_CD28} \& (\text{APC_B71} \mid \text{APC_B72})) \mid (\cap_{i=1}^{\text{THR_APC_CD40_max_IL6}=2} \text{APC_CD40}^{t-i} \& \text{T0_CD40L}) \mid (\text{TGFb} \& \text{IL23})) \& ((\text{IL4} \mid \text{IL10}))$
$\text{IL10} = (\text{Treg} \mid \text{Th2} \mid (\text{IL10} \& \text{T0_ICOS} \& \text{APC_B7H2} \& ((\cap_{i=1}^{\text{upreg}=4} \text{IL10}^{t-i} \& \cap_{i=1}^{\text{upreg}=4} \text{T0_ICOS}^{t-i} \& \cap_{i=1}^{\text{upreg}=4} \text{APC_B7H2}^{t-i}))) \mid (\text{IL10} \& \text{TNFa} \& ((\cap_{i=1}^{\text{upreg}=4} \text{IL10}^{t-i} \& \cap_{i=1}^{\text{upreg}=4} \text{TNFa}^{t-i}))) \mid (\text{IL10} \& \text{IL2} \& ((\cap_{i=1}^{\text{upreg}=4} \text{IL10}^{t-i} \& \cap_{i=1}^{\text{upreg}=4} \text{IL2}^{t-i}))) \& ((\text{T0_OX40} \& \text{APC_OX40L}) \& ((\text{IL10} \& (\text{T0_PD1} \& (\text{APC_B7H1} \mid \text{APC_B7DC}))))$
$\text{IL12} = ((\text{APC_MHCII} \& \text{T0_TCR} \& \text{APC_DLL} \& \text{T0_NOTCH3} \& \text{APC_CD40} \& \text{T0_CD40L}) \mid (\text{IL12} \& \text{T0_ICOS} \& ((\cap_{i=1}^{\text{upreg}=4} \text{IL12}^{t-i} \& \cap_{i=1}^{\text{upreg}=4} \text{T0_ICOS}^{t-i}))) \& \text{IL10}$
$\text{IL13} = \text{Th2} \mid (\text{T0_ACT} \& \text{Th1} \& \text{IL18})$

Table 4. Boolean equations (continued)

$\mathbf{IL17} = ((\text{Th17} \ \& \ \text{IL6} \ \& \ \text{TGFb} \ \& \ \text{IL23}) \ \ (\text{IL17} \ \& \ \text{T0_ICOS} \ \& \ \text{APC_B7H2} \ \& \ ! \ (\cap_{i=1}^{\text{upreg}=4} \ \text{IL17}^{t-i} \ \& \ \cap_{i=1}^{\text{upreg}=4} \ \text{T0_ICOS}^{t-i} \ \& \ \cap_{i=1}^{\text{upreg}=4} \ \text{APC_B7H2}^{t-i}))) \ \& \ ! \ (\text{IL17} \ \& \ \text{T0_CD27})$
$\mathbf{IL18} = 1$
$\mathbf{IL21} = \text{Tfh} \ \ \text{Th17} \ \ ((\text{T0_ACT} \ \& \ \text{IL6}) \ \& \ ! \ \text{IL4} \ \& \ ! \ \text{IFNG} \ \& \ ! \ \text{TGFb}) \ \ (\text{IL21} \ \& \ \text{T0_CD27} \ \& \ ! \ (\cap_{i=1}^{\text{upreg}=4} \ \text{IL21}^{t-i} \ \& \ \cap_{i=1}^{\text{upreg}=4} \ \text{T0_CD27}^{t-i}))$
$\mathbf{IL23} = \text{Ag_DLL}$
$\mathbf{IL27} = \text{Ag_DLL}$
$\mathbf{TNFa} = (((\text{Ag_DLL} \ \& \ \text{IFNG}) \ \ \text{IL2} \ \ \text{GMCSF} \ \ \text{TGFb}) \ \ ((\text{TNFa} \ \& \ \text{T0_ICOS} \ \& \ \text{APC_B7H2}) \ \& \ ! \ (\cap_{i=1}^{\text{upreg}=4} \ \text{TNFa}^{t-i} \ \& \ \cap_{i=1}^{\text{upreg}=4} \ \text{T0_ICOS}^{t-i} \ \& \ \cap_{i=1}^{\text{upreg}=4} \ \text{APC_B7H2}^{t-i}))) \ \& \ ! \ \text{IL10} \ \& \ ! \ (\text{TNFa} \ \& \ \text{IL4})$
$\mathbf{TGFb} = \text{Treg}$
$\mathbf{IFNG} = ((\text{T0_ACT} \ \ \text{Th1}) \ \ (\text{IFNG} \ \& \ \text{T0_CD40L} \ \& \ \text{APC_CD40} \ \& \ ! \ (\cap_{i=1}^{\text{upreg}=4} \ \text{IFNG}^{t-i} \ \& \ \cap_{i=1}^{\text{upreg}=4} \ \text{T0_CD40L}^{t-i} \ \& \ \cap_{i=1}^{\text{upreg}=4} \ \text{APC_CD40}^{t-i}))) \ \ (\text{IFNG} \ \& \ \text{T0_ICOS} \ \& \ \text{APC_B7H2} \ \& \ ! \ (\cap_{i=1}^{\text{upreg}=4} \ \text{IFNG}^{t-i} \ \& \ \cap_{i=1}^{\text{upreg}=4} \ \text{T0_ICOS}^{t-i} \ \& \ \cap_{i=1}^{\text{upreg}=4} \ \text{APC_B7H2}^{t-i}))) \ \ (\text{IFNG} \ \& \ \text{IL12} \ \& \ ! \ (\cap_{i=1}^{\text{upreg}=4} \ \text{IFNG}^{t-i} \ \& \ \cap_{i=1}^{\text{upreg}=4} \ \text{IL12}^{t-i}))) \ \& \ ! \ \text{Th2} \ \& \ ! \ \text{IL10} \ \& \ ! \ (\text{IFNG} \ \& \ \text{T0_PD1} \ \& \ (\text{APC_B7H1} \ \ \text{APC_B7DC}))$
$\mathbf{GMCSF} = (\text{Th1} \ \ (\text{GMCSF} \ \& \ \text{IL12} \ \& \ ! \ (\cap_{i=1}^{\text{upreg}=4} \ \text{GMCSF}^{t-i} \ \& \ \cap_{i=1}^{\text{upreg}=4} \ \text{IL12}^{t-i}))) \ \& \ ! \ (\text{IL27}) \ \& \ ! \ (\text{GMCSF} \ \& \ \text{IL6})$

3.1 Network dynamics simulations

The dynamic evolution of the network after antigen exposure can be captured by the semi-quantitative activation profiles of network nodes (Figure 4). Under the same initial conditions, different nodes exhibited different levels of relative activation and different patterns of oscillation. The immune system triggers different responses depending on the type of antigen; bacteria and viruses provoke Th1 responses while parasites or allergens trigger Th2 responses³⁹. Due the molecular structure of the antigens involved in SLE, the majority of the examples are done simulating Th1 polarizing antigens. Accordingly, in the simulations the activation profile for most nodes was dependent on the antigen type, but this dependency varied among nodes. In general, differences in activation profiles due to antigen type were larger for interleukins and smaller for early signals of activation (CD80, CD86, T-cell activation). Another condition that was studied was the FcR γ chain translocation, which is an alteration observed in some SLE patients. Simulations under this alteration produced considerable changes in the profiles of some nodes like Interleukin 2 (IL-2), while expression of most nodes remains unaltered under this condition. For some nodes like TNF α , alterations in its activation profiles due to FcR γ chain translocation were evident only for certain antigen types (Figure 4).

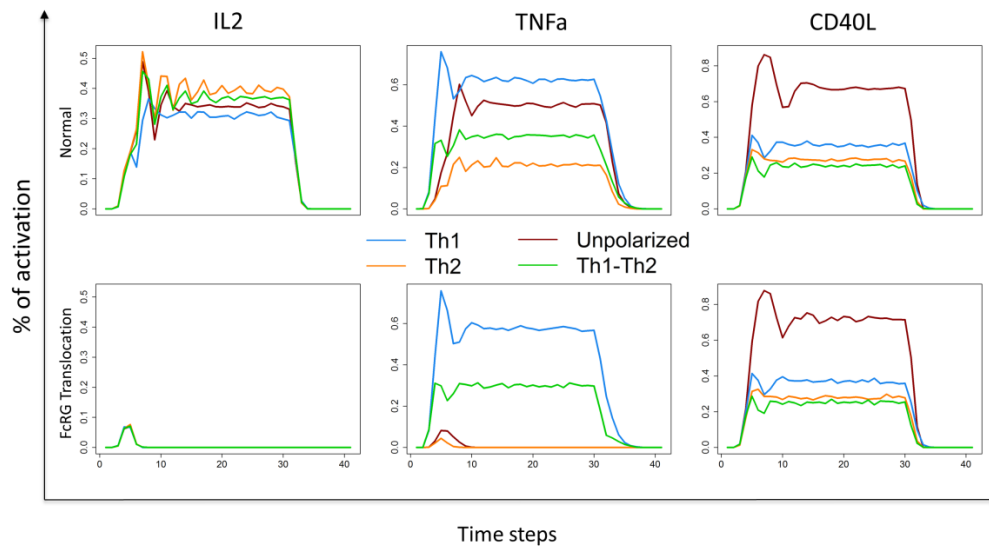


Figure 4. Differential expression of selected nodes for different conditions of antigen exposure and translocation of FcR γ chain. Chronic immune response against four different types of antigens (blue for Th1 like antigen, orange for Th2 like antigen, red for other types of antigens and green when Th1 and Th2 like antigens are present) was simulated. Lower panel displays the impact of FcR γ chain translocation on node expression.

3.2. Perturbation analysis and clustering

We performed a perturbation analysis to identify the simulated perturbations (node blockage or over-expression) that could lead to alterations exhibited in SLE patients, represented as increased or decreased activation of the 23 nodes that have been reported as altered in SLE patients. Figure 5a shows under the presence of a Th1 antigen, which knockouts produced attractors with a (i) higher activation than the unperturbed simulation for any of the 16 nodes that have been reported as upregulated in SLE patients (TNF α , APC_MHCII, T0_PD1,..., T0_CA2), (ii) lower activation for any of the 7 nodes that have been reported as downregulated in SLE (IL4, APC_B7H1,...Treg). Similar analysis was performed to identify which node over-expressions could lead to higher or lower activation probabilities of the nodes that have been reported as altered in SLE (Figure 5b). The heatmaps were combined with a hierarchical clustering method to arrange the columns according to the lupus-like manifestations that they triggered. Nodes that caused similar alterations are clustered together as it is shown in the dendrograms on top of each heatmap. Heatmaps and clusters resulted from simulation on other conditions are included in Supplementary Figure 2.

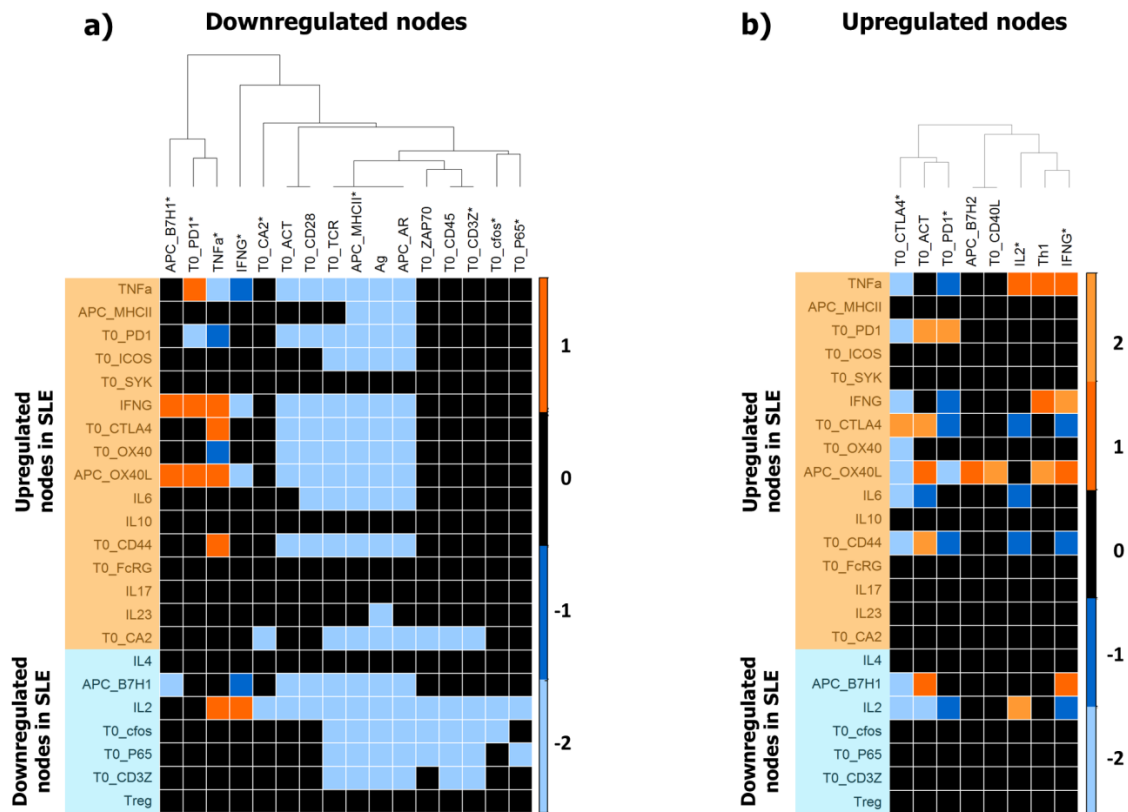


Figure 5. Clustering of perturbations according to “SLE like” alterations

Heatmaps indicate the effect of single perturbations on the nodes that have been reported as altered in SLE. The numeric scale in the legend represents different values of the nodes Perturbation Index (PI) under different perturbations. A value of 2 represents PIs greater than 2, a value of 1 PIs between 1.25 and 2, the 0 substitutes PIs close to 1, the -1 indicates PIs between 0.8 and 0.5, and the -2 PIs smaller than 0.5. Two types of perturbations were simulated, node knockouts (a) and node over-expressions (b). Each heatmap contains 23 rows, one for each node that has been reported as altered in SLE. Most perturbations did not trigger considerable changes in those 23 nodes (represented by a 0 in the numeric scale and indicated in black or absent from the heatmap). Some perturbations led to a higher activation of the 23 nodes (represented by a 1 or 2 in the numeric scale and indicated in orange in the heatmaps) while the lower activation of the 23 nodes were more common (represented by a -1 or -2 in the numeric scale and in blue in the heatmap). Perturbations were clustered according to the SLE like alterations that they provoked as can be seen in the blue and orange blocks in the heatmaps. Results shown are for Th1 type antigen conditions. Other conditions are in Supplemental Figure 2. The * in the nodes of the columns denotes that they are reported to be altered in SLE.

3.3. Evaluation of therapeutic targets

Perturbations clustered together not only triggered similar “SLE like” alterations but it was found that they also tended to respond similarly to simulated treatment. Figure 6 shows the effect of three perturbations (knockouts of TNF α , Programmed death-ligand 1 (B7H1), and Programmed cell death protein 1 (PD1), that were clustered together because they trigger upregulations in nodes that have been reported as altered in SLE (TNF α , IFN γ , and APC_OX40L). The figure also shows the effect of two different treatments (targeting components of this network that have been used in clinical trials,

i.e. anti-TNF α and anti-ICOS) on the three nodes TNF α , IFN γ , and APC_OX40L in the presence of the above mentioned alterations.

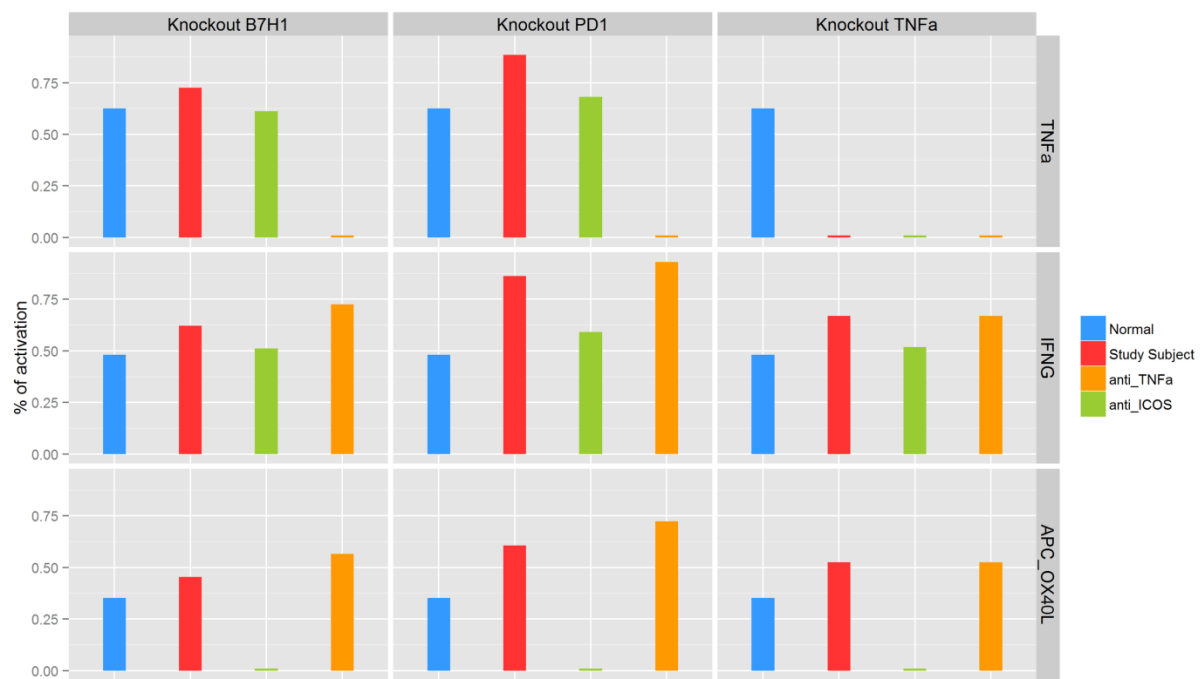


Figure 6. Anti-ICOS and anti-TNF α simulated treatments

Simulation of drug/treatment in individuals exhibiting “SLE-like” alterations in TNF α , IFN γ and APC_OX40L activation probability due to three different underlying alterations, TNF α , APC_B7H1 and T0_PD1 knockouts (grouped from the cluster analysis). Anti-ICOS treatment had different effect on the three clustered perturbations while anti-TNF α showed no effect on activation levels of IFN γ or APC_OX40L.

Simulations showed that anti-TNF α treatment decreased only the levels of TNF α . Moreover, this treatment even led to higher expression of IFN γ and APC_OX40L under the three studied perturbations. Treatment with anti-ICOS reverted the over-expression found in IFN γ and TNF α , however for the case of APC_OX40L, the response elicited was not optimal since that node was completely shut-down, despite a 40% activation was seen in the control condition (“Normal”).

Another interesting possibility is the inclusion of inhibition strength on the analysis (Figure 7). Although, this network is not yet a quantitative tool, it can evaluate what would be the required target engagement and exposure level of a monoclonal antibody (mAb) to effectively block a molecular pathway and potentially decrease the appearance of “SLE like” alterations. As drug target engagement can be measured experimentally using human cells, this information could be easily included in the model. This analysis

would be of special interest in cases in which mAbs against the same targets but from different manufactures exhibit different clinical efficacy⁴⁰.

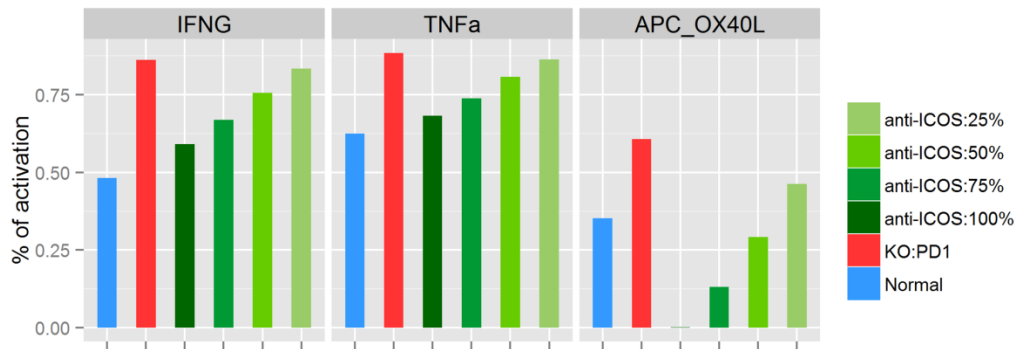


Figure 7. Effect of different levels of anti-ICOS treatment

Different levels of inhibition of T0_ICOS node were simulated (25%, 50%, 75% and 100% inhibition) in order to test its effect on IFN γ and TNF α nodes activation in a study subject with a knockout on T0_PD1 molecule (KO:PD1). It can be observed that higher levels of inhibition led to lower activation of the perturbed condition in both IFN γ and TNF α nodes, making the activation probability of these nodes similar to normal conditions when using the highest anti-ICOS treatment. Higher levels of inhibition on APC_OX40L node however, create an excessive downregulation of the node which suggests that the lowest anti-ICOS treatment may be more adequate.

4. DISCUSSION

In the current work we present a systems pharmacology model based on Boolean networks for the processes involved in the antigen presentation by the APC to the T cells, in the context of the autoimmune disease SLE. Technical aspects regarding model implementation and coding can be obtained from elsewhere²⁸. Here we provide a comprehensive workflow to help in developing and apply this type of discrete models in the area of early drug development.

The motivation to embark on this project comes from the complexity of the immune system and the lack of longitudinal data for most of its main components, hampering the development of (semi-) mechanistic pharmacokinetic/ pharmacodynamic (PK/PD) models based on ordinary differential equations. In fact there are recent examples in literature where the population PK/PD approach has been applied to analyze data from clinical trials in SLE^{9,10}. In those cases, no more than two biomarkers were considered as representative of a positive signal of the drug effects. From a proof of concept point of view such strategy is justified, but given the complexity of SLE disease (and of many others), it seems insufficient to face the current challenges in developing new therapeutic strategies: (i) identify poor and non-responders, (ii) target identification, or (iii) rational search of drug combinations.

Our system pharmacology model should not be viewed as a competitor of traditional PK/PD models and systems biology models, but rather a tool in between to bring together different views of handling in vivo systems.

SLE is characterized by its clinical heterogeneity, most likely, this pathology comprises patients with different underlying alterations and different types of autoantigens, and therefore, treatment success may vary greatly among patients. Few attempts have been made in clinical phenotyping and endotyping before clinical trials in SLE patients, even knowing that treatment success has been low in highly heterogeneous populations for other diseases⁴¹. In this work, we have simulated different alterations of the immune system that triggered molecular alterations similar to those reported for SLE patients. However, as the present model covers only a subsection of the whole SLE pathway, the “SLE like” alterations were restricted to molecular alterations of the antigen presentation process described for SLE patients, and not yet to SLE clinical

manifestations. Figure 5 shows how the same “SLE like” alterations can be provoked by different underlying univariate alterations (perturbations) and Figure 6 shows how the effect of drug treatment to control these “SLE like” alterations could be different depending on the underlying alteration (provoking perturbation). Furthermore, these examples were made simulating only one type of antigen (Th1 antigen). In Supplemental Figure 3 it can be seen that the same “SLE like” alteration may be triggered by different initial conditions. For example TNF α was upregulated between others by a downregulation of T0_PD1 when a Th1 like antigen was simulated (Figure 5). The same TNF α upregulation was triggered by a downregulation of T0_CTLA4 under a Th2 antigen simulation or by an over-expression of T0_CD40L under a simultaneous Th1 and Th2 antigen stimulation. In total 34 combinations of antigen type and underlying perturbation triggered an over-expression of TNF α . Therefore, response to treatment intended to control such “SLE like” alterations may also vary significantly depending on the underlying perturbation. This systems pharmacology approach may help to identify groups of patients that share alterations in the same molecular pathways, and could respond similarly to equal treatments, maximizing the treatment success in clinical trials by patient stratification.

Only 12 perturbations in the network were able to provoke upregulations of the 16 nodes that have been reported as upregulated in SLE patients, this is a surprisingly low number compared to the 112 perturbations that were tested (52 node blockages and 52 node over-expressions). Similarly 22 perturbations led to downregulations of the 6 nodes that have been reported as downregulated in SLE patients. Most of these 22 perturbations were downregulations of nodes involved in the initial stages of the immune response, triggering a blockage of the response, impeding the activation of all nodes except the constitutive ones. Therefore such perturbations should not be considered as a good replication of a “SLE like” alteration. Consequently, it can be said that few system perturbations triggered “SLE like” alterations under Th1 antigen conditions. This result was also observed for other antigen exposure conditions (Supplementary Figure 2).

This work evaluated the relationship between: (i) system perturbation (ii) “SLE like” alteration and (iii) response to therapy. The analysis was performed in an univariate way, meaning that underlying alterations (node perturbation) were simulated individually and no combination of perturbations were tested, mainly because of the

large number of possible combinations of perturbations, more than 12000 combinations for a bivariate perturbation analysis and exponentially more for three or more simultaneous alterations. The fact that most nodes perturbations did not affect significantly the network evolution agrees with similar observations in other works of systems biology⁴². Besides, it makes sense that critical processes as the immune response are not totally dependent on individual nodes and redundant mechanisms assure a functional physiology in case of single molecular defects.

Apart from target identification, drug development can also benefit from rapid target invalidation, avoiding costly clinical trials of predictable inefficacious drugs. The model presented in this work could be useful in this regard, for example an anti-TNF α treatment which has been successfully used in other autoimmune diseases has not shown clinical efficacy in SLE. This model, although incomplete, showed that anti-TNF α was ineffective in controlling most “SLE like” alterations and only controlled TNF α levels, results that are in agreement with the clinical data that suggest that anti-TNF α treatment is only efficacious in SLE patients with alterations related to high levels of TNF α ⁴³. Again, this type of analysis will be valid and relevant once the whole network is finished.

It must be highlighted that despite the promising applicability of this approach, the full potential of this tool cannot be asses until the whole SLE pathway is included in the network. In the same way, full model validation is not possible at this stage because activation of many nodes is also regulated by other molecules, critical to the immune physiopathology of SLE but not yet included in the model. This project was done to evaluate if a systems pharmacology approach can contribute to tackle the current challenges in drug development. Evidently, these challenges can be pursued by different types of models of different complexities, with advantages and disadvantages for each alternative. We consider that the present work support the use of Boolean networks as the right beginning to support target validation/invalidation, identification of biomarkers and patient stratification in early stages of drug development for autoimmune diseases. This is especially relevant considering the complexity of the immune system and all the technical challenges of estimating hundreds of parameters for a quantitative model, including the generation of reliable human data. Boolean networks are easily and quickly implemented, flexible and scalable to larger systems. Furthermore, this model can also identify in which subsections of the network it is worth to undertake deeper

quantitative analysis or to include further knowledge about gene expression promoters or polymorphisms.

Despite the advantages of this approach to study processes in which there is a general lack of robust data, there are several limitations that must be considered. Boolean networks are restrained to computing simple logic operations and do not capture temporal details that may be required for modeling certain aspects of regulatory networks. Additionally, the process of annotation and translation of literature into Boolean equation is very time consuming and susceptible to multiple interpretation, also the type of data necessary to perform fine validation of these networks are not easily accessible, especially from human subjects. However, these models can be used as a first attempt to understand the general dynamical properties of complex biological systems.

5. CONCLUSIONS

Heterogeneity of SLE manifestations can be modeled by different underlying altered pathways of the immune system using a systems pharmacology approach based on Boolean networks. The model seems appropriate to make the best use of the few available data in complex diseases. The reach of this approach was explored. This work constitutes a satisfactory proof of concept of this methodology and the evaluation justifies the expansion of the current model to include the whole SLE pathway in the network. These models are promising as research tools to support early stages of drug development focused on target validation/invalidation, identification of biomarkers and patient stratification.

6. REFERENCES

1. Mohan, C. & Putterman, C. Genetics and pathogenesis of systemic lupus erythematosus and lupus nephritis. *Nat. Rev. Nephrol.* (2015). doi:10.1038/nrneph.2015.33
2. Herrmann, M., Podolska, M., Biermann, M., Maueröder, C. & Hahn, J. Inflammatory etiopathogenesis of systemic lupus erythematosus: an update. *J. Inflamm. Res.* 161 (2015). doi:10.2147/JIR.S70325
3. Rahman, A. & Isenberg, D. a. Systemic lupus erythematosus. *N. Engl. J. Med.* **358**, 929–39 (2008).
4. Pons-Estel, G. J., Alarcón, G. S., Scofield, L., Reinlib, L. & Cooper, G. S. Understanding the Epidemiology and Progression of Systemic Lupus Erythematosus. *Semin. Arthritis Rheum.* **39**, 257–268 (2010).
5. Tsokos, G. C. Systemic Lupus Erythematosus. *New England Journal of Medicine* (2011). doi:10.1056/NEJMra1100359
6. Bernknopf, a, Rowley, K. & Bailey, T. A review of systemic lupus erythematosus and current treatment options. *Formulary* **46**, 178–194 (2011).
7. Merrill, J. T. Treatment of Systemic Lupus Erythematosus. **70**, 172–176 (2012).
8. Belmont, H. M. Treatment of systemic lupus erythematosus - 2013 update. *Bull. Hosp. Jt. Dis.* **71**, 208–13 (2013).
9. Budu-Grajdeanu, P., Schugart, R. C., Friedman, A., Birmingham, D. J. & Rovin, B. H. Mathematical framework for human SLE Nephritis: disease dynamics and urine biomarkers. *Theor. Biol. Med. Model.* **7**, 14 (2010).
10. Chen, P. *et al.* Pharmacokinetic and Pharmacodynamic Relationship of AMG 811, An Anti-IFN- γ IgG1 Monoclonal Antibody, in Patients with Systemic Lupus Erythematosus. *Pharm. Res.* **32**, 640–653 (2014).
11. Bai, J. P. F., Fontana, R. J., Price, N. D. & Sangar, V. Systems pharmacology modeling: an approach to improving drug safety. *Biopharm. Drug Dispos.* **35**, 1–14 (2014).

12. Geerts, H., Roberts, P. & Spiros, A. Assessing the synergy between cholinomimetics and memantine as augmentation therapy in cognitive impairment in schizophrenia. A virtual human patient trial using quantitative systems pharmacology. *Front. Pharmacol.* **6**, (2015).
13. Goryanin, Igor I., Goryachev, A. *Advances in Systems Biology*. (Springer Sciences & Business Media, 2012).
14. Lu, Y., Griffen, S. C., Boulton, D. W. & Leil, T. A. Use of systems pharmacology modeling to elucidate the operating characteristics of SGLT1 and SGLT2 in renal glucose reabsorption in humans. *Front. Pharmacol.* **5**, 1–13 (2014).
15. Palmér, R. *et al.* Effects of il-1 β -blocking therapies in type 2 diabetes mellitus: A quantitative systems pharmacology modeling approach to explore underlying mechanisms. *CPT Pharmacometrics Syst. Pharmacol.* **3**, 1–8 (2014).
16. van der Graaf, P. H. & Benson, N. Systems pharmacology: bridging systems biology and pharmacokinetics-pharmacodynamics (PKPD) in drug discovery and development. *Pharm. Res.* **28**, 1460–4 (2011).
17. Wang, Y. *et al.* Multi-scale modeling of cell survival and death mediated by the p53 network: A systems pharmacology framework. *Mol. Biosyst.* **11**, 3011–3021 (2015).
18. Younesi, E. *et al.* PDON: Parkinson’s disease ontology for representation and modeling of the Parkinson’s disease knowledge domain. *Theor. Biol. Med. Model.* **12**, 1–17 (2015).
19. Ait-Oudhia, S., Straubinger, R. M. & Mager, D. E. Systems pharmacological analysis of paclitaxel-mediated tumor priming that enhances nanocarrier deposition and efficacy. *J. Pharmacol. Exp. Ther.* **344**, 103–12 (2013).
20. Benson, N. *et al.* Systems pharmacology of the nerve growth factor pathway: use of a systems biology model for the identification of key drug targets using sensitivity analysis and the integration of physiology and pharmacology. *Interface Focus* **3**, 20120071 (2013).

21. Birtwistle, M. R., Mager, D. E. & Gallo, J. M. Mechanistic vs. Empirical network models of drug action. *CPT pharmacometrics Syst. Pharmacol.* **2**, e72 (2013).
22. Chudasama, V. L., Ovacik, M. A., Abernethy, D. R. & Mager, D. E. Logic-Based and Cellular Pharmacodynamic Modeling of Bortezomib Responses in U266 Human Myeloma Cells. *J. Pharmacol. Exp. Ther.* **354**, 448–458 (2015).
23. Geerts, H., Roberts, P. & Spiros, A. A quantitative system pharmacology computer model for cognitive deficits in schizophrenia. *CPT Pharmacometrics Syst. Pharmacol.* **2**, 1–8 (2013).
24. Gulati, a, Isbister, G. K. & Duffull, S. B. Scale reduction of a systems coagulation model with an application to modeling pharmacokinetic-pharmacodynamic data. *CPT pharmacometrics Syst. Pharmacol.* **3**, e90 (2014).
25. Klinken, D. J. Enhancing the discovery and development of immunotherapies for cancer using quantitative and systems pharmacology: Interleukin-12 as a case study. *J. Immunother. Cancer* **3**, (2015).
26. Wajima, T., Isbister, G. K. & Duffull, S. B. A comprehensive model for the humoral coagulation network in humans. *Clin. Pharmacol. Ther.* **86**, 290–8 (2009).
27. Steinway, S. N., Biggs, M. B., Loughran, T. P., Papin, J. a. & Albert, R. Inference of Network Dynamics and Metabolic Interactions in the Gut Microbiome. *PLOS Comput. Biol.* **11**, e1004338 (2015).
28. Irurzun-Arana, I. *Methodology for Boolean Modeling of Biological Networks Applied to Systems Pharmacology.* (2015). at <<https://www.page-meeting.org/default.asp?abstract=3377>>
29. Poll, T. Van Der *et al.* Effects of 11-10 on Systemic Inflammatory Responses During Sublethal Primate Endotoxemia'. (1997).
30. Takahashi, N. *et al.* Impaired CD4 and CD8 effector function and decreased memory T cell populations in ICOS-deficient patients. *J. Immunol.* **182**, 5515–27 (2009).
31. Thakar, J., Pilione, M., Kirimanjeswara, G., Harvill, E. T. & Albert, R. Modeling

- systems-level regulation of host immune responses. *PLoS Comput. Biol.* **3**, e109 (2007).
32. Kauffman, S. A. Metabolic stability and epigenesis in randomly constructed genetic nets. *J. Theor. Biol.* **22**, 437–467 (1969).
 33. Saadatpour, A., Albert, I. & Albert, R. Attractor analysis of asynchronous Boolean models of signal transduction networks. *J. Theor. Biol.* **266**, 641–56 (2010).
 34. Wang, R.-S., Saadatpour, A. & Albert, R. Boolean modeling in systems biology: an overview of methodology and applications. *Phys. Biol.* **9**, 55001 (2012).
 35. Enyedy, E. J. *et al.* Fc epsilon receptor type I gamma chain replaces the deficient T cell receptor zeta chain in T cells of patients with systemic lupus erythematosus. *Arthritis Rheum.* **44**, 1114–1121 (2001).
 36. Hopfensitz, M., Müssel, C., Maucher, M. & Kestler, H. A. Attractors in Boolean networks: A tutorial. *Comput. Stat.* **28**, 19–36 (2013).
 37. Wynn, M. L., Consul, N., Merajver, S. D. & Schnell, S. Logic-based models in systems biology: a predictive and parameter-free network analysis method. *Integr. Biol.* **4**, 1323 (2012).
 38. Maimon, Oded, R. L. *Data Mining and Knowledge Discovery Handbook*. (Springer, 2005).
 39. Amsen, D., Spilianakis, C. G. & Flavell, R. a. How are T(H)1 and T(H)2 effector cells made? *Curr. Opin. Immunol.* **21**, 153–60 (2009).
 40. Auer, K. & Trachter, R. efficacy of biologics in Crohn ' s disease : a cautionary tale. 219–229 (2014).
 41. Posey Norris, S. M., Pankevich, D. E., Davis, M. & Altevogt, B. M. *Improving and Accelerating Therapeutic Development for Nervous System Disorders. The National Academic Press, Washington, D.C.* (National Academies Press, 2014). doi:10.17226/18494
 42. Fortelny, N. *et al.* Network analyses reveal pervasive functional regulation

- between proteases in the human protease web. *PLoS Biol.* **12**, e1001869 (2014).
43. Zhu, L.-J., Yang, X. & Yu, X.-Q. Anti-TNF- α Therapies in Systemic Lupus Erythematosus. *J. Biomed. Biotechnol.* **2010**, 1–8 (2010).

SUPPLEMENTARY MATERIAL

Supplementary data 1: Boolean equations Justification

$$\text{APC_MHCII} = (\text{Ag} \ \& \ \text{APC_AR})$$

The autoantigen is recognized by the receptor on the APC, it is processed and the MHCII activates to present the autoantigen to the Th0 cell¹.

$$\text{T0_TCR} = 1$$

T0_TCR has a constitutive expression, in other words, it is always activated².

$$\text{APC_B71} / \text{APC_B72} = (\text{APC_MHCII} \ \& \ \text{T0_TCR} \ \& \ \text{Ag})$$

On most APC populations, B7-2 is expressed constitutively at low levels and is rapidly upregulated, whereas B7-1 is expressed after activation³.

$$\text{T0_NOTCH3} = 1$$

Constitutive expression.

$$\text{T0_NOTCH1_2} = 1$$

Constitutive expression.

$$\text{APC_DLL} = \text{APC_AR} \ \& \ \text{Ag_DLL}$$

Members of the DLL family of Notch ligands are expressed on APC in response to microbial stimuli that promote TH1-cell induction by APC⁴.

$$\text{APC_JAGGED} = \text{APC_AR} \ \& \ \text{Ag_JAGGED}$$

Expression of Jagged family members is induced on APC by Th2 promoting microbial and pro-inflammatory stimuli⁴.

$$\text{APC_CD40} = \text{Ag_DLL} \ \& \ \text{T0_TCR} \ \& \ \text{APC_MHCII}$$

Some antigens (like LPS) can promote the expression of APC_CD40 in APC while some antigens do not⁵.

$$\begin{aligned} \mathbf{T0_CD40L} = & ((\mathbf{APC_MHCII} \ \& \ \mathbf{T0_TCR} \ \& \ \mathbf{Ag} \ \& \ \mathbf{T0_ICOS} \ \& \ \mathbf{APC_B7H2}) \ | \ ((\mathbf{T0_CD40L} \ \& \ \mathbf{Th1} \ \& \\ & (\mathbf{IL2} \ | \ \mathbf{IL12}))) \ \& \ ! \ (\cap_{i=1}^{\text{upreg}=4} \ \mathbf{T0_CD40L}^{t-i} \ \& \ \cap_{i=1}^{\text{upreg}=4} \ \mathbf{Th1}^{t-i} \ \& \ (\cap_{i=1}^{\text{upreg}=4} \ \mathbf{IL2}^{t-i} \ | \ \cap_{i=1}^{\text{upreg}=4} \ \mathbf{IL12}^{t-i}))) \\ & | \ ((\mathbf{T0_CD40L} \ \& \ \mathbf{T0_CD28} \ \& \ (\mathbf{APC_B71} \ | \ \mathbf{APC_B72})) \ (\cap_{i=1}^{\text{upreg}=4} \ \mathbf{T0_CD40L}^{t-i} \ \& \\ & \cap_{i=1}^{\text{upreg}=4} \ \mathbf{T0_CD28} \ \& \ (\cap_{i=1}^{\text{upreg}=4} \ \mathbf{APC_B71}^{t-i} \ | \ \cap_{i=1}^{\text{upreg}=4} \ \mathbf{APC_B72}^{t-i}))) \ \& \ ! \ ((\mathbf{APC_CD40} \ \& \\ & \mathbf{T0_CD40L} \ \& \ ! \ \mathbf{Th1}) \ | \ (\mathbf{T0_CD40L} \ \& \ \mathbf{IL4})) \end{aligned}$$

T0_CD40L expression on activated T cells occurs in two phases, one between 0 and 24 hours after activation and the other after 24 hours, which is regulated by the cytokines IL4 (represses T0_CD40L expression) and IL12 (sustains T0_CD40L expression). ICOS cross-linking with its receptor, APC_B7H2, results in the expression of T0_CD40L⁶. Furthermore it has been seen that IL2 induce T0_CD40L on previously activated CD4 cells⁷ and the activation of the molecules T0_CD28 and APC_B71 or APC_B72, enhance CD40L expression⁸. T0_CD40L is internalized after contact with its receptor CD40 but when Th1 is present, T0_CD40L expression is more important than its internalization⁹.

$$\begin{aligned} \mathbf{T0_ICOS} = & (\mathbf{T0_TCR} \ \& \ \mathbf{APC_MHCII} \ \& \ \mathbf{Ag}) \ | \ \mathbf{TNFa} \ | \ ((\mathbf{T0_ICOS} \ \& \ (\mathbf{T0_CD28} \ \& \ (\mathbf{APC_B71} \ | \\ & \mathbf{APC_B72}))) \ \& \ ! \ (\cap_{i=1}^{\text{upreg}=4} \ \mathbf{T0_ICOS}^{t-i} \ \& \ (\cap_{i=1}^{\text{upreg}=4} \ \mathbf{T0_CD28}^{t-i} \ \& \ (\cap_{i=1}^{\text{upreg}=4} \ \mathbf{APC_B71}^{t-i} \ | \\ & \cap_{i=1}^{\text{upreg}=4} \ \mathbf{APC_B72}^{t-i}))) \ | \ ((\mathbf{T0_ICOS} \ \& \ (\mathbf{IL12} \ | \ \mathbf{IL23})) \ \& \ ! \ \mathbf{IL4}) \ \& \ ! \ (\cap_{i=1}^{\text{upreg}=4} \ \mathbf{T0_ICOS}^{t-i} \ \& \\ & (\cap_{i=1}^{\text{upreg}=4} \ \mathbf{IL12}^{t-i} \ | \ \cap_{i=1}^{\text{upreg}=4} \ \mathbf{IL23}^{t-i}))) \end{aligned}$$

ICOS is not expressed constitutively on naive T cells but is induced rapidly on T cells after TCR engagement^{3,6}. Also TNFa can promote T0_ICOS expression on T cells when stimulation via TCR/CD3 complex is weak¹⁰. The activation of the nodes T0_CD28 and APC_B71 or APC_B72 upregulates T0_ICOS expression^{11,12}. IL-12 and IL-23 enhance ICOS expression on activated Th cells, but IL4 reduce the upregulatory effects of these interleukins¹³.

$$\mathbf{APC_B7H2} = (\mathbf{T0_ICOS} \ \& \ \mathbf{IFNG}) \ \& \ ! \ (\mathbf{APC_B7H2} \ \& \ \mathbf{IL10})$$

IFNG increased APC_B7H2 expression after incubation for 24 hours¹⁴. APC_B7H2 expression may be negatively regulated by IL-10¹⁵.

$$\mathbf{T0_CD44} = \mathbf{T0_ACT}$$

Th0 activation, allows T0_CD44 recognizes and binds hyaluronan, activating the node T0_CD44¹⁶.

$$\mathbf{T0_CD28} = ! \ (\cap_{i=1}^{\text{THR_CTLA4_max_CD28}=2} \ \mathbf{T0_CTLA4}^{t-i} \ | \ (\mathbf{T0_CD28} \ \& \ \cap_{i=1}^{\text{THR_TNFa_max}=3} \ \mathbf{TNFa}^{t-i}))$$

CD28 is constitutively expressed on the surface of T cells, whereas CTLA-4 expression is rapidly upregulated following T cell activation^{8,12}. CTLA-4 is then capable of directly competing with CD28 for binding of B7. CTLA-4 may also exert a direct negative effect on CD28 signaling, mediated by the binding of the phosphatases PP2A and SHP-2¹⁷. TNFa downregulates CD28 expression when the levels of the TNFa are high¹⁸.

$$\mathbf{T0_CTLA4} = \cap_{i=1}^{\text{THR_T0_ACT_max_CTLA4}=2} \ \mathbf{T0_ACT}^{t-i}$$

T0_CTLA4 expression is rapidly upregulated following T cell activation, but it is located in the intracellular compartment, so some time is required to express this molecule in the T cell surface^{12,17,19}.

$$\mathbf{T0_OX40} = \cap_{i=1}^{THR_T0_ACT_max_OX40=2} \mathbf{T0_ACT}^{t-i} \mid \mathbf{TNFa} \mid (\mathbf{T0_OX40} \ \& \ \mathbf{IL2} \ \& \ ! (\cap_{i=1}^{upreg=4} \mathbf{T0_OX40}^{t-i} \ \& \ \cap_{i=1}^{upreg=4} \mathbf{IL2}^{t-i})) \mid ((\mathbf{T0_OX40} \ \& \ \mathbf{T0_CD28} \ \& \ (\mathbf{APC_B71} \ \mid \ \mathbf{APC_B72})) \ \& \ ! (\cap_{i=1}^{upreg=4} \mathbf{T0_OX40}^{t-i} \ \& \ \cap_{i=1}^{upreg=4} \mathbf{T0_CD28}^{t-i} \ \& \ (\cap_{i=1}^{upreg=4} \mathbf{APC_B71}^{t-i} \ \mid \ \cap_{i=1}^{upreg=4} \mathbf{APC_B72}^{t-i})))$$

The optimal expression of T0_OX40 occurs 24-48 hours after the activation of naïve T cells and requires strong TCR ligation, CD28 engagement and IL-2/IL-2R signaling²⁰. On the other hand, exogenous TNF can promote the expression of T0_OX40, on T cells when stimulation via the TCR/CD3 complex is relatively weak¹⁰.

$$\mathbf{APC_OX40L} = \mathbf{APC_CD40} \ \& \ \mathbf{T0_CD40L} \ \& \ \mathbf{APC_MHCII}$$

APC_OX40L is not constitutively expressed but can be induced on professional antigen- presenting cells (APC) following antigen recognition by APC_MHCII²¹ and also, the expression of OX40L is dependent upon signaling through CD40²².

$$\mathbf{APC_B7H1} = (\cap_{i=1}^{THR_T0_ACT_max_B7H1=2} \mathbf{T0_ACT}^{t-i} \mid \mathbf{IFNG} \ \mid \ (\mathbf{APC_B7H1} \ \& \ \mathbf{TNFa} \ \& \ ! (\cap_{i=1}^{upreg=4} \mathbf{APC_B7H1}^{t-i} \ \& \ \cap_{i=1}^{upreg=4} \mathbf{TNFa}^{t-i})) \mid (\mathbf{APC_B7H1} \ \& \ \mathbf{IL12} \ \& \ ! (\cap_{i=1}^{upreg=4} \mathbf{APC_B7H1}^{t-i} \ \& \ \cap_{i=1}^{upreg=4} \mathbf{IL12}^{t-i})) \mid (\mathbf{APC_B7H1} \ \& \ \mathbf{IL4} \ \& \ ! (\cap_{i=1}^{upreg=4} \mathbf{APC_B7H1}^{t-i} \ \& \ \cap_{i=1}^{upreg=4} \mathbf{IL4}^{t-i}))) \ \& \ ! (\mathbf{APC_B7H1} \ \& \ \mathbf{TGFb})$$

APC_B7H1 is activated after activation²³, and is rapidly activated upon IFNG treatment²⁴. TNF-a has been associated with increased APC_B7H1 expression, while TGF-b suppressed induction of the APC_B7H1 in healthy control cells²⁵. On the other hand, the addition of IL12 or IL4 led to up-regulate APC_B7H1 ligand²⁶.

$$\mathbf{APC_B7DC} = \cap_{i=1}^{THR_T0_ACT_max_B7DC=2} \mathbf{T0_ACT}^{t-i} \ \mid \ (\mathbf{APC_B7DC} \ \& \ \mathbf{GMCSF} \ \& \ ! (\cap_{i=1}^{upreg=4} \mathbf{APC_B7DC}^{t-i} \ \& \ \cap_{i=1}^{upreg=4} \mathbf{GMCSF}^{t-i})) \mid (\mathbf{APC_B7DC} \ \& \ \mathbf{IL12} \ \& \ ! (\cap_{i=1}^{upreg=4} \mathbf{APC_B7DC}^{t-i} \ \& \ \cap_{i=1}^{upreg=4} \mathbf{IL12}^{t-i})) \mid (\mathbf{APC_B7DC} \ \& \ \mathbf{IL4} \ \& \ ! (\cap_{i=1}^{upreg=4} \mathbf{APC_B7DC}^{t-i} \ \& \ \cap_{i=1}^{upreg=4} \mathbf{IL4}^{t-i})) \mid (\mathbf{APC_B7DC} \ \& \ \mathbf{IL13} \ \& \ ! (\cap_{i=1}^{upreg=4} \mathbf{APC_B7DC}^{t-i} \ \& \ \cap_{i=1}^{upreg=4} \mathbf{IL13}^{t-i}))$$

The interleukins IL-4 and IL-13 upregulate APC_B7DC²⁷; In other study, the addition of IL-12 or IL-4 led to further up-regulation of APC_B7DC²⁶.

$$\mathbf{T0_PD1} = \cap_{i=1}^{THR_T0_ACT_max_PD1=2} \mathbf{T0_PD1}^{t-i} \ \mid \ (\mathbf{T0_PD1} \ \& \ \mathbf{TNFa} \ \& \ ! (\cap_{i=1}^{upreg=4} \mathbf{T0_PD1}^{t-i} \ \& \ \cap_{i=1}^{upreg=4} \mathbf{TNFa}^{t-i}))$$

PD-1 is highly upregulated following TCR stimulation^{19,23}. Exogenous TNF can promote the expression of T0_PD-1 on T cells when stimulation via the TCR/CD3 complex is relatively weak¹⁰.

$$\mathbf{T0_CD27} = \mathbf{T0_ACT} \ \& \ ! \cap_{i=1}^{THR_T0_ACT_max_CD27=4} \mathbf{T0_CD27}^{t-i}$$

T cell activation via TCR/CD3 complex, induces T0_CD27 expression²⁸. However, in humans, T0_CD27 expression distinguishes between naïve and effector/memory stages of T cells; The differentiation into effector T cells is accompanied by loss of T0_CD27 expression²⁹.

T0_ZAP70 = APC_MHCII & T0_TCR & T0_CD3Z

Once the antigen is present to the T cell by the APC_MHCII, T0_TCR becomes activated and the T0_CD3ζ chain recruits the zeta associated protein of 70 kDa (T0_ZAP70) kinase³⁰.

T0_SYK = APC_MHCII & Ag & T0_TCR & T0_FcRG

Upon stimulation of SLE T cells, the T0_FcRG chain recruits the spleen tyrosine kinase (T0_Syk) instead of the normally recruited ZAP70³⁰.

T0_cfos = T0_ZAP70

When T0_ZAP70 is activated, then it phosphorylates other molecules, thus transmitting the signal downstream into three distinct pathways. One of these pathways is Ras-MAPK cascade, which induces and activates T0_cfos protein, a component of the transcription factor Activated protein 1 (AP1)³⁰.

T0_CD3Z = (APC_MHCII & Ag & T0_TCR & T0_CD45) &! T0_FcRG

Once APC_MHCII and T0_TCR are activated by the presence of the antigen, T0_CD45 is the responsible to remove inhibitory phosphates from the Src family lymphocyte kinase (Lck), and the T0_CD3Z chain is phosphorylated, resulting in their activation³⁰.

T0_CA2 = T0_ZAP70 | T0_SYK

When T0_ZAP70 is activated, then it phosphorylates other molecules, thus transmitting the signal downstream into three distinct pathways. After phosphorylation of some molecules, inositol trisphosphate leads to opening of the calcium channels, increased intracellular calcium concentrations and activation of the phosphatase calcineurin, which dephosphorylates and activates the transcription factor Nuclear factor of activated T cells (NFAT), one of the pathways to transmit the signal downstream³⁰.

T0_FcRG = APC_MHCII & Ag & T0_TCR & Lupus

SLE T cells display a unique rewiring of the surface T0_TCR-CD3 complex wherein expression of the T0_CD3Z chain is decreased in cells from a majority of patients. The lack of the T0_CD3Z chain in the T0_TCR-CD3 complex is structurally and functionally replaced by the homologous Fc receptor gamma (T0_FcRG) chain³⁰.

T0_P65 = T0_ZAP70

When T0_ZAP70 is activated, then it phosphorylates other molecules, thus transmitting the signal downstream into three distinct pathways. Other pathway is the NFκB pathway, which after some signals activates; NF-κB is a heterodimer of the p65/p50 subunits³⁰.

T0_CD45 = 1

Constitutive expression.

$$\begin{aligned} \mathbf{T0_ACT} = & ((\mathbf{APC_MHCII} \ \& \ \mathbf{T0_TCR} \ \& \ (\mathbf{T0_CD28} \ \& \ (\mathbf{APC_B71} \ | \ \mathbf{APC_B72}))) \ | \ (\mathbf{T0_ACT} \ \& \ \\ \mathbf{T0_ICOS} \ \& \ \mathbf{APC_B7H2} \ \& \ ! \ (\cap_{i=1}^{upreg=4} \ \mathbf{T0_ACT}^{t-i} \ \& \ \cap_{i=1}^{upreg=4} \ \mathbf{T0_ICOS} \ \& \ \cap_{i=1}^{upreg=4} \ \mathbf{APC_B7H2}^{t-i})) \\ | \ & (\mathbf{T0_ACT} \ \& \ \mathbf{T0_CD40L} \ \& \ \mathbf{APC_CD40} \ \& \ ! \ (\cap_{i=1}^{upreg=4} \ \mathbf{T0_ACT}^{t-i} \ \& \ \cap_{i=1}^{upreg=4} \ \mathbf{T0_CD40L}^{t-i} \ \& \ \\ \cap_{i=1}^{upreg=4} \ & \ \mathbf{APC_CD40}^{t-i})) \ | \ (\mathbf{T0_ACT} \ \& \ \mathbf{T0_OX40} \ \& \ \mathbf{APC_OX40L} \ \& \ ! \ (\cap_{i=1}^{upreg=4} \ \mathbf{T0_ACT}^{t-i} \ \& \ \\ \cap_{i=1}^{upreg=4} \ & \ \mathbf{T0_OX40}^{t-i} \ \& \ \cap_{i=1}^{upreg=4} \ \mathbf{APC_OX40L}^{t-i})) \ \& \ ! \ ((\mathbf{T0_CTLA4} \ \& \ (\mathbf{APC_B71} \ | \ \mathbf{APC_B72})) \ | \ \\ (\mathbf{T0_PD1} \ \& \ & \ (\mathbf{APC_B7DC} \ | \ \mathbf{APC_B7H1}))) \end{aligned}$$

T0_ACT needs two signals to activate. The first one is provided by the interaction of the APC_MHCII with T0_TCR and the second by the interaction of the T0_CD28 with APC_B71 or APC_B72. This signal augments and sustains a T cell response^{3,31}. Other molecules enhance T0_ACT expression, like the interaction of T0_CD40L with APC_CD40³², T0_OX40 with APC_OX40L³³ and T0_ICOS with APC_B7H2^{3,34}. However the interaction of T0_CTLA4 with APC_B71 or APC_B72^{3,27,35} and the interaction of T0_PD1 with APC_B7H1 or APC_B7DC^{24,36}, deliver a negative signal, inhibiting T0_ACT.

$$\mathbf{Th1} = ((\mathbf{T0_ACT} \ \& \ \mathbf{APC_CD40} \ \& \ \mathbf{T0_CD40L} \ \& \ \mathbf{IL12} \ \& \ \mathbf{IFNG}) \ | \ (\mathbf{Th1} \ \& \ \mathbf{T0_CD44} \ \& \ ! \ (\cap_{i=1}^{upreg=4} \ \mathbf{Th1}^{t-i} \ \& \ \cap_{i=1}^{upreg=4} \ \mathbf{T0_CD44}^{t-i}))) \ \& \ ! \ (\mathbf{Th1} \ \& \ \mathbf{Treg}) \ \& \ ! \ \mathbf{Th2} \ \& \ ! \ \mathbf{TGFb}$$

T0_CD40L is necessary to Th1 development, this could be because the lack of T0_CD40L fail to produce IL12 cytokine from the APC, and IL12 and IFNG are required for Th1 differentiation^{4,32}. Furthermore Guan et al. found that in CD44^{-/-} mice, Th1 immune response was down-regulated³⁷, so CD44 has an influence in Th1 differentiation.

Contrary Treg have an inhibitory effect on Th1 proliferation, reducing the magnitude of the immune response³⁸ and on the other hand Th2 cell differentiation and Th2 cytokine secretion inhibits Th1 development³⁹; TGFb also blocks Th1 differentiation in mice⁴⁰. Some of these studies are performed in mice, but it has been found that differentiation of Th1 and Th2 cells follows similar rules in humans as in mice⁴¹.

$$\mathbf{Th2} = (\mathbf{T0_ACT} \ \& \ (\mathbf{T0_CD28} \ \& \ (\mathbf{APC_B71} \ | \ \mathbf{APC_B72})) \ \& \ \mathbf{IL4}) \ \& \ ! \ (\mathbf{Th2} \ \& \ (\mathbf{Treg} \ | \ \mathbf{T0_CD44})) \ \& \ ! \ \mathbf{IL12} \ \& \ ! \ \mathbf{TGFb}$$

It has been seen that T0_CD28 is necessary for Th2 development³²; also IL4 promotes Th2 differentiation⁴. As same as in the Th1, Tregs inhibit the proliferation of the Th2 cells, reducing the magnitude of the immune response, moreover in the case of the Th2 cell, Tregs also enhance its apoptosis³⁸, but in this case, Guan et al. found that in CD44^{-/-} mice, Th2 immune response was up-regulated³⁷, so CD44 has a negative influence in Th1 differentiation. Furthermore, IL-12³⁹ and TGFb³⁹ inhibits Th2 development. Some of these studies are performed in mice, but it has been found that differentiation of Th1 and Th2 cells follows similar rules in humans as in mice⁴¹.

$$\begin{aligned} \mathbf{Th17} = & (((\mathbf{T0_ACT} \ \& \ \mathbf{TGFb} \ \& \ (\mathbf{IL21} \ | \ \mathbf{IL6} \ | \ \mathbf{IL23})) \ | \ (\mathbf{Th17} \ \& \ \mathbf{T0_ICOS} \ \& \ \mathbf{APC_B7H2} \ \& \ ! \ \\ (\cap_{i=1}^{upreg=4} \ & \ \mathbf{Th17}^{t-i} \ \& \ \cap_{i=1}^{upreg=4} \ \mathbf{T0_ICOS}^{t-i} \ \& \ \cap_{i=1}^{upreg=4} \ \mathbf{APC_B7H2}^{t-i})) \ | \ (\mathbf{Th17} \ \& \ \mathbf{T0_CD40L} \ \& \ \\ \mathbf{APC_CD40} \ \& \ ! \ & \ (\cap_{i=1}^{upreg=4} \ \mathbf{Th17}^{t-i} \ \& \ \cap_{i=1}^{upreg=4} \ \mathbf{T0_CD40L}^{t-i} \ \& \ \cap_{i=1}^{upreg=4} \ \mathbf{APC_CD40}^{t-i}))) \ \& \ ! \ (\mathbf{Treg} \\ \& \ ! \ & \ (\mathbf{IL21} \ | \ \mathbf{IL6}))) \ \& \ ! \ (\mathbf{IL12} \ | \ \mathbf{IFNG} \ | \ \mathbf{IL4}) \end{aligned}$$

Once Th0 is activated, in the presence of TGF- β plus IL-6 or IL-21 or IL23, the Treg developmental pathway is abrogated, and instead T cells develop into Th17 cells^{41,42}. Gao et al.¹⁵ study demonstrates that T0_ICOS-APC_B7H2 interaction is critical for Th17. Also development of Th17 critically depends on APC_CD40-T0_CD40L cross-talk⁴³. However IL-12, IFN- γ , and IL-4 can inhibit Th17 differentiation in humans⁴¹.

$$\mathbf{Tfh} = (\mathbf{T0_ACT \& IL12 \& IL21 \& IL6}) \mid ((\mathbf{Tfh \& APC_CD40 \& T0_CD40L \& T0_ICOS \& APC_B7H2}) \&! (\cap_{i=1}^{upreg=4} \mathbf{Tfh}^{t-i} \& \cap_{i=1}^{upreg=4} \mathbf{APC_CD40}^{t-i} \& \cap_{i=1}^{upreg=4} \mathbf{T0_CD40L}^{t-i} \& \cap_{i=1}^{upreg=4} \mathbf{T0_ICOS}^{t-i} \& \cap_{i=1}^{upreg=4} \mathbf{APC_B7H2}^{t-i}))$$

The cytokines IL21, IL6 and IL12 are necessary for Tfh generation^{44,45}. Also, Bossaller et al.⁴⁶ have found that human T0_ICOS and T0_CD40L deficiency results in a significant reduction of circulating Tfh cells, so these costimulation molecules upregulates Tfh expression.

$$\mathbf{Treg} = ((\mathbf{T0_ACT \& TGFb}) \mid (\mathbf{Treg \& T0_PD1 \& APC_B7H1 \&! (\cap_{i=1}^{upreg=4} \mathbf{Treg}^{t-i} \& \cap_{i=1}^{upreg=4} \mathbf{T0_PD1}^{t-i} \& \cap_{i=1}^{upreg=4} \mathbf{APC_B7H1}^{t-i}))) \&! (\mathbf{IL6 \mid IL21}))$$

Once Th0 is activated and the cytokine TGFb is present, Th0 differentiates to Treg⁴⁷. Furthermore, Yao et al. found that the cross-linking between APC_B7H1 with T0_PD1 enhances and sustains Treg expression⁴⁸. However IL6, which is a pro-inflammatory cytokine, inhibits Treg differentiation⁴⁹. Also the cytokine IL21 can inhibit its differentiation⁵⁰.

$$\mathbf{IL2} = \mathbf{T0_ACT \& T0_cfos \& T0_P65 \& T0_CA2 \&! (T0_CTLA4 \& (APC_B71 \mid APC_B72))}$$

T0_P65, T0_cfos and T0_CA2 are components involved in the routes which mediate IL2 transcription³⁰. T0_CTLA4 inhibits IL2 synthesis and progression through the cell cycle and terminates T cell responses³.

$$\mathbf{IL4} = (\mathbf{Th2} \mid (\mathbf{T0_ACT \& APC_JAGGED \& T0_NOTCH1_2}) \mid ((\mathbf{IL4 \& T0_ICOS \& APC_B7H2}) \&! (\cap_{i=1}^{upreg=4} \mathbf{IL4}^{t-i} \& \cap_{i=1}^{upreg=4} \mathbf{T0_ICOS}^{t-i} \& \cap_{i=1}^{upreg=4} \mathbf{APC_B7H2}^{t-i})) \mid ((\mathbf{IL4 \& APC_OX40L \& T0_OX40}) \&! (\cap_{i=1}^{upreg=4} \mathbf{IL4}^{t-i} \& \cap_{i=1}^{upreg=4} \mathbf{APC_OX40L}^{t-i} \& \cap_{i=1}^{upreg=4} \mathbf{T0_OX40}^{t-i})) \mid (\mathbf{IL4 \& T0_CD27} \&! (\cap_{i=1}^{upreg=4} \mathbf{IL4}^{t-i} \& \cap_{i=1}^{upreg=4} \mathbf{T0_CD27}^{t-i}))) \&! (\mathbf{IL4 \& (T0_PD1 \& APC_B7DC)})$$

Th2-cell lineage produces IL4^{4,6}. Human ICOS deficiency significantly reduces the production of cytokine IL4⁵¹. Also T0_OX40 ligation with its ligand (APC_OX40L) increases four times the expression of IL-4⁵² and IL-4 expression is increased upon CD27 costimulation⁵³. However, in the presence of APC_B7DC IL4 production is markedly reduced³⁶.

$$\mathbf{IL6} = ((\mathbf{T0_CD28 \& (APC_B71 \mid APC_B72)}) \mid (\cap_{i=1}^{THR_APC_CD40_max_IL6=2} \mathbf{APC_CD40}^{t-i} \& \mathbf{T0_CD40L}) \mid (\mathbf{TGFb \& IL23})) \&! (\mathbf{IL4 \mid IL10})$$

IL6 has a dose-dependent effect in response to T0_CD28⁵⁴. It has been seen that APC_CD40 acts to trigger IL6 release from dendritic cells (DC)^{43,55}, on the other hand it has found seen that IL-6 production was mostly dependent on TGF-b and IL-23⁵⁶. However IL4 and IL10 cytokines suppressed IL6 secretion⁵⁷⁻⁵⁹.

$$\mathbf{IL10} = (\mathbf{Treg} \mid \mathbf{Th2} \mid (\mathbf{IL10 \& T0_ICOS \& APC_B7H2} \&! (\cap_{i=1}^{upreg=4} \mathbf{IL10}^{t-i} \& \cap_{i=1}^{upreg=4} \mathbf{T0_ICOS}^{t-i} \& \cap_{i=1}^{upreg=4} \mathbf{APC_B7H2}^{t-i})) \mid (\mathbf{IL10 \& TNFa} \&! (\cap_{i=1}^{upreg=4} \mathbf{IL10}^{t-i} \& \cap_{i=1}^{upreg=4} \mathbf{TNFa}^{t-i})) \mid (\mathbf{IL10 \& IL2} \&! (\cap_{i=1}^{upreg=4} \mathbf{IL10}^{t-i} \& \cap_{i=1}^{upreg=4} \mathbf{IL2}^{t-i}))) \&! (\mathbf{T0_OX40 \& APC_OX40L}) \&! (\mathbf{IL10 \& (T0_PD1 \& (APC_B7H1 \mid APC_B7DC))})$$

Although Treg cells are the main producers of IL10 it has been seen that it can be produced by Th2 cells⁶⁰. T0_ICOS activation upregulates IL10 production⁵¹, TNFa⁶¹ and IL2⁶² also induce the secretion of IL10. On the other hand OX40L inhibits its generation⁶³ and in the presence of APC_B7H1 or APC_B7DC the secretion of IL10 is decreased^{24,36,64}.

IL12 = ((APC_MHCII & T0_TCR & APC_DLL & T0_NOTCH3 & APC_CD40 & T0_CD40L) | (IL12 & T0_ICOS & ! (∩_{i=1}^{upreg=4} IL12^{t-i} & ∩_{i=1}^{upreg=4} T0_ICOS^{t-i}))) & ! IL10

Certain antigens, like LPS, promotes IL12 enhance⁶⁵. Furthermore IL-12 has been found to be secreted by DC upon antigen-specific interaction with T cells. The antigen-driven induction of IL-12 secretion requires interaction via peptide/ MHC class II-TCR and APC_CD40- T0_CD40 ligand molecules⁶⁶ and also others researchers have found that APC_CD40 and T0_CD40L interaction is essential for IL12 production by dendritic cells^{32,67,68}. T0_ICOS enhance the induction of IL12⁵¹ (Takahashi et al., 2009) However, Ria and et al. found that IL-10 produced by Th2 cells appears to be solely responsible for the inhibition of Th1-induced IL-12 secretion⁶⁶.

IL13 = Th2 | (T0_ACT & Th1 & IL18)

Th2 cell lineage produces IL13 cytokine^{4,6}, however, when Th1 cells are stimulated with IL18, they produce IL-13⁶⁹.

IL17 = ((Th17 & IL6 & TGFb & IL23) | (IL17 & T0_ICOS & APC_B7H2 & ! (∩_{i=1}^{upreg=4} IL17^{t-i} & ∩_{i=1}^{upreg=4} T0_ICOS^{t-i} & ∩_{i=1}^{upreg=4} APC_B7H2^{t-i}))) & ! (IL17 & T0_CD27)

Th17 lineage cells produces IL17 cytokine⁴² together with IL6, TGFb and IL23⁵⁶. Moreover, Takahashi and et al.⁵¹ found that in T0_ICOS deficient patients, the IL17 secretion was impaired. On the other hand, IL17 expression is dramatically reduced in Th17 upon T0_CD27 costimulation⁷⁰.

IL18 = 1

Constitutive expression.

IL21 = Tfh | Th17 | ((T0_ACT & IL6) & ! IL4 & ! IFNG & ! TGFb) | (IL21 & T0_CD27 & ! (∩_{i=1}^{upreg=4} IL21^{t-i} & ∩_{i=1}^{upreg=4} T0_CD27^{t-i})))

Tfh and Th17 cells secrete IL21 cytokine^{42,44}. When Suto et al.⁷¹ stimulated naive CD4+ T cells with anti-CD3mAb/anti-CD28mAb in the presence of IL6, anti-IL4 mAb, and anti-IFNG mAb with or without TGFb, they found that IL6 together with the blocking antibodies to IL-4 and IFNG strongly induced the development of IL21 – producing CD4 + T cells; Diehl et al.⁷² also show that IL6 increased IL21 production by human CD4+ T cells. On the other hand T0_CD27 costimulation increased IL21 expression⁵³.

IL23 = Ag_DLL

Some pathogens and Toll-like receptor agonists, like LPS, CpG and Polyl:C, enhance expression of the p40, p35, and p19 subunits, resulting in the release of bioactive IL-23⁷³.

IL27 = Ag_DLL

Some pathogens and Toll-like receptor agonists, like LPS, CpG and Polyl:C, enhance expression of the p40, p35, and p19 subunits, resulting in the release of bioactive IL-27; The production of this cytokine can be further augmented by T cell CD40L/CD40 interactions that drive potent positive feedback responses for DC activation⁷³.

TNFa = (((Ag_DLL & IFNG) | IL2 | GMCSF | TGFb) | ((TNFa & T0_ICOS & APC_B7H2) &! (∩_{i=1}^{upreg=4} TNFa^{t-i} & ∩_{i=1}^{upreg=4} T0_ICOS^{t-i} & ∩_{i=1}^{upreg=4} APC_B7H2^{t-i}))) &! IL10 &! (TNFa & IL4)

IFNG augments TNFa production in response to LPS (antigen) stimulation⁶¹. Also IL-2, GMCSF and TGFb have been reported to induce TNF release^{61,74}. Human ICOS deficiency significantly reduces the expression of cytokine TNFa⁵¹. However, treatment with IL10 causes significant reductions in TNFa⁶⁵. Furthermore its production is attenuated by IL-4⁷⁴.

TGFb = Treg

TGFb is produced by Treg cells⁴² and other multiple lineages of leukocytes and stromal cells, but they are not included on the network.

IFNG = ((T0_ACT | Th1) | (IFNG & T0_CD40L & APC_CD40 &! (∩_{i=1}^{upreg=4} IFNG^{t-i} & ∩_{i=1}^{upreg=4} T0_CD40L^{t-i} & ∩_{i=1}^{upreg=4} APC_CD40^{t-i})) | (IFNG & T0_ICOS & APC_B7H2 &! (∩_{i=1}^{upreg=4} IFNG^{t-i} & ∩_{i=1}^{upreg=4} T0_ICOS^{t-i} & ∩_{i=1}^{upreg=4} APC_B7H2^{t-i})) | (IFNG & IL12 &! (∩_{i=1}^{upreg=4} IFNG^{t-i} & ∩_{i=1}^{upreg=4} IL12^{t-i}))) &! Th2 &! IL10 &! (IFNG & T0_PD1 & (APC_B7H1 | APC_B7DC))

The IFNG genes are transcribed in naïve T cells within 3 to 24 hours after initial activation⁴. Also, Th1 cells produce IFNG⁶. Howland et al. found that in the absence of T0_CD40L, T cells had a selective defect in IFNG production, but the addition of IL-12 enhanced IFNG production³² also, Takahashi et al. showed T0_ICOS expression enhances IFNG expression⁵¹. On the other hand, Th2 inhibits IFN-g secretion⁷⁵ and in the presence of T0_PD1, APC_B7H1 and APC_B7DC the secretion of IFNG is decreased^{23,24,36,64}.

GMCSF = (Th1 | (GMCSF & IL12 &! (∩_{i=1}^{upreg=4} GMCSF^{t-i} & ∩_{i=1}^{upreg=4} IL12^{t-i}))) &! (IL27) &! (GMCSF & IL6)

GMCSF is promoted by the Th1 cells. Noster et al.⁷⁶ have found that the addition of IL12 enhances significantly GMCSF production; while other interleukins like IL27 or IL6 inhibits or downregulate GMCSF expression respectively in humans

Supplementary Methods

R framework

In order to minimize the effort to implement models, run simulations and analyze the results, we developed a framework consisting on a series of R and C++ scripts to perform Boolean modeling of Systems Biology or Pharmacology networks. The main features of this framework are: a parallelized simulation algorithm, an attractor search algorithm, a perturbation analysis method and its graphical representation and the clustering of the perturbation analysis result. To facilitate execution from R Studio because of its user-friendly interface, we used the Rcpp R package to communicate from R to the C++ algorithm and get the result back to the R environment again. The algorithms written in R use additional R packages like data.table and corrplot (Wie, 2013).

The framework is called AutoImmune Targeting On R (AITOR), although it can be implemented for any other disease or biological network. Another manuscript with all the details about the AITOR framework is being prepared for publication and it will be soon available.

Attractor analysis

The attractor search was computed via exhaustive repetitions of the simulation algorithm. Because of the large-scale network, the estimation of the attractor is very slow if computed in the R environment. We coded the simulation algorithm on C++ in order to increase the simulation speed in 60 fold. To guarantee that all attractors of a network with n nodes are found, it is necessary to test all the 2^n possible states as initial states. Due to the exponential relationship, this search becomes unmanageable at around 30 nodes (Hopfensitz et al., 2012). Fortunately, we were not interested in testing all the possible start states, as we defined a few possible initial conditions for our SLE networks (Table 3).

To obtain all the attractor states a great computing effort is required because some of these states very rarely occur. However, we found that the activation probabilities of the nodes almost did not change if those “unusual” states were ignored, suggesting that these rare states can be excluded from the analysis to decrease the number of repetitions needed for the attractor search algorithm. Therefore, the 8 initial conditions of the SLE

network were evolved for 5000 time steps in asynchronous mode and repeated 40 times in order to obtain a satisfactory approximation of the activation probabilities of the system nodes.

Hierarchical clustering

The result of the univariate perturbation analysis is a square matrix in which the number of rows and columns is equal to the number of nodes in the network. The value in each cell of the matrix corresponds to the Perturbation Index (PI) of the “row node” under a perturbation from the “column node”. We transformed the resulting matrix to store only 5 possible values: a value of 2 represents PIs greater than 2, a 1 indicates PIs between 1.25 and 2, the 0 substitutes PIs close to 1, the -1 indicates PIs between 0.5 and 0.8 and the -2 PIs smaller than 0.5. Values of 1 and 2 are used to represent perturbations that cause a higher activation of the nodes in the system. On the contrary, values of -1 and -2 indicate lower activations of the nodes.

To group the system perturbations according to the lupus-like alterations that they provoked the next steps were followed: i) A new matrix was created in which the number of rows and columns was equal to the number of nodes in the network (52). ii) For each node, we listed all the alterations that they provoked on the 23 nodes that have been reported as altered in SLE (“SLE like” alterations), that is, we summed the number of 2,1,-1 and -2 that each node provokes. iii) The value in each cell of the matrix was filled with the ratio between the number of “SLE like” alterations that the “column” and “row” node shared over the number of “SLE like” alterations provoked by the “row” perturbation. For example, if a perturbation on node A provoked 4 “SLE like” alterations, a perturbation in node B led to 5 “SLE like” alterations and both perturbation shared 3 of those “SLE like” alterations, a value of $\frac{3}{4}=0.75$ was stored in the row A column B position of the matrix, while a value of $\frac{3}{5}=0.6$ was stored in the row B column A position. The diagonal of this matrix is a vector of 1s. iv) Rows and columns of nodes which perturbations did not provoke any “SLE like” alteration were removed from the matrix. v) Hierarchical clustering analysis was applied over the outcome matrix of the previous step.

We used the Euclidean metric to measure distance between the alterations that each node shared with the rest of the nodes of the network. For the previous example, the distance between the alterations that node A and B shared is:

$D(A, B) = \sqrt{\sum_{i=1}^n (B_i - A_i)^2} = \sqrt{(1 - 0.6)^2 + (0.75 - 1)^2} = 0.4717$, where n is the number of nodes in the network (2 for this example).

All these operations can be computed in the R framework automatically with the help of the R scripts that the group developed.

Supplementary Table 1

Supplementary table 1. Altered nodes in SLE

Node	Alteration in SLE patients	Reference
APC_MHCII	Upregulated	77
APC_B7H1 (PDL1)	Downregulated	25,78
APC_OX40L	Upregulated	33,79
T0_CTLA4	Upregulated	80
T0_CD44	Upregulated	81
T0_PD1	Upregulated	82
T0_ICOS	Upregulated	83
T0_OX40	Upregulated	63,84
T0_CD3Z	Downregulated	30,85
T0_FcRG	Upregulated	30,85,86
T0_SYK	Upregulated	30
T0_cfos	Downregulated	30,87
T0_CA2	Upregulated	30
T0_P65	Downregulated	30,88
IL2	Downregulated	30
IL4	Downregulated	89
IL10	Upregulated	90
IL6	Upregulated	91
IFNG	Upregulated	92,93
TNFa	Upregulated	25
IL23	Upregulated	94
IL17	Upregulated	95
Treg	Downregulated	96

Supplementary Table 2

Supplementary table 2. Node localization, type and function.

Name	Localization	Type	Function	Reference
Antigen			Autoantigen in SLE.	97
Antigen receptor	APC	Surface molecule	Antigen receptor in the Antigen Presenting Cell.	
MHCII	APC	Surface molecule	The main function of MHCII (major histocompatibility complex class II) molecule is to present processed antigens to CD4 (+) T-lymphocytes. It is critical for the initiation of the antigen-specific immune response.	98
B71	APC	Surface molecule	B71 (CD80) is a B7 family member that has dual specificity for the stimulatory receptor CD28 and the inhibitory receptor CTLA-4.	3
B72	APC	Surface molecule	B72 (CD86) is a B7 family member, that has dual specificity for the stimulatory receptor CD28 and the inhibitory receptor CTLA-4.	3
DLL	APC	Surface molecule	DLL is expressed on APC in response to bacteria, viruses and TLR-ligands that promote TH1-cell induction by APC.	4
JAGGED	APC	Surface molecule	JAGGED is expressed on APC in response to parasites and allergens that promote TH2-cell induction by APC.	4
CD40	APC	Surface molecule	CD40 is a type I transmembrane protein of the TNFR superfamily. CD40-CD40L engagement on the surface of DCs promotes their cytokine production, the induction of costimulatory molecules on their surface, and facilitates the cross-presentation of antigen.	99
B7H1	APC	Surface molecule	B7H1 (Programmed death-ligand 1) and B7DC (Programmed death-ligand 2) strongly inhibit both T-cell proliferation and cytokine production even in the presence of strong B7-CD28 signals.	3
B7DC	APC	Surface molecule	B7H1 (Programmed death-ligand 1) and B7DC (Programmed death-ligand 2) strongly inhibit both T-cell proliferation and cytokine production even in the presence of strong B7-CD28 signals.	3
B7H2	APC	Surface molecule	B7H2 (ICOS ligand) is a member of the CD28/CD152 receptor family. ICOS-B7H2 engagement, enhances T cell proliferation, secretion of cytokines, and up-regulation of cell surface molecules.	51
OX40L	APC	Surface molecule	OX40L (CD252) is a member of the TNFR/TNF superfamily and is expressed on activated CD4. It regulates cytokine production from T cells and modulates cytokine receptor signaling.	21
TCR	T cell	Surface molecule	TCR (T cell receptor) recognizes the antigen presented by the MHCII molecule.	100
T0_ACT		Th0 activated	Th0 activated.	

Supplementary Table 2 (continued)

NOTCH1_2	T cell	Surface molecule	Notch1 or notch2 have been implicated in Th2-cell differentiation.	4
NOTCH3	T cells	Surface molecule	Notch3 has been implicated in Th1-cell differentiation.	4
CD27	T cell	Surface molecule	CD27 is a lymphocyte-specific member of the TNFR which is expressed in T cells after activation via TCR/CD3 complex.	28
CD28	T cell	Surface molecule	CD28 delivers signals important for T cell activation and survival.	12
CTLA4	T cell	Surface molecule	CTLA-4 (cytotoxic T lymphocyte associated protein 4) inhibits T cell responses and regulates peripheral T cell tolerance.	12
CD45	T cell	Surface molecule	CD45 (lymphocyte common antigen) acts as a positive regulator of Src family protein tyrosine kinases.	101
CD44	T cell	Surface molecule	CD44 is a transmembrane glycoprotein. It acts as a co-stimulus for T cell activation in association with triggering through the TCR.	102
CD40L	T cell	Surface molecule	CD40L (CD154) is a type II transmembrane protein of the TNF superfamily. CD40-CD40L engagement on the surface of DCs promotes their cytokine production, the induction of costimulatory molecules on their surface, and facilitates the cross-presentation of antigen.	99
PD1	T cell	Surface molecule	PD1 (Programmed cell death protein 1) is an inhibitory molecule expressed by activated T cells. Engagement of PD1 by B7H1 (PDL1) or B7DC (PDL2) inhibits TCR-mediated proliferation and cytokine production by previously activated T cells.	3
ICOS	T cell	Surface molecule	ICOS (Inducible T-cell costimulator) enhances T cell proliferation, secretion of cytokines, and upregulation of cell surface molecules.	51
OX40	T cell	Surface molecule	OX40 (CD134) is a member of the TNFR/TNF superfamily and is expressed on activated CD4. OX40 Regulates cytokine production from antigen-presenting cells and modulates cytokine receptor signaling. Promotes division and survival of conventional T cells, augmenting the clonal expansion of effector and memory populations.	21
CD3Z	T cell	Intracellular molecule	CD3 ζ (T-cell receptor T3 zeta chain) mediates intracellular signaling through ZAP70.	85
FcRG	T cell	Intracellular molecule	FcR γ (Fc receptor gamma) mediates intracellular signaling through SYK.	85
ZAP70	T cell	Intracellular molecule	ZAP70 (Zeta-chain-associated protein kinase 70) mediates intracellular signaling.	30
SYK	T cell	Intracellular molecule	Syk (Spleen Tyrosine Kinase) mediates TCR signaling independently of CD45 and of Lck.	101
cfos	T cell	Intracellular molecule	cfos is a component of the AP1 transcription factor.	30

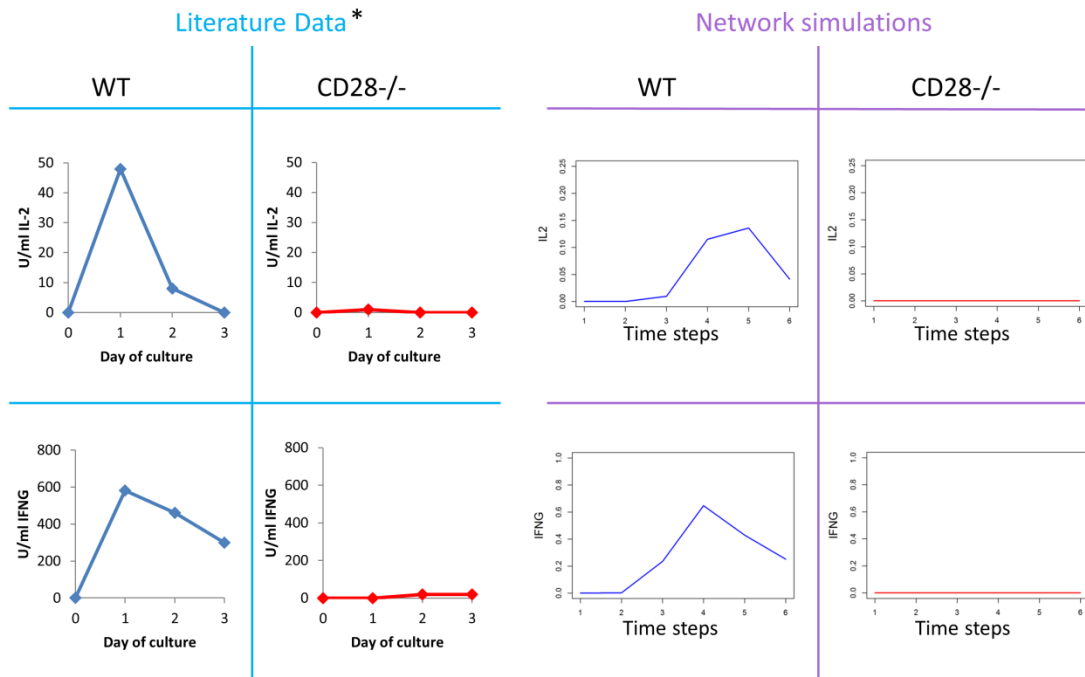
Supplementary Table 2 (continued)

CA2	T cell	Intracellular molecule	CA2 (Calcium) is present in NFAT transcription factor.	30
P65	T cell	Intracellular molecule	p65 is a subunit of NF- κ B transcription factor.	30
IL2		Cytokine	IL-2 (Interleukin 2) plays a crucial role in immune activation and homeostasis.	103
Th2		Differentiated T cell	Th2 cells evoke strong antibody responses (including those of the IgE class) and eosinophil accumulation, but inhibit several functions of phagocytic cells (phagocyte-independent inflammation).	104
IL4		Cytokine	IL-4 (Interleukin 4) has an important role in regulating antibody production.	105
IL10		Cytokine	IL-10 (Interleukin 10) modulates expression of cytokines, soluble mediators and cell surface molecules by cells of myeloid origin, with important consequences for their ability to activate and sustain immune and inflammatory responses.	106
IL13		Cytokine	IL-13 (Interleukin 13) induces immunoglobulin production and proliferation of B cells and the differentiation of cells of the monocytic lineage.	107
IL6		Cytokine	IL-6 (Interleukin 6) is a pleiotropic cytokine which induces terminal differentiation of B lymphocytes into antibody-forming cells and the differentiation of T cells into effector cells. IL-6 also has multiple potent proinflammatory effects.	108
IL12		Cytokine	IL-12 (Interleukin 12) induces cytokine production (IFN- γ) acts as a growth factor for activated NK and T cells, enhances the cytotoxic activity of NK cells, and favors cytotoxic T lymphocyte generation.	109
IFNG		Cytokine	IFN- γ (Interferon gamma) is the chief cytokine involved in the protective immune response against mycobacterial infection.	110
Th1		Differentiated T cell	Th1 cells evoke cell-mediated immunity and phagocyte-dependent inflammation.	104
TNFα		Cytokine	TNF α (tumor necrosis factor alpha) provokes inflammation, necrosis, cell proliferation, differentiation, and apoptosis.	111
TGFβ		Cytokine	TGF β (transforming growth factor beta) regulates the proliferation and differentiation of cells, embryonic development, wound healing, and angiogenesis.	112
IL21		Cytokine	IL-21 (Interleukin 21) modulates the functions of T, B, and NK cells. It is also a potent antitumor agent.	113
IL23		Cytokine	IL-23 (Interleukin 23) is a proinflammatory cytokine which is involved in differentiation of Th17 cells in a pro-inflammatory context.	114
Th17		Differentiated T cell	Th17 cells are potent inducers of tissue inflammation and have been associated with the pathogenesis of many experimental autoimmune diseases.	42

Supplementary Table 2 (continued)

IL17	Cytokine	IL-17 (Interleukin 17) family plays a crucial role in host defense against microbial organisms and in the development of inflammatory diseases.	115
GMCSF	Cytokine	GM-CSF (Granulocyte macrophage colony stimulating factor) is an important hematopoietic growth factor and immune modulator.	116
Treg	Differentiated T cell	Treg (regulatory T cells) prevents autoimmune diseases by establishing and maintaining immunologic self-tolerance.	117
Tfh	Differentiated T cell	Tfh (T follicular helper cells) specialize in providing cognate help to B cells and are fundamentally required for the generation of T cell-dependent B cell responses.	118
IL18	Cytokine	IL-18 (Interleukin 18) is a proinflammatory cytokine which induces IFN- γ and Th1 responses.	119
IL27	Cytokine	IL-27 (Interleukin 27) is a heterodimeric cytokine of the IL-12 family that plays an important role in the regulation of T and B cells responses.	120

Supplementary Figure 1

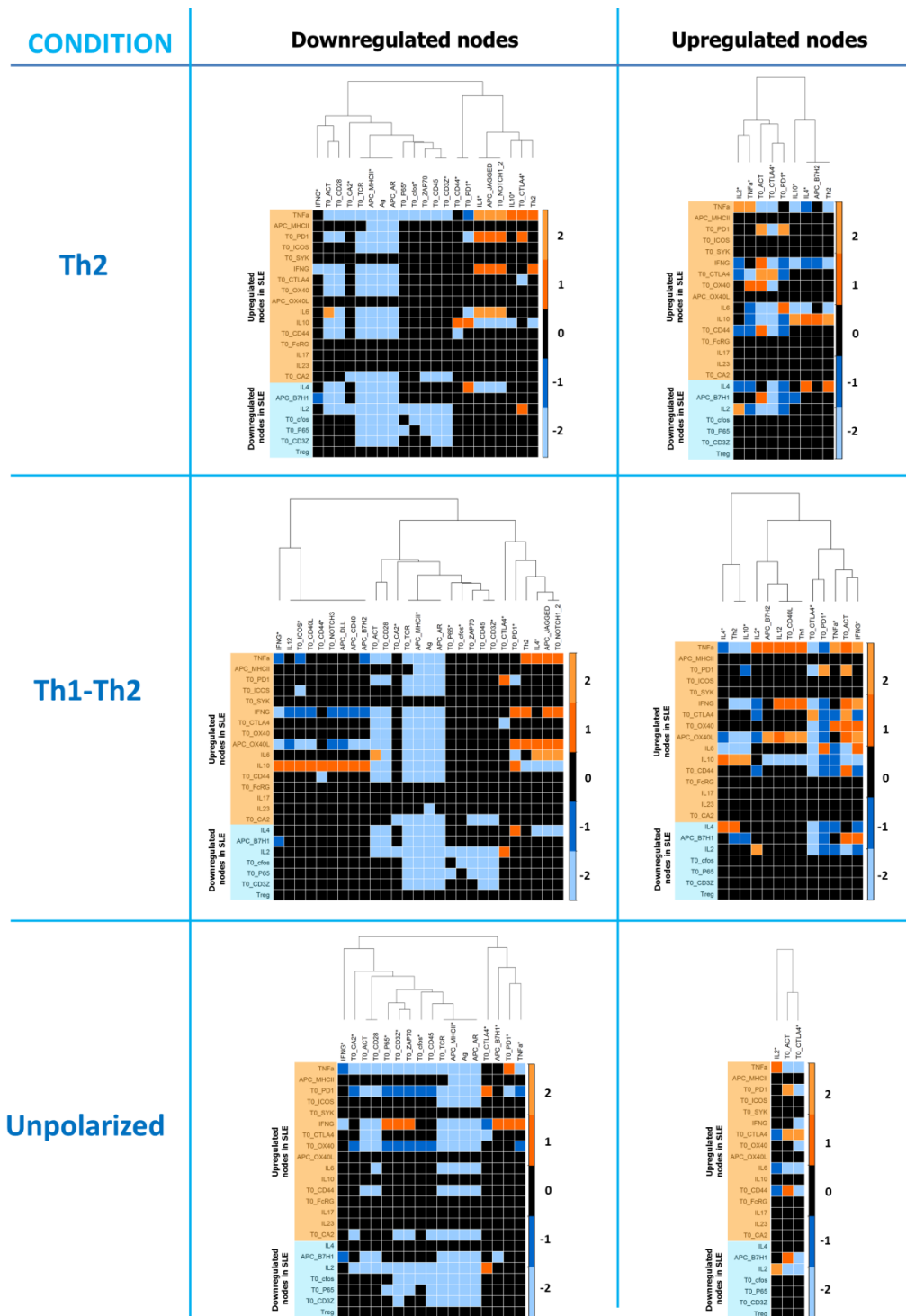


* Adapted from Howland et al. 2000

Supplementary Figure 1. Network validation

It must be highlighted that despite the promising applicability of this approach, the full potential of this tool cannot be assessed until the whole SLE pathway is included in the network. In the same way, full model validation is not possible at this stage because expression of many nodes is also regulated by other molecules, critical to the immune pathophysiology of SLE but not yet included in the model. Because of that validation attempts of this network were limited to early signals of immune activation in normal and perturbed conditions. Activation profiles of nodes from *ex vivo* (left) and *in silico* (right) were similar. The greatest difference was on the onset of activation that is immediate in the *ex vivo* conditions because T-cells are cultured directly with the antigen while in the simulations a time-step for Antigen APC encounter and other for APC migration to lymph nodes were included. Although, agreement between simulations and results from clinical trials may also be considered part of validation, the full effect of a treatment cannot be evaluated in the model until the network is completed. Furthermore, at the moment only one mAb has been approved for the treatment of SLE (Belimumab) under certain conditions, therefore there is only one usable example to validate and effective treatment, unfortunately the target of Belimumab (B-cell activating factor) is not yet included in this model.

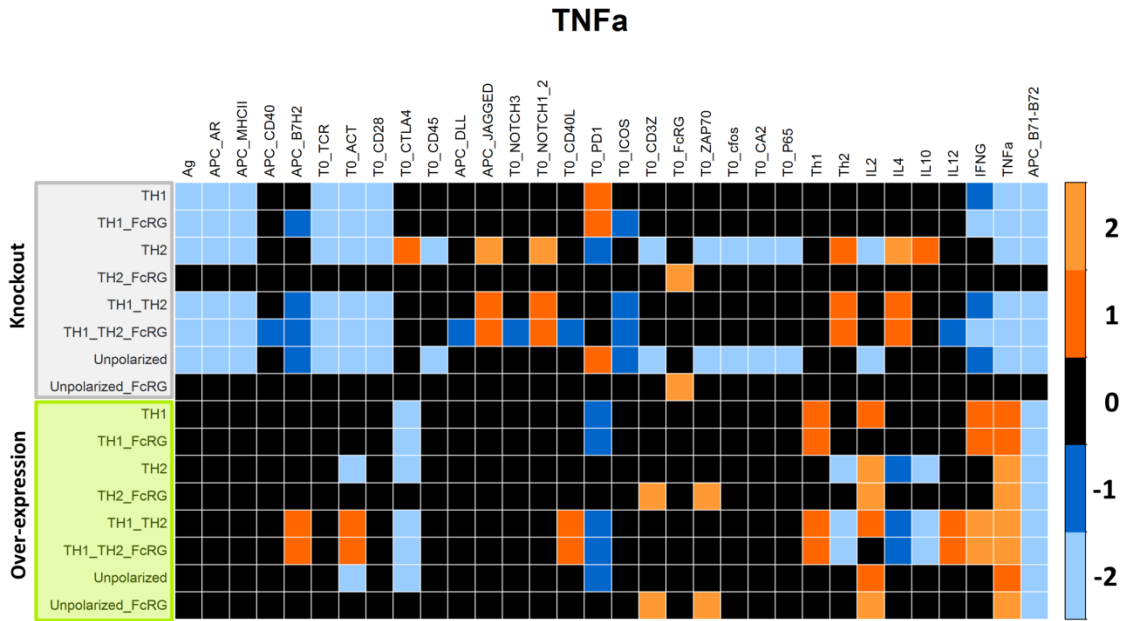
Supplementary Figure 2



Supplementary Figure 2. Clustering of perturbations according to “SLE like” alterations.

Clustering of perturbations according to “SLE like” alterations depending on different initial conditions. Heatmaps indicate the effect of single perturbations on the nodes that have been reported as altered in SLE. Two types of perturbations were simulated, node knockouts (left) and node over-expressions (right). Each heatmap contains 23 rows, one for each node that has been reported as altered in SLE. Most perturbations did not trigger considerable changes in those 23 nodes (indicated in black or absent from the heatmap). Some perturbations led to upregulations of the 23 nodes (represented in orange) while downregulation of the 23 nodes were more common (blue). Perturbations were clustered according to SLE like alterations that they provoked as can be seen in the blue and orange blocks in the heatmaps. Th2 and Th1-Th2 antigen simulation grouped the majority of the alterations reported in SLE while perturbation in simulation under unpolarized antigen conditions were not able to reproduce these alterations.

Supplementary Figure 3



Supplementary Figure 3. TNF α alteration triggered by different initial conditions.

TNF α alteration may be triggered by different initial conditions (knockouts in grey and over-expressions in green). TNF α was upregulated by a downregulation of T0_PD1 when a Th1 like antigen was simulated. The same TNF α upregulation was triggered by a downregulation of T0_CTLA4, IL4 or IL10 under a Th2 antigen simulation; or IL4 under a Th1-Th2 antigen simulation. Also, TNF α was upregulated by an over-expression of IL2 or IFN- γ under a Th1 antigen simulation; IL2 under a Th2 antigen simulation; APC_B7H2, T0_CD40L, IL-2 or IFN- γ under a Th1-Th2 antigen simulation; or Th2 or IFN- γ when an unpolarized simulation was made.

Supplementary References

1. Ford, M. L. & Larsen, C. P. Translating costimulation blockade to the clinic: Lessons learned from three pathways. *Immunol. Rev.* **229**, 294–306 (2009).
2. Saunders, a E. & Johnson, P. Modulation of immune cell signalling by the leukocyte common tyrosine phosphatase, CD45. *Cell. Signal.* **22**, 339–48 (2010).
3. Sharpe, A. H. & Freeman, G. J. The B7-CD28 superfamily. *Nat. Rev. Immunol.* **2**, 116–126 (2002).
4. Amsen, D., Spilianakis, C. G. & Flavell, R. a. How are T(H)1 and T(H)2 effector cells made? *Curr. Opin. Immunol.* **21**, 153–60 (2009).
5. Wu, W., Alexis, N. E., Bromberg, P. A., Jaspers, I. & Peden, D. B. Mechanisms of LPS-induced CD40 expression in human peripheral blood monocytic cells. *Biochem. Biophys. Res. Commun.* **379**, 573–577 (2009).
6. Zygmunt, B. & Veldhoen, M. *T helper cell differentiation more than just cytokines. Advances in immunology* **109**, (Elsevier inc., 2011).
7. Skov, S., Bonyhadi, M., Odum, N. & Ledbetter, J. a. IL-2 and IL-15 Regulate CD154 Expression on Activated CD4 T Cells. *J. Immunol.* **164**, 3500–3505 (2000).
8. Podojil, J. R. & Miller, S. D. Targeting the B7 family of co-stimulatory molecules: successes and challenges. *BioDrugs* **27**, 1–13 (2013).
9. Lee, B. O., Haynes, L., Eaton, S. M., Swain, S. L. & Randall, T. D. The Biological Outcome of CD40 Signaling Is Dependent on the Duration of CD40 Ligand Expression: Reciprocal Regulation by Interleukin (IL)-4 and IL-12. *J. Exp. Med.* **196**, 693–704 (2002).
10. Nakae, S. *et al.* Mast Cells Enhance T Cell Activation: Importance of Mast Cell Costimulatory Molecules and Secreted TNF. *J. Immunol.* **176**, 2238–2248 (2006).
11. Hutloff, a *et al.* ICOS is an inducible T-cell co-stimulator structurally and functionally related to CD28. *Nature* **397**, 263–266 (1999).
12. Greenwald, R. J., Freeman, G. J. & Sharpe, A. H. The B7 family revisited. *Annu. Rev. Immunol.* **23**, 515–48 (2005).
13. Wassink, L. *et al.* ICOS expression by activated human Th cells is enhanced by IL-12 and IL-23: increased ICOS expression enhances the effector function of both Th1 and Th2 cells. *J. Immunol.* **173**, 1779–1786 (2004).
14. Aicher, a. *et al.* Characterization of Human Inducible Costimulator Ligand

- Expression and Function. *J. Immunol.* **164**, 4689–4696 (2000).
15. Gao, X., Zhao, L., Wang, S., Yang, J. & Yang, X. Enhanced inducible costimulator ligand (ICOS-L) expression on dendritic cells in interleukin-10 deficiency and its impact on T-cell subsets in respiratory tract infection. *Mol. Med.* **19**, 346–56 (2013).
 16. Ariel, a. *et al.* Induction of interactions between CD44 and hyaluronic acid by a short exposure of human T cells to diverse pro-inflammatory mediators. *Immunology* **100**, 345–351 (2000).
 17. Salama, A. K. S. & Hodi, F. S. Cytotoxic T-lymphocyte-associated antigen-4. *Clin. Cancer Res.* **17**, 4622–8 (2011).
 18. Bryl, E., Vallejo, a. N., Weyand, C. M. & Goronzy, J. J. Down-Regulation of CD28 Expression by TNF-. *J. Immunol.* **167**, 3231–3238 (2001).
 19. Fife, B. T. & Pauken, K. E. The role of the PD-1 pathway in autoimmunity and peripheral tolerance. *Ann. N. Y. Acad. Sci.* **1217**, 45–59 (2011).
 20. Redmond, W. L., Ruby, C. E. & Weinberg, A. D. The role of OX40-mediated co-stimulation in T-cell activation and survival. *Crit. Rev. Immunol.* **29**, 187–201 (2009).
 21. Croft, M., So, T., Duan, W. & Soroosh, P. The significance of OX40 and OX40L to T-cell biology and immune disease. *Immunol. Rev.* **229**, 173–91 (2009).
 22. Jenkins, S. J., Perona-Wright, G., Worsley, A. G. F., Ishii, N. & MacDonald, A. S. Dendritic cell expression of OX40 ligand acts as a costimulatory, not polarizing, signal for optimal Th2 priming and memory induction in vivo. *J. Immunol.* **179**, 3515–23 (2007).
 23. Keir, M. E., Butte, M. J., Freeman, G. J. & Sharpe, A. H. PD-1 and its ligands in tolerance and immunity. *Annu. Rev. Immunol.* **26**, 677–704 (2008).
 24. Freeman, B. G. J. *et al.* Engagement of the PD-1 Immunoinhibitory Receptor by a Novel B7 Family Member Leads to Negative Regulation of Lymphocyte Activation. **192**, (2000).
 25. Ou, J.-N., Wiedeman, A. E. & Stevens, A. M. TNF- α and TGF- β counter-regulate PD-L1 expression on monocytes in systemic lupus erythematosus. *Sci. Rep.* **2**, 295 (2012).
 26. Liang, S. C. *et al.* Regulation of PD-1, PD-L1, and PD-L2 expression during normal and autoimmune responses. *Eur. J. Immunol.* **33**, 2706–16 (2003).
 27. Collins, M., Ling, V. & Carreno, B. M. The B7 family of immune-regulatory ligands. *Genome Biol.* **6**, 223 (2005).

28. Lens, S. M., Tesselaar, K., van Oers, M. H. & van Lier, R. a. Control of lymphocyte function through CD27-CD70 interactions. *Semin. Immunol.* **10**, 491–499 (1998).
29. Tesselaar, K. *et al.* Expression of the Murine CD27 Ligand CD70 In Vitro and In Vivo. *J. Immunol.* **170**, 33–40 (2003).
30. Moulton, V. R. & Tsokos, G. C. Abnormalities of T cell signaling in systemic lupus erythematosus. *Arthritis Res. Ther.* **13**, 207 (2011).
31. Bour-Jordan, H. *et al.* Intrinsic and extrinsic control of peripheral T-cell tolerance by costimulatory molecules of the CD28/ B7 family. *Immunol. Rev.* **241**, 180–205 (2011).
32. Howland, K. C., Ausubel, L. J., London, C. a. & Abbas, a. K. The Roles of CD28 and CD40 Ligand in T Cell Activation and Tolerance. *J. Immunol.* **164**, 4465–4470 (2000).
33. Manku, H., Graham, D. S. C. & Vyse, T. J. Association of the co-stimulator OX40L with systemic lupus erythematosus. *J. Mol. Med. (Berl)*. **87**, 229–34 (2009).
34. Beier, K. C. *et al.* Induction, binding specificity and function of human ICOS. *Eur. J. Immunol.* **30**, 3707–3717 (2000).
35. Romo-Tena, J., Gómez-Martín, D. & Alcocer-Varela, J. CTLA-4 and autoimmunity: new insights into the dual regulator of tolerance. *Autoimmun. Rev.* **12**, 1171–6 (2013).
36. Latchman, Y. *et al.* PD-L2 is a second ligand for PD-1 and inhibits T cell activation. **2**, (2001).
37. Guan, H., Nagarkatti, P. S. & Nagarkatti, M. Role of CD44 in the differentiation of Th1 and Th2 cells: CD44-deficiency enhances the development of Th2 effectors in response to sheep RBC and chicken ovalbumin. *J. Immunol.* **183**, 172–80 (2009).
38. Tian, L. *et al.* Foxp3⁺ regulatory T cells exert asymmetric control over murine helper responses by inducing Th2 cell apoptosis. *Blood* **118**, 1845–1853 (2011).
39. Gorelik, L., Fields, P. E. & Flavell, R. a. Cutting Edge: TGF- Inhibits Th Type 2 Development Through Inhibition of GATA-3 Expression. *J. Immunol.* **165**, 4773–4777 (2000).
40. Gorelik, L., Constant, S. & Flavell, R. a. Mechanism of transforming growth factor beta-induced inhibition of T helper type 1 differentiation. *J. Exp. Med.* **195**, 1499–1505 (2002).
41. Tesmer, L. A., Lundy, S. K., Sarkar, S. & Fox, D. A. Th17 cells in human

- disease. *Immunological Reviews* **223**, 87–113 (2008).
42. Korn, T., Bettelli, E., Oukka, M. & Kuchroo, V. K. IL-17 and Th17 Cells. *Annu. Rev. Immunol.* **27**, 485–517 (2009).
 43. Iezzi, G. *et al.* CD40-CD40L cross-talk integrates strong antigenic signals and microbial stimuli to induce development of IL-17-producing CD4⁺ T cells. *Proc. Natl. Acad. Sci. U. S. A.* **106**, 876–81 (2009).
 44. Nurieva, R. I. *et al.* Generation of follicular helper T cells is mediated by IL-21 but independent of TH1, TH2 or TH17 lineages. **29**, 138–149 (2009).
 45. Ma, C. S. *et al.* Early commitment of naïve human CD4⁽⁺⁾ T cells to the T follicular helper (T(FH)) cell lineage is induced by IL-12. *Immunol. Cell Biol.* **87**, 590–600 (2009).
 46. Bossaller, L. *et al.* ICOS deficiency is associated with a severe reduction of CXCR5⁺CD4 germinal center Th cells. *J. Immunol.* **177**, 4927–4932 (2006).
 47. Wan, Y. Y. & Flavell, R. A. ‘ Yin-Yang ’ functions of TGF- β and Tregs in immune regulation. **2216**, 199–213 (2007).
 48. Yao, S. & Chen, L. PD-1 as an Immune Modulatory Receptor. **1**, 262–264 (2014).
 49. Kimura, A. & Kishimoto, T. IL-6: regulator of Treg/Th17 balance. *Eur. J. Immunol.* **40**, 1830–5 (2010).
 50. Battaglia, A. *et al.* Interleukin-21 (IL-21) synergizes with IL-2 to enhance T-cell receptor-induced human T-cell proliferation and counteracts IL-2 / transforming growth factor- β -induced regulatory T-cell development. **21**, (2012).
 51. Takahashi, N. *et al.* Impaired CD4 and CD8 effector function and decreased memory T cell populations in ICOS-deficient patients. *J. Immunol.* **182**, 5515–27 (2009).
 52. Ohshima, Y. *et al.* OX40 costimulation enhances interleukin-4 (IL-4) expression at priming and promotes the differentiation of naive human CD4⁽⁺⁾ T cells into high IL-4-producing effectors. *Blood* **92**, 3338–3345 (1998).
 53. Coquet, J. M. *et al.* The CD27 and CD70 costimulatory pathway inhibits effector function of T helper 17 cells and attenuates associated autoimmunity. *Immunity* **38**, 53–65 (2013).
 54. Orabona, C. *et al.* CD28 induces immunostimulatory signals in dendritic cells via CD80 and CD86. *Nat. Immunol.* **5**, 1134–1142 (2004).
 55. Perona-Wright, G. *et al.* A pivotal role for CD40-mediated IL-6 production by dendritic cells during IL-17 induction in vivo. *J. Immunol.* **182**, 2808–2815

- (2009).
56. Volpe, E. *et al.* A critical function for transforming growth factor-beta, interleukin 23 and proinflammatory cytokines in driving and modulating human T(H)-17 responses. *Nat. Immunol.* **9**, 650–657 (2008).
 57. Linker-israeli, M. *et al.* Exogenous IL-10 and IL-4 Down-regulate IL-6 Production by SLE-Derived PBMC. **91**, 6–16 (1999).
 58. Donnelly, R. P. *et al.* Tissue-Specific Regulation of IL-6 Production. **151**, (1993).
 59. Heyen, J. R. R., Ye, S. M., Finck, B. N. & Johnson, R. W. Interleukin (IL)-10 inhibits IL-6 production in microglia by preventing activation of NF- κ B. *Mol. Brain Res.* **77**, 138–147 (2000).
 60. Liu, Z. *et al.* Interleukin (IL)-23 suppresses IL-10 in inflammatory bowel disease. *J. Biol. Chem.* **287**, 3591–3597 (2012).
 61. Papadakis, K. a. & Targan, S. R. Tumor necrosis factor: Biology and therapeutic inhibitors. *Gastroenterology* **119**, 1148–1157 (2000).
 62. Tsuji-Takayama, K. *et al.* The production of IL-10 by human regulatory T cells is enhanced by IL-2 through a STAT5-responsive intronic enhancer in the IL-10 locus. *J. Immunol.* **181**, 3897–3905 (2008).
 63. Kow, N. Y. & Mak, A. Costimulatory Pathways: Physiology and Potential Therapeutic Manipulation in Systemic Lupus Erythematosus. **2013**, (2013).
 64. Messal, N., Serriari, N.-E., Pastor, S., Nunès, J. a & Olive, D. PD-L2 is expressed on activated human T cells and regulates their function. *Mol. Immunol.* **48**, 2214–9 (2011).
 65. Poll, T. Van Der *et al.* Effects of IL-10 on Systemic Inflammatory Responses During Sublethal Primate Endotoxemia'. (1997).
 66. Ria, F., Penna, G. & Adorini, L. Th1 cells induce and Th2 inhibit antigen-dependent IL-12 secretion by dendritic cells. *Eur. J. Immunol.* **28**, 2003–16 (1998).
 67. Ruedl, C., Bachmann, M. F. & Kopf, M. The antigen dose determines T helper subset development by regulation of CD40 ligand. *Eur. J. Immunol.* **30**, 2056–2064 (2000).
 68. Magee, C. N., Boenisch, O. & Najafian, N. The role of costimulatory molecules in directing the functional differentiation of alloreactive T helper cells. *Am. J. Transplant* **12**, 2588–600 (2012).
 69. Hayashi, N. *et al.* T helper 1 cells stimulated with ovalbumin and IL-18 induce

- airway hyperresponsiveness and lung fibrosis by IFN-gamma and IL-13 production. *Proc. Natl. Acad. Sci. U. S. A.* **104**, 14765–14770 (2007).
70. Coquet, J. M. *et al.* The CD27 and CD70 costimulatory pathway inhibits effector function of T helper 17 cells and attenuates associated autoimmunity. *Immunity* **38**, 53–65 (2013).
71. Suto, A. *et al.* Development and characterization of IL-21-producing CD4+ T cells. *J. Exp. Med.* **205**, 1369–79 (2008).
72. Diehl, S. A., Schmidlin, H., Nagasawa, M., Blom, B. & Spits, H. IL-6 Triggers IL-21 production by human CD4+ T cells to drive STAT3-dependent plasma cell differentiation in B cells. *Immunology and Cell Biology* **90**, 802–811 (2012).
73. Kastelein, R. a, Hunter, C. a & Cua, D. J. Discovery and biology of IL-23 and IL-27: related but functionally distinct regulators of inflammation. *Annu. Rev. Immunol.* **25**, 221–242 (2007).
74. Zelová, H. & Hošek, J. TNF- α signalling and inflammation: interactions between old acquaintances. *Inflamm. Res.* **62**, 641–51 (2013).
75. Biedermann, T., Röcken, M. & Carballido, J. M. TH1 and TH2 lymphocyte development and regulation of TH cell-mediated immune responses of the skin. *J. Investig. Dermatol. Symp. Proc.* **9**, 5–14 (2004).
76. Noster, R. *et al.* IL-17 and GM-CSF expression are antagonistically regulated by human T helper cells. *Sci. Transl. Med.* **6**, 241ra80 (2014).
77. Robak, E., Smolewski, P. & Woz, A. Clinical significance of circulating dendritic cells in patients with systemic lupus erythematosus. **13**, (2004).
78. Mozaffarian, N., Wiedeman, a E. & Stevens, a M. Active systemic lupus erythematosus is associated with failure of antigen-presenting cells to express programmed death ligand-1. *Rheumatology (Oxford)*. **47**, 1335–41 (2008).
79. Graham, D. S. C. *et al.* Polymorphism at the TNF superfamily gene TNFSF4 confers susceptibility to systemic lupus erythematosus. *Nat. Genet.* **40**, 83–89 (2008).
80. Jury, E. C. *et al.* Abnormal CTLA-4 function in T cells from patients with systemic lupus erythematosus. *Eur. J. Immunol.* **40**, 569–78 (2010).
81. Crispín, J. C. *et al.* Expression of CD44 variant isoforms CD44v3 and CD44v6 is increased on T cells from patients with systemic lupus erythematosus and is correlated with disease activity. *Arthritis Rheum.* **62**, 1431–7 (2010).
82. Jiao, Q. *et al.* Upregulated PD-1 expression is associated with the development of systemic lupus erythematosus, but not the PD-1.1 Allele of the PDCD1 gene. *Int. J. Genomics* **2014**, 10–12 (2014).

83. Yang, J.-H. *et al.* Expression and function of inducible costimulator on peripheral blood T cells in patients with systemic lupus erythematosus. *Rheumatology (Oxford)*. **44**, 1245–1254 (2005).
84. Patschan, S. *et al.* CD134 expression on CD4+ T cells is associated with nephritis and disease activity in patients with systemic lupus erythematosus. *Clin. Exp. Immunol.* **145**, 235–242 (2006).
85. Enyedy, E. J. *et al.* Fc epsilon receptor type I gamma chain replaces the deficient T cell receptor zeta chain in T cells of patients with systemic lupus erythematosus. *Arthritis Rheum.* **44**, 1114–1121 (2001).
86. Krishnan, S., Warke, V. G., Nambiar, M. P., Tsokos, G. C. & Farber, D. L. The FcR gamma subunit and Syk kinase replace the CD3 zeta-chain and ZAP-70 kinase in the TCR signaling complex of human effector CD4 T cells. *J. Immunol.* **170**, 4189–4195 (2003).
87. Kyttaris, V. C., Juang, Y.-T., Tenbrock, K., Weinstein, a. & Tsokos, G. C. Cyclic Adenosine 5'-Monophosphate Response Element Modulator Is Responsible for the Decreased Expression of c-fos and Activator Protein-1 Binding in T Cells from Patients with Systemic Lupus Erythematosus. *J. Immunol.* **173**, 3557–3563 (2004).
88. Wong, H. K., Kammer, G. M., Dennis, G. & Tsokos, G. C. Abnormal NF-kappa B activity in T lymphocytes from patients with systemic lupus erythematosus is associated with decreased p65-RelA protein expression. *J. Immunol.* **163**, 1682–1689 (1999).
89. Sugimoto, K. *et al.* Decreased IL-4 producing CD4+ T cells in patients with active systemic lupus erythematosus-relation to IL-12R expression. *Autoimmunity* **35**, 381–7 (2002).
90. Park, Y. B. *et al.* Elevated interleukin-10 levels correlated with disease activity in systemic lupus erythematosus. *Clin. Exp. Rheumatol.* **16**, 283–8
91. Linker-Israeli, M. *et al.* Elevated levels of endogenous IL-6 in systemic lupus erythematosus. A putative role in pathogenesis. *J. Immunol.* **147**, 117–23 (1991).
92. Harigai, M. *et al.* Excessive production of IFN-gamma in patients with systemic lupus erythematosus and its contribution to induction of B lymphocyte stimulator/B cell-activating factor/TNF ligand superfamily-13B. *J. Immunol.* **181**, 2211–9 (2008).
93. al-Janadi, M., Al-Balla, S., Al-Dalaan, A. & Raziuddin, S. Cytokine profile in systemic lupus erythematosus, rheumatoid arthritis, and other rheumatic diseases. *J. Clin. Immunol.* **13**, 58–67 (1993).
94. Du, J., Li, Z., Shi, J. & Bi, L. Associations between serum interleukin-23 levels

- and clinical characteristics in patients with systemic lupus erythematosus. *J. Int. Med. Res.* **42**, 1123–1130 (2014).
95. Talaat, R. M., Mohamed, S. F., Bassyouni, I. H. & Raouf, A. A. Th1/Th2/Th17/Treg cytokine imbalance in systemic lupus erythematosus (SLE) patients: Correlation with disease activity. *Cytokine* **72**, 146–53 (2015).
 96. Dolff, S. *et al.* Disturbed Th1, Th2, Th17 and T(reg) balance in patients with systemic lupus erythematosus. *Clin. Immunol.* **141**, 197–204 (2011).
 97. Riemekasten, G. & Hahn, B. H. Key autoantigens in SLE. *Rheumatology (Oxford)*. **44**, 975–82 (2005).
 98. Holling, T. M., Schooten, E. & van Den Elsen, P. J. Function and regulation of MHC class II molecules in T-lymphocytes: of mice and men. *Hum. Immunol.* **65**, 282–90 (2004).
 99. Elgueta, R. *et al.* Molecular mechanism and function of CD40/CD40L engagement in the immune system. *Immunol. Rev.* **229**, 152–72 (2009).
 100. Sundberg, E. J., Deng, L. & Mariuzza, R. A. TCR recognition of peptide/MHC class II complexes and superantigens. *Semin. Immunol.* **19**, 262–71 (2007).
 101. Chu, D. H. *et al.* The Syk protein tyrosine kinase can function independently of CD45 or Lck in T cell antigen receptor signaling. *EMBO J.* **15**, 6251–61 (1996).
 102. Graham, V. A., Marzo, A. L. & Tough, D. F. A role for CD44 in T cell development and function during direct competition between CD44+ and CD44- cells. *Eur. J. Immunol.* **37**, 925–34 (2007).
 103. Gaffen, S. L. & Liu, K. D. Overview of interleukin-2 function, production and clinical applications. *Cytokine* **28**, 109–23 (2004).
 104. Romagnani, S. T-cell subsets (Th1 versus Th2). *Ann. Allergy. Asthma Immunol.* **85**, 9-18, 21 (2000).
 105. Brown, M. A. & Hural, J. Functions of IL-4 and control of its expression. *Crit. Rev. Immunol.* **17**, 1–32 (1997).
 106. Moore, K. W., de Waal Malefyt, R., Coffman, R. L. & O'Garra, A. Interleukin-10 and the interleukin-10 receptor. *Annu. Rev. Immunol.* **19**, 683–765 (2001).
 107. McKenzie, A. N. *et al.* Interleukin 13, a T-cell-derived cytokine that regulates human monocyte and B-cell function. *Proc. Natl. Acad. Sci. U. S. A.* **90**, 3735–9 (1993).
 108. Tackey, E., Lipsky, P. E. & Illei, G. G. Rationale for interleukin-6 blockade in systemic lupus erythematosus. *Lupus* **13**, 339–343 (2004).

109. Trinchieri, G. Interleukin-12: a proinflammatory cytokine with immunoregulatory functions that bridge innate resistance and antigen-specific adaptive immunity. *Annu. Rev. Immunol.* **13**, 251–76 (1995).
110. Cavalcanti, Y. V. N., Brelaz, M. C. A., Neves, J. K. de A. L., Ferraz, J. C. & Pereira, V. R. A. Role of TNF-Alpha, IFN-Gamma, and IL-10 in the Development of Pulmonary Tuberculosis. *Pulm. Med.* **2012**, 745483 (2012).
111. Liu, Z. G., Hsu, H., Goeddel, D. V & Karin, M. Dissection of TNF receptor 1 effector functions: JNK activation is not linked to apoptosis while NF-kappaB activation prevents cell death. *Cell* **87**, 565–76 (1996).
112. Blobe, G. C., Schiemann, W. P. & Lodish, H. F. Role of Transforming Growth Factor β in Human Disease. *N. Engl. J. Med.* **342**, 1350–1358 (2000).
113. Pelletier, M. & Girard, D. Biological functions of interleukin-21 and its role in inflammation. *ScientificWorldJournal.* **7**, 1715–35 (2007).
114. Duvallet, E., Semerano, L., Assier, E., Falgarone, G. & Boissier, M.-C. Interleukin-23: a key cytokine in inflammatory diseases. *Ann. Med.* **43**, 503–11 (2011).
115. Gu, C., Wu, L. & Li, X. IL-17 family: cytokines, receptors and signaling. *Cytokine* **64**, 477–85 (2013).
116. Shi, Y. *et al.* Granulocyte-macrophage colony-stimulating factor (GM-CSF) and T-cell responses: what we do and don't know. *Cell Res.* **16**, 126–133 (2006).
117. Corthay, A. How do regulatory T cells work? *Scand. J. Immunol.* **70**, 326–36 (2009).
118. Ma, C. S., Deenick, E. K., Batten, M. & Tangye, S. G. The origins, function, and regulation of T follicular helper cells. *J. Exp. Med.* **209**, 1241–53 (2012).
119. Dinarello, C. A. Interleukin-18, a proinflammatory cytokine. *Eur. Cytokine Netw.* **11**, 483–6 (2000).
120. Larousserie, F. *et al.* Differential effects of IL-27 on human B cell subsets. *J. Immunol.* **176**, 5890–7 (2006).

CHAPTER 2

COAGULATION OVERVIEW

1. Coagulation generalities

Hemostasis is a defense mechanism of the body that encompasses the processes by which a hemorrhagic process ceases. The hemostasis is divided into primary hemostasis and secondary hemostasis¹.

Primary hemostasis

This process corresponds with platelet activation, aggregation and platelet plug formation at the site of injury.

Secondary hemostasis

This process consists of coagulation cascade activation by which the insoluble fibrin clot is formed. Both processes, primary and secondary hemostasis occurs simultaneously.

2. Coagulation mechanisms

Several bibliographical sources show that coagulation is regulated by different pathways, the intrinsic, extrinsic and common pathways. This theory is known as the classic model of coagulation². Although it is very useful to interpret the results obtained from some “*in vitro*” coagulation tests like prothrombin time (PT) or activated partial thromboplastin time (aPTT), it fails to explain the coagulation process taking place “*in vivo*”. Currently, the so called cellular model of coagulation is the most accepted theory³, which divides the coagulation into three simultaneous steps which happen in different cell surfaces.

Classic model:

The classic model of coagulation consists of two different pathways, the intrinsic and the extrinsic pathways that converge in the common pathway by which the fibrin clot is formed (Figure 1)².

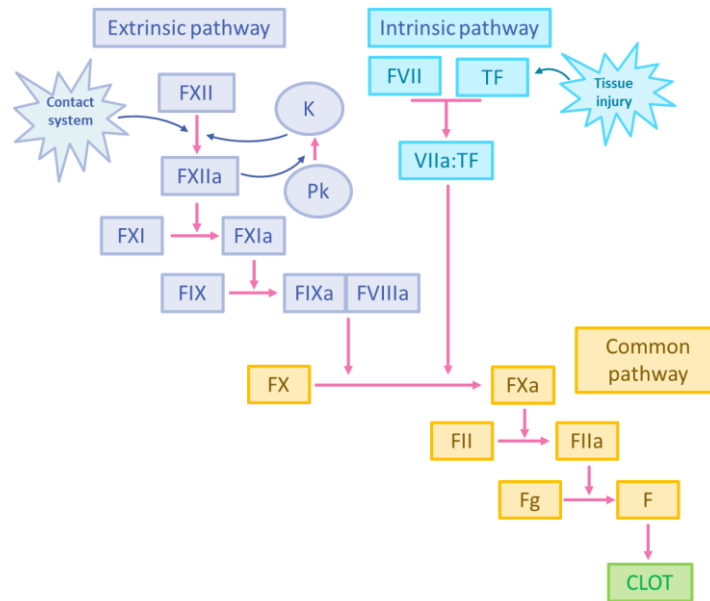


Figure 1. Representation of the coagulation process according to the classic model of coagulation. TF (tissue factor), FXII (factor XII), FXIIa (activated factor XII), Pk (prekallikrein), K (kallikrein), FXI (factor XI), FXIa (activated factor XI), FIX (factor IX), FIXa (activated factor IX), FVIIIa (activated factor VIII), FVII (factor VII), FVIIa (activated factor VII), FX (factor X), FXa (activated factor X), FII (factor II, prothrombin), FIIa (activated factor II, thrombin), Fg (fibrinogen) and F (fibrin).

- (i) **Extrinsic pathway:** It begins as a response triggered by a tissue injury which induces the binding between the extravascular tissue factor (TF) and the circulating factor VII (FVII), forming a complex which in turn will activate factor X (FX).
- (ii) **Intrinsic pathway:** This pathway begins when the blood comes in contact with a negatively charged system, activating the FXII. Then, the activated FXII (FXIIa) promotes the activation of prekallikrein (Pk) protein to kallikrein (K) and further reciprocal activation of FXII by kallikrein results in coagulation cascade activation. Then, the FXIIa acts on FXI to form FXIa, which activates FIX. After that, FIXa binds to FVIIIa to form the tenase complex (FIXa: FVIIIa) which will activate FX.
- (iii) **Common pathway:** Once the FX is activated by one of the previous pathways, FXa converts prothrombin (FII) into thrombin (FIIa), which by several processes will transform circulating fibrinogen (Fg) into insoluble fibrin (F), forming a stable clot in the injury site.

Cellular model:

The cellular model proposed by Hoffman in 2003³ will be explained later in the chapter.

3. Coagulation regulation

The coagulation system also has several regulation/control mechanisms to keep hemostasis, where the following endogenous anticoagulants² play a key role:

- (i) Antithrombin III (ATIII): This small protein can bind to activated factors FIIa, FXa, and FIXa and inactivate them. The action of certain drugs can enhance the activity of this protein as heparins.

- (ii) Tissue factor pathway inhibitor (TFPI): This anticoagulant is a polypeptide able to inhibit FXa reversibly, through the formation of the corresponding complex (FXa-TFPI). This complex inhibits FVIIa-TF complex, blocking coagulation initiation.

- (iii) Protein C system: This system is formed by protein C, thrombomodulin, activated protein C (APC) and protein S. APC and protein S form a complex with a proteolytic capacity which breaks the peptide bonds from FVa and FVIIIa that have pro-coagulant properties.

4. Coagulation tests

Some of the most relevant *in vitro* coagulation tests are: (i) prothrombin time (PT), (ii) activated partial thromboplastin time (aPTT) and (iii) calibrated automated thrombogram (CAT)⁴.

Prothrombin time

PT, introduced by Armand Quick in 1935⁵, is one of the most used tests in clinical practice. It evaluates the extrinsic and common pathways of the coagulation, i.e., the activity of the factors VII, V, XII and fibrinogen. It is expressed in seconds, quantifying the time required for clot formation in a citrated plasma (blood + sodium citrate) sample obtained from a patient after adding thromboplastin (tissue factor (TF) + phospholipids) and calcium.

PT represents the test of choice to monitor oral anticoagulant therapy. The main disadvantage is that the PT values obtained from the same sample can vary largely across laboratories due to the different sensitivities of the thromboplastin reagents. To

overcome this limitation, the international normalized ratio (INR) was introduced⁶. INR is described in equation 1 as follows:

$$INR = \left(\frac{\text{patient PT}}{\text{mean PT}} \right)^{ISI} \quad \text{Equation 1}$$

where patient PT is the PT value corresponding to the blood sample of interest obtained from a particular laboratory, mean PT is the mean of the PT values from 20 healthy individuals blood samples of both sexes measured in the same laboratory, and ISI is the international sensitivity index, which is given by the manufacturer.

The normal PT value in the healthy population ranges from 10 to 20 seconds, and the value of INR can vary between 0.8-1.2^{aa}.

Activated partial thromboplastin time

aPTT test was introduced by Langdell in 1953⁷. This test evaluates the intrinsic and common pathways of the coagulation process. As well as PT, aPTT quantifies the time required for clot formation measured in seconds, but the procedure is different. First, partial thromboplastin reagent (phospholipids without TF) is added to a citrated plasma sample of the patient. Then, the plasma sample is incubated with a surface contact activator, which can be kaolin, ellagic acid, celite among others, to obtain a controlled activation. Finally, calcium chloride is added. Normal values range between 30-45 seconds^{bb}. This test is widely used to monitor the effect of heparins treatment⁸. Furthermore, it has been observed that people with short aPTT have more possibilities to suffer thromboembolic events^{9,10}.

Calibrated automated thrombogram

Thrombin generation assay (TGA) was introduced by MacFarlane and Biggs in 1953¹¹. They measured thrombin concentration over the time in whole blood. However, the procedure resulted too laborious and time consuming. On the other hand, in the same year, Pitney and Dacie¹² performed the test in plasma. Several years later, Hemker et al¹³ in 2003, developed the calibrated automated thrombogram (CAT) which improved the efficiency and accuracy of the previous tests.

^{aa} <https://www.fda.gov/downloads/ICECI/Inspections/IOM/UCM135835.pdf>

^{bb} <https://www.fda.gov/downloads/ICECI/Inspections/IOM/UCM135835.pdf>

This test measures the concentration of thrombin produced over time after the addition of TF to a plasma sample. The resultant thrombogram, as well as the parameters which describe the curve¹⁴, are represented in Figure 2. This test is used to analyze thrombotic or hemorrhagic disorders. The main disadvantage is that it requires about an hour to be completed limiting its application in urgent care.

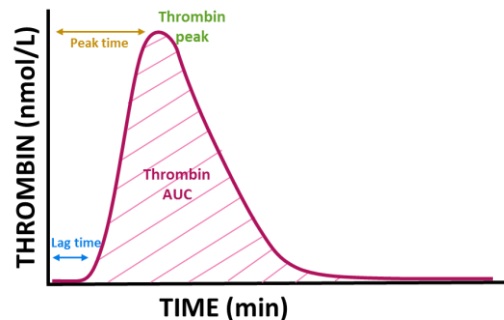
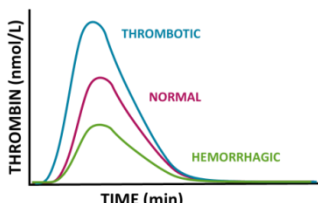


Figure 2. Representation of the curve obtained with the CAT method and thrombin curve parameters.

The test can be performed in platelet-poor plasma (PPP) or platelet-rich plasma (PRP)⁴. When PPP is used, procoagulant phospholipids, normally in a concentration of 4 μ M to enhance TF effects have to be added to the sample. Contrary, when the sample is PRP, the platelets are responsible for TF amplification. In both cases, TF concentration can vary depending on the laboratory. The shape of the curve depends on the experimental conditions (the type of plasma, phospholipid concentration, and TF concentration) and the lack of standardization of reference ranges of those conditions makes it difficult the comparison between curves generated from different experiments.

Differences between PT and aPTT tests and TGA

PT and aPTT	CAT
<p>Evaluates the extrinsic, intrinsic and common pathways, quantifying the time required for clot formation</p> <p>Allow predicting bleeding in patients</p> <p>They have been standardized for monitoring therapy:</p> <ul style="list-style-type: none"> • PT: vitamin K antagonist • aPTT: heparins <p>Not suited to represent the balance of coagulation that occurs “in vivo”</p> <p>Minutes to complete</p>	<p>Quantitative evaluation of thrombin formation</p> <p>Distinguished between hemorrhagic or thrombotic conditions</p>  <p>Reveals the endogenous thrombin levels in plasma</p> <p>About 1 hour to complete</p>

5. Coagulation alterations

The coagulation system is regulated by a strict homeostatic control to keep the balance between pro- and anticoagulant activities. A disorder in this balance will lead to hemorrhagic or thrombotic diseases respectively. Coagulation diseases can be divided into hereditary or acquired disorders. Hereditary disorders are genetic diseases, generally caused by chromosomal and gene mutations and pass from generation to generation. While acquired disorders are caused by risk factors like smoking, pregnancy, obesity, immobility among others. Table 1 lists some bleeding as well as some thrombotic disorders.

Table 1. Coagulation disorders. (BP) Birth prevalence. (P) Prevalence.

COAGULATION DISORDERS				
	DISEASE	PREVALENCE	COAGULATION TESTS PT	aPTT
BLEEDING DISORDERS				
HEREDITARY	Haemophilia A	BP) 1 in 4,000 to 5,000 males ^{cc}	Normal	Prolonged ¹⁵
	Haemophilia B	(BP) 1 in 20,000 males	Normal	Normal/prolonged ¹⁶
	von Willebrand disease	(P) 1 in 100 to 10,000 ^{dd}	Normal ¹⁷	Normal/prolonged ¹⁷
	Factor V deficiency	(P) 1 in 1,000,000 ^{ee}	Prolonged ¹⁸	Prolonged ¹⁸
	Factor VII deficiency	(P) 1 in 300,000 to 500,000 ^{ff}	Prolonged ¹⁹	Prolonged ¹⁹
	Factor X deficiency	(P) 1 in 1,000,000 ^{gg}	Prolonged ²⁰	Prolonged ²⁰
	Factor XIII deficiency	(P) 1 to 3 in 1,000,000 ^{hh}	Normal ²¹	Normal ²¹
	Prothrombin deficiency	(P) 1 in 2,000,000 ⁱⁱ	Prolonged ²²	Normal/prolonged ²²
ACQUIRED	Afibrinogenemia	(BP) 1 in 1,000,000 ^{jj}	No clot detected ²³	No clot detected ²³
	Disseminated intravascular coagulation	Unknown	Normal/prolonged ²⁴	Normal/prolonged ²⁴
	Vitamin K deficiency	Unknown	Normal/prolonged ²⁵	Normal ²⁶
	Liver disease	Unknown	Normal/prolonged ²⁵	Prolonged ²⁶
THROMBOTIC DISORDERS				
HEREDITARY	Protein C deficiency	(P) 1 in 500 ^{kk}	-	-
	Protein S deficiency	(P) 1 in 500 ^{ll}	-	-
	Antithrombin III deficiency	(P) 1 in 2,000 to 3,000 ^{mmm}	Normal/reduced ²⁷	Reduced ²⁷
	Factor V Leiden	3 - 8 % of people with European ancestry ⁿⁿ	Normal	Normal
	Prothrombin mutation	(P) 1 in 50 ^{oo}	Normal	Normal
ACQUIRED	Antiphospholipid antibody syndrome	Antiphospholipid antibodies in 1% to 5% of young healthy control subjects ^{pp}	-	-
	Increased levels of factors VIII, IX, XI or fibrinogen	Unknown	-	-
	Fibrinolysis defects	Unknown	-	-
	Homozygous homocystinuria	(P) 1 in 200,000 to 335,000	-	-

^{cc} <https://ghr.nlm.nih.gov/condition/hemophilia#statistics>

^{dd} <https://ghr.nlm.nih.gov/condition/von-willebrand-disease#statistics>

^{ee} <https://ghr.nlm.nih.gov/condition/factor-v-deficiency#statistics>

^{ff} <https://ghr.nlm.nih.gov/condition/factor-vii-deficiency#statistics>

^{gg} <https://ghr.nlm.nih.gov/condition/factor-x-deficiency#statistics>

^{hh} <https://ghr.nlm.nih.gov/condition/factor-xiii-deficiency#statistics>

ⁱⁱ <https://ghr.nlm.nih.gov/condition/prothrombin-deficiency#statistics>

^{jj} <https://ghr.nlm.nih.gov/condition/congenital-afibrinogenemia#statistics>

^{kk} <https://ghr.nlm.nih.gov/condition/protein-c-deficiency#statistics>

^{ll} <https://ghr.nlm.nih.gov/condition/protein-s-deficiency#statistics>

^{mmm} <https://ghr.nlm.nih.gov/condition/hereditary-antithrombin-deficiency#statistics>

ⁿⁿ <https://ghr.nlm.nih.gov/condition/factor-v-leiden-thrombophilia#statistics>

^{oo} <https://ghr.nlm.nih.gov/condition/prothrombin-thrombophilia#statistics>

^{pp} <https://ghr.nlm.nih.gov/condition/antiphospholipid-syndrome#statistics>

6. Therapeutic alternatives

Treatments for bleeding disorders

Due to the fact that most bleeding disorders are caused by some factor deficiencies, usually the treatment consists on the supplementation of those factors that are lacking or reduced. Although treatments are not curative, they help to alleviate the symptoms and reducing the bleeding risk²⁸. Currently, the treatments involving factor concentrates are very safe and are indicated for a wide variety of bleeding disorders (including those under the category of rare diseases). Coagulation factor plasma concentrates are derived from human plasma and are available for FI, FVII, FVIII, FXI and FXIII⁹⁹. Additionally, it is possible to synthesize recombinant factor VIII and recombinant factor VIIa using recombinant technology²⁹. Also, coagulation factors can be administered in combination, for example prothrombin complex concentrate is composed of factors II, VII, IX and X^{rr}.

When the factor required is not available as plasma concentrate, fresh frozen plasma is administered to the patient³⁰. Another possibility is the administration of a cryoprecipitate which contains factor VIII, fibrinogen and other coagulation proteins. The advantage concerning fresh frozen plasma is that as it is concentrated, the administered volume is less, but the disadvantage is that not all coagulation factors are contained, being only suitable for a few deficiencies.

The use of desmopressin, a synthetic hormone, increases factor VIII and von Willebrand factor levels, and it is used to treat patients with mild to moderate haemophilia A and von Willebrand disease³¹.

Vitamin K can be used in patients with deficiency of vitamin K dependent factors but it is not always effective.

Finally, antifibrinolytic drugs can be used in bleeding disorders. Usually, they are used in minor surgeries like dental operations and to control excessive menstrual bleeding. Two examples are tranexamic acid and aminocaproic acid³².

All these options are summarized in Table 2.

qq <https://www.wfh.org/en/sslpage.aspx?pid=668>
rr <https://www.wfh.org/en/sslpage.aspx?pid=668>

Table 2. Options for hemorrhagic disorders.

ANTHEMORRHAGIC TREATMENT	
Option	Description
FI, FVII, FVIII, FXI and FXIII	As plasma concentrate
FVIII and FVIIa	Recombinant technology
Fresh frozen plasma	The factor required is not available as plasma concentrated
Cryoprecipitate	Contains factor VIII, fibrinogen and other coagulation proteins
Desmopressin	Increases factor VIII levels
Vitamin K	Increase vitamin K dependent factors
Antifibrinolytic drugs	Tranexamic acid and aminocaproic acid

Treatments for thrombotic disorders

Treatments used in thrombotic disorders are summarized in Table 3^{33,34}. The mechanism of action of vitamin K antagonist drugs is the inhibition of vitamin K epoxide reductase, inhibiting initially the proteins C and S and later, inhibiting the coagulation factors II, VII, IX and X. For this reason, when a rapid anticoagulation effect is needed, they are administered together with rapid acting parenteral anticoagulant, normally heparins. Warfarin is the most used anticoagulant drug in venous thromboembolism. On the other hand, heparins bind to ATIII enhancing its activation and thus inhibiting coagulation. They are divided into unfractionated heparin (UH) and low molecular weight heparins (LMWH). Heparins can be administered parentally or subcutaneously and they are used in prophylaxis, for example in pre-operative and post-operative thrombosis or patients with venous thromboembolism. LMWHs are more predictable dose-response than UH. Finally, the most recent drugs are the new oral anticoagulants which are directed against two coagulation activated factors: factors IIa and Xa. Among the advantages of these new drugs are that they do not have a narrow therapeutic margin and they do not need to be monitored.

Overview

Table 3. Possible treatments for thrombotic disorders with their respective indications. UH (unfractionated heparin), LMWH (low molecular weight heparins), DIC (disseminated intravascular coagulation), DVT (deep vein thrombosis), PE (pulmonary embolism).

ANTICOAGULATION TREATMENT				
Drug	Mechanism of action		Indications	Laboratory monitoring
Vitamin K antagonists				
Warfarin	Vitamin K antagonists inhibit vitamin K-epoxide reductase thus decreasing the reduced form of vitamin K (VKH ₂). Therefore, inhibiting the synthesis of biologically active forms of vitamin k-dependent coagulation factors (II, VII, IX and X) and regulator proteins S and C		<ul style="list-style-type: none"> • Prophylaxis /treatment of venous thrombosis • Pulmonary embolism • Atrial fibrillation • Cardiac valve replacement • Myocardial infarction • Treatment of deep vein thrombosis and myocardial infarction • Prevention of cerebral embolism, pulmonary embolism, and transient ischemic attacks. 	PT, INR
Acenocoumarol				PT, INR
Heparins				
Unfractionated heparin	UH binds reversibly to the natural anticoagulant ATIII, accelerating the rate at which ATIII inactivates thrombin and factor Xa		<ul style="list-style-type: none"> • Treatment of venous thromboembolism • Thromboprophylaxis in general surgery and trauma • Venous Thromboembolism in Pediatric Patients • Cardioversion of Atrial Fibrillation • Arterial Thromboembolism • DIC ... 	aPPT
LMWH	Enoxaparin	As well as UH, LMWH bind to ATIII to enhance its activity	<ul style="list-style-type: none"> • Prophylaxis of deep vein thrombosis in abdominal surgery, hip replacement surgery, knee replacement surgery, or medical patients with severely restricted mobility during acute illness 	Anti-Xa level
	Dalteparin		<ul style="list-style-type: none"> • Inpatient treatment of acute DVT with or without pulmonary embolism 	Anti-Xa level
	Tinzaparin		<ul style="list-style-type: none"> • Prophylaxis of ischemic complications of unstable angina • Treatment of acute ST-segment elevation myocardial infarction 	Anti-Xa level
New oral anticoagulants				
Xa inhibitors	Apixaban	Direct inhibition of FXa, blocking the conversion of prothrombin to thrombin	<ul style="list-style-type: none"> • Reduction of risk of stroke and systemic embolism in patients with non-valvular atrial fibrillation 	Not required
	Rivaroxaban		<ul style="list-style-type: none"> • Reduction of risk of stroke and systemic embolism in patients with non-valvular atrial fibrillation • Treatment of DVT and pulmonary embolism • Prophylaxis of DVT following hip or knee replacement surgery 	Not required
	Edoxaban		<ul style="list-style-type: none"> • Reduction of risk of stroke and systemic embolism in patients with non-valvular atrial fibrillation • Treatment of DVT and PE 	Not required
Ila inhibitors	Dabigatran	Direct inhibition of FIIa, blocking the conversion of fibrinogen to fibrin	<ul style="list-style-type: none"> • Reduction of risk of stroke and systemic embolism in patients with non-valvular atrial fibrillation • Treatment of DVT and pulmonary embolism in patients who have been treated with a parenteral anticoagulant for 5-10 • Prophylaxis of DVT and PE in patients who have undergone hip replacement surgery 	Not required

7. REFERENCES

1. Gale, A. Current understanding of hemostasis. *Toxicol Pathol.* **39**, 273–280 (2011).
2. Palta, S., Saroa, R. & Palta, A. Overview of the coagulation system. *Indian J. Anaesth.* **58**, 515–523 (2014).
3. Hoffman, M. A cell-based model of coagulation and the role of factor VIIa. *Blood Rev.* **17**, 51–55 (2003).
4. Lancé, M. D. A general review of major global coagulation assays: Thrombelastography, thrombin generation test and clot waveform analysis. *Thromb. J.* **13**, 1–6 (2015).
5. Quick AJ. The prothrombin time in haemophilia and in obstructive jaundice. *J. Biol. Chem.* **109:73-4**, (1935).
6. Troulis, M. J., Head, T. W. & Leclerc, J. R. What is the INR? *J. Can. Dent. Assoc.* **62**, 428–30 (1996).
7. LANGDELL, R. D., WAGNER, R. H. & BRINKHOUS, K. M. Effect of antihemophilic factor on one-stage clotting tests; a presumptive test for hemophilia and a simple one-stage antihemophilic factor assay procedure. *J. Lab. Clin. Med.* **41**, 637–47 (1953).
8. Levy, J. H., Szlam, F., Wolberg, A. S. & Winkler, A. Clinical use of the activated partial thromboplastin time and prothrombin time for screening: A review of the literature and current guidelines for testing. *Clin. Lab. Med.* **34**, 453–477 (2014).
9. Tripodi, A., Chantarangkul, V., Martinelli, I., Bucciarelli, P. & Mannucci, P. M. A shortened activated partial thromboplastin time is associated with the risk of venous thromboembolism. **104**, 3631–3634 (2004).
10. Pilgeram, L. O., Chee, A. N. & Bussche, G. Von Dem. Evidence for abnormalities in clotting and thrombolysis as a risk factor for stroke. *Stroke* **4**, 643–657 (1973).
11. Macfarlane, R. & Biggs, R. A Thrombin Generation Test. The application in haemophilia and Thrombocytopenia. *J. Clin. Pathol.* **6**, 3–9 (1953).
12. PITNEY, W. R. & DACIE, J. V. A simple method of studying the generation of thrombin in recalcified plasma; application in the investigation of haemophilia. *J. Clin. Pathol.* **6**, 9–14 (1953).
13. Hemker, H. C. *et al.* Calibrated automated thrombin generation measurement in clotting plasma. *Pathophysiol. Haemost. Thromb.* **33**, 4–15 (2003).
14. Duarte, R. C. F., Ferreira, C. N., Rios, D. R. A., Reis, H. J. dos & Carvalho, M. das G. Thrombin generation assays for global evaluation of the hemostatic system: perspectives and limitations. *Rev. Bras. Hematol. Hemoter.* **39**, 259–265 (2017).
15. Bakija, A. T. *et al.* Specific and global coagulation tests in patients with mild haemophilia A with a double mutation (Glu113Asp, Arg593Cys). *Blood Transfus.* **13**, 622–630 (2015).
16. Park, C.-H., Seo, J.-Y., Kim, H.-J., Jang, J. H. & Kim, S.-H. A diagnostic challenge: mild hemophilia B with normal activated partial thromboplastin time. *Blood Coagul. Fibrinolysis* **21**, 368–371 (2010).
17. James, P. D. & Goodeve, A. C. von Willebrand disease. *Genet. Med.* **13**, 365–376 (2011).
18. Hirai, D. *et al.* Acquired Factor V Inhibitor. *Intern. Med.* **55**, 3039–3042 (2016).
19. Napolitano, M., Siragusa, S. & Mariani, G. Factor VII Deficiency: Clinical Phenotype, Genotype and Therapy. *J. Clin. Med.* **6**, 38 (2017).
20. Chatterjee, T. *et al.* Inherited Factor X (Stuart-Prower Factor) deficiency and its management.

- Med. J. Armed Forces India* **71**, S184–S186 (2015).
21. Martinuzzo, M. *et al.* Effects of factor XIII deficiency on thromboelastography. Thromboelastography with calcium and streptokinase addition is more sensitive than solubility tests. *Mediterr. J. Hematol. Infect. Dis.* **8**, 1–8 (2016).
 22. Imane, S., Laalej, Z., Faez, S. & Oukkache, B. Congenital factor II deficiency: Moroccan cases. *Int. J. Lab. Hematol.* **35**, 416–420 (2013).
 23. Verhovsek, M., Moffat, K. A. & Hayward, C. P. M. Laboratory testing for fibrinogen abnormalities. *Am. J. Hematol.* **83**, 928–931 (2008).
 24. Arora, M. M. *et al.* Diagnosing disseminated intravascular coagulation in acute infection: Can we do without FDP & D-dimer. *Med. J. Armed Forces India* **58**, 13–17 (2002).
 25. Triplett, D. A. Coagulation and bleeding disorders: Review and update. *Clin. Chem.* **46**, 1260–1269 (2000).
 26. Journeycake, J. M. & George, R. Coagulation Disorders AT : F : **24**, (2003).
 27. Bhakuni, T. *et al.* Antithrombin III deficiency in Indian patients with deep vein thrombosis: Identification of first India based at variants including a novel point mutation (T280A) that leads to aggregation. *PLoS One* **10**, 1–18 (2015).
 28. Cohen, A. J. & Kessler, C. M. Treatment of inherited coagulation disorders. *Am. J. Med.* **99**, 675–82 (1995).
 29. Coppola, A. *et al.* Treatment of hemophilia: a review of current advances and ongoing issues. *J. Blood Med.* **1**, 183–95 (2010).
 30. Arya, R. C., Wander, G. & Gupta, P. Blood component therapy: Which, when and how much. *J. Anaesthesiol. Clin. Pharmacol.* **27**, 278–84 (2011).
 31. Ozgönel, B., Rajpurkar, M. & Lusher, J. M. How do you treat bleeding disorders with desmopressin? *Postgrad. Med. J.* **83**, 159–63 (2007).
 32. van Galen, K. P. M., Engelen, E. T., Mauser-Bunschoten, E. P., van Es, R. J. J. & Schutgens, R. E. G. Antifibrinolytic therapy for preventing oral bleeding in patients with haemophilia or Von Willebrand disease undergoing minor oral surgery or dental extractions. *Cochrane database Syst. Rev.* CD011385 (2015). doi:10.1002/14651858.CD011385.pub2
 33. Harter, K., Levine, M. & Henderson, S. Anticoagulation Drug Therapy: A Review. *West. J. Emerg. Med.* **16**, 11–17 (2015).
 34. Franchini, M., Liumbruno, G. M., Bonfanti, C. & Lippi, G. The evolution of anticoagulant therapy. *Blood Transfus.* **14**, 175–184 (2016).

Describing the coagulation cascade: from a systems pharmacology model to a semi- mechanistic PKPD approach

**M. Leire Ruiz-Cerdá^{1,2}, Eduardo Asín Prieto^{1,2}, Annabel Blasi³, Joan Carles
Reverter⁴ and Iñaki F. Trocóniz^{1,2}**

Manuscript in preparation

¹Pharmacometrics & Systems Pharmacology, Department of Pharmacy and Pharmaceutical Technology, School of Pharmacy, University of Navarra, Pamplona 310890, Spain

²IdiSNA, Navarra Institute for Health Research; Pamplona, Spain.

³ Anesthesia Department. Hospital Clinic. Barcelona. Institut per a la recerca biomedica Agusti Pi i Sunyé (IDIBAPS).

⁴ Haemostasis and haemotherapy. Hospital Clinic. Barcelona.

1. INTRODUCTION

Hemostasis is the physiologic response that involves the processes by which a hemorrhagic process ceases. The hemostasis is divided into primary and secondary hemostasis¹. After a blood vessel injury, the vessel is constricted to reduce blood flow, and circulating platelets adhere to the vessel wall at the lesion site where they are aggregated and activated (primary hemostasis)². In the surface of these activated platelets take place several enzymatic reactions by which the coagulation factors are activated to form the insoluble fibrin clot. This process is known as coagulation cascade (secondary hemostasis)².

The “*in vivo*” coagulation process can be explained by the cellular model proposed by Hoffman³⁻⁵. This model is composed of three consecutive steps occurring in different cellular surfaces (Figure 1).

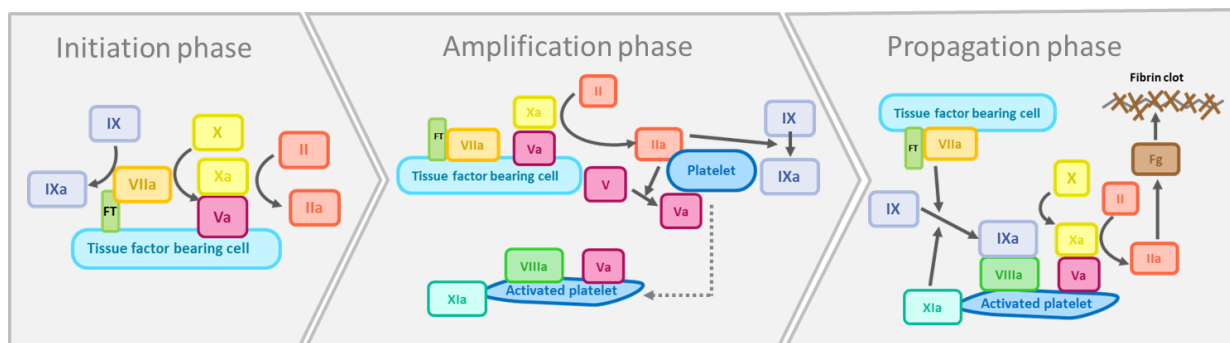


Figure 1. Representation of the coagulation process according to the cellular model of coagulation. TF (tissue factor), FXII (factor XII), FXIIa (activated factor XII), FXI (factor XI), FXIa (activated factor XI), FIX (factor IX), FIXa (activated factor IX), FVIIIa (activated factor VIII), FVII (factor VII), FVIIa (activated factor VII), FX (factor X), FXa (activated factor X), FII (factor II, prothrombin), FIIa (activated factor II, thrombin) and Fg (fibrinogen).

- (i) The initiation phase takes place on the surface of cells that contain the tissue factor (TF), like fibroblasts or macrophages among others. The TF is a protein able to initiate the coagulation cascade. On the other hand, some coagulation factors like factor VII (FVII), FX, FII can permeate through tissue spaces leaving the vascular space, coming in contact with TF in the extravascular space generating a little thrombin burst.
- (ii) The amplification phase starts after a tissue injury with vessel damage. Because of the lesion, the components that were not able to permeate through tissue spaces like FVIII, platelets and so on, can now pass to the

extravascular space establishing contact with the small amounts of thrombin generated in the initiation phase. This thrombin has several functions like platelet activation, FV and FXI activation.

- (iii) Finally, in the propagation phase, which occurs on the surface of activated platelets through the activation of different factors, the amount of thrombin necessary to form the coagulation clot is generated.

However, the classic model of coagulation, which divides the process into extrinsic, intrinsic and common pathways is more appropriated to explained the prothrombin time⁶ (PT) and the activated partial thromboplastin time⁷ (aPTT) “*in vitro*” coagulation tests. These tests are the most used measurements of coagulation activity in the clinical setting, measuring the time between the addition of activators to a plasma sample and the sufficient production of thrombin. Although these tests have a huge diagnostic value, they are not able to characterize all thrombin formation process during coagulation. In fact, they only identify the thrombin generated in the initiation phase, ignoring more than 90% of the thrombin formed⁸. To overcome this limitation, the thrombin generation assay (TGA) introduced by MacFarlane and Biggs in 1953⁹ or the calibrated automated thrombogram (CAT) by Hemker et al.¹⁰ in 2003, measure the amount of thrombin produced over time after the addition of TF to a blood or plasma sample, respectively. This test, contrary to PT and aPTT, provides information about the amplification and propagation phases of the hemostatic system. The main limitation is that it is not well standardized and thus, the possibly different experimental conditions make difficult the comparison between patient’s thrombin profiles in different experiments.

Due to the large numbers of components involved in the coagulation cascade and the different possible experimental conditions that can be used in coagulation tests, the development of mathematical models can be very useful to explore and predict different scenarios to better adjust and personalize patient treatments.

Modelling approaches:

Several models for part or whole blood coagulation process have been developed and are available in the literature¹¹⁻²². Through this type of models, it is possible to simulate the time profiles of the different components of the coagulation cascade and reproduce the endpoints of PT, aPTT and TGA tests. Also, they allow simulating different type of patients and therapies.

Systems pharmacology (SP) models are based on the bottom-up approach (Figure 2), which builds an exhaustive computational structure based on the knowledge available of the physiologic system. The main advantage of these models is that they are not limited by the type of data, which can be qualitative or quantitative, longitudinal or not, from one or different experiments, with the same or different experimental conditions²³. Once built, they represent a very useful tool to understand *in silico*, how the system behaves under different perturbations as polymorphisms or potential treatment. In addition, they serve as the starting point to develop other types of models^{24,25} that constitute a reduced version of the full model but maintaining the principal mechanisms involved. However, when fitting experimental data, and due to the elevated number of processes involved, in most cases it is not possible to estimate all the parameters defined in the model, being necessary to fix some from the literature. Furthermore, the obtaining of measures characterizing all the processes involved represents an unaffordable enterprise.

On the other spectrum of the modeling paradigm, the population pharmacokinetic-pharmacodynamic (PKPD) models describe the observed data accurately through simpler models where all model parameters are identifiable. These models follow a top-down approach (Figure 2), which treats the whole organism as a single system incorporating possible covariates²⁶. One of the limitations of this type of models is that they lack of deep mechanistic characterization of the physiologic processes limiting their application outside of controlled disease and treatment scenarios.

Compared to the previous type of models a better option is the development of semi-mechanistic PKPD models that, besides to provide good data description, their structure resembles the mechanism of the key processes. Usually, this type of models uses the middle-out approach (Figure 2), which includes the most relevant components of the system in order to describe the available clinical data²⁷ accurately.

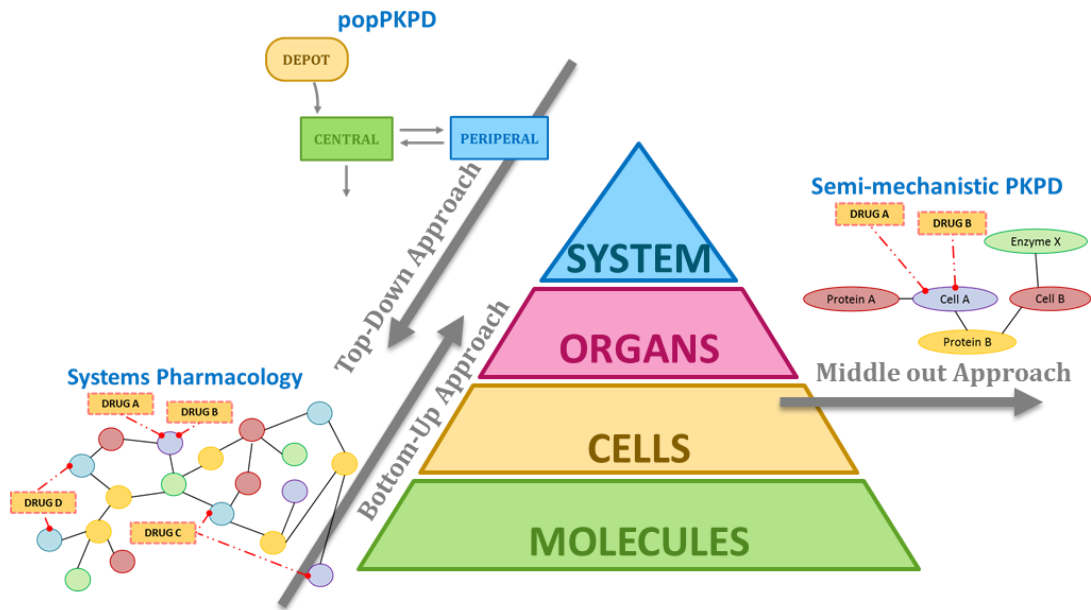


Figure 2. Different modelling perspectives regard to data requirements and mechanistic structure. Top-down approach, top-down approach and middle out approach.

The first objective in this article was to implement and evaluate two SP models found in the literature for the whole coagulation process^{19,21}. Because an unavoidable step is the evaluation of these SP models and their capacity to mimic the pathophysiological behavior, the second objective was to evaluate the performance of both models concerning longitudinal data of FIIa available in literature²⁸. Finally, a more manageable model able to reproduce the clinical data including inter-individual variability and covariate effects was built based on clinical data gathered from the literature.

2. METHODS

Literature search of quantitative systems pharmacology models for coagulation

Several coagulation models were identified through a systematic search in PubMed database. These models describe the whole coagulation process or characterize parts of coagulation cascade to describe the time courses of some coagulation factors or blood coagulation tests¹¹⁻²². Among the first group, two models were finally selected which characterize the entire coagulation network based on the inclusion of the relevant components and reactions^{19,21}.

Model implementation and evaluation

Both models were implemented using SimBiology (v. 5.6) software, which is a MATLAB (MathWorks, v. 2017a) toolbox²⁹.

The model developed by Wajima and co-authors¹⁹ (referred to hereafter as model 1) was established in a way that longitudinal profiles of the coagulation factors can be generated, and the results according to the PT or aPTT tests can be calculated under different experimental in silico scenarios.

The model consists of 51 components and 48 reactions. The components include coagulation factors, coagulation activators, natural anticoagulants, the vitamin K and its reduced and oxidized forms. The effect of the anticoagulant drugs warfarin, unfractionated heparin (UFH) and low molecular weight heparins (LMWHs) were simulated. A scheme of the model can be seen in supplementary material Figure S1A.

The dynamics of the system was described by algebraic and ordinary differential equations (ODEs) resembling mechanisms of synthesis, degradation, activation, and complex formation. Warfarin effect was incorporated using an I_{MAX} model and heparin effect using complex formation, resulting in the removal of the participating factors. An example of FIIa is presented below (Figure 3):

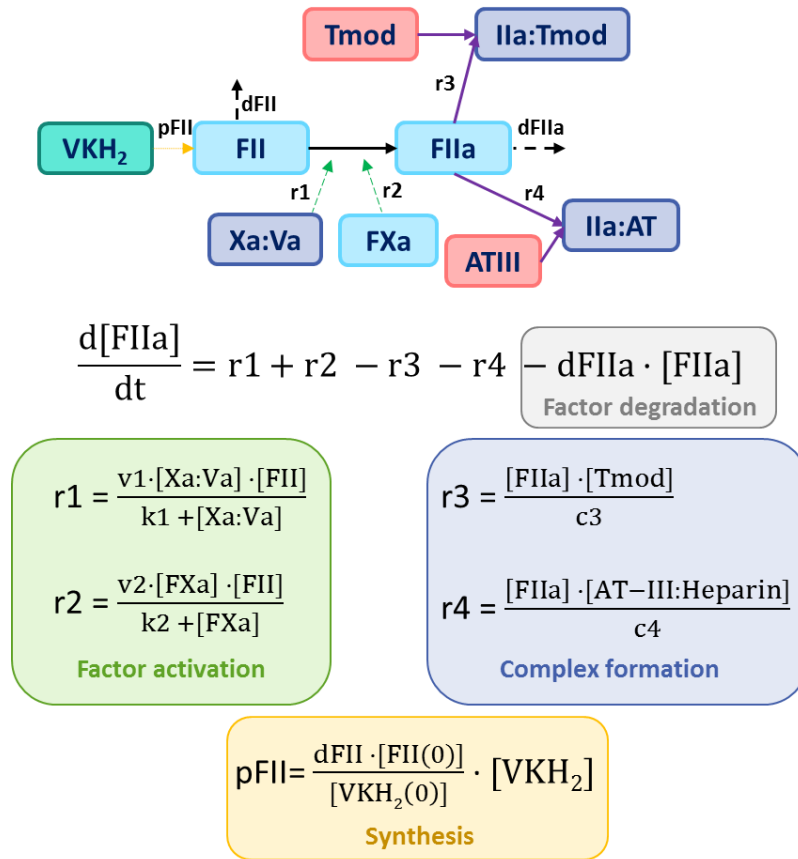
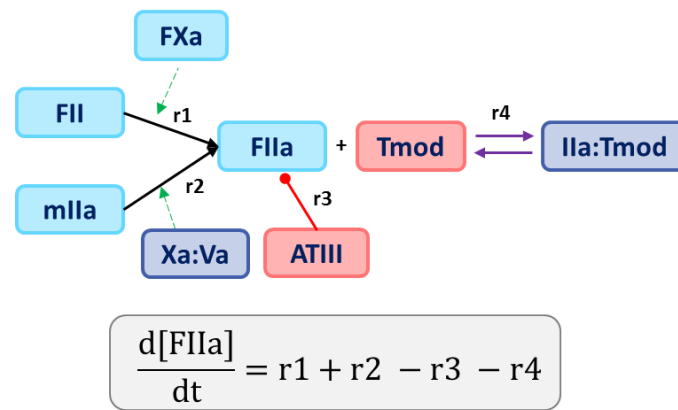


Figure 3. Corresponding ODE for the FIIa indicating the different types of reaction. v and k parameters represent V_{max} and k_m Michaelis-Menten constants and they are expressed in h^{-1} and nM respectively. p_{FII} is the production rate of FII based on a turn-over model expressed in nM . d_{FIIa} is the degradation rate constant of FIIa. Complex formation is a stoichiometric reaction in which the components are assumed to combine in a molar ratio of 1:1 and are divided by the parameter c , which is expressed in $nM \cdot h$. $[]$ denotes concentration and (0) initial concentration. Tmod (thrombomodulin), VKH_2 (vitamin K hydroquinone) and AT (antithrombin III).

In the supplementary tables 2, 3 and 4 of Wajima, et al. article¹⁹ parameters values, initial conditions for each component and degradation rate constants respectively are presented.

The model by Nayak and co-authors²¹ (referred to hereafter as model 2) was built to match in-house in vitro calibrated automated thrombogram (CAT) and aPTT data and therefore synthesis or degradation rates are not considered. This model consists of 61 components and 62 reactions as it is shown in supplementary material Figure S1B. Model equations are based in association-dissociation kinetics and reactions of first and second order. The example for FIIa is presented below in Figure 4.



$$r1 = k1 \cdot [\text{FXa}] \cdot [\text{FII}]$$

$$r2 = k2 \cdot [\text{mIIa}] \cdot [\text{Xa:Va}]$$

$$r3 = k3 \cdot [\text{FIIa}] \cdot [\text{ATIII}]$$

$$r4 = k4 \cdot [\text{FIIa}] \cdot [\text{Tmod}] - k5 \cdot [\text{FIIa:Tmod}]$$

Figure 4. Corresponding ODE for FIIa in model 2. k_1 , k_2 , k_3 and k_4 are rate constant of second order and k_5 of first order. [] denotes concentration. Tmod (thrombomodulin), and ATIII (antithrombin III).

In the supporting information of Nayak, et al. article²¹ is possible to find parameter values as well as the initial concentration of the model components.

In both models, the parameters were taken from the literature to later be adjusted based on the assumption of 30% fibrinogen reduction occurred at 10-15 seconds in PT test simulation and at 27-39 seconds in the aPTT test simulation for standard plasma samples in the case of model 1 or to fit in-house in vitro data in the case of model 2.

Once implemented, the models were curated analyzing whether or not they were capable of reproducing the key quantitative results shown in the original publications.

Clinical data

To explore the performance of the two systems pharmacology models described above, beyond the conditions used in the original publications, the dataset available from Menezes and co-workers²⁸, which includes raw individual longitudinal data of thrombin measured in 20 normal subjects and 40 patients with trauma, was integrated. Additional information gathered from each subject during the study was the baseline activation percentage of factors II, V, VII, VIII, IX, X, and ATIII, and the PT and aPTT values.

Simulations

For all the patients, CAT profiles, PT (implemented only in model 2) and aPTT values were obtained simulating with the two selected models. In case of the factors measured in each of the subjects (see above), their initial concentrations were calculated converting the reported percentage into concentration using the initial concentrations of the original models. Table 1 shows this conversion. For initial concentrations per individual check supplementary material table S2 and S3. Initial conditions for factors and proteins that were not reported in the experimental data of Menezes, et al.²⁸ article, were assumed to have a 100% activity percentage.

Table 1. Mean blood factors percentage transformed into concentrations (nM).

	II	V	VII	VIII	IX	X	ATIII
Mean activation percentage from normal subjects reported in Menezes et al. article	78.7%	50.65%	81.6%	32.5%	115.2%	74.6%	83.3%
Mean activation percentage from trauma patients reported in Menezes et al. article	76.6%	48.32%	124.7%	114.57%	104.77%	75.65	87.67%
Initial conditions from model 1	1394.4	26.7	10	0.7	89.6	174.3	-
Normal mean blood factors concentration	1097.39	13.52	8.16	0.23	103.21	130.02	-
Trauma mean blood factors concentration	1068.11	12.90	12.47	0.80	93.8784	131.85795	-
Initial conditions from model 2	1400	20	10	0.7	90	160	3400
Normal mean blood factors concentration	1101.8	10.13	8.16	0.23	103.68	119.36	2832.2
Trauma mean blood factors concentration	1072.4	9.67	12.47	0.80	94.29	121.04	2980.95

The initial conditions to simulate the different coagulation tests are summarized in Table 2. To generate thrombin profiles TF concentration was set to the corresponding value used in Menezes, et al.²⁸. Moreover, the parameters quantifying endogenous production rates of all components of the system were set to 0.

PT and aPTT values were calculated as the time at which 30% of the fibrinogen was transformed to fibrin^{19,21}. Initial concentrations of all components of the models were diluted by one third as described in Wajima, et al. and Nayak, et al articles^{19,21}. Additionally, the endogenous production rates of all components were set to 0. In the

case of aPTT test simulation, the initial concentrations for XIa and XI were set to $0.148 \times XI(0)$ and $0.339 \times XI(0)$, respectively, where $XI(0)$ is the physiologic concentration of factor XI in a plasma sample.

Table 2. Initial conditions for coagulation tests simulations. FXI(0) factor XI initial concentration.

Test/Initial condition	TF	CA	Model components
CAT	0.005 nM	0 nM	Initial concentration
PT	100 nM	0 nM	Initial concentration/3
aPTT	0 nM	100nM	Initial concentration/3 FXI=FXI(0) \times 0.339 FXIa=FXI(0) \times 0.148

Semi-mechanistic PKPD model building

Data analysis

Thrombin concentration versus time profiles were described based on the population approach using Nonlinear Mixed Effect Models (NONMEM) version 7.4³⁰ and First Order Conditional Estimation (FOCE) method with INTERACTION option. Data corresponding to normal subjects and trauma patients were analyzed simultaneously. The observed data recorded at times greater than 25 minutes were excluded from the analysis due to experimental noise. Also, trauma patient 2818 was ignored in the analysis as the associated time profile corresponded to an outlier.

Thrombin experimental data in normal scale as well as logarithmically transformed were used for the analysis. Between subject variability (BSV) was modelled exponentially and residual variability was modelled considering an additive error for time >15 min and a combined error for times < 15 min.

Model building

Models were based on ordinary differential equations and resulted in a simplified version of the systems pharmacology models 1 and 2 which were used as a guide to maintain the mechanistic perspective in the current evaluation.

In the following, the first model fit to the data is described as an example. Figure 5 shows both the schematic and mathematical representation of the model.

The first model probed was the simplest one, where the tissue factor directly activates thrombin synthesis.

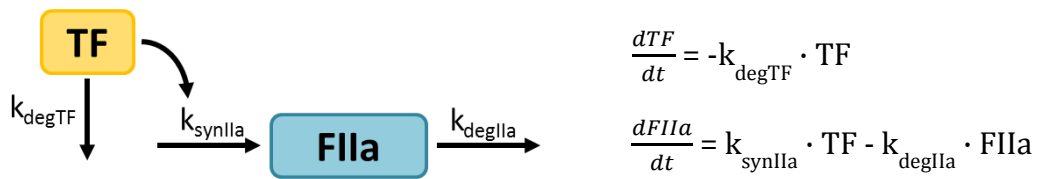


Figure 5. Schematic and mathematical model representation. k_{degTF} is the degradation constant of TF, k_{synIIa} is the synthesis constant of FIIa and k_{degIIa} is the degradation constant of FIIa.

The model assumes that TF (i) is degraded through a first order process characterized by the first order rate constant k_{degTF} , and (ii) triggers the activation of factor II, represented by the first order rate constant k_{synIIa} . The process governed by the first order rate constant k_{degIIa} represents the degradation of FIIa.

Model selection

The log-likelihood ratio test was performed to compare nested models and assist in model selection. It is based on the minimum objective function value (OFV) provided by NONMEM³⁰ for each run. The OFV is approximately equal to -2 times the logarithm of the likelihood of the data and the difference in OFV between two nested models is approximately χ^2 distributed. On the other hand, to compare non-nested models the Akaike Information Criteria (AIC) was used, which was calculated as $AIC = -2LL + 2 \times NP$, where NP is the number of parameters in the model³¹. Other criteria used in the choice of the final model were the precision of parameter estimates and the results for model performance by visual inspection of goodness-of-fit plots (GOFs)³².

Covariate selection

Once the base population model for thrombin profiles of normal subjects and trauma patients was developed, a covariate analysis was performed. As the supplementary material of Menezes, et al²⁸ paper reported blood factors percentage of factors V, VII, VIII, IX, X and ATIII, they were considered for inclusion as covariates in the model. Additionally, the disease condition (normal or trauma) was also considered as categorical covariate.

Covariate selection was performed using the stepwise covariate modelling (SCM) implemented in the Perl-speaks-Nonmem (PsN) software (v.4.4.8)³³ with a level of

significance of 0.05 during the forward inclusion and of 0.01 during the backward deletion.

Model evaluation

Thrombin model was evaluated through visual predictive checks (VPCs). A total of 500 datasets with the same characteristics as the original dataset were simulated. The 5th, 50th and 95th percentiles of simulated observations in each dataset were computed. Then, the 90% confidence interval of each calculated percentile was obtained and plotted against the 5th, 50th and 95th of raw thrombin data. On the other hand, parameter estimates precision was obtained from the analysis of 500 bootstrap datasets using PsN software³³.

3. RESULTS

Model implementation and evaluation of the implementation

Both models were satisfactorily implemented, as shown by the exact reproduction of the results presented in both manuscripts (Figure 6). The rest of the graphics that appear in the articles along with their simulated version obtained in the current evaluation are shown supplementary material S4.

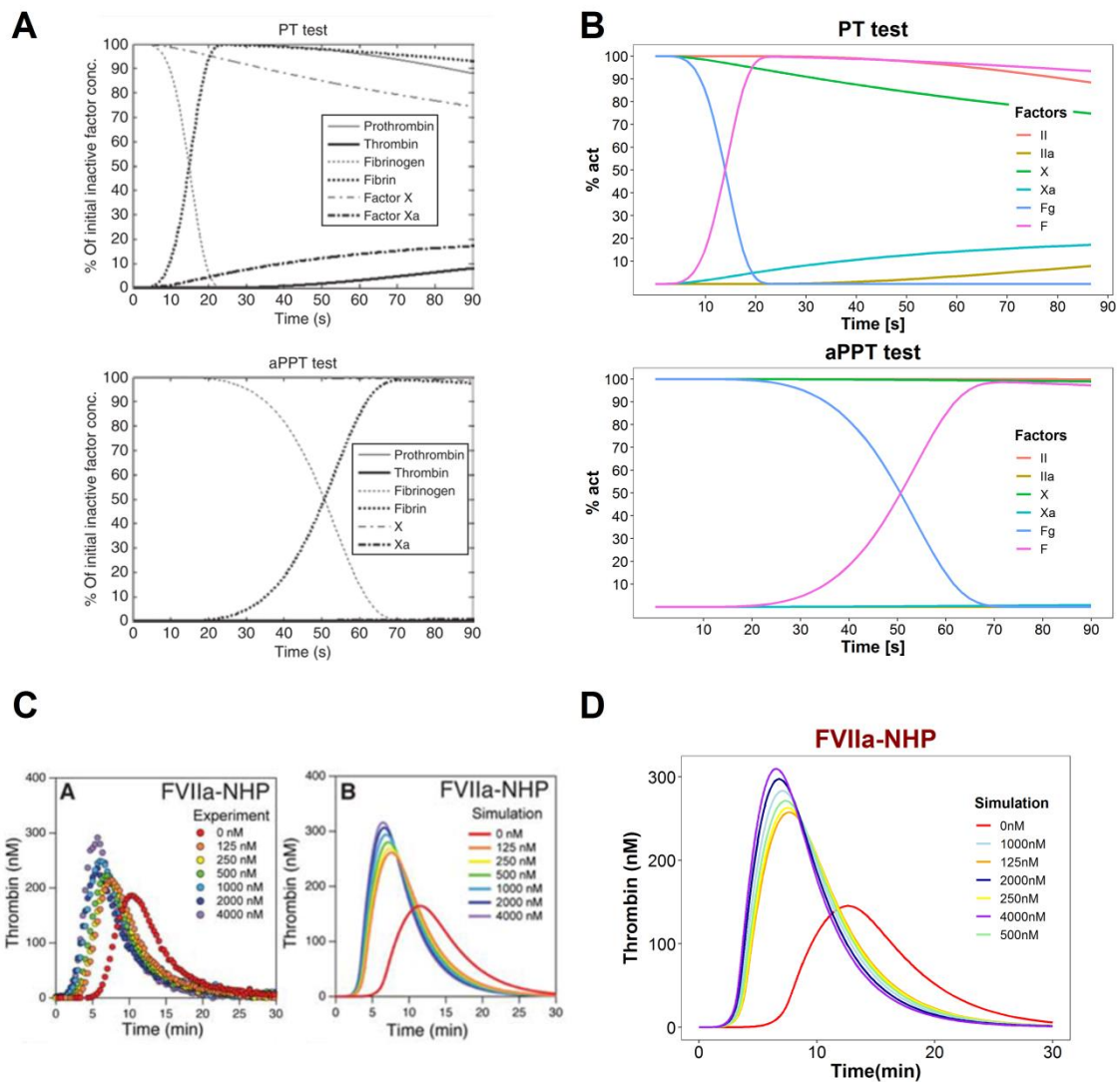


Figure 6. Graphical representation for the simulated profiles from Wajima et al. and Nayak et al. articles and their respective representation after implementation using Simbiology. A. Graphics obtained from Wajima, et al. article. B. Simulations performed with Simbiology with model 1. C. Graphics obtained from Nakay, et al. article. D. Simulations performed with Simbiology with model 2.

Clinical data integration in the models and simulation

CAT simulations

Figure 7 shows the thrombin raw data reported by Menezes et al.²⁸, for normal subjects (upper panel) and trauma patients (lower panel). The blue line represents the mean of the raw data. In general, the values of thrombin are higher in trauma patients concerning normal individuals. In panel 7B the subject with a profile considered to be outlier is highlighted in red.

The corresponding simulated profiles using (i) the mean values obtained with the reported percentage of activation for factors II, V, VII, VIII, IX, X, and ATIII (Table 1) and (ii) the initial conditions reported in each model for the rest of components, appear superimposed in Figure 7.

As it can be observed, there are apparent discrepancies between the mean of the observed and simulated profiles.

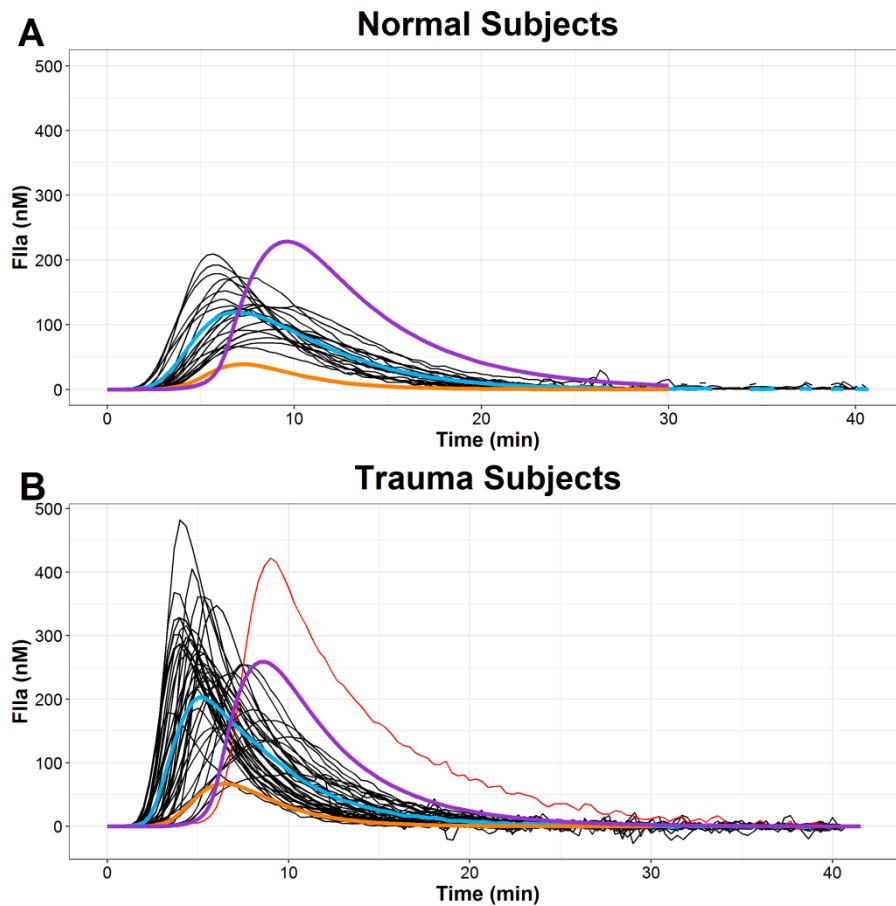


Figure 7. CAT profiles of the experimental data for A normal subjects and B trauma patients. Black lines represent the individual raw data. Blue line the mean of the raw data, the orange and purple line the simulations obtained with model 1 and model 2 respectively. Red line represents the outlier.

Simulations obtained from model 1 provided profiles showing lower levels of thrombin for both type of patients. On the contrary, the results obtained after the application of model 2, pointed in the other direction, especially for normal subjects. In the trauma patients, the two mean curves are quite similar in magnitude but delayed in the case of the simulated profile. Supplementary material S5 shows the individual observed and simulated profiles.

Table 3 lists the values of maximal thrombin levels in the studied scenarios (observed and simulated) where the differences seen in the full profiles are summarized. Relative errors (RE) were calculated as it is shown in equation 1.

$$\% \text{ RE} = \frac{\text{Sim value} - \text{Ref value}}{\text{Ref value}} \times 100 \quad \text{Equation 1}$$

where Sim value represents the simulated thrombin peak obtained with model 1 or model 2 and Ref value the thrombin peak of Menezes, et al. mean data.

Table 3. Thrombin peak concentration in different situations with corresponding relative errors.

		Thrombin peak (nM)	Relative error (%)
Normal subjects	Menezes	119.20	-
	Wajima	38.89	-67.37
	Nayak	228.38	91.59
Trauma patients	Menezes	202.81	-
	Wajima	67.16	-66.89
	Nayak	259.14	27.77

Sensitivity analysis

To explore the impact of the initial conditions of those coagulation factors that were not measured in the Menezes, et al., manuscript¹⁹ on the thrombin vs time profiles, a sensitivity analysis was performed. That univariate analysis consisted of simulating the thrombin profiles modifying the initial condition of each factor $\pm 30\%$ of the value originally reported^{19,21}.

Results shown in Figure 8 indicate that in general, the impact of initial conditions was negligible except for the TF in both models and TFPI in the case of model 2, but in any case not enough to explain the discrepancies represented in Figure 7.

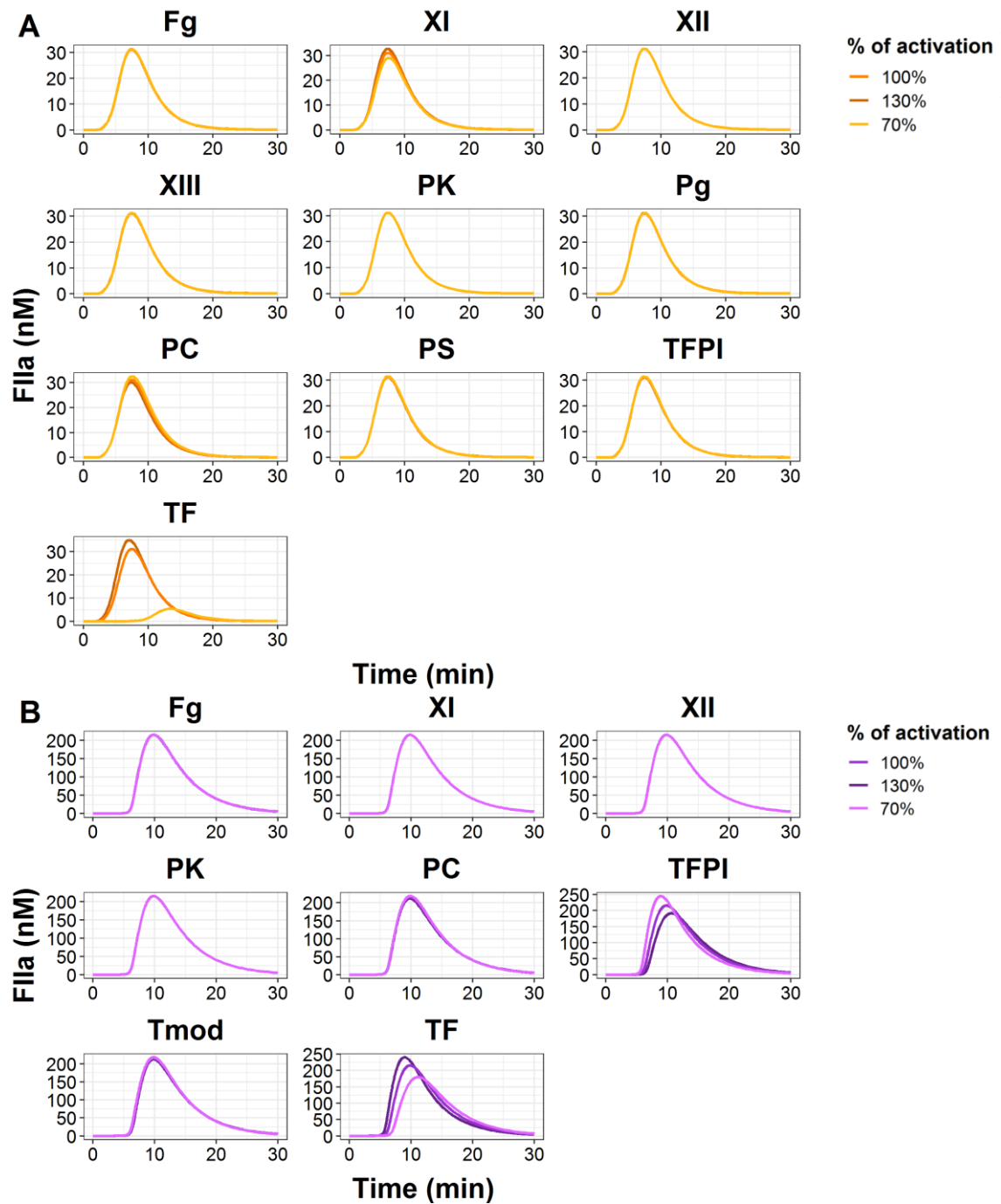


Figure 8. Results from the sensitivity analysis, A (model 1), B (model 2). The top of each panel indicates the factor in which initial conditions were changed $\pm 30\%$ of the reported values in each model.

PT and aPTT simulations

Figure 9 compares the PT and aPTT values reported by Menezes, et al.²⁸ with those obtained from model 1 (PT and aPTT) and model 2 (aPTT). For the case of PT, mean simulated values agreed well with the mean of the observations for normal subjects and patients, being all the values within the normal range.

aPTT resulted overpredicted in models 1 and 2 with respect the mean observed value in normal subjects and in patients with trauma as well, although both models predicted a reduction in aPTT in trauma patients with respect to normal subjects as seen with the mean observed values.

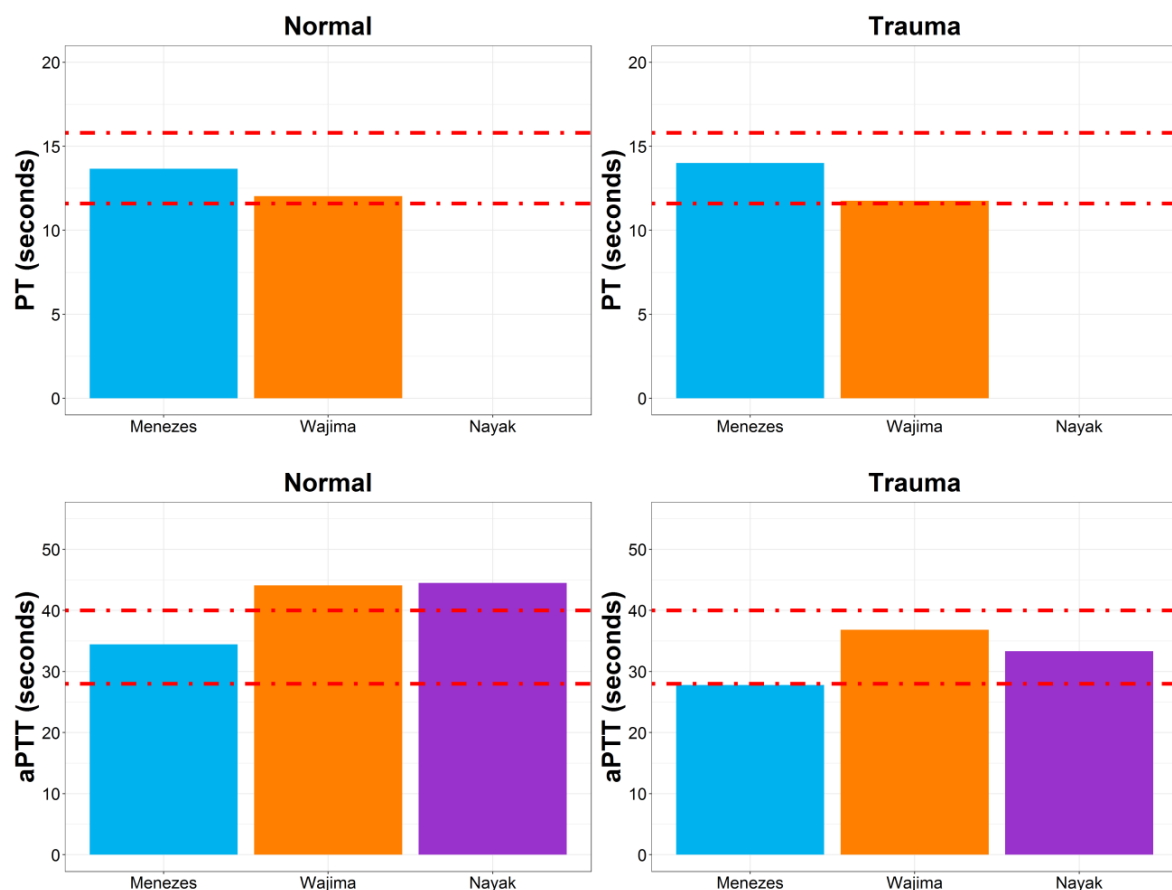


Figure 9. Mean PT (upper) and aPTT (lower) values for normal subjects (left) and trauma patients (right). Histograms in blue, orange and purple represent observations, and simulated values from models 1 and 2, respectively. The red dotted dashed lines represent the range values of PT and aPTT metrics in normal subjects.

Supplementary material S5 shows the individual PT and aPTT values obtained by simulation for normal subjects.

Modelling thrombin profiles

General description of the data

Figure 10 shows the individual thrombin vs time profiles with and without logarithmic transformation. A latency time, likely associated with all mechanisms preceding thrombin formation, was observed. In addition, a greater magnitude of noise from time 25 min onwards was detected, justifying the decision to not consider those latter points for the analysis.

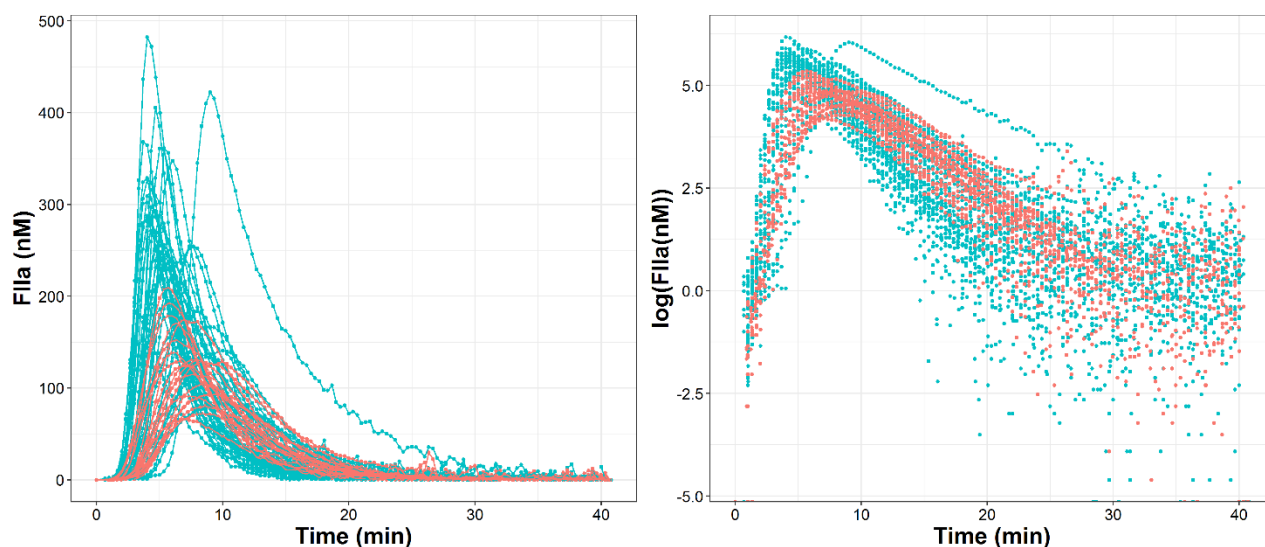


Figure 10. Observed vs time profiles of thrombin (blue for normal subjects and red for trauma patients) used during the population pharmacokinetic/pharmacodynamics analysis shown in natural scale (left) and after logarithmic transformation (right).

Table 4 provides a summary of the covariates gathered in the normal and patient population in Menezes et al. We can observe some differences between trauma and normal subjects, which only reach significance for FVIII, probably due to the large variability in the data.

Table 4. Summary of coagulation factor values per subject condition.

Factors (nM)	Normal subjects		Trauma patients		Total individuals	
	Median	Min-Max	Median	Min-Max	Median	Min-Max
FII	1108.5	725.1-1338.06	1052.8	474.09-1784.83	1066.71	474.09-1784.83
FV	11.61	8.81-25.63	12.95	0.27-25.63	12.54	0.27-25.63
FVII	7.75	4.6-11.2	7.85	4.8-59.7	7.85	4.6-59.7
FVIII	0.22 ****	0.15-0.34	0.55 ****	0.24-3.71	0.47	0.15-3.71
FIX	102.59	53.76-136.19	85.57	26.88-178.30	93.63	26.88-178.30
FX	129.85	78.44-162.1	129.85	61.01-207.42	129.85	61.01-207.42
ATIII	2805	2244-3332	2907	1768-5100	2873	1768-5100

**** p<0.0001 Significant differences between normal subjects and trauma patients. For the comparison a Wilcoxon test was used.

Figure 11 shows the scatterplot matrix of the covariates listed in Table 4, where for several pairs correlations showed values greater than 0.3³⁴.

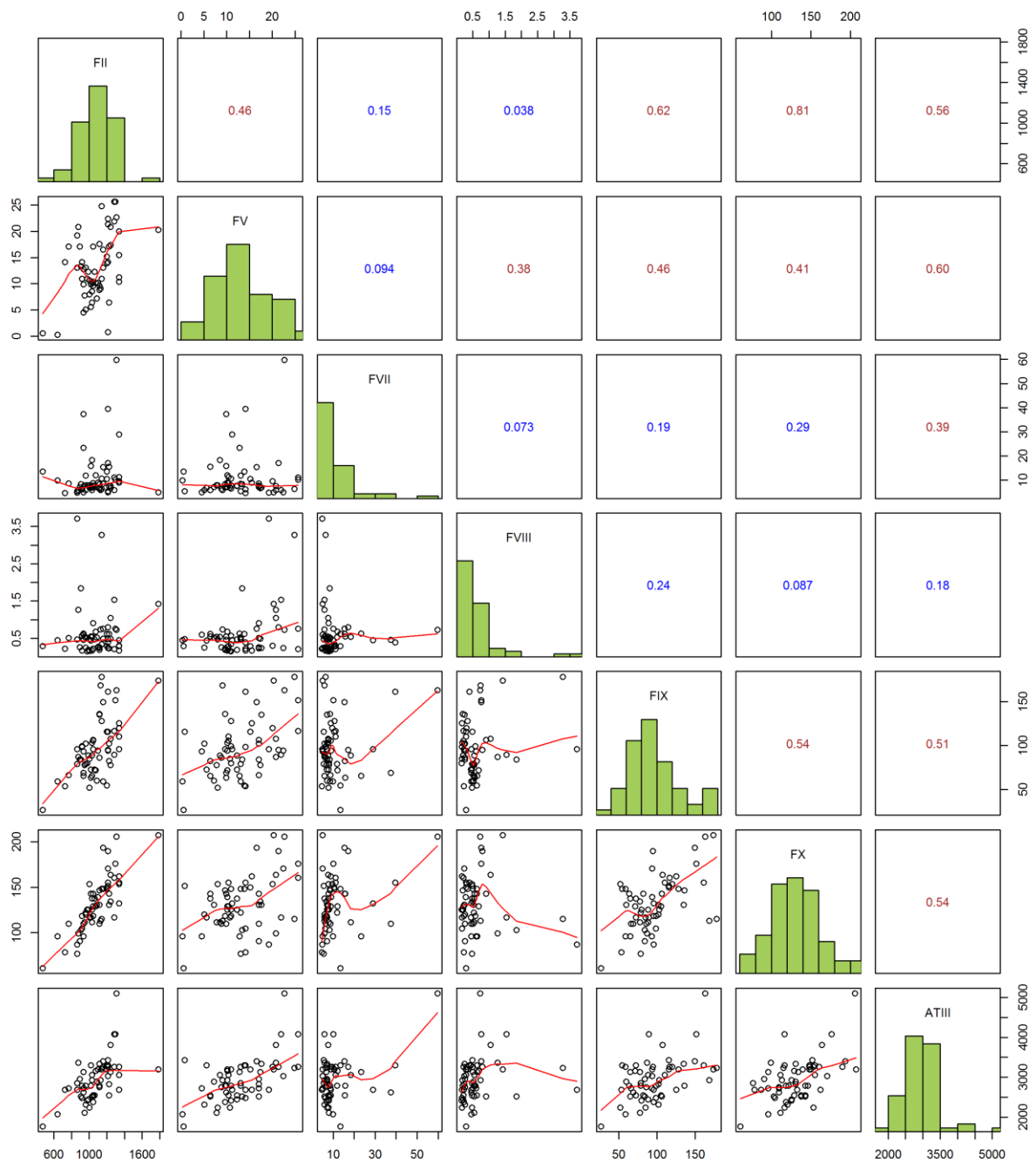


Figure 11. Scatterplot matrix of the coagulation factors gathered for the subject population in Menezes and co-authors.

Semi-mechanistic PKPD model for the coagulation process

Figure 12 provides a schematic representation of the model finally selected between different candidates based on the previously described criteria for model selection.

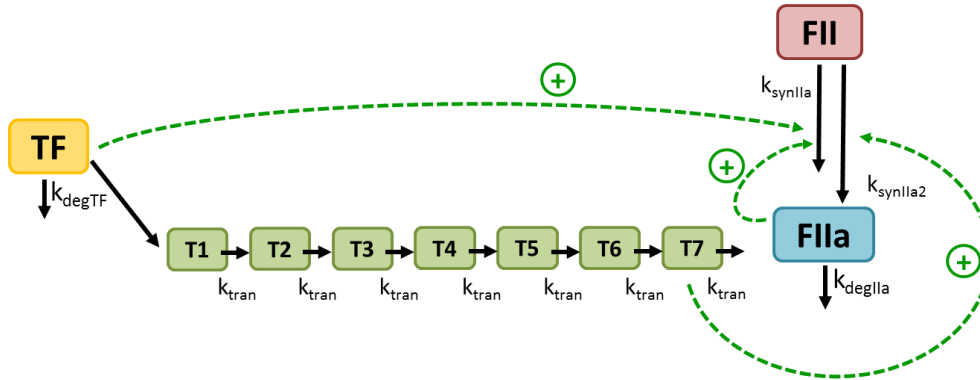


Figure 12. Schematic representation of the population pharmacokinetic/pharmacodynamic model selected describing the time course of thrombin levels “*in vivo*”.

Briefly, the model assumes that once TF is present (i) a direct activation effect is triggered characterized by the second order rate constant k_{synIIa} and (ii) a second activation pathway is initiated which appears with a certain delay with respect to TF characterized by a chain of seven transit compartments and the second order rate constant $k_{synIIa2}$. In addition, the model includes a regulatory mechanism depending on the thrombin generated.

The following set of differential equations represents mathematically the model shown in Figure 12:

$$\frac{dTF}{dt} = -k_{degTF} \cdot TF$$

$$\frac{dT1}{dt} = k_{tran} \cdot TF - k_{tran} \cdot T1$$

$$\frac{dT2}{dt} = k_{tran} \cdot T1 - k_{tran} \cdot T2$$

$$\frac{dT3}{dt} = k_{tran} \cdot T2 - k_{tran} \cdot T3$$

$$\frac{dT4}{dt} = k_{tran} \cdot T3 - k_{tran} \cdot T4$$

$$\frac{dT5}{dt} = k_{tran} \cdot T4 - k_{tran} \cdot T5$$

$$\frac{dT6}{dt} = k_{tran} \cdot T5 - k_{tran} \cdot T6$$

$$\frac{dT7}{dt} = k_{tran} \cdot T6 - k_{tran} \cdot T7$$

$$\frac{dFII}{dt} = -k_{synIIa} \cdot TF \cdot FII \cdot (1 + FIIa) - k_{synIIa2} \cdot T7 \cdot FII$$

$$\frac{dFIIa}{dt} = k_{synIIa} \cdot TF \cdot FII \cdot (1 + FIIa) + k_{synIIa2} \cdot T7 \cdot FII - k_{degIIa} \cdot FIIa$$

where k_{degTF} is the first order degradation rate constant of TF, k_{tran} is the first order rate constant of transfer between transit compartments, k_{synIIa} and k_{synIIa2} are the second order rate constants of thrombin synthesis and k_{degIIa} is the first order degradation rate constant of FIIa.

Once the final model was established the covariate study was performed to test significant effects. The set of continuous covariates tested for each parameter in the model were FII, FV, FVII, FVIII, FIX, FX and ATIII, exploring linear and nonlinear relationships. Also, patient condition (normal or trauma) was tested as categorical covariate. The selected full covariate model obtained in the forward-inclusion approach comprised the following covariate effects: FVIII on k_{synIIa} categorizing FVIII concentration and FX on k_{tran} as continuous covariate. Since the categorical covariate, patient condition was significantly correlated with FVIII, its inclusion was tested separately. In this sense, patient condition resulted significant for k_{synIIa} , k_{degIIa} and k_{tran} . Due to convergence problems in the estimation, we decided to estimate separately normal and trauma model parameters, and consequently, a substantial improvement of fit was shown compared with the base model, as reflected in the decrease of OFV and the diagnostics plots (data not shown).

When comparing normal subject and trauma patient parameter estimates, a significant change was observed in the k_{synIIa} value. As abovementioned, FVIII covariate effect was shown to be significant for k_{synIIa} and correlated with patient condition, however, when the relationship between them was studied more deeply (Figure 13), no clear relationship was observed (probably due to the high variability on FVIII levels within the two populations), therefore the covariate was not included.

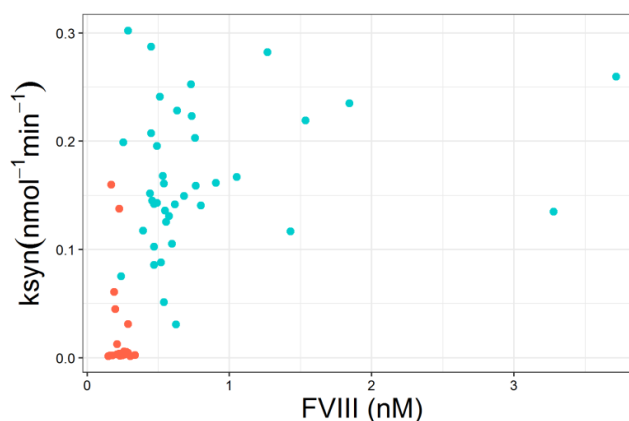


Figure 13. Graphical representation of the relationship between k_{synIIa} parameter and FVIII for normal subjects (red) and trauma patients (blue).

Modelling the coagulation cascade

Table 5 lists the estimates of model parameters and their corresponding precision represented by 95% confidence interval computed from the bootstrap analysis. It is worth noting that in none of the cases the 95% confidence intervals include the zero value, indicating that parameters were significant for the model. All estimates lie within the 95% confidence interval obtained by bootstrap, what denotes the model robustness. However, k_{synIIa} for normal subjects elicits a wide range, reflecting the poor precision in parameter estimation. The BSV was estimated for k_{synIIa} , k_{degIIa} , k_{tran} and k_{synIIa2} , which ranged from 0.02 to 5.73, reflecting the high dispersion in the data. K_{degTF} parameter was fixed to 0 min^{-1} due to the slow degradation in vitro ($0.05 \text{ h}^{-1} = 0.0008 \text{ min}^{-1}$)¹⁹ assuming that TF concentrations were constant over the experiment.

Table 5. Estimates for the final model parameters and their variability with their corresponding confidence intervals.

Parameter	Estimate	95%CI*	BSV	95%CI*	Shrinkage (%)
kdegTF (min^{-1})	0	NA	NA	NA	0
ksynIIa($\text{nmol}^{-1}\text{min}^{-1}$) (Normal)	0.0047	(0.0002-0.0179)	5.73	(2.11-39.94)	63
ksynIIa ($\text{nmol}^{-1}\text{min}^{-1}$) (Trauma)	0.15	(0.118-0.178)	0.26	(0.09-0.81)	25
kdegIIa (min^{-1}) (Normal)	1.04	(0.949-1.139)	0.041	(0.02-0.06)	38
kdegIIa (min^{-1}) (Trauma)	0.79	(0.744-0.856)	0.064	(0.04-0.08)	14
ktran (min^{-1}) (Normal)	1.38	(1.24-1.53)	0.055	(0.03-0.07)	38
ktran (min^{-1}) (Trauma)	1.8	(1.59-2.072)	0.176	(0.012-0.23)	14
ksynIIa2($\text{nmol}^{-1}\text{min}^{-1}$) (Normal)	46.7	(43.53-50.24)	0.02	(0.002-0.03)	41
ksynIIa2($\text{nmol}^{-1}\text{min}^{-1}$) (Trauma)	44.6	(39.89-49.92)	0.113	(0.06-0.15)	18
Correlations					
BSV k_{degIIa} -BSV k_{tran} (normal)	-	-	-0.03	-	-
BSV k_{tran} -BSV k_{synIIa2} (normal)	-	-	0.015	-	-
BSV k_{degIIa} -BSV k_{tran} (trauma)	-	-	-0.07	-	-
BSV k_{degIIa} -BSV k_{synIIa2} (trauma)	-	-	0.064	-	-
Residual error (Time>15)	2.06 (additive)	(1.97-3.09)	-	-	2
Residual error (Time<15)	2.43 (additive)	(1.29-2.8)	-	-	2
	0.178 (proportional)	(0.14-0.21)	-	-	2

*95% confidence interval calculated from 500 bootstrap datasets.

Figure 14 shows the individual observed and model predicted profiles indicating an excellent model performance at the individual level.

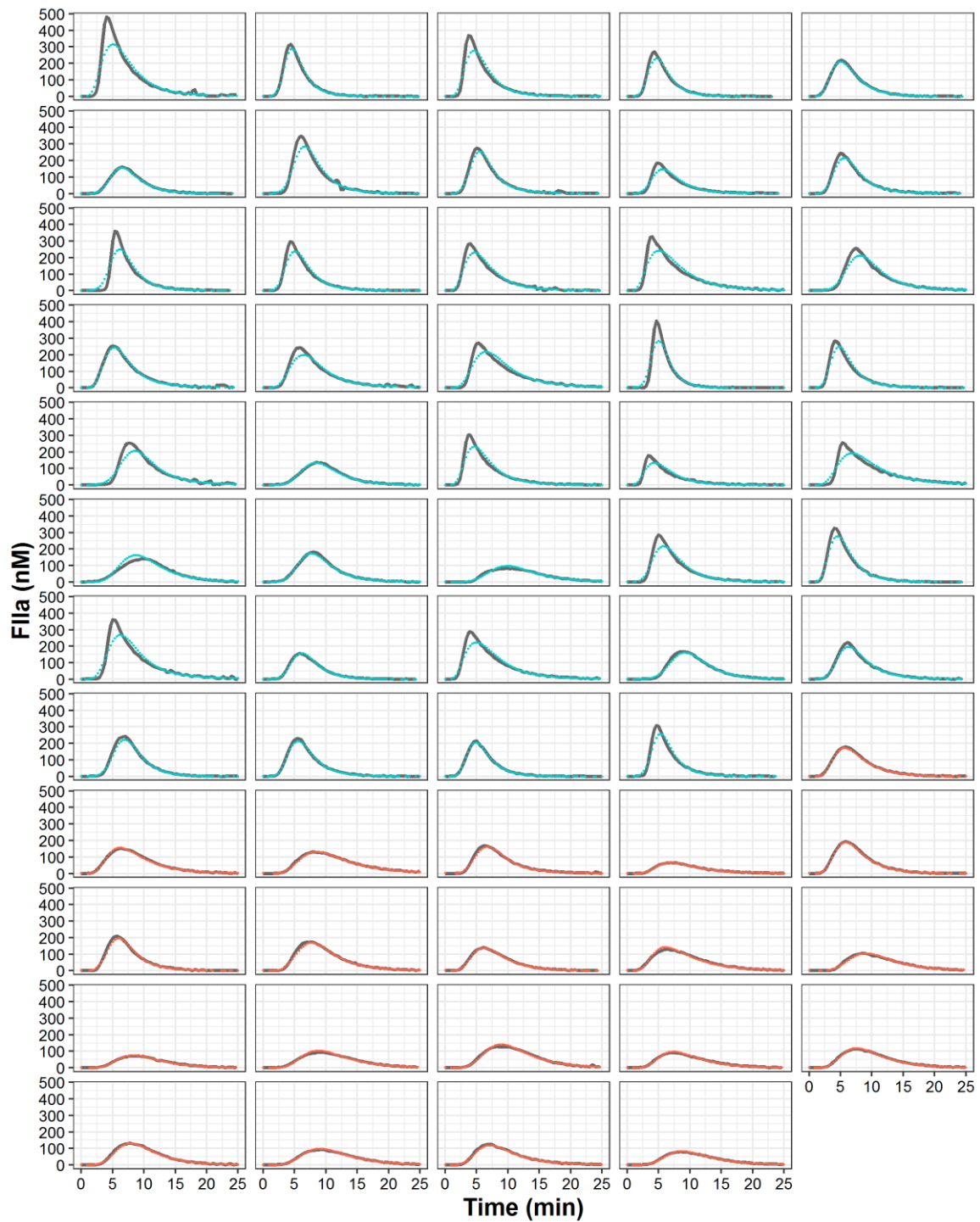


Figure 14. Individual thrombin observations (red dots, normal subjects; blue dots, trauma patients) and individual model predictions (gray lines) versus time.

Figure 15 shows the goodness of fit plots and Figure 16 shows the results of the VPC corresponding to thrombin profile stratify by subject population (normal vs trauma). The model performs adequately in capturing the central trend, and the dispersion of the data.

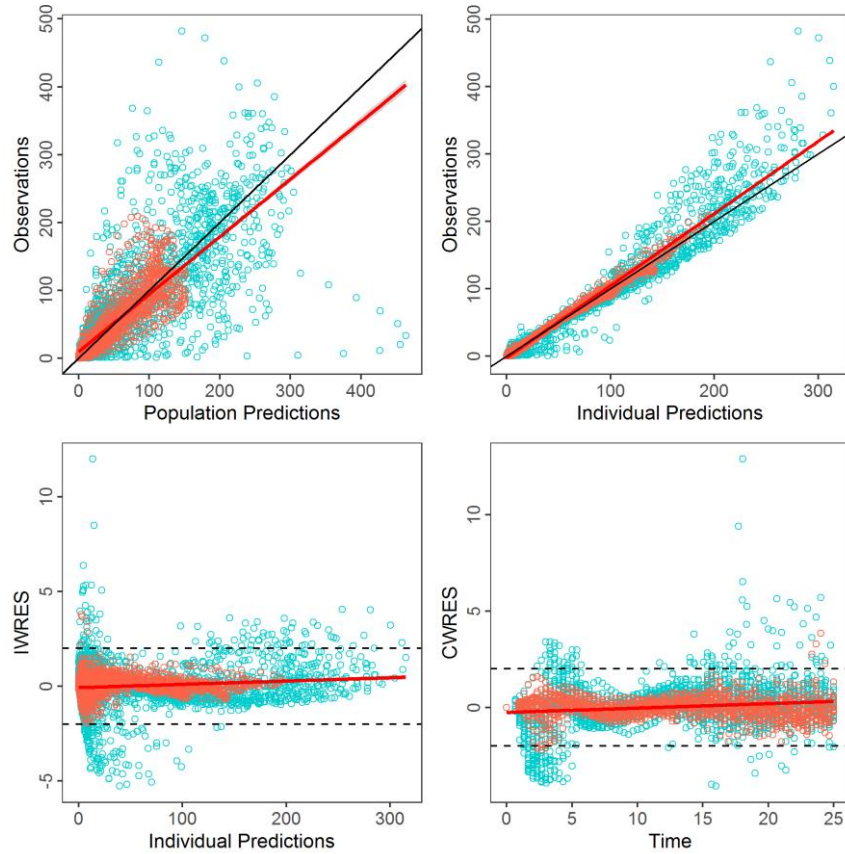


Figure 15. Goodness of fit plots corresponding to the selected semi-mechanistic model. Circles are the observed data (red normal and blue trauma). Black lines represent the perfect fit. Solid red lines represent a smooth curve through the data.

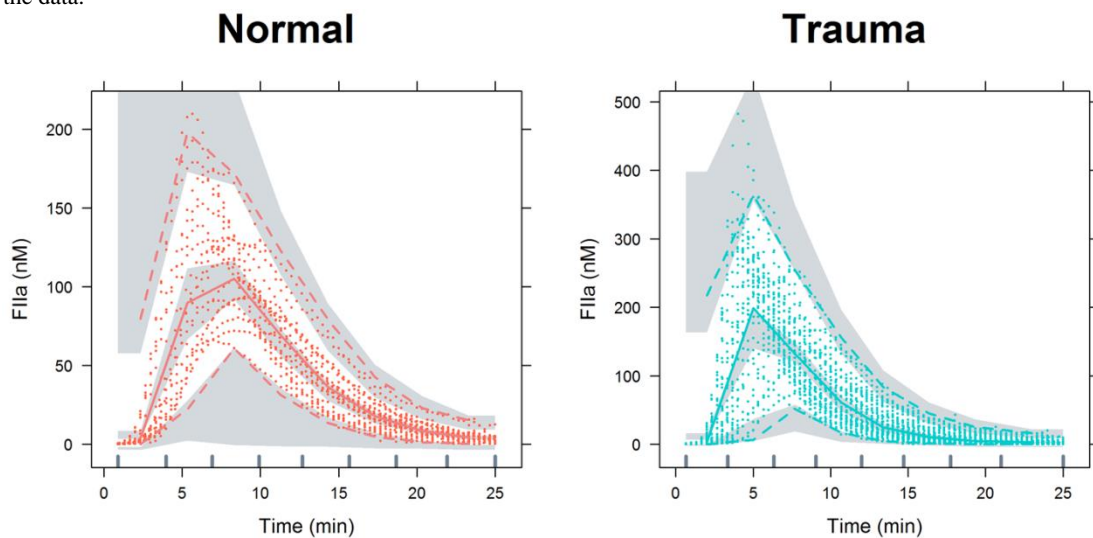


Figure 16. Visual predictive checks corresponding to thrombin profiles in normal subjects and trauma patients. Red and blue dots represent thrombin observations; the solid red and blue lines correspond to the median of the observed data while the dashed red and blue lines the 5 and 95 percentiles of the observations. Shaded grey areas are the 90% predicted intervals for corresponding percentiles obtained from 500 simulated studies.

4. DISCUSSION

The coagulation process is crucial for human life. For this reason, understanding the different elements and key players and the associated pathologies is needed to individualize the therapy and optimize the patient prognosis. In this sense, mathematical models are a very useful tool that can help to predict the coagulation dynamics and simulate different scenarios.

The objective of this work was to implement and compare two systems pharmacology models publicly available to finally challenge them against raw data consisting on individual thrombin profiles measured “*in vitro*” from normal subjects and patients with trauma. To the best of our knowledge, this evaluation is the first time that the capabilities of two models from the point of view of describing individual data have been compared.

Both models were adequately implemented in the Simbiology platform, as all the results shown in the original publications were reproduced almost exactly. However, disappointing results were obtained when simulated thrombin profiles generated from the two models were compared. Discrepancies were far from negligible questioning which model should be used in the future to explore *in silico* scenarios regarding drug development or patient management. Moreover, both models failed to describe raw thrombin time profiles. Noteworthy is the fact that the results from the local sensitivity analysis could not make the observed and simulated profiles closer.

Different possibilities can be considered to explain those results. First, the systems pharmacology models were adjusted to describe *ex-vivo* experimental data, and therefore the experimental conditions should be controlled tightly and reported carefully. In this context, for example, one of the models can be used to calculate both PT and aPTT values, whereas for the other calculation of PT is not possible. The main differences regarding assumptions and structure of both systems pharmacology models are shown in the supplementary material S7.

The fact that none of the models could describe the full thrombin vs time profiles in the vast majority of the subjects might be explained by the use of typical parameters and typical initial conditions for the rest of coagulation factor not measured. Nevertheless, some results obtained during this evaluation deserve discussion. For example relative changes in aPTT found in trauma patients with respect normal subjects could be reproduced by both models.

The outcome of our simulations motivated us to develop a semi-mechanistic PKPD model to describe thrombin concentration profiles over time after adding TF. The developed model successfully describes the experimental observations in normal subjects as well as in trauma patients. This resembles main mechanisms represented with much higher granularity in the models 1 and 2.

In models 1 and 2 the conversion of prothrombin to thrombin is governed by the FXa and the complex Xa:Va reactions. In line with these models, the developed semi-mechanistic model describes two different mechanisms for thrombin formation. The reaction ruled by the k_{synIIa} constant (responsible for a quick burst of thrombin) would correspond with the FXa reaction in models 1 and 2. On the other hand, the k_{synIIa2} constant, responsible for generating large thrombin concentrations, would correspond with Xa:Va reaction. These two mechanisms are in agreement with the cell-based model of the coagulation proposed by Hoffmann⁴, in which the first thrombin synthesis corresponds with the initiation phase and the second one with the propagation phase. Nevertheless, when relating parameter values, due to differences in the structure of the models, it is difficult to compare the estimates even though the mechanisms and involved entities are similar. The degradation rate constant of FIIa was the only parameter subject for comparison providing similar values for the developed model and model 1 (1.04 min^{-1} for normal subjects and 1.12 min^{-1} , respectively). Moreover, Gulati, et al.³⁴ obtained a comparable value for degradation rate constant of FIIa (0.97 min^{-1}). These authors reduced Wajima, et al. systems pharmacology model¹⁹ through proper lumping to estimate parameters for describing fibrinogen concentrations vs time profiles obtained from venom-induced consumption coagulopathy patients data.

Regarding k_{degTF} parameter, it was fixed to 0 in our model because of the assumed slow degradation rate “*in vitro*” from model 1 (reflected by a half-life of 831 min) compared

to the length experimental procedure (40 min), therefore assuming constant TF concentrations over the experiment.

However, our model presents some limitations. Firstly, the analysis was performed in a little fraction of population, including only normal subjects and trauma patients, with a high between-subject variability. This limitation inquiries model predictability and generalization. Nevertheless, the simulations performed with the VPC suggest that the model performs adequately and predicts well the raw data. The second limitation is that the model was built based on Menezes, et al. data, which only provided the concentration for some coagulation factors. The possibility of including the concentration of activated factors could represent an opportunity in order to discern between normal subjects and trauma patients, and therefore provide more accurate predictions depending on the patient condition.

In conclusion, systems pharmacology models are very useful when understanding processes involve in biological systems. However, up-to-date they tend to fail at the time to describe and predict individual data. Nevertheless, their structure facilitates the development of mechanistic-based models that can be fit to the data providing meaningful and precise model parameters as well as adequate model predictions. This type of models can result very useful at the time to treat particular individuals personalizing their dosage.

5. REFERENCES

1. Gale, A. Current understanding of hemostasis. *Toxicol Pathol.* **39**, 273–280 (2011).
2. Palta, S., Saroa, R. & Palta, A. Overview of the coagulation system. *Indian J. Anaesth.* **58**, 515–523 (2014).
3. Hoffman, M. A cell-based model of coagulation and the role of factor VIIa. *Blood Rev.* **17**, 51–55 (2003).
4. Hoffman, M. & Monroe, D. M. A cell-based model of hemostasis. *Thromb. Haemost.* **85**, 958–65 (2001).
5. Hoffman, M. M. & Monroe, D. M. Rethinking the coagulation cascade. *Curr. Hematol. Rep.* **4**, 391–6 (2005).
6. Quick A.J. The prothrombin time in haemophilia and in obstructive jaundice. *J. Biol. Chem.* **109:73-4**, (1935).
7. LANGDELL, R. D., WAGNER, R. H. & BRINKHOUS, K. M. Effect of antihemophilic factor on one-stage clotting tests; a presumptive test for hemophilia and a simple one-stage antihemophilic factor assay procedure. *J. Lab. Clin. Med.* **41**, 637–47 (1953).
8. Lancé, M. D. A general review of major global coagulation assays: Thrombelastography, thrombin generation test and clot waveform analysis. *Thromb. J.* **13**, 1–6 (2015).
9. Macfarlane, R. & Biggs, R. A Thrombin Generation Test. The application in haemophilia and Thrombocytopenia. *J. Clin. Pathol.* **6**, 3–9 (1953).
10. Hemker, H. C. *et al.* Calibrated automated thrombin generation measurement in clotting plasma. *Pathophysiol. Haemost. Thromb.* **33**, 4–15 (2003).
11. Ataullakhanov, F. I. & Panteleev, M. A. Mathematical Modeling and Computer Simulation in Blood Coagulation. *Pathophysiol. Haemost. Thromb.* **34**, 60–70 (2005).
12. Qiao, Y., Liu, J. & Zeng, Y. A kinetic model for simulation of blood coagulation and inhibition in the intrinsic path. *J. Med. Eng. Technol.* **29**, 70–74 (2005).
13. Qiao, Y. H. *et al.* The kinetic model and simulation of blood coagulation—the kinetic influence of activated protein C. *Med. Eng. Phys.* **26**, 341–347 (2004).
14. Mann, K. G., Butenas, S. & Brummel, K. The dynamics of thrombin formation. *Arterioscler. Thromb. Vasc. Biol.* **23**, 17–25 (2003).
15. Chatterjee, M. S., Denney, W. S., Jing, H. & Diamond, S. L. Systems biology of coagulation initiation: Kinetics of thrombin generation in resting and activated human blood. *PLoS Comput. Biol.* **6**, (2010).
16. Zhou, X., Huntjens, D. R. H. & Gilissen, R. A. H. J. A systems pharmacology model for predicting effects of Factor Xa inhibitors in healthy subjects: Assessment of pharmacokinetics and binding kinetics. *CPT Pharmacometrics Syst. Pharmacol.* **4**, 650–659 (2015).
17. Hartmann, S., Biliouris, K., Lesko, L. J., Nowak-Göttl, U. & Trame, M. N. Quantitative Systems Pharmacology Model to Predict the Effects of Commonly Used Anticoagulants on the Human Coagulation Network. *CPT Pharmacometrics Syst. Pharmacol.* **5**, 554–564 (2016).
18. Mann, K. G., Brummel-Ziedins, K., Orfeo, T. & Butenas, S. Models of blood coagulation. *Blood Cells, Mol. Dis.* **36**, 108–117 (2006).
19. Wajima, T., Isbister, G. K. & Duffull, S. B. A comprehensive model for the humoral coagulation network in humans. *Clin. Pharmacol. Ther.* **86**, 290–298 (2009).

20. Hockin, M. F., Jones, K. C., Everse, S. J. & Mann, K. G. A model for the stoichiometric regulation of blood coagulation. *J. Biol. Chem.* **277**, 18322–18333 (2002).
21. Nayak, S. *et al.* Using a Systems Pharmacology Model of the Blood Coagulation Network to Predict the Effects of Various Therapies on Biomarkers. *CPT Pharmacometrics Syst. Pharmacol.* **4**, 396–405 (2015).
22. Lee, D. *et al.* A quantitative systems pharmacology model of blood coagulation network describes in vivo biomarker changes in non-bleeding subjects. *J. Thromb. Haemost.* **14**, 2430–2445 (2016).
23. Wang, R. S., Saadatpour, A. & Albert, R. Boolean modeling in systems biology: An overview of methodology and applications. *Phys. Biol.* **9**, (2012).
24. Chudasama, V. L., Ovacik, M. A., Abernethy, D. R. & Mager, D. E. Logic-Based and Cellular Pharmacodynamic Modeling of Bortezomib Responses in U266 Human Myeloma Cells. *J. Pharmacol. Exp. Ther.* **354**, 448–458 (2015).
25. Ramakrishnan, V. & Mager, D. E. Network-Based Analysis of Bortezomib Pharmacodynamic Heterogeneity in Multiple Myeloma Cells. *J. Pharmacol. Exp. Ther.* **365**, 734–751 (2018).
26. Bloomingdale, P., Nguyen, V. A., Niu, J. & Mager, D. E. Boolean network modeling in systems pharmacology. *J. Pharmacokinet. Pharmacodyn.* **45**, 159–180 (2018).
27. Tylutki, Z., Polak, S. & Wiśniowska, B. Top-down, Bottom-up and Middle-out Strategies for Drug Cardiac Safety Assessment via Modeling and Simulations. *Curr. Pharmacol. Reports* **2**, 171–177 (2016).
28. Menezes, A. A., Vilardi, R. F., Arkin, A. P. & Cohen, M. J. Targeted clinical control of trauma patient coagulation through a thrombin dynamics model. *Sci. Transl. Med.* **9**, 1–12 (2017).
29. MATLAB and Statistics Toolbox Release 2017a, The MathWorks, Inc., Natick, Massachusetts, U. S. No Title.
30. R., B. NONMEM Users Guide Introduction to NONMEM 7.4.0. ICON Development Solutions Ellicott City, MD 2011.
31. H., A. FACTOR ANALYSIS AND AIC. *PSYCHOMETRIK* **52**, 317–332 (1987).
32. Mould, D. R. & Upton, R. N. Basic Concepts in Population Modeling, Simulation, and Model-Based Drug Development—Part 2: Introduction to Pharmacokinetic Modeling Methods. *CPT Pharmacometrics Syst. Pharmacol.* **2**, e38 (2013).
33. Lindbom, L., Pihlgren, P., Jonsson, E. N. & Jonsson, N. PsN-Toolkit--a collection of computer intensive statistical methods for non-linear mixed effect modeling using NONMEM. *Comput. Methods Programs Biomed.* **79**, 241–57 (2005).
34. Gulati, a, Isbister, G. K. & Duffull, S. B. Scale reduction of a systems coagulation model with an application to modeling pharmacokinetic-pharmacodynamic data. *CPT pharmacometrics Syst. Pharmacol.* **3**, e90 (2014).

SUPPLEMENTARY MATERIAL

Figure S1A. The scheme of the model for coagulation process developed by Wajima and co-authors (Adapted from the original article)¹⁹.

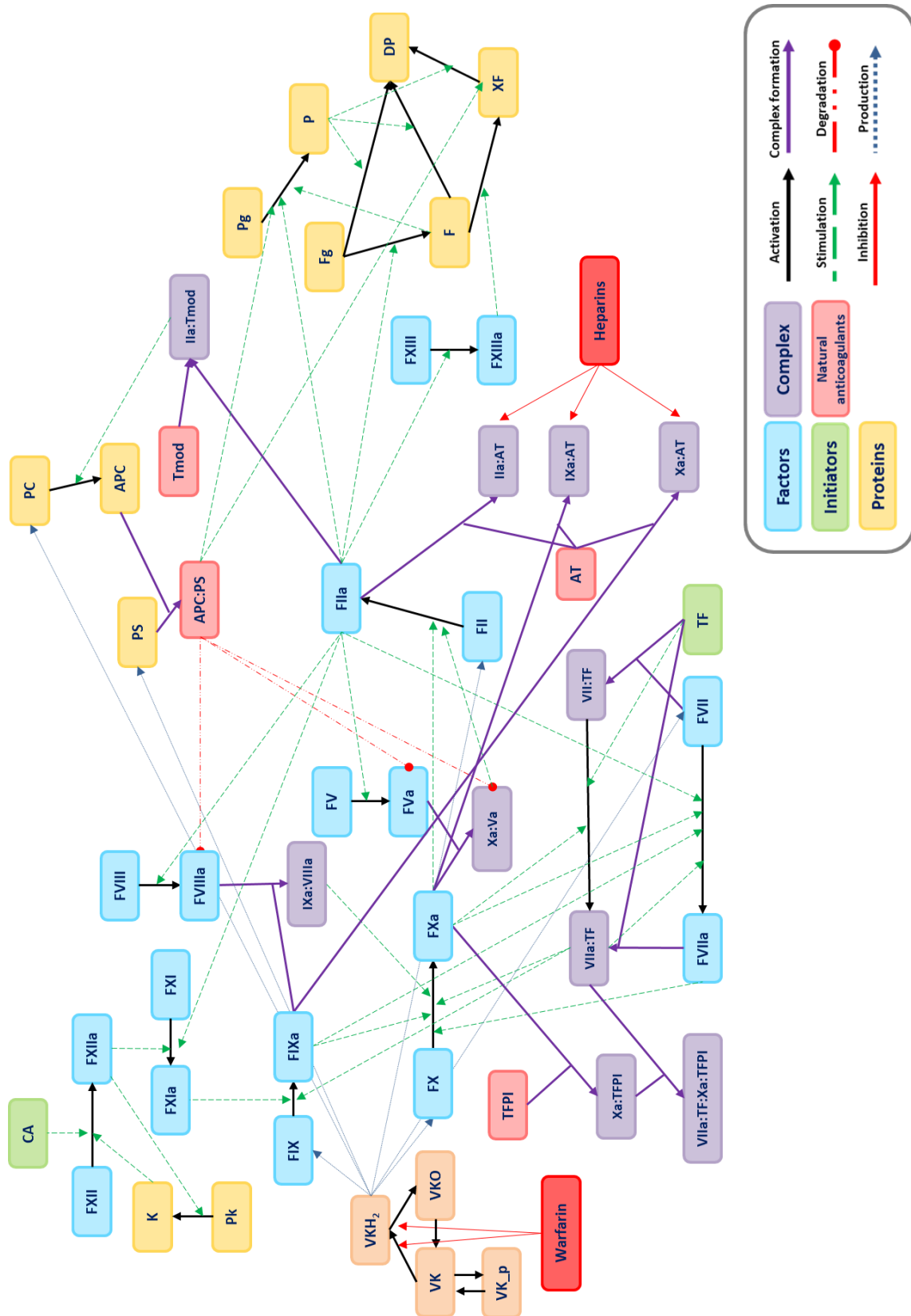


Figure S1B. The scheme of the model for coagulation process developed by Nayak and co-authors.

Figure obtained from the original article²¹.

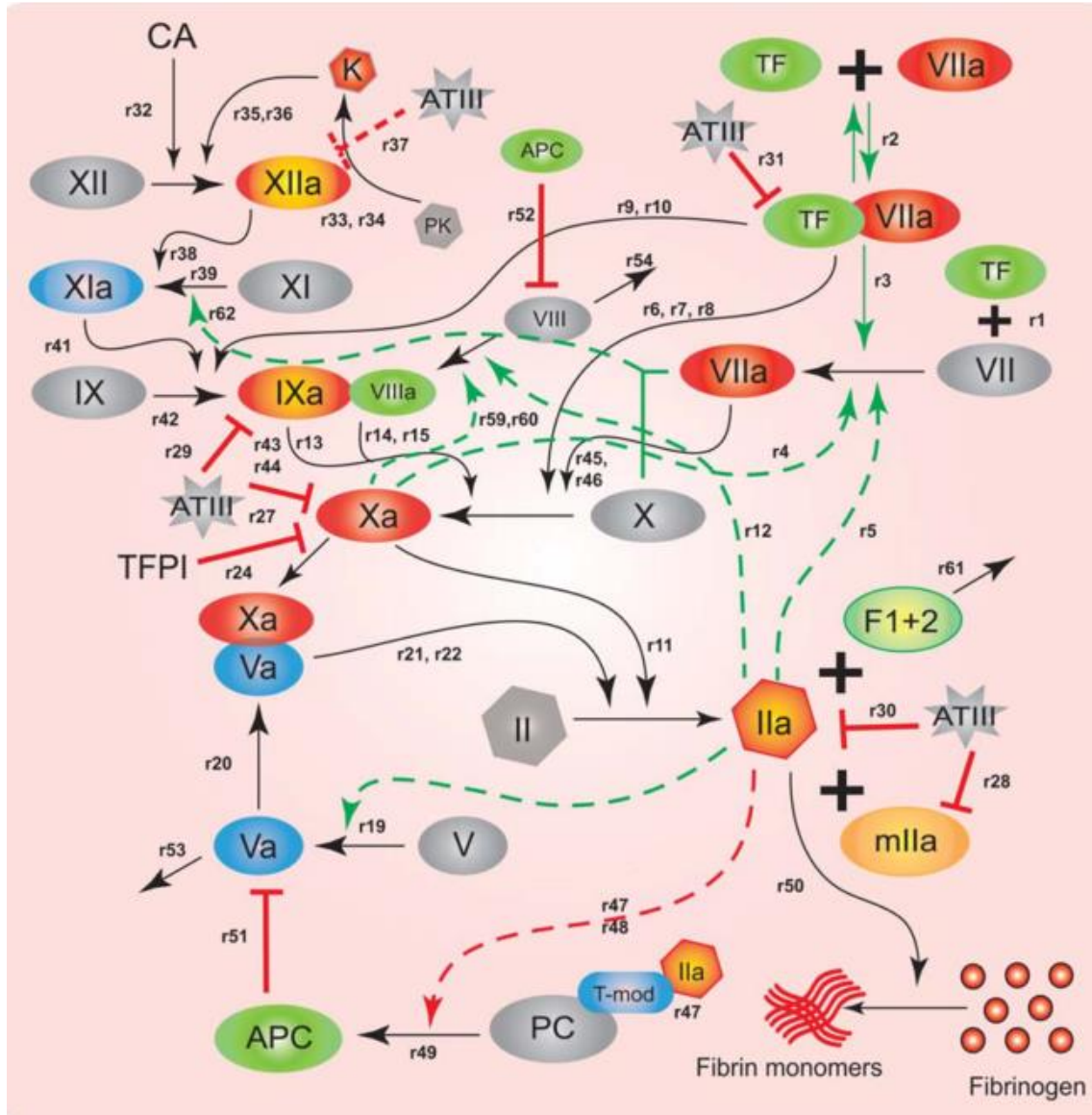


Table S2. Blood factors percentage transformed into concentration for Wajima, et al. model simulations

ID	II	V	VII	VIII	IX	X	ATIII
14488	990.024	12.282	7.6	0.196	88.704	125.496	2448
14489	1003.968	10.68	7	0.161	85.12	116.781	2244
14490	1338.624	15.486	8.9	0.168	125.44	162.099	2686
14491	1045.8	9.612	6.9	0.224	95.872	118.524	2380
14492	725.088	14.151	4.6	0.224	53.76	78.435	2686
14493	1199.184	15.219	10.4	0.287	115.584	149.898	3196
14494	920.304	14.151	6.1	0.168	98.56	104.58	2482
14495	1115.52	9.612	8.4	0.189	136.192	146.412	2788
14496	1101.576	10.146	9	0.273	94.08	139.44	3196
14497	976.08	10.947	7.9	0.147	79.744	125.496	2414
14498	1338.624	10.413	11.2	0.287	110.208	155.127	3060
14499	892.416	17.088	7.1	0.259	84.224	90.636	2958
14500	1338.624	20.025	9.6	0.301	120.064	153.384	3264
14501	1227.072	17.088	7.6	0.231	102.144	130.725	2822
14502	1031.856	10.146	7.1	0.175	103.04	125.496	2924
14503	1143.408	10.947	10.6	0.336	128.128	148.155	3196
14504	1115.52	8.811	6.3	0.259	86.016	109.809	2754
14505	1115.52	17.622	7	0.245	135.296	130.725	3332
14506	1045.8	10.413	8.8	0.21	105.728	128.982	2550
14507	1282.848	25.632	11.1	0.21	116.48	160.356	3264
2543	1143.408	24.831	6.3	3.276	178.304	115.038	3230
2575	1282.848	21.894	5.9	1.533	89.6	116.781	4080
2580	864.528	19.224	4.8	3.717	95.872	87.15	2686
2597	878.472	20.826	5.8	1.267	86.912	99.351	3366
2624	864.528	13.083	5.4	0.469	78.848	76.692	2856
2634	920.304	10.947	6.5	0.574	99.456	118.524	2788
2665	1241.016	20.826	7.6	1.05	107.52	163.842	3808
2668	1296.792	25.632	10.1	0.756	151.424	176.043	4080
2675	641.424	0.267	9.8	0.448	59.136	95.865	2074
2711	962.136	5.073	5.8	0.252	102.144	120.267	2312
2714	1129.464	9.078	5.8	0.735	168.448	113.295	2924
2716	906.36	13.35	8.3	1.841	84.224	102.837	2516
2743	934.248	9.879	37.4	0.455	68.992	109.809	2618
2751	1059.744	12.282	7.7	0.469	72.576	137.697	2550
2771	1199.184	13.884	13.5	0.616	54.656	148.155	3298
2772	948.192	7.743	7.9	0.539	77.952	111.552	2108
2784	1213.128	22.428	4.9	0.238	94.08	170.814	3026
2797	1310.736	22.695	59.7	0.728	163.072	205.674	5100
2814	1157.352	13.083	8.5	0.49	59.136	148.155	3264
2816	1045.8	17.088	7.7	0.903	106.624	142.926	2516
2817	1003.968	8.01	7.8	0.469	51.968	153.384	2244
2819	962.136	13.083	11.8	0.532	78.848	122.01	2788
2827	474.096	0.534	13.5	0.287	26.88	61.005	1768
2829	1087.632	7.209	7.1	0.518	60.032	130.725	2890
2841	1031.856	8.544	18.3	0.539	88.704	111.552	3060
2843	766.92	17.088	8.7	0.511	66.304	109.809	2720
2860	934.248	12.816	23.3	0.63	65.408	95.865	3128
2881	934.248	4.539	4.9	0.595	93.184	95.865	2720
2883	1784.832	20.292	5	1.428	173.824	207.417	3196
2885	1031.856	6.408	5.9	0.546	65.408	137.697	2516
2892	1157.352	16.554	15.4	0.763	149.632	193.473	3400
2924	1338.624	11.214	28.9	0.448	95.872	132.468	2686
2767	1213.128	21.36	17.1	0.798	94.976	189.987	3264
2818	1213.128	0.801	5.4	0.483	115.584	151.641	3434
2830	1227.072	6.408	15.5	0.623	82.432	142.926	2550
2840	1017.912	9.879	15.8	0.553	63.616	142.926	2788
2872	1213.128	14.151	39.5	0.392	161.28	155.127	3298
2878	1241.016	17.355	6.7	0.49	77.952	134.211	3128
2895	1073.688	10.146	12	0.679	71.68	128.982	3162
2901	1017.912	5.607	6.8	0.441	72.576	116.781	3298

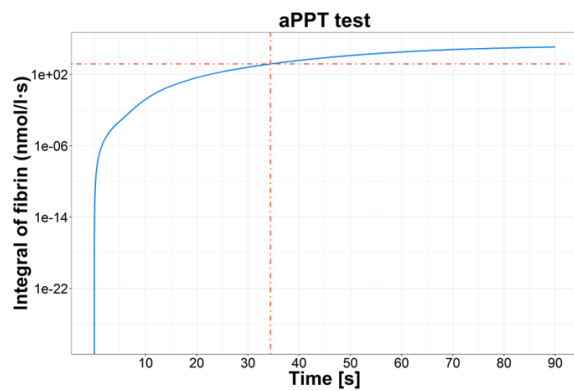
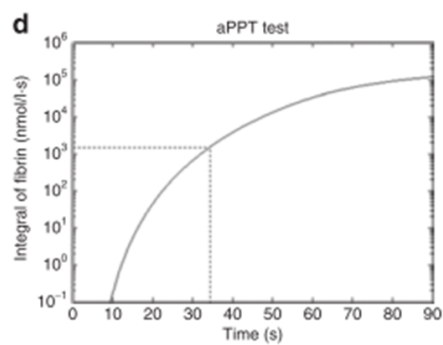
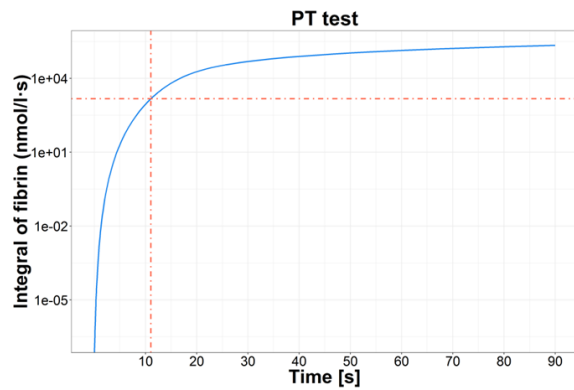
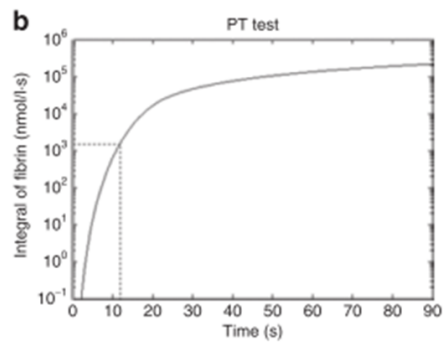
Table S3. Blood factors percentage transformed into concentration for Nayak, et al. model simulations

ID	II	V	VII	VIII	IX	X	ATIII
14488	994	9.2	7.6	0.196	89.1	115.2	2448
14489	1008	8	7	0.161	85.5	107.2	2244
14490	1344	11.6	8.9	0.168	126	148.8	2686
14491	1050	7.2	6.9	0.224	96.3	108.8	2380
14492	728	10.6	4.6	0.224	54	72	2686
14493	1204	11.4	10.4	0.287	116.1	137.6	3196
14494	924	10.6	6.1	0.168	99	96	2482
14495	1120	7.2	8.4	0.189	136.8	134.4	2788
14496	1106	7.6	9	0.273	94.5	128	3196
14497	980	8.2	7.9	0.147	80.1	115.2	2414
14498	1344	7.8	11.2	0.287	110.7	142.4	3060
14499	896	12.8	7.1	0.259	84.6	83.2	2958
14500	1344	15	9.6	0.301	120.6	140.8	3264
14501	1232	12.8	7.6	0.231	102.6	120	2822
14502	1036	7.6	7.1	0.175	103.5	115.2	2924
14503	1148	8.2	10.6	0.336	128.7	136	3196
14504	1120	6.6	6.3	0.259	86.4	100.8	2754
14505	1120	13.2	7	0.245	135.9	120	3332
14506	1050	7.8	8.8	0.21	106.2	118.4	2550
14507	1288	19.2	11.1	0.21	117	147.2	3264
2543	1148	18.6	6.3	3.276	179.1	105.6	3230
2575	1288	16.4	5.9	1.533	90	107.2	4080
2580	868	14.4	4.8	3.717	96.3	80	2686
2597	882	15.6	5.8	1.267	87.3	91.2	3366
2624	868	9.8	5.4	0.469	79.2	70.4	2856
2634	924	8.2	6.5	0.574	99.9	108.8	2788
2665	1246	15.6	7.6	1.05	108	150.4	3808
2668	1302	19.2	10.1	0.756	152.1	161.6	4080
2675	644	0.2	9.8	0.448	59.4	88	2074
2711	966	3.8	5.8	0.252	102.6	110.4	2312
2714	1134	6.8	5.8	0.735	169.2	104	2924
2716	910	10	8.3	1.841	84.6	94.4	2516
2743	938	7.4	37.4	0.455	69.3	100.8	2618
2751	1064	9.2	7.7	0.469	72.9	126.4	2550
2771	1204	10.4	13.5	0.616	54.9	136	3298
2772	952	5.8	7.9	0.539	78.3	102.4	2108
2784	1218	16.8	4.9	0.238	94.5	156.8	3026
2797	1316	17	59.7	0.728	163.8	188.8	5100
2814	1162	9.8	8.5	0.49	59.4	136	3264
2816	1050	12.8	7.7	0.903	107.1	131.2	2516
2817	1008	6	7.8	0.469	52.2	140.8	2244
2819	966	9.8	11.8	0.532	79.2	112	2788
2827	476	0.4	13.5	0.287	27	56	1768
2829	1092	5.4	7.1	0.518	60.3	120	2890
2841	1036	6.4	18.3	0.539	89.1	102.4	3060
2843	770	12.8	8.7	0.511	66.6	100.8	2720
2860	938	9.6	23.3	0.63	65.7	88	3128
2881	938	3.4	4.9	0.595	93.6	88	2720
2883	1792	15.2	5	1.428	174.6	190.4	3196
2885	1036	4.8	5.9	0.546	65.7	126.4	2516
2892	1162	12.4	15.4	0.763	150.3	177.6	3400
2924	1344	8.4	28.9	0.448	96.3	121.6	2686
2767	1218	16	17.1	0.798	95.4	174.4	3264
2818	1218	0.6	5.4	0.483	116.1	139.2	3434
2830	1232	4.8	15.5	0.623	82.8	131.2	2550
2840	1022	7.4	15.8	0.553	63.9	131.2	2788
2872	1218	10.6	39.5	0.392	162	142.4	3298
2878	1246	13	6.7	0.49	78.3	123.2	3128
2895	1078	7.6	12	0.679	72	118.4	3162
2901	1022	4.2	6.8	0.441	72.9	107.2	3298

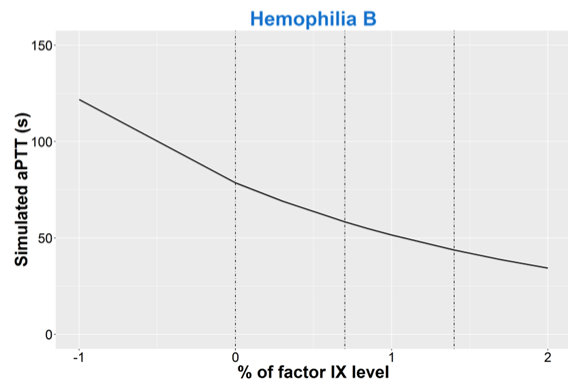
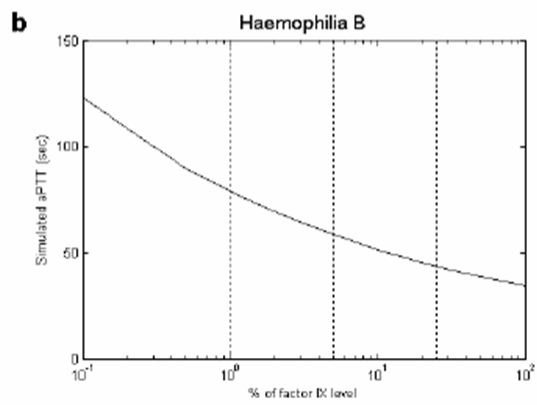
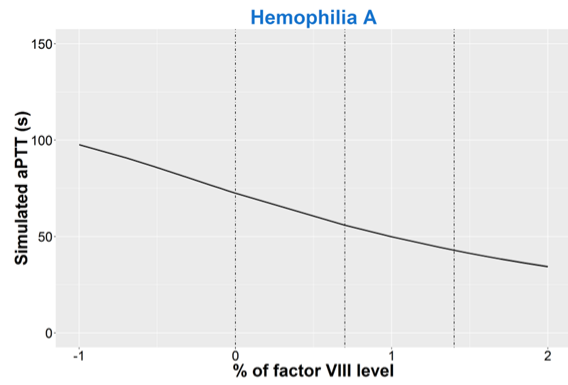
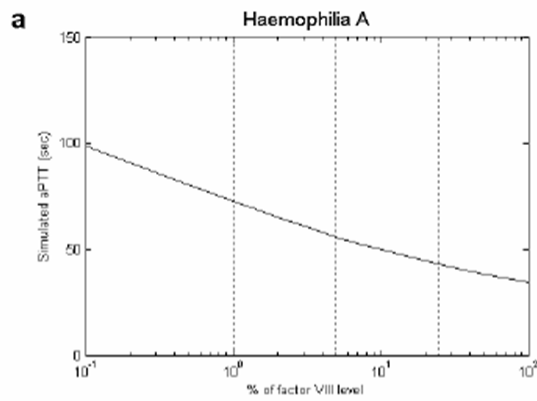
S.4 Graphic validation

Wajima, et al. model:

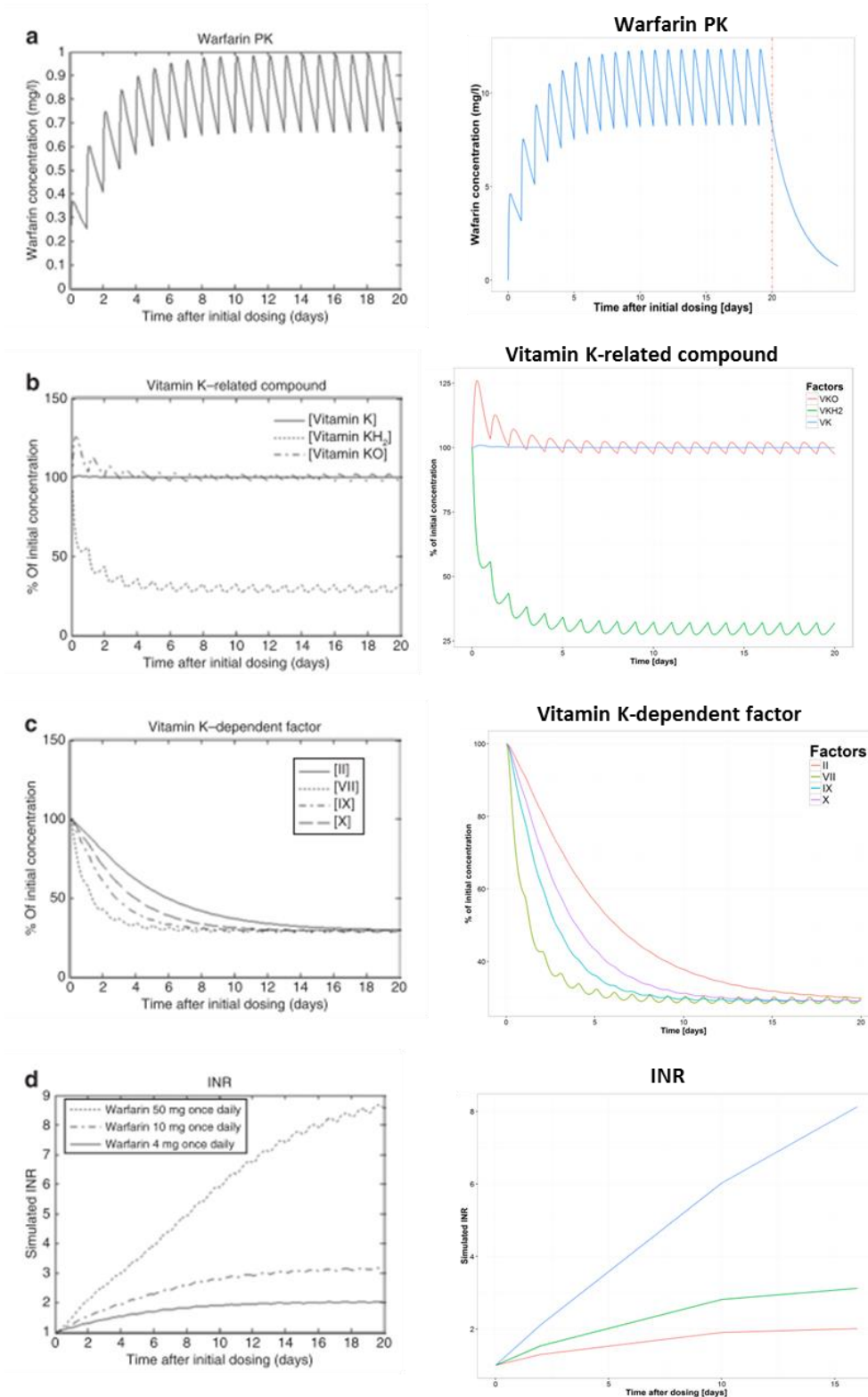
- The integral of fibrin in the PT test and in the aPTT test. The dotted lines show 1,500 nmol/l·s of the integral of fibrin, which we take as the clotting point in the study. The clotting times are 11.8 s in the INR test simulation and 34.4 s



- The Simulated aPTT for Hemophilia A and Hemophilia B

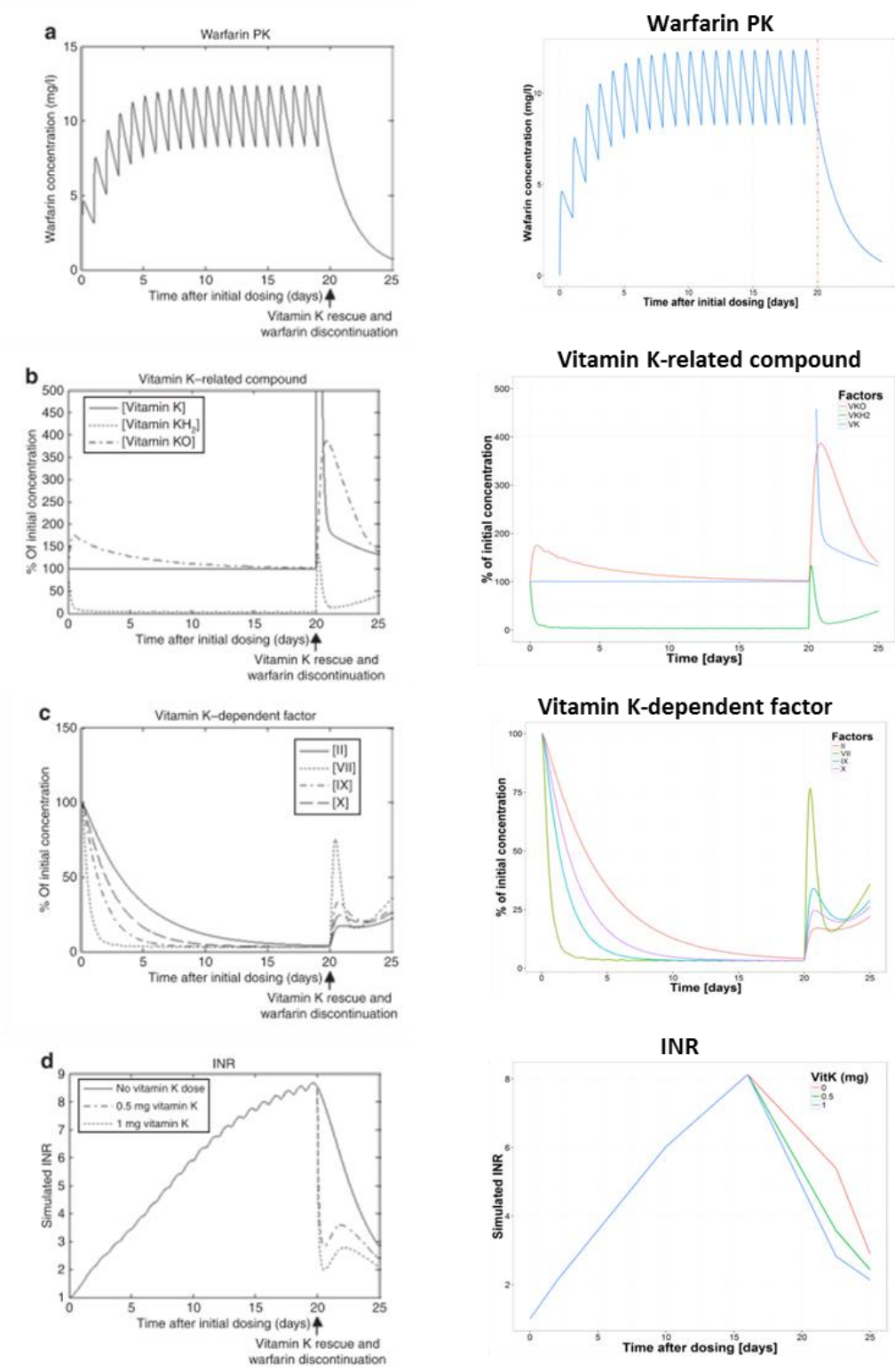


- Time courses of warfarin plasma concentration, vitamin K-related compounds, vitamin K-dependent coagulation factors, and international normalized ratio (INR) after warfarin therapy.

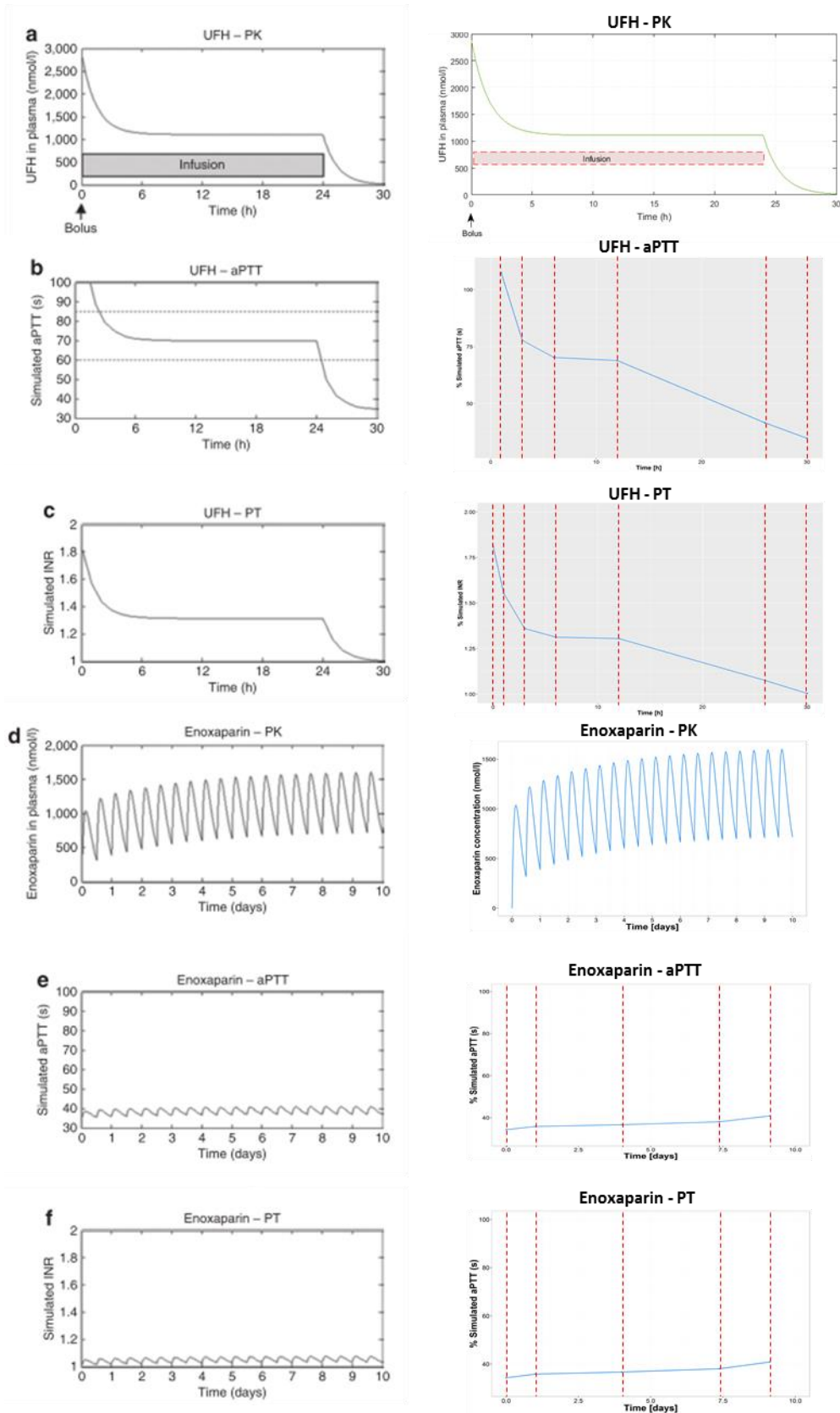


Modelling the coagulation cascade

- Time courses of warfarin plasma concentration, vitamin K–related compounds, vitamin K–dependent coagulation factors, and international normalized ratio (INR) after vitamin K therapy for excessive exposure to warfarin.

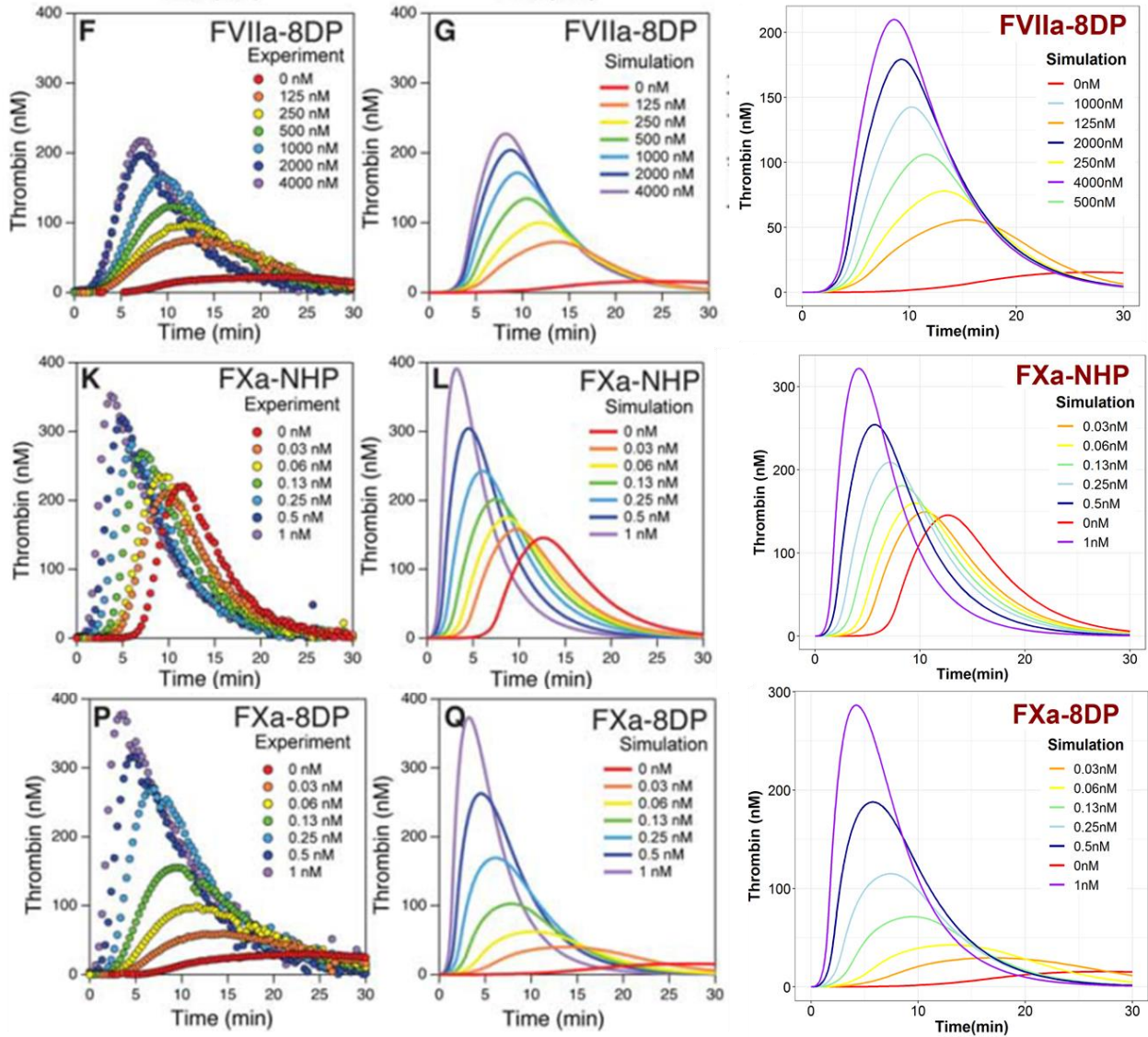


- Time courses of plasma concentrations of UFH and LMWH (enoxaparin), INR, and aPTT.



Nayak, et al. model:

- TGAs for various concentration of FVIIa or FXa added to normal human plasma (NHP) or FVIII deficient plasma (8DP). The first column corresponds with experimental data, the second with Nayak’s model simulations and the third one with the simulations obtained with the implemented model in Simbiology.

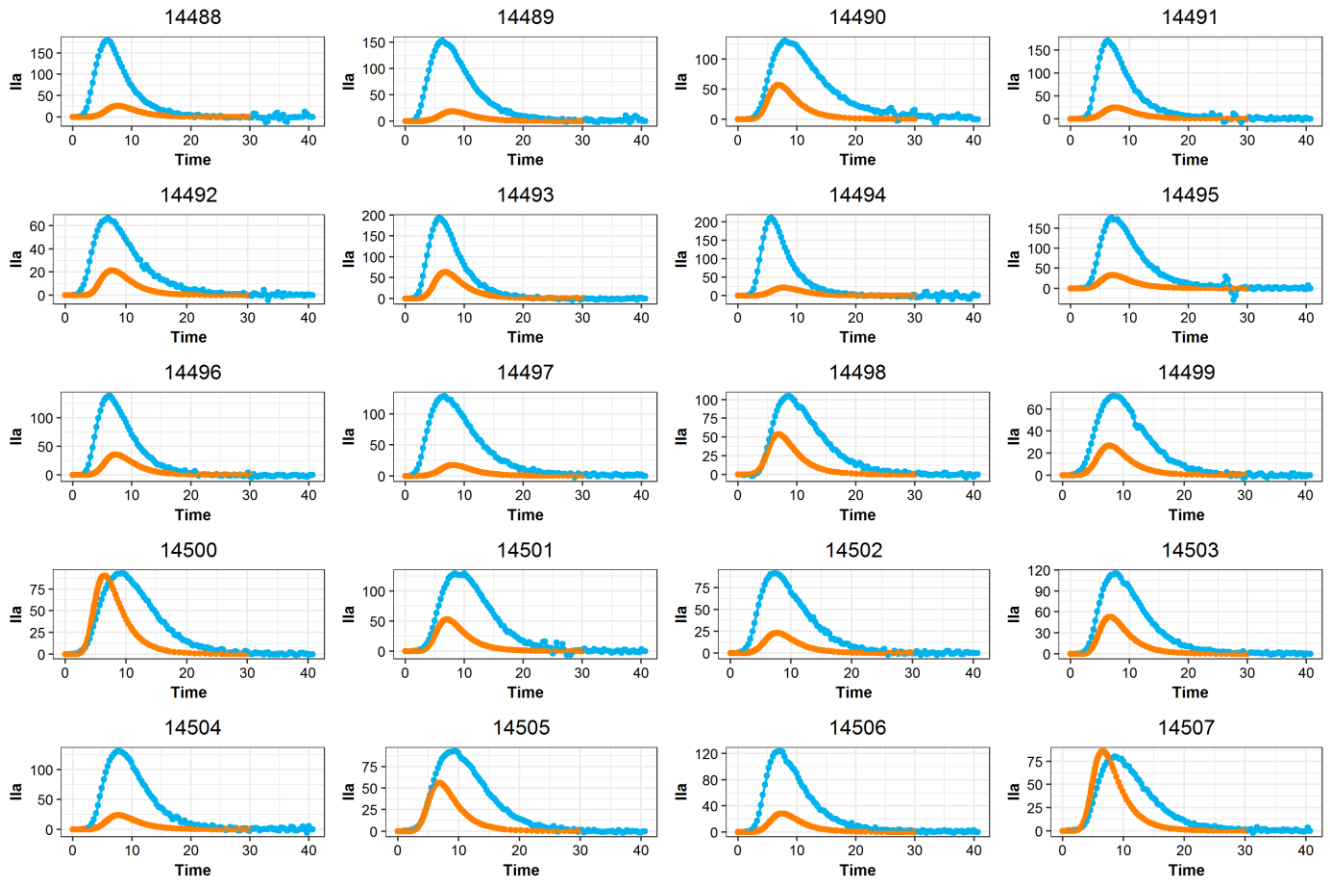


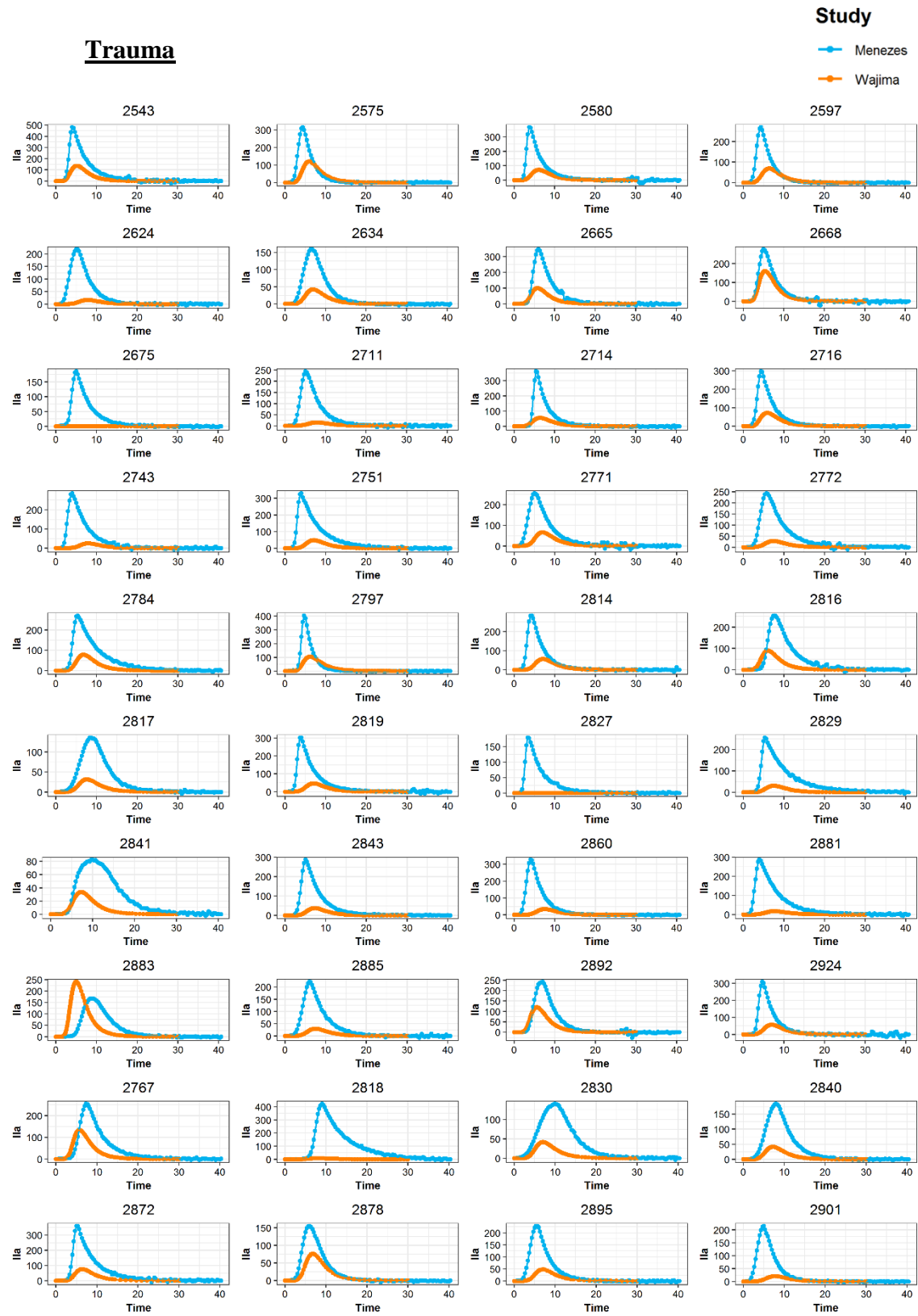
S5. TGA simulations with individual initial conditions reported in Menezes, et al. article.

Wajima, et al. model:

Normal

Study



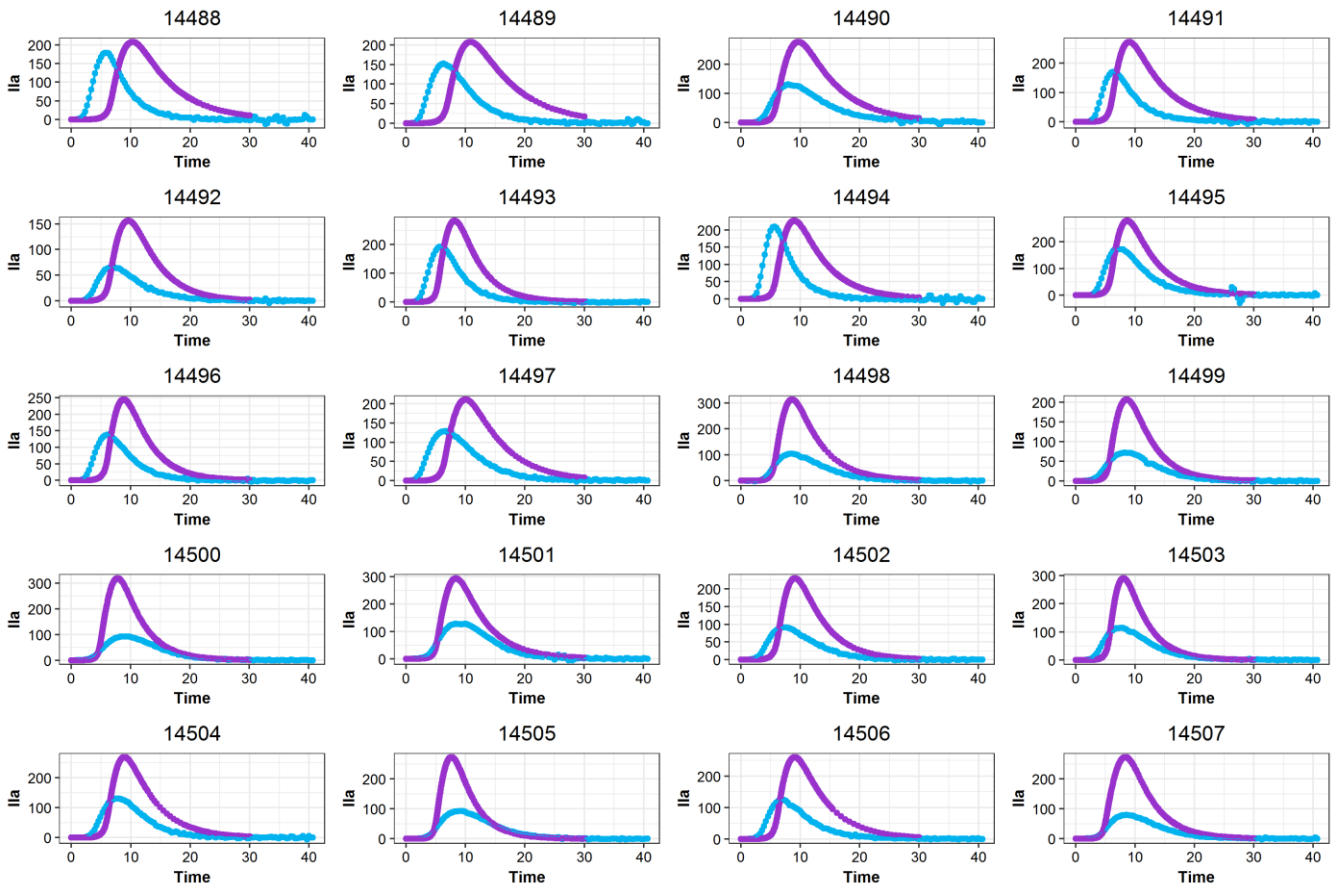


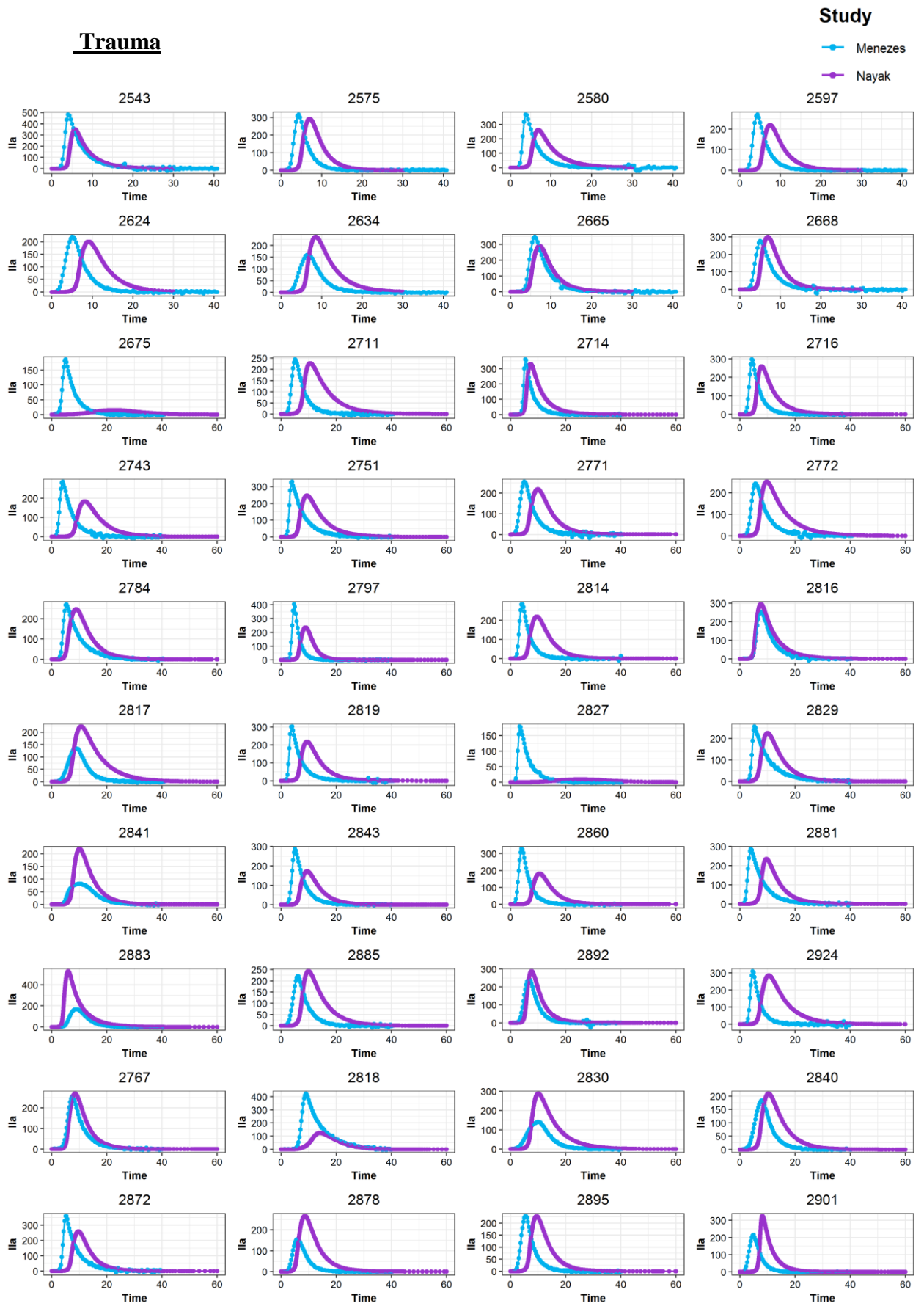
Nayak, et al. model:

Normal

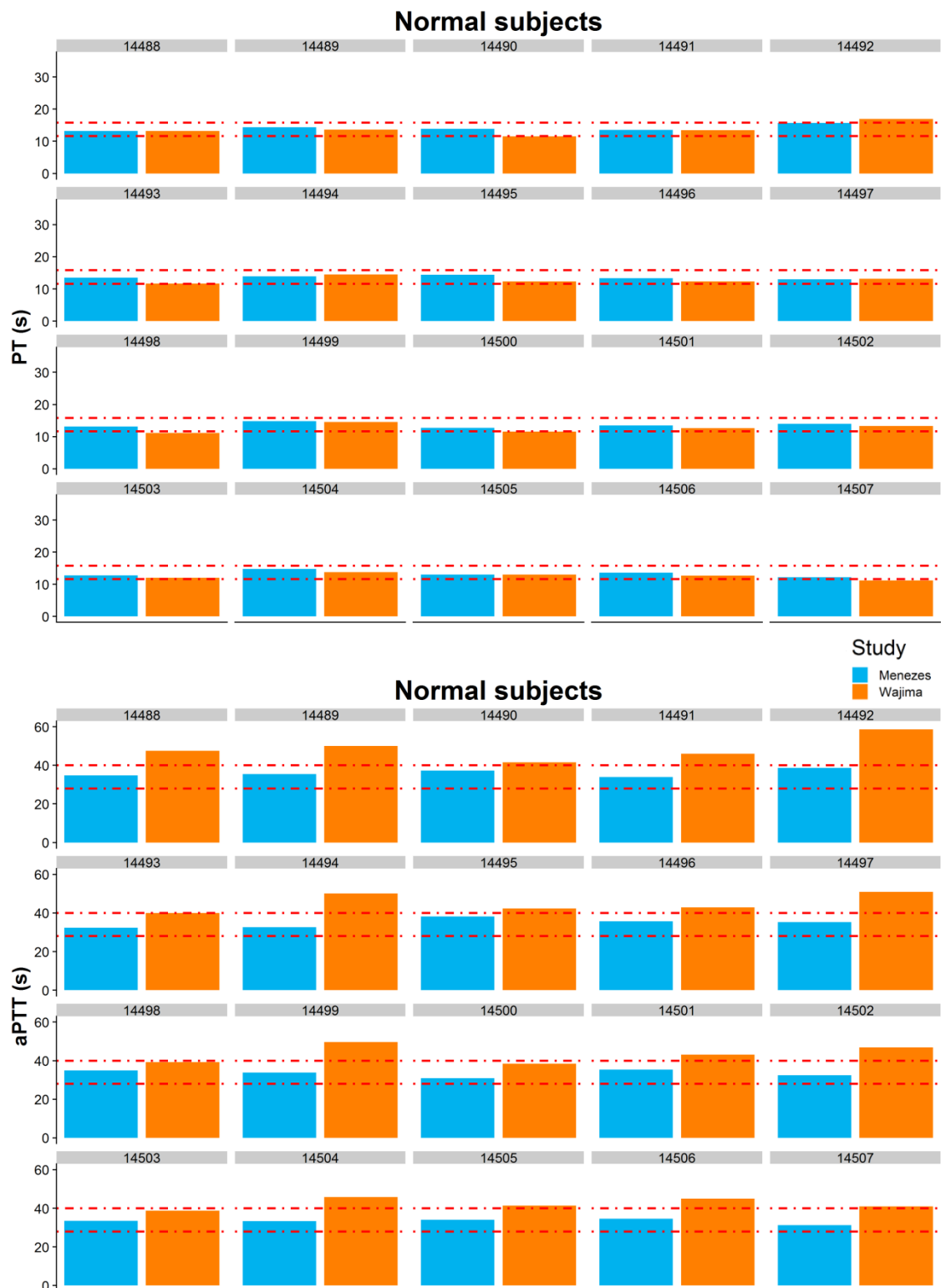
Study

- Menezes
- Nayak





S6. PT and aPTT simulations with individual initial conditions in normal subjects with Wajima et al. model reported in Menezes, et al. article.



S7. Differences between Wajima, et al. model and Nayak, et al. model.

Coagulation models		
	Wajima, et al.	Nayak, et al.
Approximation	Bottom-up approach	Bottom-up approach
Components / Reactions	51/48	61/62
Parameters	134	87
Equations type	Activation: $\frac{Vmax \cdot [enzyme]}{km + [enzyme]} \cdot [inactivated\ factor]$ Complex formation: $\frac{[factor\ 1] \cdot [factor\ 2]}{c}$ Degradation: $-\frac{Vmax \cdot [enzyme]}{km + [enzyme]} \cdot [inactivated\ factor]$ Inhibition: $1 - \frac{Imax \cdot [Drug]}{IC50 + [Drug]}$	Activation: $k \cdot [enzyme] \cdot [inactivated\ factor]$ Complex formation: $kon \cdot A \cdot B - koff \cdot AB$
Output	PT (INR), aPTT and factor profiles	TGAs and aPTT
Data for validation	Snakebite data obtained from Tanos, et al. Measured PT and aPTT obtained from Pohl, et al.	In-house data
Assumptions	<ul style="list-style-type: none"> Model parameters were started with the values from the literature and adjusted based on the assumption of 30% fibrinogen reduction occurred at 10-15 seconds in INR test simulation and at 27-39 seconds in the aPTT test simulation for standard plasma samples. The criteria for clotting was based on the integral of fibrin, being a value of 1500nmol/L·s the clotting point. Each component was assumed to follow a first-order degradation rate with a degradation rate constant. The inactivated factors and proteins were assumed to have natural production rates. Complex formation was represented as a stoichiometric reaction in which the components are assumed to combine in a molar ratio of 1:1. Extrinsic pathway activation was assumed to be initiated by exposing plasma to TF. Intrinsic pathway activation was assumed to be initiated by plasma coming in contact with a negatively charged surface, which activates factor XII to XIIa. The natural anticoagulant effects of AT-III without heparin acceleration are assumed to be included in the natural degradation rate for each factor. The initial concentrations of all activated factors, complexes, and products were assumed, to be 0. 	<ul style="list-style-type: none"> The model assumed a well-mixed system for in vitro experiments. The criteria for clotting was based on the integral of fibrin, being a value of 1500nmol/L·s the clotting point. Extrinsic pathway activation was assumed to be initiated by exposing plasma to TF. Intrinsic pathway activation was assumed to be initiated by plasma coming in contact with a negatively charged surface, which activates factor XII to XIIa.

CHAPTER 3

The long neglected player: modeling tumor uptake to guide optimal dosing

**Leire Ruiz-Cerdá^{1,2}, Eduardo Asín-Prieto^{1,2}, Zinnia P Parra-Guillen^{1,2}
and Iñaki F Troconiz^{1,2}**

Clin Cancer Res. 2018 Jul 15;24(14):3236-3238

(doi: 10.1158/1078-0432.CCR-18-0580)

¹ Pharmacometrics & Systems Pharmacology, Department of Pharmacy and Pharmaceutical Technology, School of Pharmacy, University of Navarra, Pamplona 310890, Spain

² IdiSNA, Navarra Institute for Health Research, Pamplona, Spain

Running title: Modeling tumor uptake to guide dose selection

ABSTRACT

Pharmacokinetic modeling is widely used to support decision making in translational medicine and patient care, traditionally using circulating drug exposure. The development of mechanistic computational models that integrate drug concentrations at the site of action making use of existing knowledge opens a new paradigm in optimal dosing.

MAIN TEXT

In the current issue of *Clinical Cancer Research*, Ribba and colleagues¹ applied the Model Informed Drug Discovery & Development (MID3) paradigm to optimize dosing regimens of Cergutuzumab amunaleukin (CEA-IL2v), a bivalent carcinoembryonic antigen (CEA)-specific antibody fused to a modified interleukin 2 (IL2) capable to activate the immune response in the tumor microenvironment. Their contribution, which relies on the fundamental premise that drug exposure represents the major driver of patient's response (at least at early stages of the progression of the disease), goes far beyond the MID3 standards.

In this commentary, we aim to bring the attention of the reader to the concepts of tumor exposure, mechanistic conceptualization of the system to treat, data integration, knowledge re-usability, and virtual scenarios. These concepts are key to understand and predict patient's response in the tight frames of decision making during drug development, as illustrated in the commented manuscript¹.

The use of models to establish dosage regimens has been present in drug development and patient care during the last three decades. With the arrival of biologics, specifically monoclonal antibodies, these models have gained mechanistic insights leading to the term of target-mediated drug disposition (TMDD)², accounting among other phenomena for time dependent pharmacokinetics. Indeed, the TMDD framework has been used by Ribba and colleagues¹ to characterize the reduction of circulating drug exposure during treatment triggered by the increasing target levels.

On the other hand, there is an arsenal of models linking systemic circulating drug exposure to response. One drawback of these approaches comes from the fact that tumor exposure is inferred from the time course of systemic drug levels and response, and therefore, variability in response due to target bioavailability cannot be accounted for (scenario a, Figure 1). Gathering tumor exposure appears as an obvious solution to overcome this important limitation, however, accessing tumor biopsies or intra-tumor microdialysis are not always possible. In the commented article, CEA-IL2v longitudinal tumor uptake was assessed through imaging data, which likely implied a significant amount of resources as indicated by the fact that a small cohort of 14 patients received ⁸⁹Zr-labeled CEA-IL2 and only three measurements up to eight hours post-dose were obtained per subject. The additional costs may pay off in the long term if this

methodology proves to be more precise to select the “optimal dosing regimen” for efficacy studies, therefore maximizing the chances of clinical success and reducing the alarming rates of late phases failure, one of the major hurdles in current oncology drug development.

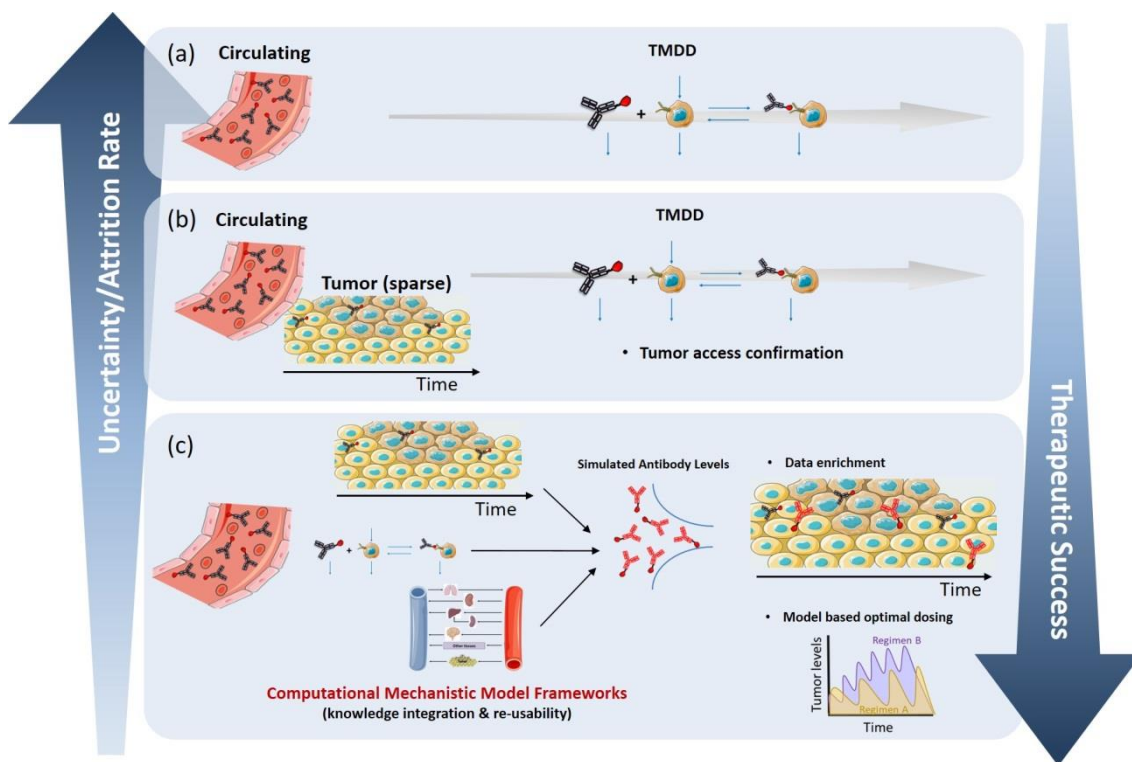


Figure 1. Expected impact of study design driving data availability and data processing approaches on attrition rates and therapeutic success in oncology drug development and patient care. (a) Circulating antibodies measurements coupled with semi-mechanistic modeling efforts; (b) circulating antibodies and sparse tumor measurements coupled with semi-mechanistic modeling efforts using tumor uptake information to confirm target uptake; and (c) circulating antibodies and sparse tumor measurements coupled with mechanistic modeling efforts using publicly available computational tools and Bayesian modeling. TMDD, target mediated drug disposition

It should be highlighted that those raw data would have been sufficient to simply confirm tumor access, but certainly it would have not permitted the prediction of exposure at the site of action in untested dosing scenarios (scenario b, Figure 1). How to deal with that type of information to get robust and trustful exposure predictions is a very relevant as well as a non-trivial question to answer related to extrapolation. We need scientifically sound tools to constrain prediction outcomes within reliable bounds, which can be achieved considering the system (tumor) as an entity with a dynamism governed by physiological processes, rather than a black box. This mechanistic

perspective is not exempted from complexities though, as it is quite data and computational demanding.

Interestingly, the strategy followed by Ribba and colleagues¹ minimized data and computation requirements upon the adaptation of a mechanistic computational model publicly available (scenario c, Figure 1). One fundamental property of mechanistic models is that processes (and their corresponding parameters) inherent to the system are isolated from those that are treatment-specific, therefore, enabling the integration of physicochemical characteristics of the compound, which are independent from the type of disease and its progression and frequently available from early stages of the discovery phase. This approach ensures and promotes model re-usability in other therapeutics, as well as it reduces the data acquisition needs permitting the use of sparse measurements in the target tissue.

The results obtained by Ribba and colleagues¹ using the above mechanistic approach and integrating data from different sources (intrinsic drug properties, temporal profiles of drug levels in peripheral blood and tumor, and immune cell counts) are impressive if one compares the lack of meaningful trends shown in panel E of their Figure 2 with the predictions generated and shown in bottom panels of their Figure 3. Given those results, it will not be surprising that the same modeling paradigm can be applied by others in the case of different antibodies and cancer indications.

So far, the commentary has been focused on the drug development arena, however, this approach opens the avenue of translating MID3 efforts to model informed drug use in patient care. The authors made use of a powerful modeling technique, the Bayesian approach³. In brief, given a population model and individual (sparse) patient data, individual exposure profiles can be generated. Therefore, the modeling framework that Ribba and colleagues¹ present in this journal should not be diluted in time, and we highly encourage to carry forward and re-use those computational tools at the time when patient data are gathered and the therapeutic is available for medicine personalization.

Consequently, the end-product of the modeling effort we are discussing is the simulation outcome showing how a change in the dosing schema can overcome the reduced availability of circulating CEA-IL2v result of the model predicted peripheral target expansion. Focusing on drug exposure and leaving efficacy and toxicity apart,

there are at least two variables that need to be taken into consideration for dose optimization at the typical patient, which are dose level and dosing interval. The pharmacometric discipline provides tools to find, from a formal perspective, optimal dosing and design scenarios in order to extract the most from clinical trials. Nevertheless, publicly available information on these therapies indicates that one of the main obstacles in clinical phases of drug development of these compounds is dose selection and optimization, which is still mainly driven by classical maximum tolerated dose (MTD) schemas and non-compartmental analysis⁴. To the best of our knowledge, there is only one publication where pharmacokinetic/pharmacodynamic modeling efforts were undertaken to develop a translation model integrating information across the different phases of drug development to finally support decision making⁵ in the immune-oncology arena.

To summarize, Ribba and colleagues¹ have applied the MID3 paradigm during the clinical development program of a new immune modulator in oncology therapy. In their work, circulating levels of CEA-IL2v and imaging data were embedded in a computational modeling framework using publicly available information. This strategy, based on sparse data, allowed for an *in silico* optimization of dosing schedules with focus on tumor uptake as an alternate/complementary paradigm to MTD. It should not be ignored that selection of the right dosage regimen is ultimately driven by the balance between efficacy and toxicity. Remarkably, the authors found a strong positive correlation between predicted target levels and interleukin 2 receptor (IL2-R) positive cells, supporting drug mechanism of action and adding robustness to the developed model. Therefore, we are eager to see how tumor uptake drives CEA-IL2v patient's response.

In conclusion, the contribution of Ribba and colleagues highlights the enormous potential of modeling and simulation as a pillar in drug development and translational medicine supporting dosing optimization and decision making.

REFERENCES

1. Ribba, B. *et al.* Prediction of the Optimal Dosing Regimen Using a Mathematical Model of Tumor Uptake for Immunocytokine-Based Cancer Immunotherapy. *Clin. Cancer Res.* **24**, 3325–3333 (2018).
2. Levy, G. Pharmacologic target-mediated drug disposition. *Clin. Pharmacol. Ther.* **56**, 248–52 (1994).
3. Barbolosi, D., Ciccolini, J., Lacarelle, B., Barlési, F. & André, N. Computational oncology--mathematical modelling of drug regimens for precision medicine. *Nat. Rev. Clin. Oncol.* **13**, 242–54 (2016).
4. Mathijssen, R. H. J., Sparreboom, A. & Verweij, J. Determining the optimal dose in the development of anticancer agents. *Nat. Rev. Clin. Oncol.* **11**, 272–81 (2014).
5. Lindauer, A. *et al.* Translational Pharmacokinetic/Pharmacodynamic Modeling of Tumor Growth Inhibition Supports Dose-Range Selection of the Anti-PD-1 Antibody Pembrolizumab. *CPT pharmacometrics Syst. Pharmacol.* **6**, 11–20 (2017).

GENERAL DISCUSSION

During the drug development process, especially in the context of complex diseases, it would be of a great help to have available tools facilitating key and relevant tasks, for example identifying (i) the right therapeutic targets for the addressed condition, (ii) underlying alterations involved in the disease etiopathogenesis and prognosis, (iii) different subpopulations of patients with specific treatment considerations, and (iv) key biomarkers that can assist in the decision making process by quickly and accurately predicting and evaluating the progression the disease of particular subjects.

The Food and Drug Administration (FDA), has suggested some strategies and tools with the purpose of facilitating and accelerating the drug development process. One of these strategies describes the potential benefit of the use of pharmacometrics and systems pharmacology disciplines. Under the name of “Model Informed Drug Discovery and Development” (MID3), this strategy aims to enhance drug discovery productivity and efficiency targeting the abovementioned objectives using mathematical models throughout all the stages of the process¹.

Throughout this thesis, systems pharmacology and pharmacometrics were applied to different pathologies covering a broad spectrum of methodologies and objectives. On the one hand, systems pharmacology was used to develop a framework that could help to identify targets, biomarkers and patients subpopulations, especially in cases of complex diseases by linking the already available knowledge of complex biological systems with qualitative or quantitative pharmacology data. On the other hand, pharmacometrics allowed us to build a semi-mechanistic PKPD model to describe and predict experimental data, which, in the future, will serve to individualize treatments, explore different scenarios and predict drug behavior.

Along the different chapters of this thesis, different qualitative and quantitative systems pharmacology models as well as semi-mechanistic PKPD models are shown and have been already discussed with special mention to their advantages and limitations. Therefore, in this section, a summary, general discussion and overview of the whole work is provided.

Systems pharmacology based on Boolean networks

In Chapter 1, it is shown how, in cases of complex diseases with limited longitudinal or quantitative data, systems pharmacology based on Boolean networks represents an interesting and useful approach.

Systemic Lupus Erythematosus (SLE) is a very complex autoimmune disease, which is characterized by a high between patient heterogeneity. Due to this heterogeneity, it would not seem reasonable to treat different patients with the same pharmacological treatment, as the expected outcome is difficult to predict and might vary significantly.

For such a reason, and through a systems pharmacology approach applied to SLE disease, we tried to identify different subpopulations of patients in order to predict the likely progression, and thus, be able to develop individualized therapies that guarantee a high probability of therapeutic success.

The first step in this type of approaches represents a literature survey integrating all the available knowledge. A great general interest in biomedicine on this disease was detected as a huge amount of available discrete data is found in the literature including several papers reporting alterations in patients, as well as public and private datasets from -omics experiments.

In detail, this chapter aimed to build a systems pharmacology model based on Boolean networks to characterize the co-stimulation process in SLE disease. This model integrates all the available knowledge to group SLE patients according to their molecular alterations to find out whether there are, indeed, different subpopulations of patients that may require different treatments.

The resultant network was composed of 52 components and 296 governing relationships between them which were divided into activation, deactivation, upregulation and downregulation processes. Twenty three out of 52 nodes had already been reported to be altered in SLE. Once the logic network was established, we can obtain semi-quantitative profiles and the attractors of the system. For the semi-quantitative profiles, we ran 5,000 model simulations of 40 time steps (30 of antigen exposure and 10 of washout) and then, calculated the average of all simulations at each time step for all the nodes. For the attractor analysis, we ran 40 simulations with 5,000 time steps. In both cases, to mimic

biologic conditions and increase robustness on the results, we decided to incorporate variability by randomly updating the nodes in each time step (asynchronous method), which resulted in different progressions of the network.

An interesting feature of this approach is that perturbations can be introduced in the network, recreating knockouts or upregulations by setting a node to 0 or 1, respectively. By perturbing all network components, it is possible to study which the most likely perturbations are that may cause SLE reported alterations, and then, apply a clustering analysis to group together underlying alterations according to the lupus-like manifestations they provoke.

Those possibilities show important implications in the case of evaluating potential treatments. As we have already evaluated, different perturbations can lead to very similar alterations, which would either react similarly to the same treatments or, on the contrary, elicit different effects.

The main limitation of this network is that it only describes a fraction of the immune response, and therefore, until all SLE pathways and immune alterations were included into the model we would not be able to assess its full potential. Moreover, the building process of the relationships between the nodes is challenging, because of the published controversial results, unsupported affirmations, questionable experiments and unanswered questions about the immune dynamics. Finally, another limitation that should be highlighted is that full model validation is not feasible at this stage because activation of many nodes is also regulated by other molecules, critical to the immune physiopathology of SLE, but not currently available for inclusion in the model.

Nevertheless, these limitations suppose new opportunities to improve the already developed immune Boolean network in order to provide better assistance in drug development and clinical care in the case of SLE patients.

Quantitative systems pharmacology

In the previous chapter, a Boolean network was developed for SLE disease due to the limited longitudinal data available from the literature. On the contrary, when adequate longitudinal data is available, quantitative systems pharmacology models can be

developed that describes the full longitudinal profile of the elements and pathways involved in a disease.

In Chapter 2, the objective was to develop a framework that could assist in the individualization/optimization of factor administration for patients with coagulation disorders undergoing surgery. To fulfill the previous goal, two quantitative systems pharmacology models for the coagulation cascade process^{2,3} found in the literature were presented, implemented and evaluated. Both models incorporated most of the components involved in the coagulation process and were developed using parameters searched in the literature and optimized to describe in-house data.

In our case, both models were satisfactorily implemented and reproduced. The models were able to replicate factor profiles as well as different coagulation tests (TGA, PT and aPTT) results provided in the original publications. Nevertheless, one of the main advantages of modeling is the predictive performance required for study design and treatment optimization. To prove the model performance for both models with external data, experimental data was obtained from a published article. This data includes the percentage of activation for different factors, PT and aPTT tests results and longitudinal thrombin profiles for normal subjects and trauma patients⁴. It is noteworthy to highlight the high variability observed in the experimental data.

After simulating and comparing the individual profiles as well as the mean population profiles obtained for the published and the simulated data, the models were deemed not to be good enough to describe the experimental data. This event points out the existing challenge for quantitative systems pharmacology models when dealing with data with high variability⁵.

For this reason and keeping in mind the objective of this work, we decided to move from a systems pharmacology approach to a semi-mechanistic PKPD modelling (i.e., from a knowledge-driven to a data-driven modeling approach) reducing considerably the number of parameters achieving an identifiable model.

Semi-mechanistic PKPD modelling

A semi-mechanistic population PKPD model for thrombin formation was developed according to the individual raw longitudinal data obtained from Menezes, et al.⁴.

The semi-mechanistic model consists of three main compartments. The first one is the tissue factor (TF), which is the stimulus for initiating the coagulation process to form thrombin. The second one is the prothrombin, essential factor for thrombin formation. The last compartment is representative of the thrombin levels. The model incorporates two mechanisms for thrombin formation in accordance with the cellular model of coagulation by Hoffman, et al.⁶. One of them provokes a quick but weak burst of thrombin and the other one a large thrombin peak regulated by a transit compartment model.

The model accurately describes the profiles of thrombin concentration over time after the addition of TF to plasma samples from normal subjects and trauma patients, as a main outcome of the coagulation process. The high variability between individuals and the typical profile are well captured by the model as shown by visual inspection of model simulations versus observations.

The model allows differentiating thrombin dynamics between the two different populations included. The inclusion of more data and different patient conditions might enrich the proposed coagulation model, what would improve model performance and generalization. Consequently, it could be used in clinic to manage appropriately the administration of coagulation factors as treatment for several coagulopathies minimizing risks and improving the prognosis of these patients.

The use of models to establish dosage regimens

As we have seen previously, one of the aims that systems pharmacology and pharmacometrics address is treatment individualization to enhance patient response, improving efficacy and reducing toxicity. In Chapter 3, it is shown an approach that opens an avenue in the model informed drug use in patient care.

Usually, pharmacokinetic models use blood drug concentrations to infer drug exposure in the site of action. In this chapter, we have presented a brief perspective discussing the impact of considering exposure at the target site concerning systemic concentrations. To

address this, we referred to Ribba, et al.⁷ article where a model for drug uptake by tumor tissue that integrates a target-mediated drug disposition approach (TMDD) was presented. The model was used to optimize dosing regimens in patients with advanced and/or metastatic solid carcinoembryonic antigen positive (CEA⁺) tumors, overcoming the increase in the synthesis of the target triggered by the therapeutic agents increasing its clearance and reducing tumor concentrations.

In this contribution, a novel immunocytokine, which is formed by an antibody against CEA and a variant of interleukin 2 (IL2, not able to bind to IL2 receptor of the T regulatory cells), is presented. Once the drug is administered, it enhances the expansion of immune cells positive to IL2 receptor, resulting in faster depletion of available drug. For this reason, the incorporation of peripheral immune cells concentrations to the model allowed predicting the real drug uptake in the tumor cells, confirmed by intratumoral sparse measurements. Interestingly, the authors used for the model building publicly available models^{8,9} which emphasizes the importance of knowledge reusing that can be achieved using the model based approach. Below, a representation of the model developed by these authors is presented (Figure 1). As a result of this, the authors concluded through model simulations that increasing the dose or shortening the time interval between doses led to a higher drug uptake by the tumor.

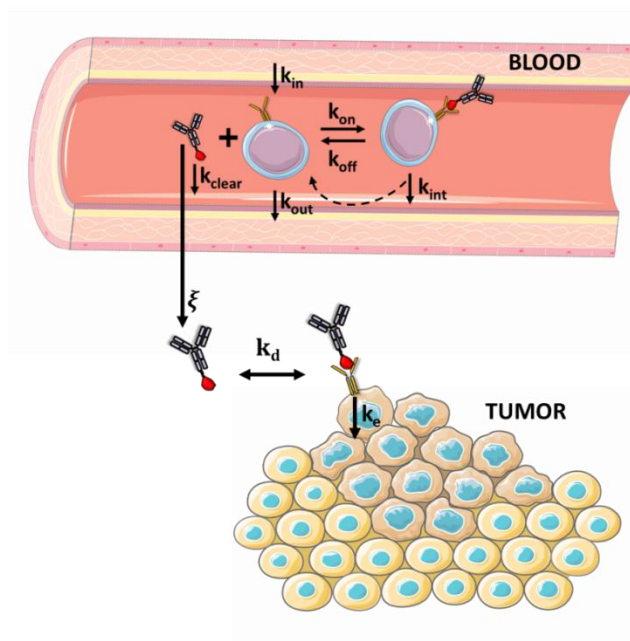


Figure 1. Model representation of drug uptake developed by Ribba, et al.

This example highlights the enormous potential of pharmacometrics modeling and simulation as a pillar in drug development and translational medicine, supporting dosing optimization and decision-making.

In summary, this thesis constitutes an effort of learning and application of a broad spectrum of modeling techniques and tools from the qualitative and quantitative systems pharmacology models (knowledge-driven) to the PKPD models (data-driven) applied to both drug development and clinical care. Across the different chapters, we present examples on the application of these techniques to situations with limited longitudinal data (chapter 1), longitudinal data from the literature (chapter 2) and experimental data from plasma, imaging and scarce data from the site of action (chapter 3).

REFERENCES

1. Marshall, S. *et al.* Model-informed Drug Discovery and Development (MID3): Current Industry Good Practice & Regulatory Expectations and Future Perspectives. *CPT Pharmacometrics Syst. Pharmacol.* (2018). doi:10.1002/psp4.12372
2. Wajima, T., Isbister, G. K. & Duffull, S. B. A comprehensive model for the humoral coagulation network in humans. *Clin. Pharmacol. Ther.* **86**, 290–298 (2009).
3. Nayak, S. *et al.* Using a Systems Pharmacology Model of the Blood Coagulation Network to Predict the Effects of Various Therapies on Biomarkers. *CPT Pharmacometrics Syst. Pharmacol.* **4**, 396–405 (2015).
4. Menezes, A. A., Vilaridi, R. F., Arkin, A. P. & Cohen, M. J. Targeted clinical control of trauma patient coagulation through a thrombin dynamics model. *Sci. Transl. Med.* **9**, 1–12 (2017).
5. Rogers, K. V., Bhattacharya, I., Martin, S. W. & Nayak, S. Know Your Variability: Challenges in Mechanistic Modeling of Inflammatory Response in Inflammatory Bowel Disease (IBD). *Clin. Transl. Sci.* **11**, 4–7 (2018).
6. Hoffman, M. & Monroe, D. M. A cell-based model of hemostasis. *Thromb. Haemost.* **85**, 958–65 (2001).
7. Ribba, B. *et al.* Prediction of the Optimal Dosing Regimen Using a Mathematical Model of Tumor Uptake for Immunocytokine-Based Cancer Immunotherapy. *Clin. Cancer Res.* **24**, 3325–3333 (2018).
8. Schmidt, M. M. & Wittrup, K. D. A modeling analysis of the effects of molecular size and binding affinity on tumor targeting. *Mol. Cancer Ther.* **8**, 2861–71 (2009).
9. Thurber, G. M. & Dane Wittrup, K. A mechanistic compartmental model for total antibody uptake in tumors. *J. Theor. Biol.* **314**, 57–68 (2012).

CONCLUSIONS/ CONCLUSIONES

- (1) A systems pharmacology model based on Boolean Network was built for the co-stimulation process, in the autoimmune disease Systems Lupus Erythematosus (SLE) disease, constituting proof of concept for this methodology in the context of Systems Pharmacology. The model allows identifying drug targets, optimal combinatorial regimens and subpopulations of responders and non-responders to drug treatment.
- (2) Two quantitative systems pharmacology models of coagulation process found in the literature were well implemented in Simbiology. Clinical data also found in the literature was simulated with both models. The models seem not to be appropriate to describe individual data due to the large number of parameters and equations making impossible the introduction of inter-individual variability in the models.
- (3) A semi-mechanistic PKPD model for coagulation process was successfully developed in order to describe individual clinical data. The model was able to describe individual thrombin profiles from normal subjects as well as trauma patients.
- (4) Considering drug exposure at the target site aside from systemic concentrations represent a powerful complement in drug development and translational medicine supporting dosing optimization and decision making.

- (1) Un modelo de Farmacología de Sistemas basado en redes Boleanas fue construido para el proceso de la co-estimulación, en la enfermedad autoinmune Lupus Eritematoso Sistémico (LES), constituyendo una prueba de concepto de esta metodología en el contexto de la farmacología de sistemas. El modelo permite la identificación de dianas terapéuticas, regímenes óptimos en combinación y subpoblaciones de pacientes de respondedores y no respondedores al tratamiento farmacológico.
- (2) Dos modelos de farmacología de sistemas cuantitativos del proceso de la coagulación encontrados en la literatura fueron bien implementados en Simbiology. Los datos clínicos que también fueron encontrados en la literatura se simularon con ambos modelos. Los modelos parecen no ser apropiados para describir datos individuales debido a la gran cantidad de parámetros y ecuaciones que hacen imposible la introducción de la variabilidad interindividual en los modelos.
- (3) Se desarrolló con éxito un modelo PKPD semi-mecanístico para el proceso de coagulación con el fin de describir datos clínicos individuales. El modelo fue capaz de describir los perfiles de trombina individuales de sujetos normales y de pacientes con traumatismo encontrados en la literatura.
- (4) Considerar la exposición al fármaco en lugar de acción a parte de las concentraciones a nivel sistémico, representa un potente complemento en el desarrollo de fármacos y la medicina traslacional, apoyando la optimización de la dosificación y la toma de decisiones.

ANNEX I

RESEARCH ARTICLE

A systems pharmacology model for inflammatory bowel disease

Violeta Balbas-Martinez^{1,2}, Leire Ruiz-Cerdá^{1,2}, Itziar Irurzun-Arana^{1,2}, Ignacio González-García^{1^{na}}, An Vermeulen^{3,4}, José David Gómez-Mantilla^{1^{nb}}, Iñaki F. Trocóniz^{1,2*}

1 Pharmacometrics & Systems Pharmacology, Department of Pharmacy and Pharmaceutical Technology, School of Pharmacy and Nutrition, University of Navarra, Pamplona, Spain, **2** IdiSNA, Navarra Institute for Health Research, Pamplona, Spain, **3** Janssen Research and Development, a division of Janssen Pharmaceutical NV, Beerse, Belgium, **4** Laboratory of Medical Biochemistry and Clinical Analysis, Faculty of Pharmaceutical Sciences, Ghent, Belgium

^{na} Current address: PharmaMar, Colmenar Viejo, Madrid, Spain.

^{nb} Current address: Boehringer Ingelheim, Ingelheim am Rhein, Germany.

* itroconiz@unav.es



OPEN ACCESS

Citation: Balbas-Martinez V, Ruiz-Cerdá L, Irurzun-Arana I, González-García I, Vermeulen A, Gómez-Mantilla JD, et al. (2018) A systems pharmacology model for inflammatory bowel disease. PLoS ONE 13(3): e0192949. <https://doi.org/10.1371/journal.pone.0192949>

Editor: Shree Ram Singh, National Cancer Institute, UNITED STATES

Received: October 17, 2017

Accepted: February 1, 2018

Published: March 7, 2018

Copyright: © 2018 Balbas-Martinez et al. This is an open access article distributed under the terms of the [Creative Commons Attribution License](https://creativecommons.org/licenses/by/4.0/), which permits unrestricted use, distribution, and reproduction in any medium, provided the original author and source are credited.

Data Availability Statement: All relevant data are within the paper and its Supporting Information files.

Funding: Development of the computational model was supported by a fellowship grant from the Navarra Government to Violeta Balbás-Martínez of 61.965 Euros (http://www.navarra.es/home_es/Actualidad/BON/Boletines/2017/18/Anuncio-5/) and Janssen Research and Development. The funders had no role in study design, data collection and analysis, decision to publish, or preparation of

Abstract

Motivation

The literature on complex diseases is abundant but not always quantitative. This is particularly so for Inflammatory Bowel Disease (IBD), where many molecular pathways are qualitatively well described but this information cannot be used in traditional quantitative mathematical models employed in drug development. We propose the elaboration and validation of a logic network for IBD able to capture the information available in the literature that will facilitate the identification/validation of therapeutic targets.

Results

In this article, we propose a logic model for Inflammatory Bowel Disease (IBD) which consists of 43 nodes and 298 qualitative interactions. The model presented is able to describe the pathogenic mechanisms of the disorder and qualitatively describes the characteristic chronic inflammation. A perturbation analysis performed on the IBD network indicates that the model is robust. Also, as described in clinical trials, a simulation of anti-TNF α , anti-IL2 and Granulocyte and Monocyte Apheresis showed a decrease in the Metalloproteinases node (MMPs), which means a decrease in tissue damage. In contrast, as clinical trials have demonstrated, a simulation of anti-IL17 and anti-IFN γ or IL10 overexpression therapy did not show any major change in MMPs expression, as corresponds to a failed therapy. The model proved to be a promising *in silico* tool for the evaluation of potential therapeutic targets, the identification of new IBD biomarkers, the integration of IBD polymorphisms to anticipate responders and non-responders and can be reduced and transformed in quantitative model/s.

the manuscript. Janssen Research and Development provided support in the form of salaries for author AV, but did not have any additional role in the study design, data collection and analysis, decision to publish, or preparation of the manuscript. The specific role of this author is articulated in the 'author contributions' section.

Competing interests: We have the following interests. This study was partly funded by Janssen Research and Development, the employer of An Vermeulen. There are no patents, products in development or marketed products to declare. This does not alter our adherence to all the PLOS ONE policies on sharing data and materials, as detailed online in the guide for authors.

Introduction

Inflammatory bowel disease (IBD) is a complex gastrointestinal tract disorder characterized by a functional impairment of the gut wall affecting patients' quality of life [1,2]. IBD includes ulcerative colitis (UC) and Crohn's disease (CD). The natural course of IBD is highly variable [3–6] and its etiology is still unknown. The incidence of IBD has dramatically increased worldwide over the past 50 years [7], reaching levels of 24.3 per 100,000 person-years in UC and 20.2 per 100,000 person-years in CD in the developed countries [8].

There is current evidence that Interleukin 6 (IL6), Tumour necrosis factor-alpha (TNF α), Interferon Gamma (IFN γ), Interleukin 1 beta (IL1 β), Interleukin 22 (IL22), Interleukin 17 (IL17) and Natural Killer cells (NK), among other signalling pathways, play relevant roles in the pathogenesis of IBD, which is a reflection of the complexity of that physiological system [9–12]. That complexity indicates that a universal treatment for IBD may not be feasible for the vast majority of patients [13,14]. In fact, current biological approved treatments are only palliative with a high percentage of non-responders. For example, around 50% of IBD patients treated with the current standard of care, Infliximab (an anti-TNF α) or Vedolizumab (an anti- α 4 β 7 integrin) do not respond satisfactorily to therapy [15,16]. One characteristic of the current IBD biological treatments is that approved therapies target just one signalling pathway, which might explain the high rate of non-responders and the long-term inefficiency of most treatments [15,17]. In addition, there is evidence to suggest that optimal treatment for IBD should involve a combination of different drugs [18,19]. Therefore, there is a need, especially for complex alterations such as immune-mediated diseases, to change the paradigm of drug development, considering the main aspects (targets, cross-talking between pathways, therapy combination) from an integrative and computational perspective.

Given the aforementioned biological complexity of immune-mediated diseases and the fact that current longitudinal data associated with the most relevant elements of the system are scarce, a full parameterization of IBD related systems based on a differential equation model does not yet seem feasible. However, some attempts have been made to describe quantitatively the IBD systems. For example, Wendelsdorf et al., [20] built a quantitative model based on ordinary differential equations. However, some key disease elements, such as cytokines and T cells, were incorporated non-specifically (i.e., all types of cytokine were grouped under the generic element active cytokines) in the model structure, limiting its use to explore potential therapeutic targets. More recently, Dwivendi et al., [21], based on the results of a clinical trial with the anti-IL6R antibody, Tocilizumab, have developed a multiscale systems model in Crohn's disease, limited to the IL6-mediated immune regulation pathway.

Network analysis represents a promising alternative in such data limited circumstances [22–24]. As many molecular pathways in IBD are qualitatively well described, interaction networks may be a suitable approach for characterizing IBD. These networks are simplified representations of biological systems in which the components of the system such as genes, proteins or cells are represented by nodes and the interactions between them by edges [25]. Boolean network models, originally introduced by Kauffman [26,27], represent the simplest discrete dynamic models. These models only assume two discrete states for the nodes of a network, ON or OFF, corresponding to the logic values 1 (active) or 0 (not active, but not necessarily absent) [28]. A well-designed logic model could generate predictive outcomes given a set of initial conditions. Qualitative, logical frameworks have emerged as relevant approaches with different applications, as demonstrated by a growing number of published models [29]. Complementing these applications, several groups have provided various methods and tools to support the definition and analysis of logical models, as it can be seen by the recent achievements of the Consortium for Logical Models and Tools (CoLoMoTo) in logical modelling [30].

There are already several tools for Boolean modeling of regulatory networks in which it is possible to define direct activation-inhibition relationships between the components of the network, such as BoolNet R [31] or GINsim [32]. More recently, the R package SPIDDOR (Systems Pharmacology for efficient Drug Development On R) among others, has implemented new types of regulatory interactions and perturbations within the system, such as positive and negative modulators and the polymorphism-like alterations, which lead to richer dynamics between the nodes [28].

In the specific case of IBD, there have been initial attempts to develop network models. The multi-state modeling tool published by Mei et al., [33,34] can be considered a proof of concept in the application of these types of networks in mucosal immune responses. However, the number of elements that this model considers and integrates is limited for IBD characterization, since only six different cytokine types are included in the inter-cellular scale.

The objective of the current manuscript is to present a Boolean based network model incorporating the main cellular and protein components known to play a key role in IBD development and progression. The model has been built on well-established experimental knowledge, mostly of human origin, and only including animal data when no other source of information was available. Our aim has been to build a model structure facilitating key aspects in the treatment of immune mediated disease, such as the selection of the most promising combination therapies and the study of the impact of polymorphisms on pathway regulation, thus allowing patient stratification and personalized medicine.

This study provides the scientific community with a (i) computational IBD model implemented in SPIDDOR R package [28], which allows translation of Boolean models (excluding models enclosing temporal operators) to a standard Markup language in Systems Biology for qualitative models (SBML qual [35]) which promotes model interoperability, and (ii) a repository with the main and updated information known of the immune system and IBD, which shows model transparency and allows model reusability. The proposed IBD model can be easily expanded in size and complexity to incorporate new knowledge, or other type of information such as proteomic data. The model presented hereafter is general enough to serve as a skeleton for other relevant immune diseases such as Rheumatoid Arthritis, Psoriasis or Multiple Sclerosis.

The manuscript is organized as follows: In the next section, Results regarding the structure of the model can be graphically visualized, and the ability of the model to recreate certain alterations that have been reported in IBD is demonstrated, as well as the model's capability to reproduce the results from recent clinical trials performed in IBD patients from a high-level perspective. Applications of the model, including its advantages and limitations are then discussed together with ideas for future research. Finally, the Methods section provides a detailed technical description (with the aid of supplementary material) of the network and a description of how simulations, collection, and representation of results have been performed.

Results

Graphical representation, repository, and Boolean functions

The graphical representation of the IBD network is shown in Fig 1. It consists of 43 nodes and 298 qualitative interactions located in three different physiological areas corresponding to (i) the lymph node, (ii) the blood and lymph circulatory system that irrigates the intestinal epithelial cells and (iii) the gut lumen.

Definition of all nodes and the full documented regulatory interactions conforming the model structure can be found in supporting information [S1 Table](#) and [S2 Table](#), respectively. The [S2 Table](#) is fundamental to understand the rationale for the selection and implementation

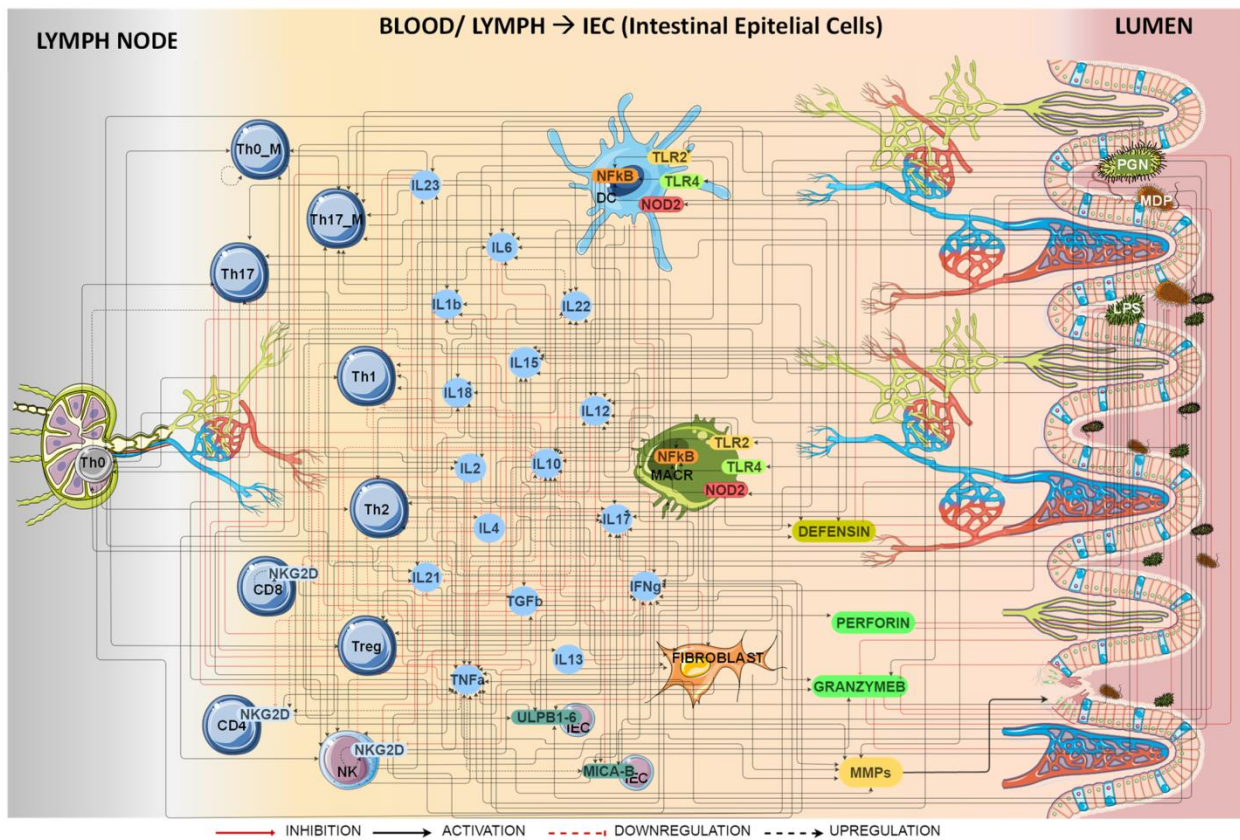


Fig 1. Graphical representation of IBD model. Nodes represent cells, proteins, bacterial antigens, receptors or ligands. Bacterial antigens trigger the IBD immune response through activation of different pattern recognition receptors (TLR2, TLR4 and NOD2) starting the innate and adaptive immune response. Reprinted from [36] under a CC BY license, with permission from the organizers of the 2016 International Conference on Systems Biology, original copyright 2016.

<https://doi.org/10.1371/journal.pone.0192949.g001>

of the Boolean functions (BF). It was organized to provide a comprehensive summary of the 301 manuscripts (published over the last three decades) used to build the model, highlighting for example whether (i) a specific pathway was reported to be altered in IBD, or (ii) information was supported by human (more than the 80% of the network structure) or animal data.

The Boolean operators used to define the network model of IBD were: the NOT operator which is noted as “!”, the AND operator which is noted as “&” and the OR operator which is noted as “|”. Recent and innovative modulators and threshold operators previously described by Irurzun-Arana et al., 2017 [28] were also part of the arsenal of Boolean elements used in the model proposed (see S1 File for a detailed description of those additional Boolean elements).

Regarding the input selection, as it is assumed that IBD is caused by intestinal dysbiosis, an environment of different bacteria was recreated selecting three different antigens which are components of most Bacterial Gram positive and Gram negative. Therefore, during the development of the proposed model the following assumptions were made: First, there is a chronic exposure to bacterial antigens: Peptidoglycan (PGN), Lipopolysaccharide (LPS) and Muramyl dipeptide (MDP). PGN is a component of the cell wall of all bacteria, but in particular of gram-positive bacteria, LPS is a component of the outer membrane of Gram-negative bacteria

Table 1. Boolean functions (BF) of the IBD model to simulate the initial conditions.

INITIAL CONDITIONS: CHRONIC EXPOSURE
$PNG = ! \left(\bigcap_{i=1}^{AG_elim-6} PERFOR^{i-1} \mid \bigcap_{i=1}^{AG_elim-6} GRANZB^{i-1} \mid \bigcap_{i=1}^{AG_elim-6} DEF^{i-1} \right)$
$MDP = ! \left(\bigcap_{i=1}^{AG_elim-6} PERFOR^{i-1} \mid \bigcap_{i=1}^{AG_elim-6} GRANZB^{i-1} \mid \bigcap_{i=1}^{AG_elim-6} DEF^{i-1} \right)$
$LPS = ! \left(\bigcap_{i=1}^{AG_elim-6} PERFOR^{i-1} \mid \bigcap_{i=1}^{AG_elim-6} GRANZB^{i-1} \mid \bigcap_{i=1}^{AG_elim-6} DEF^{i-1} \right)$

<https://doi.org/10.1371/journal.pone.0192949.t001>

[37], and MDP is a constituent of both Gram-positive and Gram-negative bacteria [38]. All three elicit strong immune responses and seem to play a critical role in the development and pathophysiology of IBD, as it has been hypothesized that the onset or relapse of IBD is triggered by an imbalance in self-microbiota composition than cannot be controlled by immune system [39]. Table 1 lists the initial conditions expressed by the corresponding BF, and shows that the nodes representing antigens are chronically expressed unless the natural antimicrobial peptides perforin (PERFOR), granzyme B (GRANZB) or defensins (DEF) become active.

Second, there is an impairment in antigen elimination in IBD patients [1,40,41], simulated with the threshold operator $Ag_elim = 6$. The threshold operator means that PERFOR, GRANZB, or DEF inhibit antigen activation when any of these three nodes have been activated for at least 6 consecutive iterations (see Table 1).

Third, the final readout of the network model is the average expression of the output node, Metalloproteinases (MMPs). There is solid evidence that this group of proteins is directly associated with intestinal fibrosis and tissue damage in IBD [42–46] supporting their use as a relevant biomarker in clinical practice as proposed by O’Sullivan et al. [47]. As it can be seen in Table 2, the nodes that directly activate MMPs are the nodes that have relevant roles in the pathogenesis of IBD [9–12,42–44,46,48].

Table 2 contains the full set of BF that modulates the signal initialized by the antigens through the activation of different pattern recognition receptors (TLR2, TLR4 and NOD2 nodes) and the impact on the output node (MMPs) as the recipient of the antigen signal internal modulation. The nodes TNF α or IFN γ have the most complex pathways as can be seen in the corresponding Boolean equations (Table 2).

With the aim of making the network model more accessible to the community it has been uploaded to “The Cell Collective” [49,50] platform (<https://www.cellcollective.org/#cb963d7f-75cb-4b2e-8987-0c7592a9c21d>). In addition, the supporting information document S2 File provides the network model in text format ready for simulation in the R-based freely available package SPIDDOR [28] and an html tutorial as a guide to reproduce the results (S3 File).

Perturbation analysis and clustering: Network robustness

The results of the network perturbation analysis are presented in Fig 2. The heatmap shows the impact of a single blockage of each node in every network node. The results indicate that most node blockages did not trigger considerable changes, suggesting that the IBD network is robust [51]. Some perturbations led to a higher activation of the nodes, while down regulations were more common. The heatmap was combined with a hierarchical clustering grouping together the nodes that caused similar alterations. Knockout of the NF κ B node appeared to be the most relevant alteration as it caused a reduction in expression of many of the nodes that were reported to be overexpressed in IBD patients. The knockout of the Th0 node (representing activated CD4+ T cells) also elicited a reduction in MMPs. The positive effects of the NF κ B and Th0 node blockades on MMPs decreased expression, resembled some of the known mechanisms of action of glucocorticoids, inhibitors of T cell activation and proinflammatory

Table 2. Boolean functions (BF) of the IBD model for the internal and the output nodes.

INTERNAL NODES
$TLR2 = PGN$
$TLR4 = LPS$
$NOD2 = MDP$
$NFkB = TLR2 NOD2 TLR4$
$IL6 = (MACR \& PGN) (DC \& (LPS PGN)) (Th17 \& IL23) (NFkB \& (ILA IL10))$
$TNF\alpha = ((NFkB \& LPS) (MACR \& (IL2 (IFN\gamma \& LPS) PGN))) (NK \& (MDP PGN LPS) \& (IL2 IL12) \& (IL2 IL15)) (FIBROBLAST \& IFN\gamma) ((CD4_NKG2D CD8_NKG2D NK_NKG2D) \& (IEC_MICA_B IEC_ULPB1_6)) \& ((\bigcap_{i=1}^{N_{reg}} IL10^{i-1} \& (\bigcap_{i=1}^{N_{reg}} TLR2^{i-1} \bigcap_{i=1}^{N_{reg}} TLR4^{i-1}) \& TNF\alpha))$
$TGFb = (Treg MACR)$
$Th0 = \bigcap_{i=1}^{N_{reg}} LPS^i \bigcap_{i=1}^{N_{reg}} MDP^i \bigcap_{i=1}^{N_{reg}} PGN^i$
$Th0_M = (Th0 \& (IL23 IL12)) Th0_M$
$IL18 = ((MACR DC) \& LPS) \& NFkB$
$IL1b = ((MACR DC) \& LPS \& NFkB) \& (IL1b \& (\bigcap_{i=1}^{N_{reg}} IL10^{i-1}))$
$IFN\gamma = ((NK \& (PGN LPS MDP \& (IL23 (IL12 \& (IL2 IL15 IL18)))) (Th0_M \& (LPS MDP PGN) \& (IL12 IL23)) Th1 ((CD8_NKG2D NK_NKG2D) \& (IEC_MICA_B IEC_ULPB1_6)) (Th17 \& (PGN LPS MDP))) ((MACR Th0) \& IL18 \& IL12) \& ((IFN\gamma \& (\bigcap_{i=1}^{N_{reg}} TGFb^{i-1} \bigcap_{i=1}^{N_{reg}} IL10^{i-1} Th2))$
$IL23 = (MACR \& IL1b) DC$
$IL22 = Th17 (NK \& ((IL18 \& IL12) IL23)) CD4_NKG2D ((IL22 \& Th0 \& IL21) \& ((\bigcap_{i=1}^{N_{reg}} IL22^{i-1} \& (\bigcap_{i=1}^{N_{reg}} Th0^{i-1} \& (\bigcap_{i=1}^{N_{reg}} IL21^{i-1})) \& TGFb))$
$IL21 = Th17 ((Th0 \& IL6) \& (ILA IFN\gamma TGFb))$
$IL17 = ((Th17 (Th17_M \& (LPS MDP PGN))) (CD4_NKG2D \& (IEC_MICA_B IEC_ULPB1_6))) \& ((\bigcap_{i=1}^{N_{reg}} TGFb^{i-1} \bigcap_{i=1}^{N_{reg}} IL13^{i-1}) \& IL17)$
$IL10 = Treg (Th2 \& IL23) ((TLR2 \& NFkB) \& (MACR \& IFN\gamma)) ((MACR \& LPS) \& IL4) (DC \& LPS)$
$Th17 = ((Th0 \& (IL1b IL23 IL6)) ((Th17 \& IL23) \& ((\bigcap_{i=1}^{N_{reg}} Th17^{i-1} \& (\bigcap_{i=1}^{N_{reg}} IL23^{i-1}))) \& ((\bigcap_{i=1}^{N_{reg}} TGFb^{i-1} \bigcap_{i=1}^{N_{reg}} IL12^{i-1} \bigcap_{i=1}^{N_{reg}} IL4^{i-1} \bigcap_{i=1}^{N_{reg}} IFN\gamma^{i-1} \bigcap_{i=1}^{N_{reg}} Treg^{i-1}) \& Th17)$
$Th17_M = ((Th0_M \& (PGN MDP LPS)) \& ((IL1b \& IL6) IL23 IL2)) Th17_M$
$Th1 = (Th0 \& ((IL12 IFN\gamma IL18) (DC \& IL12 \& IL23 \& LPS))) \& ((\bigcap_{i=1}^{N_{reg}} IL17^{i-1} \& (\bigcap_{i=1}^{N_{reg}} IL12^{i-1} \bigcap_{i=1}^{N_{reg}} Treg^{i-1} \bigcap_{i=1}^{N_{reg}} Th2^{i-1} \bigcap_{i=1}^{N_{reg}} TGFb^{i-1} \bigcap_{i=1}^{N_{reg}} IL10^{i-1} \bigcap_{i=1}^{N_{reg}} IL4^{i-1}) \& Th1)$
$Th2 = (Th0 \& (IL10 ((IL18 \& IL4) \& IL12)) ((Th2 \& IL4) \& ((\bigcap_{i=1}^{N_{reg}} Th2^{i-1} \& (\bigcap_{i=1}^{N_{reg}} IL4^{i-1}))) \& ((\bigcap_{i=1}^{N_{reg}} Treg^{i-1} \bigcap_{i=1}^{N_{reg}} IFN\gamma^{i-1} \bigcap_{i=1}^{N_{reg}} TGFb^{i-1}) \& Th2)$
$IL4 = Th2$
$IL15 = (FIBROBLAST \& (MDP LPS PGN)) (MACR \& (LPS IFN\gamma))$
$IL12 = (((MACR DC) \& (LPS PGN) \& IFN\gamma) \& (IL12 \& (\bigcap_{i=1}^{N_{reg}} TNF\alpha^{i-1}))) (DC \& IL1b) (IL12 \& (IL13 IL4)) \& ((\bigcap_{i=1}^{N_{reg}} TGFb^{i-1} \bigcap_{i=1}^{N_{reg}} IL10^{i-1}) \& IL12)$
$IL13 = Th2$
$Treg = ((\bigcap_{i=1}^{N_{reg}} Th0^{i-1} \& (TGFb TLR2)) \& ((\bigcap_{i=1}^{N_{reg}} IL6^{i-1} \bigcap_{i=1}^{N_{reg}} IL21^{i-1} \bigcap_{i=1}^{N_{reg}} IL23^{i-1} \bigcap_{i=1}^{N_{reg}} Th17^{i-1} \bigcap_{i=1}^{N_{reg}} IL22^{i-1} \bigcap_{i=1}^{N_{reg}} TNF\alpha^{i-1}) \& Treg)$
$NK = (IL15 IL2 IL12 IL23 (IL18 \& IL10)) \& ((\bigcap_{i=1}^{N_{reg}} Treg^{i-1} \& NK)$
$DEF = IL22 IL17 \bigcap_{i=1}^{N_{reg}} NOD2^{i-1}$
$IL2 = Th0 (Th0_M \& (MDP LPS PGN)) DC$
$MACR = (NFkB ((MACR \& (IFN\gamma IL15)) \& ((\bigcap_{i=1}^{N_{reg}} NFkB^{i-1} \& (\bigcap_{i=1}^{N_{reg}} IFN\gamma^{i-1} \bigcap_{i=1}^{N_{reg}} IL15^{i-1})))) \& ((\bigcap_{i=1}^{N_{reg}} IL10^{i-1} \& MACR)$
$DC = NFkB \& ((\bigcap_{i=1}^{N_{reg}} IL10^{i-1} \& DC)$
$IEC_MICA_B = ((LPS MDP PGN) (IEC_MICA_B \& TNF\alpha)) \& ((\bigcap_{i=1}^{N_{reg}} IEC_MICA_B^{i-1} \& (\bigcap_{i=1}^{N_{reg}} TNF\alpha^{i-1})) \& TGFb$
$IEC_ULPB1_6 = CD8_NKG2D \& (LPS MDP PGN)$
$CD8_NKG2D = (LPS PGN MDP) \& ((\bigcap_{i=1}^{N_{reg}} IEC_MICA_B^{i-1} \bigcap_{i=1}^{N_{reg}} IEC_ULPB1_6^{i-1} \bigcap_{i=1}^{N_{reg}} IL21^{i-1} \& (\bigcap_{i=1}^{N_{reg}} IL2^{i-1}) \& CD8_NKG2D)$
$NK_NKG2D = (LPS PGN MDP) \& ((\bigcap_{i=1}^{N_{reg}} TGFb^{i-1} \bigcap_{i=1}^{N_{reg}} IEC_MICA_B^{i-1} \bigcap_{i=1}^{N_{reg}} IEC_ULPB1_6^{i-1} \bigcap_{i=1}^{N_{reg}} IL21^{i-1} \& (\bigcap_{i=1}^{N_{reg}} IL2^{i-1}) \& NK_NKG2D)$
$CD4_NKG2D = (LPS PGN MDP (CD4_NKG2D \& (IL15 TNF\alpha))) \& ((\bigcap_{i=1}^{N_{reg}} CD4_NKG2D^{i-1} \& (\bigcap_{i=1}^{N_{reg}} IL15^{i-1} \bigcap_{i=1}^{N_{reg}} TNF\alpha^{i-1}))) \& ((\bigcap_{i=1}^{N_{reg}} IL10^{i-1} \bigcap_{i=1}^{N_{reg}} IEC_MICA_B^{i-1} \bigcap_{i=1}^{N_{reg}} IEC_ULPB1_6^{i-1} \bigcap_{i=1}^{N_{reg}} IEC_ULPB1_6^{i-1}) \& CD4_NKG2D)$
$FIBROBLAST = ((MACR \& (IL4 IL13 TGFb)) IL2) \& ((\bigcap_{i=1}^{N_{reg}} IFN\gamma^{i-1} \bigcap_{i=1}^{N_{reg}} IL12^{i-1}) \& FIBROBLAST)$
$PERFOR = NK NK_NKG2D$

(Continued)

Table 2. (Continued)

$GRANZB = CD8_NKG2D \mid NK \mid NK_NKG2D \mid (DC \& ! (LPS \mid PGN))$	OUTPUT NODE
$MMPs = (MACR \& TNF\alpha) \mid (FIBROBLAST \& (IL21 \mid IL17 \mid IL1b \mid TNF\alpha))$	

Bold text within Boolean equations indicates that the information belongs to animal data

<https://doi.org/10.1371/journal.pone.0192949.t002>

cytokines, as well as potent suppressors of the effector function of monocyte-macrophage and fibroblastic activity, interfering with the NF κ B inflammatory signal [52–54].

Network accuracy and validation

Experimental and clinical information. Simulations of chronic infection in IBD individuals show that the model reproduced satisfactorily experimental and clinical information (summarized in Table 3 and supporting information S3 Table). Fig 3 shows the results of the simulation for each network node after reaching the attractor state for virtual healthy and IBD subjects. In total, 31 upregulations in experimental studies were replicated with our simulations. Similarly, the 9 nodes reported as altered appeared upregulated in the simulations, and finally, the three nodes whose profiles were not known also proved to be upregulated.

Clinical trials. In our simulations, three drugs that have failed to prove clinical efficacy in clinical trials (anti-IL17, anti-IFN γ and rhuIL-10) also exhibited no benefit in the simulated surrogate for the disease score (Fig 4). Simulations with anti-TNF α , a biologic therapy approved for IBD, showed a decrease in the disease score. Simulations with anti-IL12-IL23, a recently approved therapy for IBD, showed a slight decrease in MMPs and anti-IL2 therapy simulation showed a decrease similar to anti-TNF α . In addition, the new promising therapy (GMA), equivalent to an anti-MACR in our model showed a decrease in MMPs similar to that for anti-TNF α .

Discussion

In the current study, we present a Systems Pharmacology (SP) network model for IBD based on the main cells and proteins involved in the disease. Our analysis appears timely, as IBD has recently been attracting increasing attention [55–59]. We attempted to meet one of the major challenges in inflammatory bowel disease (IBD) which is the integration of IBD-related information to construct a predictive model. We are not the only ones following this line of research, as Lauren A Peters et al. have very recently performed a key driver analysis to identify the genes predicted to modulate network regulatory states associated with IBD [55]. Both analyses could be integrated in the future and inform our post-transcriptomic network with the key driver genes identified by Lauren A Peters et al. [55].

In comparison with the previous quantitative approaches for IBD [20,21,33,34], our model identified Naive CD4+ T Cells, Macrophages and Fibroblasts cells as relevant in IBD. Also, in addition to the six interleukins (TGF β , IL6, IL17, IL10, IL12 and IFN γ) considered by Mei et al. [33,34] our network involves 10 interleukins more which could represent possible IBD biomarkers [60]. The procedure to evaluate the potential role of the different components on the disease as plausible biomarkers, would be equal to the one described in section 4.5 (perturbation analysis and clustering), focussing on the changes in the output node.

In the validation of network models, robustness and practical applicability represent critical aspects. The fact that the information gathered from the literature was obtained under very

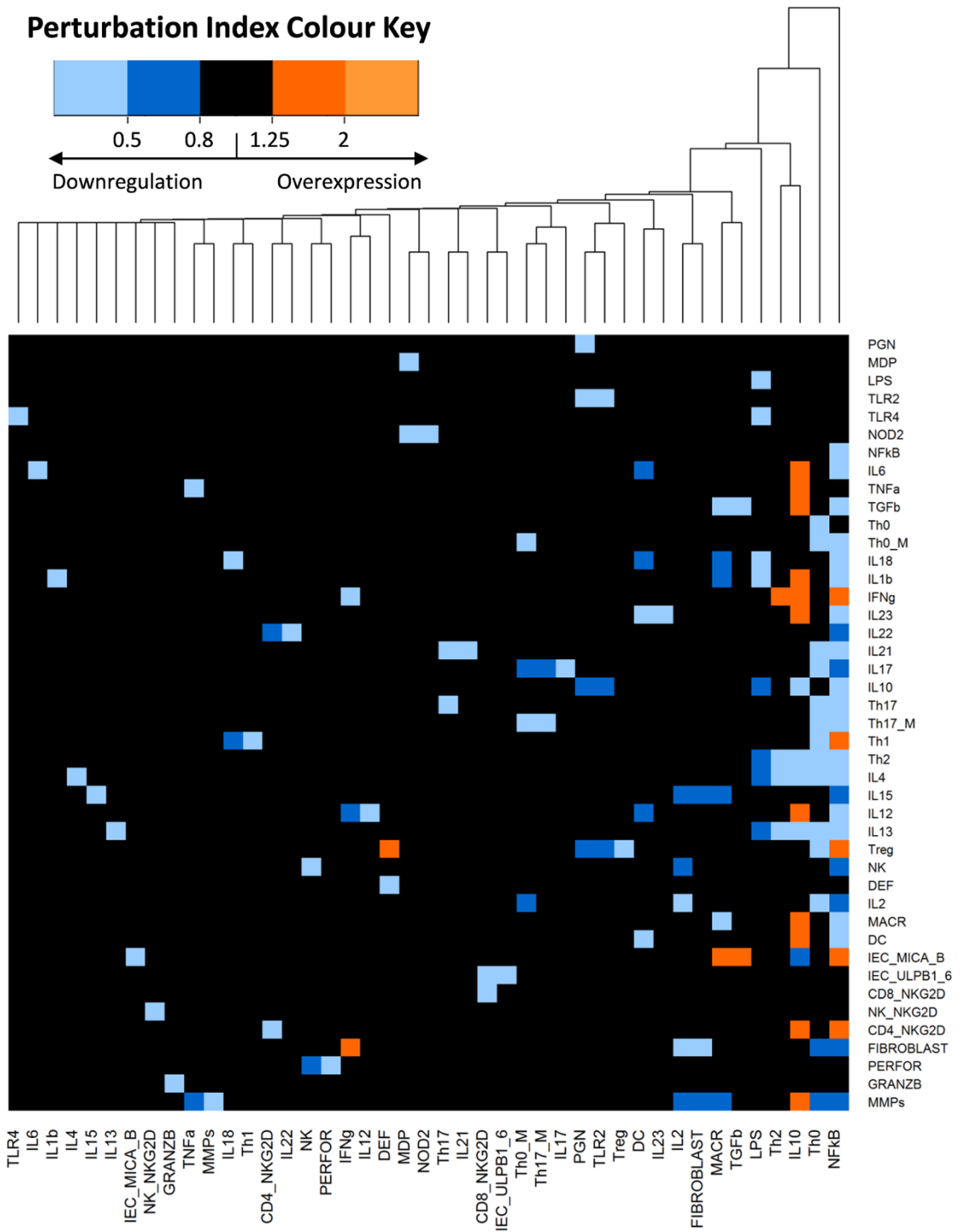


Fig 2. IBD network perturbation analysis and clustering. The heatmap indicates the effect of single blockage of each node (columns) in every network node (rows). The colour in each cell corresponds to the Perturbation Index (PI) of the nodes. When there is no change in the expression of the node, the cells of the heatmap would be black, having a value between 0.8 and 1.25 in their PIs. Otherwise, when the perturbation causes an overexpression in a node, the cell in the heatmap would be orange coloured, with PIs values greater than 1.25. On the contrary, a value of 0.8 or smaller, blue colour, indicates that the perturbation causes a downregulation of the node. The numeric scale in the legend represents different values of the nodes PI under different perturbations. Nodes that induce similar alterations are hierarchically clustered.

<https://doi.org/10.1371/journal.pone.0192949.g002>

different experimental designs/conditions/methodologies, represents a challenge with respect to validation. This led us to propose and adopt a novel strategy consisting of the comparison of the results of model-based virtual pathway simulations with those reported in the literature for IBD patients. Using this approach, we obtained a qualitative reproduction of IBD in which all the network elements that have been reported as upregulated in IBD patients appeared upregulated in our simulation results. The perturbation analysis of the network was performed by a single blockage in each node to analyse how that type of alteration propagates through the entire network reflecting the case of single polymorphisms, which represents the simplest case of IBD disease. Despite of the simplicity of this analysis, the results obtained from the model accuracy and validation procedures are encouraging. Results from the perturbation analysis indicate that the proposed network model is robust, as alteration in most nodes did not trigger considerable changes in the network [61].

Once validated and checked for robustness, the network was challenged to qualitatively reproduce the readouts of five different therapies reported in experimental and clinical studies. The outcome of this challenge was similar to the clinical output in IBD patients. By the simulation of TNF α or MACR knockout (simulating Granulocyte and Monocyte Apheresis), a decrease in MMPs node was observed, which is in line with therapy success in clinical practice by a decrease in Crohn's Disease Activity Index (CDAI) Score [42–46],[62–68]. On other hand, IL17 or IFN γ knockout or IL10 overexpression did not show major change in MMPs expression, suggested a failed therapy as was indeed found in clinical practice [69–72].

Surprisingly, the model shows that a knockout of IL2 leads to a reduction in MMPs similar to that of a knockout of TNF α , even when previous results of clinical trials with Basiliximab or Daclizumab (monoclonal antibodies that bind to the interleukin 2 receptor CD25) in Ulcerative Colitis have failed to show superiority to corticosteroids alone [73,74]. The mechanism of

Table 3. Expression of network nodes in IBD patients.

NODE	EXPRESSION	NODE	EXPRESSION	NODE	EXPRESSION	NODE	EXPRESSION
PGN MDP LPS	Altered	IL1b	Upregulated	Th2	Upregulated	DC	Downregulated in Blood-Upregulated in mucosa
TLR2	Upregulated	IFN γ	Upregulated	IL4	Altered	IEC_MICA_B	Upregulated
TLR4	Upregulated	IL23	Upregulated	IL15	Upregulated	IEC_ULPB1_6	Upregulated
NOD2	Altered	IL22	Upregulated	IL12	Upregulated	CD8_NKG2D	Upregulated
NFkB	Altered	IL21	Upregulated	IL13	Upregulated	NK_NKG2D	Unknown
IL6 TNFa	Upregulated Upregulated	IL17	Upregulated	Treg	Downregulated in Blood-Upregulated in mucosa	CD4_NKG2D	Upregulated
TGFb	Upregulated	IL10	Upregulated	NK	Upregulated	FIBROBLAST	Upregulated
Th0	Unknown	Th17	Upregulated	DEF	Altered	MMPs	Upregulated
Th0_M	Upregulated	Th17_M	Upregulated	IL2	Upregulated	PERFOR	Altered
IL18	Upregulated	Th1	Altered	MACR	Unknown	GRANZB	Upregulated

A total of 31 nodes are reported as upregulated in IBD patients, 9 are reported to be altered (when different reports from literature are inconclusive or contradictory) and 3 nodes are unknown.

<https://doi.org/10.1371/journal.pone.0192949.t003>

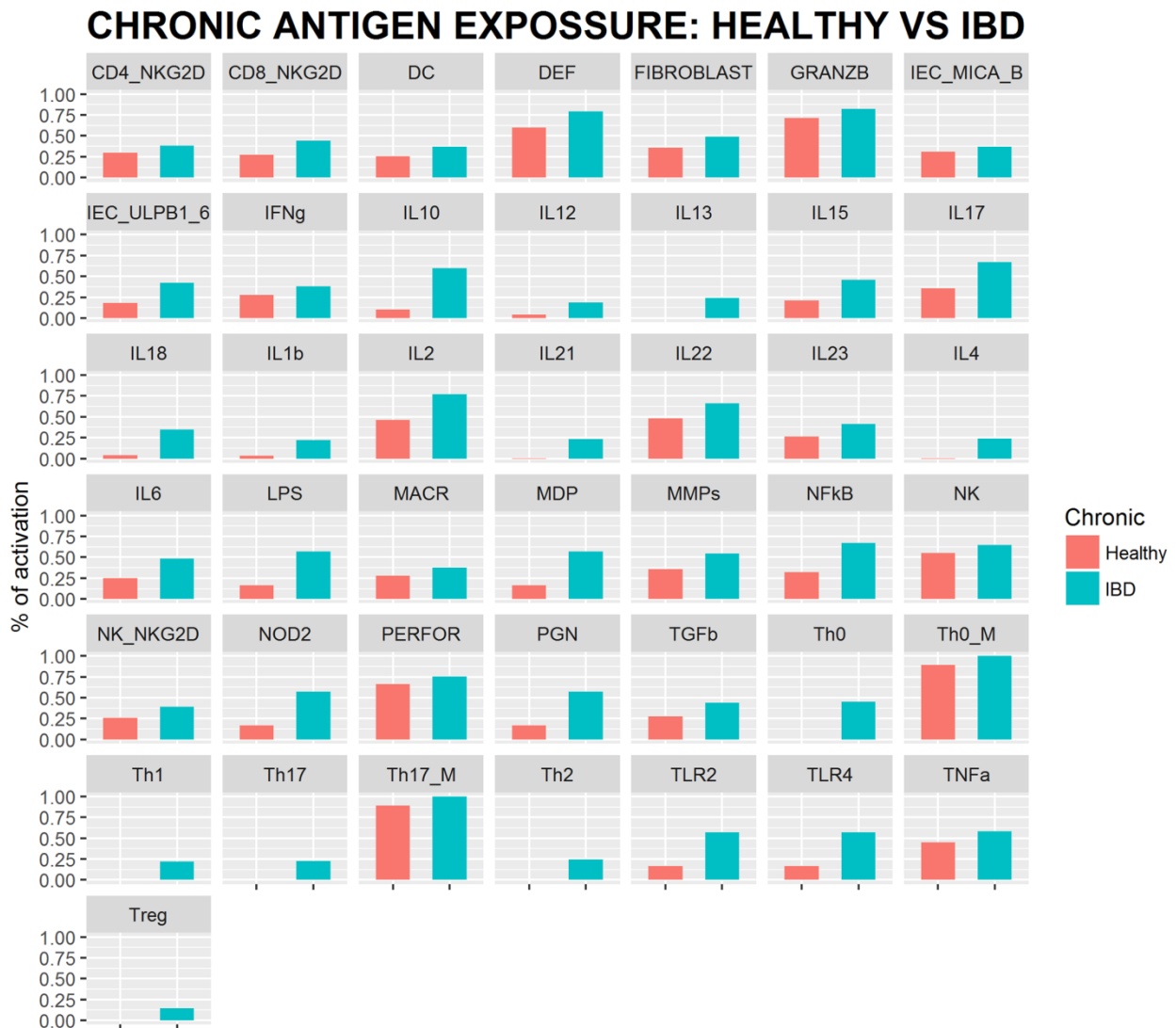


Fig 3. IBD network simulation results. Attractor state of every network node for healthy and IBD simulated individuals under chronic antigen exposure.

<https://doi.org/10.1371/journal.pone.0192949.g003>

action of corticosteroids has not been fully described, yet it is known that corticosteroids cause diminished levels of IL2 mRNA [75,76]. Together with the rest of corticosteroid inhibitory mechanisms, this would be the reason why Basiliximab or Daclizumab do not show superiority to corticosteroids alone.

Among the potential applications the current network supports: (i) biomarker selection given that the cytokines $TNF\alpha$, IL21, IL17 and IL1 β , which can be easily measured in peripheral plasma with different Enzyme-linked immunosorbent assay (ELISA) kits [77,78], are the model components directly related to MMPs activation, (ii) search for optimal combination therapy to overcome the high attrition rates in phase clinical trials with single therapies which

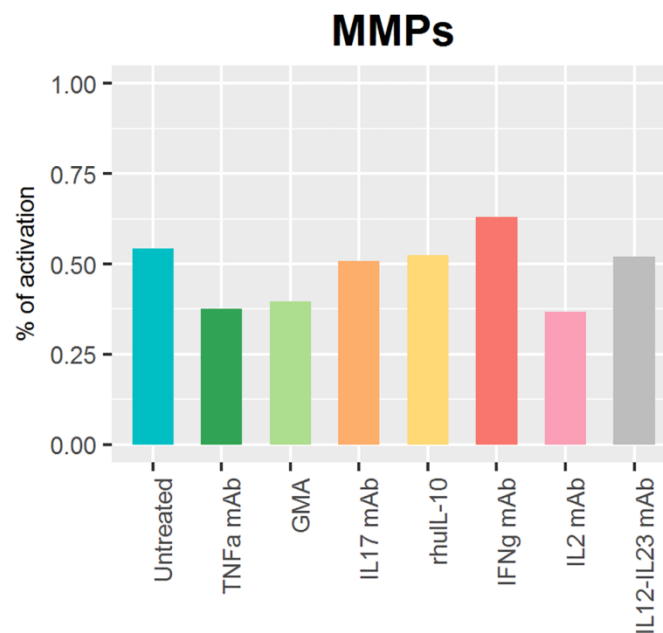


Fig 4. Comparison of MMPs expression after the simulation in IBD simulated individuals of different therapies. Simulated therapies: Anti-TNF α , GMA therapy (equivalent of knock out our MACR node), anti-IL17, human recombinant IL10 (rhIL-10), anti-IFN γ , anti-IL2 and anti-IL12-IL23. Comparing with untreated simulation, we can see a 30.7%, a 27.1%, a 31.9% and a 4.1% decrease in the MMPs expression simulating anti-TNF α , GMA therapy, anti-IL2 and anti-IL12-IL23 respectively. There is no major change in MMPs expression for the two which failed in clinical trials anti-IL17 (a 6.5% decrease) and human recombinant IL10 (a 3.2% decrease). Otherwise, anti-IFN γ therapy simulation shows an increase in MMPs expression of 16.0% compared to Untreated.

<https://doi.org/10.1371/journal.pone.0192949.g004>

are due mainly to lack of efficacy [79], and (iii) management of multiscale information such as the integration of proteomic gene expression data [55] accounting for IBD polymorphisms to anticipate responders and non-responders. With such a type of data able to correlate a genetic alteration with a decrease or an increase in protein expression, it would be possible to simulate specific genetic alteration by altering the protein expression. This would allow one of the limitations of the current network at the present time to be overcome with regard to the effects of Ustekinumab, a monoclonal antibody targeting free IL12 and IL23, which has been recently approved for moderately to severely active Crohn's disease in adults who have failed to treatment with immunomodulators, or more than one TNF α blocker [80]. Simulation results based on the known mechanisms of Ustekinumab showed just a 4.1% decrease in tissue damage. On the other hand, when simulating TNF α blocker effects, tissue damage decreased by 30.6% even though a substantial percentage of patients showed poor control of the disease after treatment with anti-TNF α antibody [15,16].

We emphasize that the proposed network model is fully accessible which allows it to undergo immediate testing and further development. In that respect it should be noted that although our model intended to include information of human origin exclusively, some critical pathways had to be complemented with animal derived data (although in the current case the percentage of human supported pathways is greater than in previous computational models [20,81,82]), but we are aware of the wide differences in the immune system between species [83–85].

This study addresses the goals of systems pharmacology by effectively encompassing prior knowledge to generate a mechanistic and predictive understanding at the systems level for IBD. Semi-quantitative understanding at the network level is necessary prior to the generation of detailed quantitative models for within-host disease dynamics. The current IBD model and the companion literature summary archive will drive the development of a dynamic (i.e., ordinary differential equation driven) model involving meaningful parameters capable of simulating longitudinal data, and allowing model reduction as well the goal of parameter estimation during the clinical stages of the drug development process. In addition, our IBD network can be extended to other inflammatory diseases, as main pathways in the model are common to most inflammatory conditions [86,87], and the outputs of our nodes could also serve as inputs to broader-scale logic models; for example, incorporating structures from available logic models of some of our nodes such as fibroblast [61], IL1b or IL6 [88].

In summary, we present a network model for inflammatory bowel disease which is available and ready to be used and can cope with (multi-scale) model extensions. It is supported by a comprehensive repository summarizing the results of the most relevant literature in the field. This model proved to be promising for the *in silico* evaluation of potential therapeutic targets, the search for pathway specific biomarkers, the integration of polymorphisms for patient stratification, and can be reduced and transformed in quantitative model/s.

Methods

Literature search and data selection

The network model is based on an exhaustive bibliographic review focusing on the essential components of IBD, as previously performed by Ruiz-Cerdá et al., in their systems pharmacology approach for lupus erythematosus [23]. Our review included around 620 papers published between October 1984 and September 2017, yet the most common reviewed articles were from 2007 or later (76%). The search of the relevant literature was made through Medical Subject Headings (MeSH) terms using different search engines such as PubMed, clinicaltrials.gov or google scholar. MeSH terms were focused on the combination of keywords and free words including: (i) relevant network components (ej. "IL6") involved in the pathogenesis of IBD, (ii) nodes that have been reported to be altered in IBD (ej. "IL6 AND IBD") and (iii) nodes directly affecting the expression of the nodes selected in (i) and (ii) (ej. "DC AND IL6"). The internal nodes selection was made according to the reported upregulated components in IBD patients together with the nodes (immune system cells) which are necessary to link the upregulated nodes, which were established as internal nodes. Only original papers with a clear description of experimental conditions were considered to identify the relationships between the components of the biological network. Due to the reported differences between animal and human immunology [83–85], in only few cases were animal data considered to connect nodes of critical pathways when no human data were available.

Annotation and system representation

Annotation was crucial to organize the available literature according to its relevance. S2 Table from supplementary information shows the way the information was organized for building the network. S2 Table includes every node definition and the relationships between the nodes. Annotation included the identification of the main elements (antigens, cytokines, cells, proteins, membrane receptors and ligands) of IBD disease.

The IBD model will be freely accessible to the public through the "The Cell Collective" repository <https://cellcollective.org/#cb963d7f-75cb-4b2e-8987-0c7592a9c21d>.

Boolean network building and R implementation

The collection of qualitative relationships extracted from the literature was transformed into a logical model as described before by Ruiz-Cerdá et al. [23]. Logic networks capture the dynamics of their components, called nodes, after selected stimuli or initial conditions [89,90] <https://paperpile.com/c/XvtklO/p0BRz+YiQ4q>. In these models the relationships of activation or inhibition between nodes are described as combinations of the logic operators: AND, OR and NOT condensed in a mathematical expression called a Boolean function for each node. Positive and negative modulators, and thresholds as previously described by Ruiz-Cerdá et al. [23] and Irurzun-Arana et al. [28] were also considered to resemble better the biological system. Boolean network building and R implementation from [S1 File](#) gives a more detailed explanation of the modulators used in the model.

Simulations

The set of combined Boolean functions for the IBD model was implemented SPIDDOR [28], using RStudio Version 0.99.442. Simulations with 25 repetitions over 5000 iterations were performed. According to preliminary experiments, these simulation conditions were required to achieve the steady state of the network called attractor [91–93]. An attractor can be a fixed-point if it composed of one state, a simple cycle if consists of more than one state that oscillates in a cycle or a complex attractor if a set of steady-states oscillate irregularly. In each simulation, a node can show two possible values in each iteration: 0 (deactivated) or 1 (activated). The percentage of activation of the output node (MMPs) calculated at the attractor state was used as the readout summary of the simulation exercises, as this group of proteins are directly associated with intestinal fibrosis and tissue damage in IBD [42–46].

Each node was updated asynchronously [94–96] according to its Boolean function that defines the dynamics of the system. Initial conditions are explained in detail in “Simulations” from [S1 File](#).

Perturbation analysis and clustering

Robustness can be defined as the system’s ability to function normally under stochastic perturbations [96]. The investigation of robustness in Boolean networks generally focuses on the dependence between robustness and network connectivity [97]. We performed a perturbation analysis in our IBD model to study robustness by simulating the effect of the single blockage of each node on every other node of the network [51]. This simulation was performed by using the *KO_matrix.f* function from SPIDDOR package with 24 repetitions over 999 iterations under asynchronous updating.

Results from the simulations described above were represented as heatmaps with dendrograms in which the number of rows and columns is equal to the number of nodes in the network (Fig 2). The colour in each cell of the heatmap corresponds to the Perturbation Index (PI) of the nodes, which is the probability ratio between the perturbed and the normal conditions as described by Irurzun-Arana et al. [28]. A hierarchical clustering method [98] was applied to further study which nodes cause similar alterations in the system.

Network accuracy and validation

Accuracy was evaluated comparing the alterations reported in the literature for IBD patients with the simulations of chronic antigen exposure for IBD or healthy individuals.

A literature search of every node expression in IBD patients was performed, and the gathered information is condensed in [S3 Table](#) including three categories: up-, down-regulated, or

altered, whether the levels in CD, UC or both (IBD) with respect to healthy volunteers are higher, lower, or inconclusive and/or contradictory, respectively.

For validation purposes, model simulations were compared against available results from clinical trials performed in IBD, CD or UC until the beginning of 2017 in <https://www.clinicaltrials.gov/>. All the molecules tested in clinical trials, whose mechanism of action is known and whose target were included in our network, were tested with the model. The network was evaluated comparing simulations and reported outcomes from clinical trials for six investigated molecules: anti-TNF α [62–65] and anti-IL12-IL23 [80], two monoclonal antibodies (mAb) approved for IBD disease, anti-IFN γ [69,70], anti-IL17 [72], anti-IL2 [73,74] and human recombinant IL10 (rhuIL-10) [71] which failed in clinical trials. Also a new promising therapy: Granulocyte and Monocyte Apheresis (GMA) [66–68] was tested. The reported CDAI (Crohn Disease Activity Index) was compared with the average expression of the MMPs output node in the attractor state.

Supporting information

S1 Table. Abbreviations. List of abbreviations.

(PDF)

S2 Table. IBD Network Repository. Table of nodes and interactions supported by references.

(PDF)

S3 Table. IBD_validation. Table of alterations in patients of IBD network nodes supported by references.

(PDF)

S1 File. Supporting_Information_Methods. Document with detailed description of the methodology.

(DOCX)

S2 File. IBD.txt. Text document with the Boolean functions written in SPIDDOR nomenclature for iBD simulation.

(TXT)

S3 File. User_Guide_SPIDDOR_IBD.html. Html tutorial about how to reproduce the results from the present manuscript with the SPIDDOR package.

(HTML)

Acknowledgments

We would like to thank The Cell Collective team, specially to Tomas Helikar, for their help in building the model in their platform and making it more accessible to the community.

Author Contributions

Conceptualization: Violeta Balbas-Martinez, José David Gómez-Mantilla, Iñaki F. Trocóniz.

Data curation: Violeta Balbas-Martinez, Leire Ruiz-Cerdá, Ignacio González-García.

Formal analysis: Violeta Balbas-Martinez, Leire Ruiz-Cerdá, Itziar Irurzun-Arana, José David Gómez-Mantilla.

Funding acquisition: An Vermeulen, Iñaki F. Trocóniz.

Investigation: Violeta Balbas-Martinez, Leire Ruiz-Cerdá, Ignacio González-García, José David Gómez-Mantilla.

Methodology: Violeta Balbas-Martinez, Itziar Irurzun-Arana, Ignacio González-García, José David Gómez-Mantilla, Iñaki F. Trocóniz.

Project administration: An Vermeulen, Iñaki F. Trocóniz.

Software: Violeta Balbas-Martinez, Itziar Irurzun-Arana, Ignacio González-García, José David Gómez-Mantilla.

Supervision: An Vermeulen, José David Gómez-Mantilla, Iñaki F. Trocóniz.

Validation: Violeta Balbas-Martinez, José David Gómez-Mantilla.

Visualization: Violeta Balbas-Martinez.

Writing – original draft: Violeta Balbas-Martinez, Iñaki F. Trocóniz.

Writing – review & editing: Violeta Balbas-Martinez, José David Gómez-Mantilla, Iñaki F. Trocóniz.

References

1. Wehkamp J, Götz M, Herrlinger K, Steurer W, Stange EF. Inflammatory Bowel Disease. *Dtsch Arztebl Int.* 2016; 113: 72–82. <https://doi.org/10.3238/arztebl.2016.0072> PMID: 26900160
2. Matricon J, Barnich N, Ardid D. Immunopathogenesis of inflammatory bowel disease. *Self Nonself.* 2010; 1: 299–309. <https://doi.org/10.4161/self.1.4.13560> PMID: 21487504
3. Solberg IC, Lygren I, Jahnsen J, Aadland E, Høie O, Cvancarova M, et al. Clinical course during the first 10 years of ulcerative colitis: results from a population-based inception cohort (IBSEN Study). *Scand J Gastroenterol.* 2009; 44: 431–440. <https://doi.org/10.1080/00365520802600961> PMID: 19101844
4. Faubion WA Jr, Loftus EV Jr, Harmsen WS, Zinsmeister AR, Sandborn WJ. The natural history of corticosteroid therapy for inflammatory bowel disease: a population-based study. *Gastroenterology.* 2001; 121: 255–260. PMID: 11487534
5. Loftus EV, Schoenfeld P, Sandborn WJ. The epidemiology and natural history of Crohn's disease in population-based patient cohorts from North America: a systematic review. *Aliment Pharmacol Ther.* Wiley Online Library; 2002; 16: 51–60. PMID: 11856078
6. Henriksen M, Jahnsen J, Lygren I, Sauar J, Kjellevoid Ø, Schulz T, et al. Ulcerative colitis and clinical course: results of a 5-year population-based follow-up study (the IBSEN study). *Inflamm Bowel Dis.* 2006; 12: 543–550. <https://doi.org/10.1097/01.MIB.0000225339.91484.fc> PMID: 16804390
7. Gasparetto M, Guariso G. Highlights in IBD Epidemiology and Its Natural History in the Paediatric Age. *Gastroenterol Res Pract.* 2013; 2013: 829040. <https://doi.org/10.1155/2013/829040> PMID: 24454343
8. Molodecky NA, Soon S, Rabi DM, Ghali WA, Ferris M. Increasing incidence and prevalence of the inflammatory bowel diseases with time, based on systematic review. *Gastroenterology.* Elsevier; 2012; Available: <http://www.sciencedirect.com/science/article/pii/S0016508511013783>
9. Brand S, Beigel F, Olszak T, Zitzmann K, Eichhorst ST, Otte J-M, et al. IL-22 is increased in active Crohn's disease and promotes proinflammatory gene expression and intestinal epithelial cell migration. *Am J Physiol Gastrointest Liver Physiol.* 2006; 290: G827–38. <https://doi.org/10.1152/ajpgi.00513.2005> PMID: 16537974
10. Yadav PK, Chen C, Liu Z. Potential role of NK cells in the pathogenesis of inflammatory bowel disease. *J Biomed Biotechnol.* 2011; 2011: 348530. <https://doi.org/10.1155/2011/348530> PMID: 21687547
11. Rovedatti L, Kudo T, Biancheri P, Sarra M, Knowles CH, Rampton DS, et al. Differential regulation of interleukin 17 and interferon gamma production in inflammatory bowel disease. *Gut.* 2009; 58: 1629–1636. <https://doi.org/10.1136/gut.2009.182170> PMID: 19740775
12. Sartor RB. Mechanisms of disease: pathogenesis of Crohn's disease and ulcerative colitis. *Nat Clin Pract Gastroenterol Hepatol.* 2006; 3: 390–407. <https://doi.org/10.1038/ncpgasthep0528> PMID: 16819502
13. Hamedani R, Feldman RD, Feagan BG. Review article: Drug development in inflammatory bowel disease: budesonide—a model of targeted therapy. *Aliment Pharmacol Ther.* 1997; 11 Suppl 3: 98–107; discussion 107–8.

14. de Lange KM, Barrett JC. Understanding inflammatory bowel disease via immunogenetics. *J Autoimmun.* 2015; <https://doi.org/10.1016/j.jaut.2015.07.013> PMID: 26257098
15. Najja N, Karoui S, Serghini M, Kallel L, Boubaker J, Filali A. [Management of failure of infliximab in inflammatory bowel disease]. *Tunis Med.* 2011; 89: 517–521. PMID: 21681712
16. Shelton E, Allegretti JR, Stevens B, Lucci M, Khalili H, Nguyen DD, et al. Efficacy of Vedolizumab as Induction Therapy in Refractory IBD Patients: A Multicenter Cohort. *Inflamm Bowel Dis.* 2015; 21: 2879–2885. <https://doi.org/10.1097/MIB.0000000000000561> PMID: 26288002
17. Raine T. Vedolizumab for inflammatory bowel disease: Changing the game, or more of the same? *United European Gastroenterol J.* 2014; 2: 333–344. <https://doi.org/10.1177/2050640614550672> PMID: 25360311
18. Coskun M, Vermeire S, Nielsen OH. Novel Targeted Therapies for Inflammatory Bowel Disease. *Trends Pharmacol Sci.* 2016; <https://doi.org/10.1016/j.tips.2016.10.014> PMID: 27916280
19. Grevenitits P, Thomas A, Lodhia N. Medical Therapy for Inflammatory Bowel Disease. *Surg Clin North Am.* 2015; 95: 1159–82, vi. <https://doi.org/10.1016/j.suc.2015.08.004> PMID: 26596920
20. Wendelsdorf K, Bassaganya-Riera J, Hontecillas R, Eubank S. Model of colonic inflammation: immune modulatory mechanisms in inflammatory bowel disease. *J Theor Biol.* 2010; 264: 1225–1239. <https://doi.org/10.1016/j.jtbi.2010.03.027> PMID: 20362587
21. Dwivedi G, Fitz L, Hegen M, Martin SW, Harrold J, Heatherington A, et al. A Multiscale Model of Interleukin-6-Mediated Immune Regulation in Crohn's Disease and Its Application in Drug Discovery and Development. *CPT: Pharmacometrics & Systems Pharmacology.* 2014; 3: 1–9.
22. Chen S, Jiang H, Cao Y, Wang Y, Hu Z, Zhu Z, et al. Drug target identification using network analysis: Taking active components in Sini decoction as an example. *Sci Rep.* 2016; 6: 24245. <https://doi.org/10.1038/srep24245> PMID: 27095146
23. Ruiz-Cerdá ML, Irurzun-Arana I, González-García I, Hu C, Zhou H, Vermeulen A, et al. Towards patient stratification and treatment in the autoimmune disease lupus erythematosus using a systems pharmacology approach. *Eur J Pharm Sci.* 2016; <https://doi.org/10.1016/j.ejps.2016.04.010> PMID: 27080094
24. Zhou W, Wang Y, Lu A, Zhang G. Systems Pharmacology in Small Molecular Drug Discovery. *Int J Mol Sci.* 2016; 17: 246. <https://doi.org/10.3390/ijms17020246> PMID: 26901192
25. Le Novère N. Quantitative and logic modelling of molecular and gene networks. *Nat Rev Genet.* 2015; 16: 146–158. <https://doi.org/10.1038/nrg3885> PMID: 25645874
26. Kauffman SA. Metabolic stability and epigenesis in randomly constructed genetic nets. *J Theor Biol.* 1969; 22: 437–467. PMID: 5803332
27. Fox RF. Review of Stuart Kauffman, *The Origins of Order: Self-Organization and Selection in Evolution.* *Biophys J.* 1993; 65: 2698–2699.
28. Irurzun-Arana I, Pastor JM, Trocóniz IF, Gómez-Mantilla JD. Advanced Boolean modeling of biological networks applied to systems pharmacology. *Bioinformatics.* 2017; <https://doi.org/10.1093/bioinformatics/btw747> PMID: 28073755
29. Naldi A, Monteiro PT, Müssel C, Consortium for Logical Models and Tools, Kestler HA, Thieffry D, et al. Cooperative development of logical modelling standards and tools with CoLoMoTo. *Bioinformatics.* 2015; 31: 1154–1159. <https://doi.org/10.1093/bioinformatics/btv013> PMID: 25619997
30. Abou-Jaoudé W, Traynard P, Monteiro PT, Saez-Rodríguez J, Helikar T, Thieffry D, et al. Logical Modeling and Dynamical Analysis of Cellular Networks. *Front Genet.* 2016; 7: 94. <https://doi.org/10.3389/fgene.2016.00094> PMID: 27303434
31. Müssel C, Hopfensitz M, Kestler HA. BoolNet—an R package for generation, reconstruction and analysis of Boolean networks. *Bioinformatics.* Oxford University Press; 2010; 26: 1378–1380. <https://doi.org/10.1093/bioinformatics/btq124> PMID: 20378558
32. Chaouiya C, Naldi A, Thieffry D. Logical Modelling of Gene Regulatory Networks with GINsim. In: van Helden J, Toussaint A, Thieffry D, editors. *Bacterial Molecular Networks: Methods and Protocols.* New York, NY: Springer New York; 2012. pp. 463–479.
33. Mei Y, Abedi V, Carbo A, Zhang X, Lu P, Philipson C, et al. Multiscale modeling of mucosal immune responses. *BMC Bioinformatics.* 2015; 16 Suppl 12: S2.
34. Bassaganya-Riera J. *Computational Immunology: Models and Tools.* Academic Press; 2015.
35. Chaouiya C, Bérenguier D, Keating SM, Naldi A, van Iersel MP, Rodríguez N, et al. SBML qualitative models: a model representation format and infrastructure to foster interactions between qualitative modelling formalisms and tools. *BMC Syst Biol.* 2013; 7: 135. <https://doi.org/10.1186/1752-0509-7-135> PMID: 24321545
36. Violeta Balbas-Martínez, Leire Ruiz-Cerdá, Itziar Irurzun-Arana, Ignacio González-García, José David Gómez-Mantilla and Iñaki F. Trocóniz. Systems Pharmacology model for Inflammatory Bowel Disease

- (IBD). In: International Conference on Systems Biology 2016, editor. <https://doi.org/10.3252/pso.eu.17ICSB.2016>
37. Smits HH, van Beelen AJ, Hesse C, Westland R, de Jong E, Soeteman E, et al. Commensal Gram-negative bacteria prime human dendritic cells for enhanced IL-23 and IL-27 expression and enhanced Th1 development. *Eur J Immunol*. 2004; 34: 1371–1380. <https://doi.org/10.1002/eji.200324815> PMID: 15114670
 38. Inohara N, Ogura Y, Fontalba A, Gutierrez O, Pons F, Crespo J, et al. Host recognition of bacterial muramyl dipeptide mediated through NOD2. Implications for Crohn's disease. *J Biol Chem*. 2003; 278: 5509–5512. <https://doi.org/10.1074/jbc.C200673200> PMID: 12514169
 39. Wehkamp J, Frick J-S. Microbiome and chronic inflammatory bowel diseases. *J Mol Med*. 2016; <https://doi.org/10.1007/s00109-016-1495-z> PMID: 27988792
 40. Buttó LF, Haller D. Dysbiosis in intestinal inflammation: Cause or consequence. *Int J Med Microbiol*. 2016; <https://doi.org/10.1016/j.ijmm.2016.02.010> PMID: 27012594
 41. Glasser A-L, Darfeuille-Michaud A. Abnormalities in the handling of intracellular bacteria in Crohn's disease: a link between infectious etiology and host genetic susceptibility. *Arch Immunol Ther Exp*. 2008; 56: 237–244.
 42. Biancheri P, Di Sabatino A, Corazza GR, MacDonald TT. Proteases and the gut barrier. *Cell Tissue Res*. 2013; 351: 269–280. <https://doi.org/10.1007/s00441-012-1390-z> PMID: 22427120
 43. Pender SLF, MacDonald TT. Matrix metalloproteinases and the gut—new roles for old enzymes. *Curr Opin Pharmacol*. 2004; 4: 546–550. <https://doi.org/10.1016/j.coph.2004.06.005> PMID: 15525541
 44. Bamba S, Andoh A, Yasui H, Araki Y, Bamba T, Fujiyama Y. Matrix metalloproteinase-3 secretion from human colonic subepithelial myofibroblasts: role of interleukin-17. *J Gastroenterol*. 2003; 38: 548–554. <https://doi.org/10.1007/s00535-002-1101-8> PMID: 12825130
 45. Lawrance IC, Rogler G, Bamias G, Breynaert C, Florholmen J, Pellino G, et al. Cellular and Molecular Mediators of Intestinal Fibrosis. *J Crohns Colitis*. 2015; <https://doi.org/10.1016/j.crohns.2014.09.008> PMID: 25306501
 46. Geremia A, Biancheri P, Allan P, Corazza GR, Di Sabatino A. Innate and adaptive immunity in inflammatory bowel disease. *Autoimmun Rev*. 2014; 13: 3–10. <https://doi.org/10.1016/j.autrev.2013.06.004> PMID: 23774107
 47. O'Sullivan S, Gilmer JF, Medina C. Matrix metalloproteinases in inflammatory bowel disease: an update. *Mediators Inflamm*. 2015; 2015: 964131. <https://doi.org/10.1155/2015/964131> PMID: 25948887
 48. Monteleone G, Caruso R, Fina D, Peluso I, Gioia V, Stolfi C, et al. Control of matrix metalloproteinase production in human intestinal fibroblasts by interleukin 21. *Gut*. 2006; 55: 1774–1780. <https://doi.org/10.1136/gut.2006.093187> PMID: 16682426
 49. Helikar T, Kowal B, Rogers JA. A cell simulator platform: the cell collective. *Clin Pharmacol Ther*. 2013; 93: 393–395. <https://doi.org/10.1038/clpt.2013.41> PMID: 23549147
 50. Helikar T, Kowal B, McClenathan S, Bruckner M, Rowley T, Madrahimov A, et al. The Cell Collective: toward an open and collaborative approach to systems biology. *BMC Syst Biol*. 2012; 6: 96. <https://doi.org/10.1186/1752-0509-6-96> PMID: 22871178
 51. Boldhaus G, Bertschinger N, Rauh J, Olbrich E, Klemm K. Robustness of Boolean dynamics under knockouts. *Phys Rev E Stat Nonlin Soft Matter Phys*. 2010; 82: 021916. <https://doi.org/10.1103/PhysRevE.82.021916> PMID: 20866846
 52. Taylor AL, Watson CJE, Bradley JA. Immunosuppressive agents in solid organ transplantation: Mechanisms of action and therapeutic efficacy. *Crit Rev Oncol Hematol*. 2005; 56: 23–46. <https://doi.org/10.1016/j.critrevonc.2005.03.012> PMID: 16039869
 53. McManus R. Mechanisms of steroid action and resistance in inflammation and disease. *J Endocrinol*. 2003; 178: 1–4. PMID: 12844329
 54. Coutinho AE, Chapman KE. The anti-inflammatory and immunosuppressive effects of glucocorticoids, recent developments and mechanistic insights. *Mol Cell Endocrinol*. 2011; 335: 2–13. <https://doi.org/10.1016/j.mce.2010.04.005> PMID: 20398732
 55. Peters LA, Perrigoue J, Mortha A, Iuga A, Song W-M, Neiman EM, et al. A functional genomics predictive network model identifies regulators of inflammatory bowel disease. *Nat Genet*. 2017; 49: 1437–1449. <https://doi.org/10.1038/ng.3947> PMID: 28892060
 56. Laffin M, Madsen KL. Fecal Microbial Transplantation in Inflammatory Bowel Disease: A Movement Too Big to Be Ignored. *Clin Pharmacol Ther*. 2017; 102: 588–590. <https://doi.org/10.1002/cpt.747> PMID: 28695658
 57. Fischer S, Neurath MF. Precision Medicine in Inflammatory Bowel Diseases. *Clin Pharmacol Ther*. 2017; 102: 623–632. <https://doi.org/10.1002/cpt.793> PMID: 28699158

58. Dipasquale V, Romano C. Vaccination strategies in pediatric inflammatory bowel disease. *Vaccine*. 2017; <https://doi.org/10.1016/j.vaccine.2017.09.031> PMID: 28967524
59. Danese S, Furfaro F, Vetrano S. Targeting S1P in Inflammatory bowel disease: new avenues for modulating intestinal leukocyte migration. *J Crohns Colitis*. 2017; <https://doi.org/10.1093/ecco-jcc/jjx107> PMID: 28961752
60. Fengming Y, Jianbing W. Biomarkers of inflammatory bowel disease. *Dis Markers*. 2014; 2014: 710915. <https://doi.org/10.1155/2014/710915> PMID: 24963213
61. Helikar T, Konvalina J, Heidel J, Rogers JA. Emergent decision-making in biological signal transduction networks. *Proc Natl Acad Sci U S A*. 2008; 105: 1913–1918. <https://doi.org/10.1073/pnas.0705088105> PMID: 18250321
62. Ben-Horin S, Vande Casteele N, Schreiber S, Lakatos PL. Biosimilars in Inflammatory Bowel Disease: Facts and Fears of Extrapolation. *Clin Gastroenterol Hepatol*. 2016; <https://doi.org/10.1016/j.cgh.2016.05.023> PMID: 27215364
63. van Dullemen HM, van Deventer SJ, Hommes DW, Bijl HA, Jansen J, Tytgat GN, et al. Treatment of Crohn's disease with anti-tumor necrosis factor chimeric monoclonal antibody (cA2). *Gastroenterology*. 1995; 109: 129–135. PMID: 7797011
64. Present DH, Rutgeerts P, Targan S, Hanauer SB, Mayer L, van Hozegand RA, et al. Infliximab for the treatment of fistulas in patients with Crohn's disease. *N Engl J Med*. 1999; 340: 1398–1405. <https://doi.org/10.1056/NEJM199905063401804> PMID: 10228190
65. Colombel J-F, Sandborn WJ, Rutgeerts P, Enns R, Hanauer SB, Panaccione R, et al. Adalimumab for maintenance of clinical response and remission in patients with Crohn's disease: the CHARM trial. *Gastroenterology*. 2007; 132: 52–65. <https://doi.org/10.1053/j.gastro.2006.11.041> PMID: 17241859
66. Yoshimura N, Yokoyama Y, Matsuoka K, Takahashi H, Iwakiri R, Yamamoto T, et al. An open-label prospective randomized multicenter study of intensive versus weekly granulocyte and monocyte apheresis in active crohn's disease. *BMC Gastroenterol*. 2015; 15: 163. <https://doi.org/10.1186/s12876-015-0390-3> PMID: 26585569
67. Liu Z, Jiang X, Sun C. The efficacy and safety of selective granulocyte and monocyte apheresis for inflammatory bowel disease: A meta-analysis. *Eur J Intern Med*. 2016; 36: e26–e27. <https://doi.org/10.1016/j.ejim.2016.08.028> PMID: 27614377
68. Di Girolamo M, Sartini A, Critelli R, Bertani A, Merighi A, Villa E. Efficacy of a Novel Granulocyte Monocyte Apheresis Adsorber Device in the Treatment of Inflammatory Bowel Diseases: A Pilot Study. *Ther Apher Dial*. 2016; 20: 668–676. <https://doi.org/10.1111/1744-9987.12453> PMID: 27921374
69. Hommes DW, Mikhajlova TL, Stoinov S, Stimac D, Vucelic B, Lonovics J, et al. Fontolizumab, a humanised anti-interferon gamma antibody, demonstrates safety and clinical activity in patients with moderate to severe Crohn's disease. *Gut*. 2006; 55: 1131–1137. <https://doi.org/10.1136/gut.2005.079392> PMID: 16507585
70. Reinisch W, Hommes DW, Van Assche G, Colombel J-F, Gendre J-P, Oldenburg B, et al. A dose escalating, placebo controlled, double blind, single dose and multidose, safety and tolerability study of fontolizumab, a humanised anti-interferon gamma antibody, in patients with moderate to severe Crohn's disease. *Gut*. 2006; 55: 1138–1144. <https://doi.org/10.1136/gut.2005.079434> PMID: 16492717
71. Schreiber S, Fedorak RN, Nielsen OH, Wild G, Williams CN, Nikolaus S, et al. Safety and efficacy of recombinant human interleukin 10 in chronic active Crohn's disease. Crohn's Disease IL-10 Cooperative Study Group. *Gastroenterology*. 2000; 119: 1461–1472. PMID: 11113067
72. Hueber W, Sands BE, Lewitzky S, Vandemeulebroecke M, Reinisch W, Higgins PDR, et al. Secukinumab, a human anti-IL-17A monoclonal antibody, for moderate to severe Crohn's disease: unexpected results of a randomised, double-blind placebo-controlled trial. *Gut*. 2012; 61: 1693–1700. <https://doi.org/10.1136/gutjnl-2011-301668> PMID: 22595313
73. Sands BE, Sandborn WJ, Creed TJ, Dayan CM, Dhanda AD, Van Assche GA, et al. Basiliximab does not increase efficacy of corticosteroids in patients with steroid-refractory ulcerative colitis. *Gastroenterology*. 2012; 143: 356–64.e1. <https://doi.org/10.1053/j.gastro.2012.04.043> PMID: 22549092
74. Van Assche G, Sandborn WJ, Feagan BG, Salzberg BA, Silvers D, Monroe PS, et al. Daclizumab, a humanised monoclonal antibody to the interleukin 2 receptor (CD25), for the treatment of moderately to severely active ulcerative colitis: a randomised, double blind, placebo controlled, dose ranging trial. *Gut*. BMJ Publishing Group Ltd and British Society of Gastroenterology; 2006; 55: 1568–1574. <https://doi.org/10.1136/gut.2005.089854> PMID: 16603634
75. Paliogianni F, Ahuja SS, Balow JP, Balow JE, Boumpas DT. Novel mechanism for inhibition of human T cells by glucocorticoids. Glucocorticoids inhibit signal transduction through IL-2 receptor. *J Immunol*. 1993; 151: 4081–4089. PMID: 8409387
76. Horst HJ, Flad HD. Corticosteroid-interleukin 2 interactions: inhibition of binding of interleukin 2 to interleukin 2 receptors. *Clin Exp Immunol*. 1987; 68: 156–161. PMID: 3115640

77. El Menyawi M, Fawzy M, Al-Nahas Z, Edris A, Hussein H, Shaker O, et al. Serum tumor necrosis factor alpha (TNF- α) level in patients with Behçet's disease: Relation to clinical manifestations and disease activity. *The Egyptian Rheumatologist*. 2014; 36: 139–143.
78. Shi M, Wei J, Dong J, Meng W, Ma J, Wang T, et al. Function of interleukin-17 and -35 in the blood of patients with hepatitis B-related liver cirrhosis. *Mol Med Rep*. 2015; 11: 121–126. <https://doi.org/10.3892/mmr.2014.2681> PMID: 25323532
79. Thomas DW, Burns J, Audette J, Carrol A, Dow-Hygelund C, Hay M. Clinical development success rates 2006–2015. San Diego: Biomedtracker/Washington, DC: BIO/Bend: Amplion. 2016;
80. Furfaro F, Gilardi D, Allocca M, Cicerone C, Correale C, Fiorino G, et al. IL-23 Blockade for Crohn's disease: next generation of anti-cytokine therapy. *Expert Rev Clin Immunol*. 2017; 1–11.
81. Palsson S, Hickling TP, Bradshaw-Pierce EL, Zager M, Jooss K, O'Brien PJ, et al. The development of a fully-integrated immune response model (FIRM) simulator of the immune response through integration of multiple subset models. *BMC Syst Biol*. 2013; 7: 95. <https://doi.org/10.1186/1752-0509-7-95> PMID: 24074340
82. Carbo A, Hontecillas R, Kronsteiner B, Viladomiu M, Pedragosa M, Lu P, et al. Systems modeling of molecular mechanisms controlling cytokine-driven CD4+ T cell differentiation and phenotype plasticity. *PLoS Comput Biol*. 2013; 9: e1003027. <https://doi.org/10.1371/journal.pcbi.1003027> PMID: 23592971
83. Laurence A O'Shea JJ. TH-17 differentiation: of mice and men. *Nat Immunol*. Nature Publishing Group; 2007; 8: 903–905. <https://doi.org/10.1038/ni0907-903> PMID: 17712339
84. Reynolds G, Haniffa M. Human and Mouse Mononuclear Phagocyte Networks: A Tale of Two Species? *Front Immunol*. 2015; 6: 330. <https://doi.org/10.3389/fimmu.2015.00330> PMID: 26124761
85. Mestas J, Hughes CCW. Of mice and not men: differences between mouse and human immunology. *J Immunol*. 2004; 172: 2731–2738. PMID: 14978070
86. Wasilewska A, Winiarska M, Olszewska M, Rudnicka L. Interleukin-17 inhibitors. A new era in treatment of psoriasis and other skin diseases. *Postepy Dermatol Alergol*. 2016; 33: 247–252. <https://doi.org/10.5114/ada.2016.61599> PMID: 27605893
87. Tan Y, Qi Q, Lu C, Niu X, Bai Y, Jiang C, et al. Cytokine Imbalance as a Common Mechanism in Both Psoriasis and Rheumatoid Arthritis. *Mediators Inflamm*. 2017; 2017: 2405291. <https://doi.org/10.1155/2017/2405291> PMID: 28239238
88. Ryll A, Samaga R, Schaper F, Alexopoulos LG, Klamt S. Large-scale network models of IL-1 and IL-6 signalling and their hepatocellular specification. *Mol Biosyst*. 2011; 7: 3253–3270. <https://doi.org/10.1039/c1mb05261f> PMID: 21968890
89. Kauffman SA. Metabolic stability and epigenesis in randomly constructed genetic nets. *J Theor Biol*. 1969; 22: 437–467. PMID: 5803332
90. Kauffman SA. The origins of order: Self organization and selection in evolution. Oxford University Press, USA; 1993.
91. Hopfensitz M, Müssel C, Maucher M, Kestler HA. Attractors in Boolean networks: a tutorial. *Comput Stat*. Springer-Verlag; 2012; 28: 19–36.
92. Saadatpour A, Albert I, Albert R. Attractor analysis of asynchronous Boolean models of signal transduction networks. *J Theor Biol*. 2010; 266: 641–656. <https://doi.org/10.1016/j.jtbi.2010.07.022> PMID: 20659480
93. Wynn ML, Consul N, Merajver SD, Schnell S. Logic-based models in systems biology: a predictive and parameter-free network analysis method. *Integr Biol*. 2012; 4: 1323–1337.
94. Saadatpour A, Albert I, Albert R. Attractor analysis of asynchronous Boolean models of signal transduction networks. *J Theor Biol*. Elsevier; 2010; 266: 641–656. <https://doi.org/10.1016/j.jtbi.2010.07.022> PMID: 20659480
95. Thakar J, Pillone M, Kirimanjeswara G, Harvill ET, Albert R. Modeling systems-level regulation of host immune responses. *PLoS Comput Biol*. 2007; 3: e109. <https://doi.org/10.1371/journal.pcbi.0030109> PMID: 17559300
96. Harvey I, Bossomaier T. Time out of joint: Attractors in asynchronous random boolean networks. *Proceedings of the Fourth European Conference on Artificial Life*. MIT Press, Cambridge; 1997. pp. 67–75.
97. Willadsen K, Triesch J, Wiles J. Understanding robustness in Random Boolean Networks. *ALIFE*. 2008. pp. 694–701.
98. Rokach L, Maimon O. Clustering Methods. In: Maimon O, Rokach L, editors. *Data Mining and Knowledge Discovery Handbook*. Springer US; 2005. pp. 321–352.